NOTICE

The quality of this microform is heavily dependent upon the quality of the original thesis submitted for microfilming. Every effort has been made to ensure the highest quality of reproduction possible.

If pages are missing, contact the university which granted the degree.

Some pages may have indistinct print especially if the original pages were typed with a poor typewriter ribbon or if the university sent us an inferior photocopy.

Reproduction in full or in part of this microform is governed by the Canadian Copyright Act, R.S.C. 1970, c. C-30, and subsequent amendments.

AVIS

La qualité de cette microforme dépend grandement de la qualité de la thèse soumise au microfilmage. Nous avons tout fait pour assurer une qualité supérieure de reproduction.

S'il manque des pages, veuillez communiquer avec l'université qui a conféré le grade.

La qualité d'impression de certaines pages peut laisser à désirer, surtout si les pages originales ont été dactylographiées à l'aide d'un ruban usé ou si l'université nous a fait parvenir une photocopie de qualité inférieure.

La reproduction, même partielle, de cette microforme est soumise à la Loi canadienne sur le droit d'auteur, SRC 1970, c. C-30, et ses amendements subséquents.

The Synthesis and Reactivity of α,β–Unsaturated Thioamide, Thioester, and Thione Iron Tricarbonyl Complexes

by

Dee Anne Brandes

Submitted in partial fulfilment
of the requirements for the degree of
Doctor of Philosophy

Faculty of Graduate Studies
University of Ottawa

ISBN 0-315-60020-9

UNIVERSITÉ D'OTTAWA
UNIVERSITY OF OTTAWA

Not to the swift, the race:

Not to the strong, the fight:

Not to the righteous, perfect grace:

Not to the wise, the light:

But often faltering feet

Come surest to the goal;

And they who walk in darkness meet

The sunrise of the soul.

Henry van Dyke, Reliance

Abstract

α,β-Unsaturated thioamide, thioester and thione iron tricarbonyl complexes **1**-**13** were prepared from the free ligands and iron pentacarbonyl using photolysis or diiron nonacarbonyl using thermolysis. X-ray crystal structures were obtained for the free ligand **2'**, [PhCH=C(Ph)C(S)NEt_2], and for complexes **1** and **2**, [$\overline{Fe(PhCH=CHC(S)NEt_2)(CO)_3}$] and [$\overline{Fe(PhCH=C(Ph)C(S)NEt_2)(CO)_3}$] respectively. Thioamide and thioester iron tricarbonyl complexes gave triphenylphosphine substituted complexes **17**-**19** resulting from loss of a carbon monoxide ligand by photolysis or thermolysis. It was not possible to substitute more than one triphenylphosphine into the complexes. Thioamide and thioester ligands could be removed from the iron tricarbonyl fragment using ceric ammonium nitrate, hydrogen peroxide, m-chloroperbenzoic acid, or thermolysis. The best results were obtained with ceric ammonium nitrate, which minimized conversion of the C=S functional group to C=O. Thioester complex **10**, [$\overline{Fe(PhCH=CHC(S)OEt)(CO)_3}$], reacted with hydrogen peroxide or m-chloroperbenzoic acid to give the sulphine complex **20**, [$\overline{Fe(PhCH=CHC(S=O)OEt)(CO)_3}$]. Nucleophiles reacted with thioamide and thioester iron tricarbonyl complexes at room temperature affording 1,4-Michael addition products free of metal coordination. At -78°C, nucleophiles reacted with thioamide iron tricarbonyl complexes forming 4-oxo-thioamide non-metal coordinated products. An electrophile reacted with thioester tricarbonyl complex **10** to give an S-alkylated cationic complex **21**, [[$\overline{Fe(PhCH=CHC(S^+\text{-}Me)OEt)(CO)_3}$][$BF_4^-$]]. Alkynes added to the metal -coordinated olefin of α,β-unsaturated thioamide iron tricarbonyl complexes **1**, **4**, [$\overline{Fe(MeCH=CHC(S)NEt_2)(CO)_3}$], and **7**, [$\overline{Fe(MeCH=CHC(S)N(Ph)(Me))(CO)_3}$], generating complexes **22**-**26** possessing a cyclopentenone ligand. An X-ray crystal structure was obtained for complex **22**.

Silicon alkoxides were used as a source of alkoxide to prepare carboxylic esters in good yields from benzylic bromides and carbon monoxide catalyzed by a rhodium (I) complex under mild conditions.

Acknowledgements

I extend my sincere gratitude to Dr. H. Alper for his guidance and encouragement.

I would also like to thank my coworkers for their friendship.

I also extend thanks to the entire faculty and staff, especially Clem Kazakoff, Raj Capoor, and Heather Dettman for their assistance.

To Eric Gabe and Ian Butler, I express my gratitude for the X-ray crystallographic determinations presented in this work.

The financial support of the University and NSERC for funding this project are gratefully acknowledged.

To my family, Mom, Dad, Kurt, Barb, and Kim,.....I MADE IT!

I offer my most sincere thanks to Phil for his continous love and support. His belief in me gave me the confidence to succeed.

To the Lord our God, I give thanks for His gift of the desire to learn.

Table of Contents

PART I

PART II

List of Tables

List of Figures

List of Abbreviations

Me = methyl

Et = ethyl

n-Bu = n-butyl

t-Bu = tert-butyl

Ph = phenyl

R = alkyl group

BDA = benzylideneacetone

PPh_3 = triphenylphosphine

ee = enantiomeric excess

DMMH = dimethyl malonate

LDA = lithium diisopropyl amine

NMR = nuclear magnetic resonance

- m = multiplet
- s = singlet
- d = doublet
- t = triplet
- q = quartet

IR = infrared

- (s) = strong
- (vs) = very strong
- (m) = medium
- (w) = weak
- (br) = broad

MS = mass spectrometry

ppm = parts per million

DEPT = distortionless enhancement polarization transfer

R_w = weight refinement

$[PPN]^+$ = bistriphenylphosphine imminium

BPK	=	sodium benzophenone ketyl
THF	=	tetrahydrofuran
C_p	=	cyclopentadienyl
M	=	transition metal
L	=	ligand
HETCOR	=	heteronuclear correlation
HMO	=	Huckel molecular orbital
LCAO	=	linear combination of atomic orbitals
SCF	=	self-consistant-field
INDO	=	neglect of differential overlap
CI	=	chemical ionization
EI	=	electron impact
DAD	=	diazo-diene
DMAD	=	dimethylacetylene dicarboxylate
mcpba	=	m-chloroperbenzoic acid
Ce(IV)	=	ceric ammonium nitrate
Nu^-	=	nucleophile
E	=	electrophile
Ar	=	aromatic
tlc	=	thin layer chromatography
●	=	impurity
B.p.	=	boiling point
M.p.	=	melting point
hυ	=	photolysis
Δ	=	thermolysis
eqv.	=	equivalents
atm	=	atmospheres

psi = pounds per square inch

decomp. = decomposition

PART I

CHAPTER 1

INTRODUCTION

This part of the thesis reports the preparation and characterization of the first α,β-unsaturated thioamide, thioester, and thione iron tricarbonyl complexes and their reactivity towards substitution, ligand removal, oxidation, electrophilic and nucleophilic attack, as well as alkyne addition. This first chapter provides a general discussion of the role of organotransition metals in organic chemistry along with a discussion of the known literature regarding α,β-unsaturated heteroatom organometallic complexes.

1.1 Organotransition Metals in Organic Chemistry

Most organic chemicals produced in bulk quantities are derived from natural gas and petroleum, usually after prior conversion of these hydrocarbons into olefins such as ethylene, propylene, or butadiene. The use of transition metal complexes for the conversion of unsaturated hydrocarbons into polymers, alcohols, ketones, carboxylic acids, and other functionalized organic molecules has been intensively studied with the result that many industrial processes utilize the technology developed from this research[1].

The use of transition metals also offers versatility to the bench organic chemist since many restrictions on chemical reactions can be overcome by metal complexation. Molecules of theoretical interest and intermediates of practical value which are too unstable to be isolated can be stabilized, protection of olefinic groups can be achieved, and the metal can be used to alter the

stereochemical outcome of many organic transformations.

The two major classes of reaction types in which transition metals are used in organic synthesis involve either catalytic or stoichiometric methods. In a catalytic reaction, a substrate A is converted into a product B in the presence of a small amount of transition metal, [M].

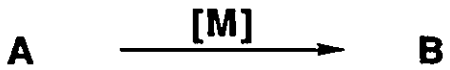

These transition metal mediated reactions utilize either a heterogeneous or a homogeneous catalyst.

Difficulties associated with the separation of the transition metal from the products in a homogeneous reaction have often made a heterogeneous process more useful in industry. Also, in the production of bulk organic chemicals, engineering and economic advantages are evident in the stability and high productivity availed by a heterogeneous system. Such systems suffer the disadvantage of being difficult to study. Homogeneous reactions, on the other hand, can be easily studied spectroscopically. In certain favourable cases intermediates in the reaction, isolated or otherwise, can be characterized. Unlike heterogeneous systems, a homogeneous reaction can provide extraordinary regio- and stereo-selective transformations owing to their operation under milder conditions of temperature and pressure or because of the nature of the transition metal. Furthermore, the common polarity of organic functional groups towards reagents can be completely reversed by complexation to a metal centre. These advantages make homogeneous reactions extremely valuable in organic synthesis.

In stoichiometric reactions, which are usually homogeneous, the transition metal is present in equal quantity to the substrate. The reaction may

proceed by a route in which there is a transient, non-stable metal complex intermediate, [A-M], or by one in which a stable metal complex, [A-M], is generated on route to product formation.

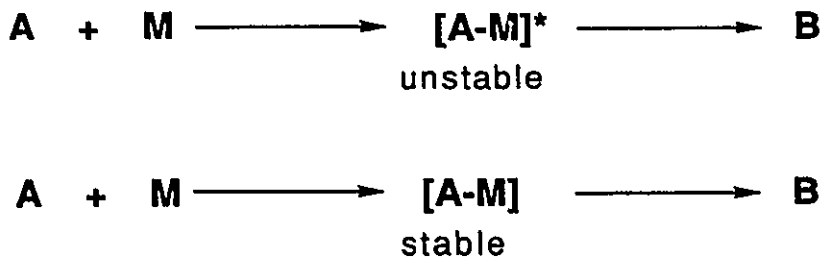

There are obvious economic advantages associated with catalytic reactions but stoichiometric reactions remain prevalent and requisite for some chemical transformations. Among the synthetically useful transition metal mediated stoichiometric reactions in organic synthesis, the most studied and commonly used are those involving carbon-carbon double bonds able to form either stable or unstable π-complexes[2].

1.2 Conjugated Dienes

Diolefin compounds are known to coordinate readily to many transition metals including iron(0)[3]. The reactivity of the organic system in complexes of conjugated dienes with tricarbonyl iron is firmly established to differ from that of the uncomplexed ligand. These differences in reactivity, particularly as applied to reactions of synthetic value, have provided organic and inorganic chemists with many fruitful research topics. A brief survey of some of the reactions of polyolefin-coordinated iron tricarbonyl complexes follows.

Many organic chemists have used the complexation of the 1,3-diene unit to protect it while carrying out reactions at other sites on the organic ligand. One

example is illustrated in Scheme 1, in which reactions occurred selectively at the aldehydic carbon[3].

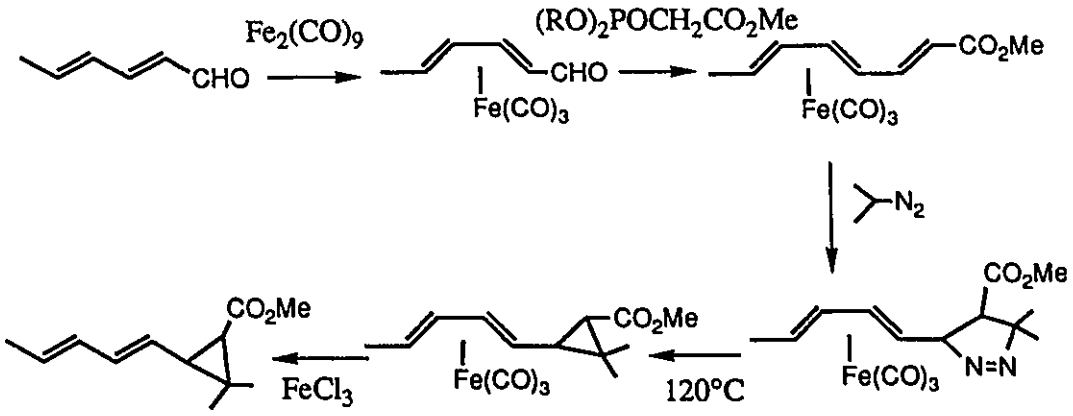

Scheme 1

Once a transformation is effected on an organic compound which is coordinated to a transition metal centre, removal of the organic ligand from the metal is necessary by some method which does not alter the organic compound, thus making the net process a synthetically viable one. Several factors contribute to the choice of method,[3] including: 1) the strength of the ligand-metal bond; 2) the oxidation state of the metal; 3) the presence of other functional groups on the organic compound, which may undergo further reaction; 4) the ability of the method to remove the organic compound in high yields; 5) the ease of separation of the organic compound from the final reaction mixture. Several methods have been developed to satisfy the above conditions and these are oxidation, protonation, and ligand exchange.

Oxidation of the metal weakens the metal carbon bonds which results in two principal modes of reaction[4]. In its oxidized state, the metal becomes a better leaving group in that the alkyl carbon is subject to S_N2 nucleophilic

substitution or solvolysis. The other mode of reaction stems from the enhanced tendency exhibited by oxidized alkyl carbonyl complexes to undergo alkyl to acyl migratory insertion followed by solvolysis of the resulting highly reactive acyl complex. A number of oxidatively induced nucleophilic metal-carbon bond cleavages are known[1].

Mild oxidative reagents are the most commonly used for ligand removal since they have been found in many examples to remove the ligand with no detrimental effect to other functional groups on the coordinated ligand. A common reagent for ligand removal uses ceric ammonium nitrate to oxidize the metal and thereby cleave the diene. Another mild oxidant, ferric chloride, has been used successfully instead of ceric ammonium nitrate for oxidative cleavage of organic ligands, and it was used in the example shown in Scheme 1[3].

Sometimes a proton source is sufficient to induce ligand removal. Most of the reactions of this type are believed to involve the initial protonation of the metal[1]. In support of this, the cleavage of the alkyl group from $[CpFe(CO)_2R]$ using $[CF_3COOH]$ has been found to occur through the intermediate $[CpFe(CO)_2(R)H][H(O_2CCF_3)_2]$ generating RH by reductive elimination[4]. A less commonly used reagent for organic ligand removal is trimethylamine oxide. This reagent is also a well known reagent for specific removal of CO ligands, so when the target organic molecule is coordinated to a tricarbonyl-iron fragment, sufficient reagent is required to remove all of the CO's as well as the ligand. For example, anionic additions to iron tricarbonyl benzenoid cations gave products I-III, which retained their configuration after removal of the $[Fe(CO)_3]$ fragment only when treated with trimethylamine oxide allowing for analysis of the stereoisomeric composition of the organic products, [2][5].

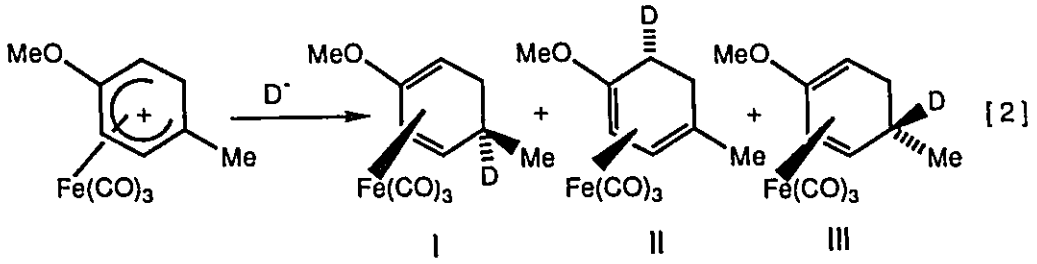

[2]

Another interesting use of a tricarbonyl iron diene system is the recent report of a chiral iron tricarbonyl complex of sorbic acid which was used as an efficient resolving agent for racemic mixtures of allylic alcohols[6]. Alcohol IV was coupled with optically pure acid (-)V affording a mixture of esters VI and VII which were readily separated by chromatography, (Scheme 2).

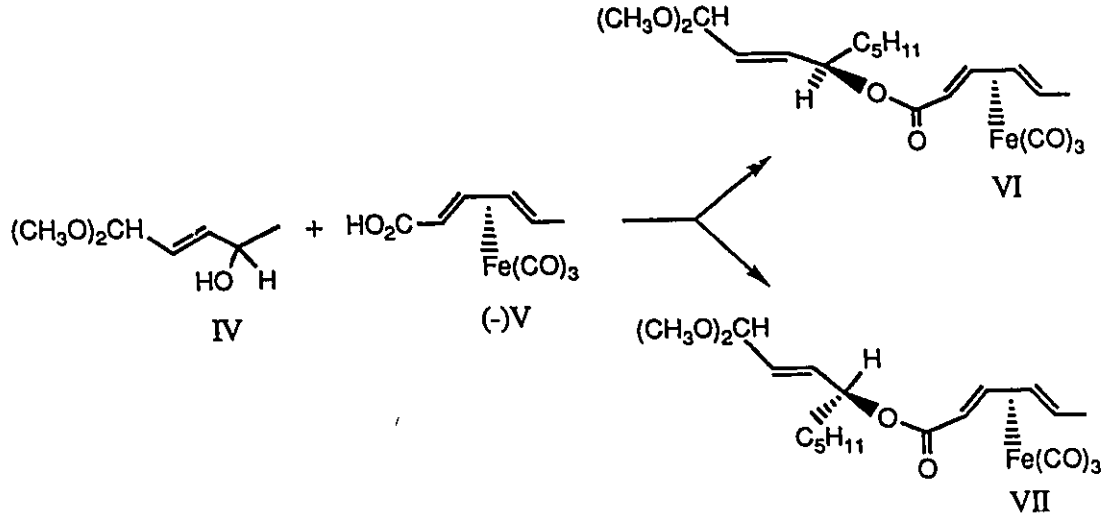

Scheme 2

The attack of nucleophiles on transition metal olefinic complexes is one of the most important classes of reactions for the preparation of new complexes and for the transformation of organic compounds that are bound to a metal centre. Nucleophiles can attack at either the metal centre or directly at the coordinated

organic ligand. Attack at the transition metal centre is a process which normally results in ligand exchange, while attack at the organic ligand coordinated to the transition metal is of major importance in the application of transition metals in organic synthesis.

Nucleophilic attack at unsaturated hydrocarbon ligands is mostly found for metals with relatively high oxidation states and having a formal positive charge or having several electron withdrawing ligands such as carbon monoxide. The reaction of nucleophiles with π-olefin complexes produces σ-alkyl metal complexes. Nucleophiles which directly attack the olefinic ligand do so from the face opposite the metal (trans attack) and usually at the more substituted olefin terminus. In contrast, initial nucleophilic reaction at the metal centre followed by insertion into the olefin gives cis addition products which occur at the least substituted olefin terminus, (Scheme 3)[1].

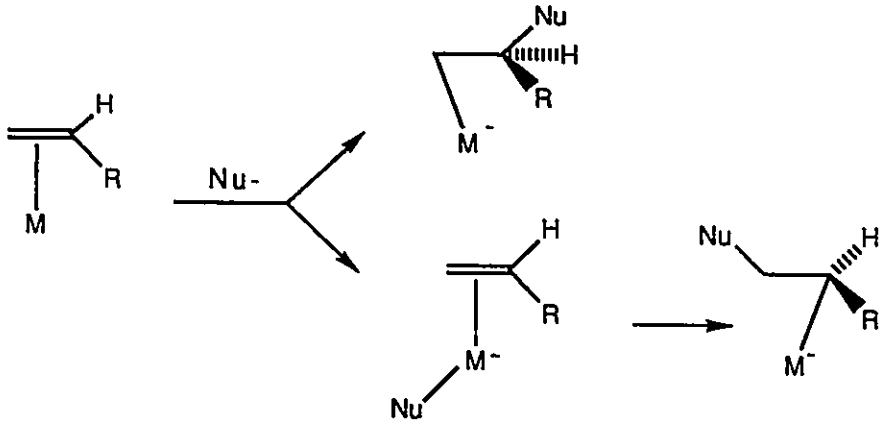

Scheme 3

Nucleophilic attack at η^4-diene complexes have been investigated for several metals. Cationic molybdenum complex VIII reacts with nucleophiles at a terminal position and exclusively from the face opposite to the metal generating η^3-allyl complex IX.

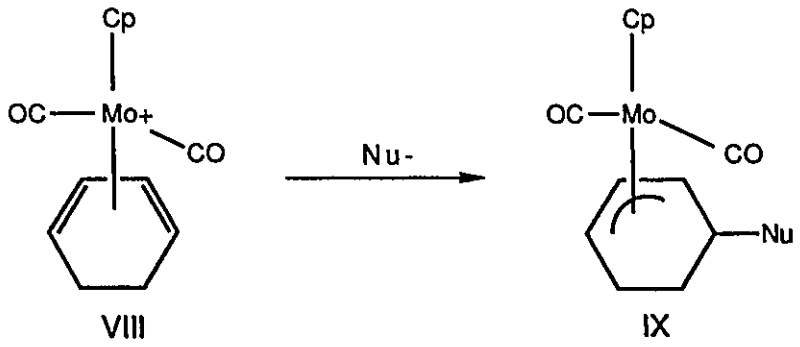

VIII IX

Such a molybdenum complex was recently used by Pearson which led to an efficient entry into trichothecene[7]. Mixtures of dienes were converted to diene-molybdenum cationic complexes X which then reacted with a variety of carbanion nucleophiles, (Scheme 4). Reaction of complex X with the lithium enolate of trimethylsilyl propionate, followed by acidic work-up gave the π-allyl complex XI in 93% yield. This was converted to the lactone XII which can be used as an intermediate for the synthesis of (±)-trichodermin XIII and (±)-trichodiene XIV. The great advantage of this synthetic route towards the lactone XII lies in its 5-step conversion from p-xylene, as compared to the traditional organic synthetic routes requiring 8-steps from 4-methylanisole or 10-steps from 2,5-dimethylcyclohexanone.

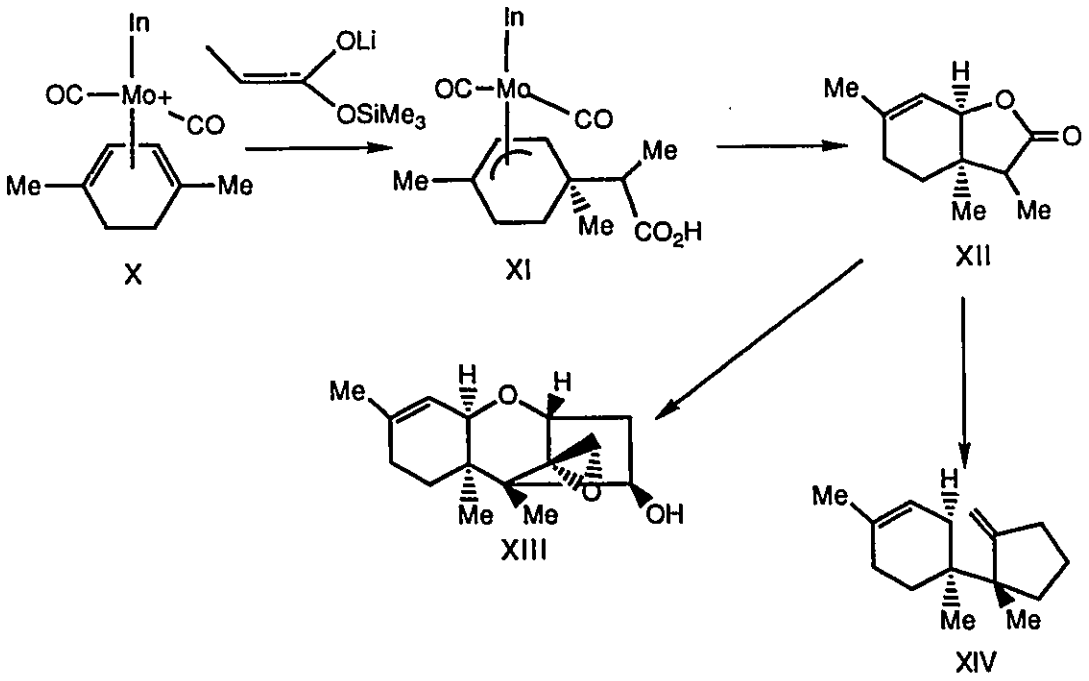

Scheme 4

Earlier Pearson used cyclohexadienyl-iron complexes similar to molybdenum complex X to synthesize compounds of type XIII and XIV (Scheme 4)[8,9,10].

The regioselectivity in the addition of nucleophiles to metal coordinated polyene systems offers two sites of possible attack, terminal or internal. Semmelhack reported a systematic study of selectivity with (η^4-1,3-diene)tricarbonyl iron complexes which showed that kinetically-controlled addition at -78°C primarily gave only anion addition at an unsubstituted internal position but at temperatures near 0°C, this addition was rapidly reversible and the thermodynamically favoured product results from nucleophilic addition at a terminal position[11]. Scheme 5 illustrates the reaction pathways.

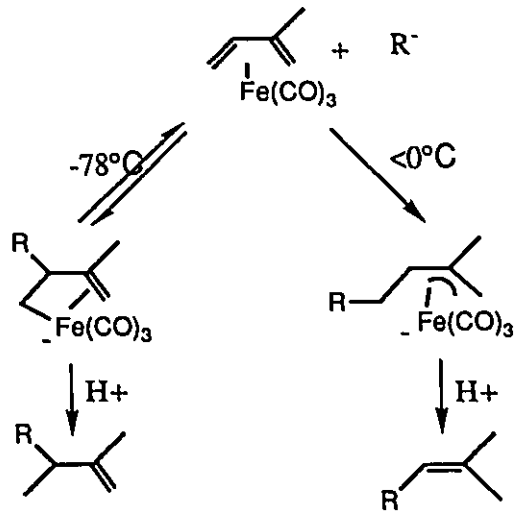

Scheme 5

The thermodynamically preferred formation of an η^3-allyl complex was due to its greater stability at temperatures above -78°C.

Earlier Semmelhack found that anion addition to (η^4-1,3-cyclohexadiene) and (η^4-1,3-diene) complexes of iron tricarbonyl under a carbon monoxide atmosphere gave CO-insertion products[12]. Cyclohexadienes gave ketones while dienes gave aldehydes, [2], and cyclopentanones, [3].

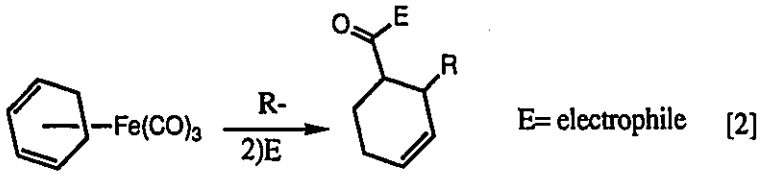

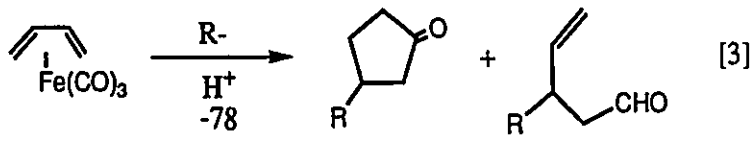

Many more applications of diene-tricarbonyl iron complexes to organic synthesis have been reported[6].

1.3 Complexes of Conjugated Heteroatoms

A logical extention to the ease of formation of diene-hydrocarbon ligands with transition metal centres is to investigate α,β-unsaturated heterodienes as ligands. The number of investigations into the reactivity of diene-like ligands containing heteroatoms are few compared with those of hydrocarbon ligands. In heteroatom-containing dienes, the presence of a heteroatom has the potential to alter the reactivity both at the metal and at the ligand. Studies of the effects of heteroatoms could lead to an increased general knowledge of organotransition metal chemistry as well as offering the potential to modify the organic ligand in a selective manner so as to generate novel organic compounds.

Heterodiene complexes that have been prepared include α,β-unsaturated ketones, aldehydes, amides, esters, imines, thioamides, and thioaldehydes. These conjugated heterodiene metal complexes may be considered to be derived from butadiene-metal π-complexes by replacing one of the sp^2 carbon atoms by a heteroatom. Other heterodiene systems are known including [O=C-C=N-], [-N=C-C=N-], and [-N=N-N=N-][13].

The first report of an α,β-unsaturated aldehyde complex was published in 1964. It was generated by heating cinnamaldehyde iron tetracarbonyl at 60°C for 15h, [4][14].

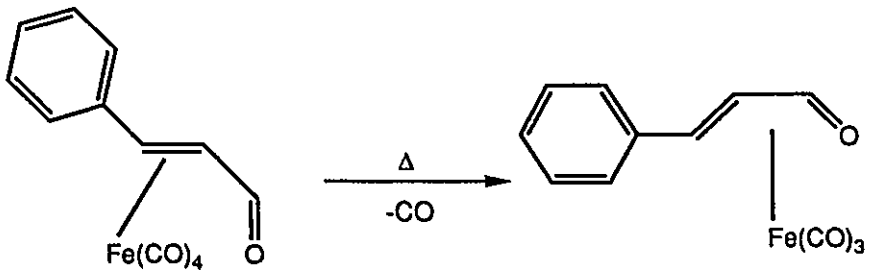

[4]

Following the same procedure, Howell, Johnson, Josty, and Lewis reported the first synthesis of complexes of α,β-unsaturated ketones, namely benzylideneacetone (BDA), chalcone, and 2,4-dibenzylidene-cyclohexanone[13].

The number of studies of the chemistry of these α,β-unsaturated ketones and aldehydes far exceeds that of any other heterodiene-metal system. Ketone complexes have the advantage that they are easy to prepare in high yields. In particular, the focus has been on the use of such complexes as a convenient source of the $[Fe(CO)_3]$ moiety for the preparation of $[(\eta^4\text{-polyolefin})Fe(CO)_3]$ complexes. The ketone is readily displaced by dienes allowing for exchange to occur under mild conditions which are usually not detrimental to other substituents on the diene molecule. Because of this, the complex $[(BDA)Fe(CO)_3]$ has been used as a trapping agent for stabilizing highly reactive polyolefins[15].

Also, Birch, Raverty, and Stephenson prepared optically active enone-iron tricarbonyl complexes from $[(BDA)Fe(CO)_3]$ and reacted them with prochiral dienes producing complexes of the type $[Fe(CO)_3(diene)]$ with some retained optical activity[16]. The chirality transfer which took place between the auxiliary α,β-unsaturated ketone having chiral centres and a prochiral diene gave planar chirality to cyclic dienes. The degree of asymmetric induction depended on the selectivity between the two enantiofaces of the diene during complexation.

Recently a novel chiral phosphite complex containing an α,β-unsaturated ketone moiety (XV) was synthesized permitting high diastereofacial selective coordination of the conjugated enone moiety to transition metals, [5][17].

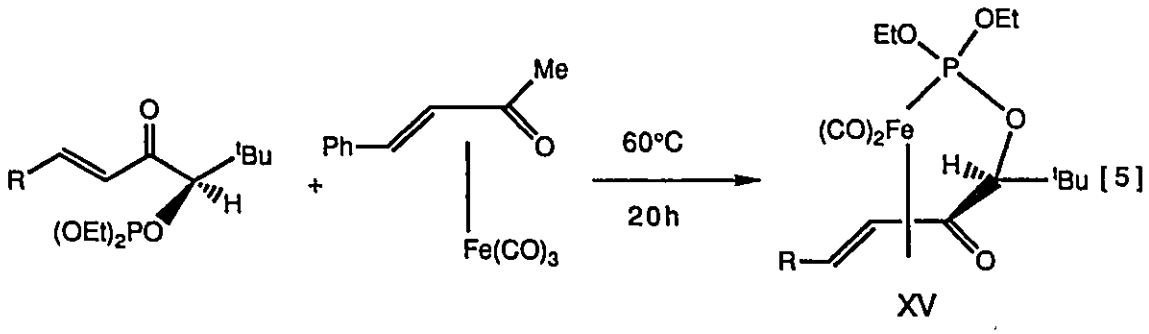

XV [5]

Carbanionic addition reactions with complex XV using α–lithioisobutyronitrile, gave a Michael-type addition product with 99% enantiomeric excess, [6].

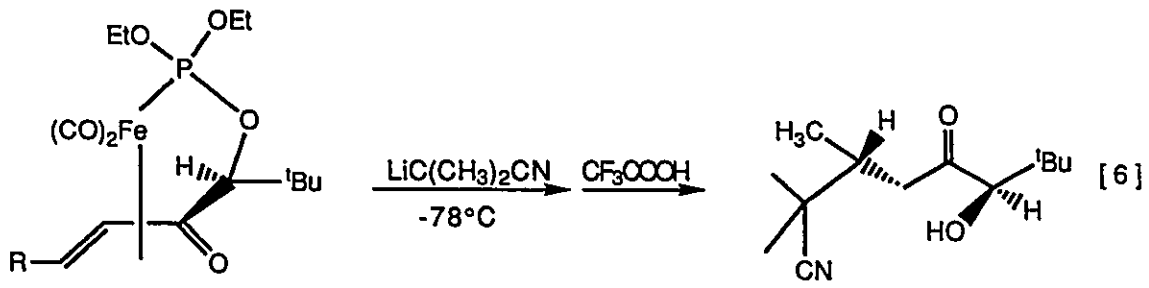

[6]

Tetracarbonyl iron complexes of α,β-unsaturated esters and amides have been reported but their tricarbonyl iron analogues are not known. The reaction of these tetracarbonyl iron complexes with nucleophiles is known forming 1,4-diketones[18,19].

Iron tricarbonyl complexes of α,β-unsaturated heteroatoms are known to undergo electrophilic addition and do so at the heteroatom because the heteroatom has a lone pair of electrons that is sterically more available than the metal centre. α,β-Unsaturated ketones and aldehydes are protonated at the

oxygen using H_2SO_4 producing complexes of type XVI.

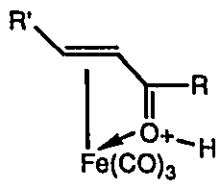

XVI

Acetylium tetrafluoroborate also reacts at the oxygen of iron tetracarbonyl and tricarbonyl complexes of α,β-unsaturated aldehydes and ketones with the products being either A or B, [7][20]. A comparison of spectral data with other allylic tricarbonyl iron complexes made the proposed structure "A" the more favoured representation of the product.

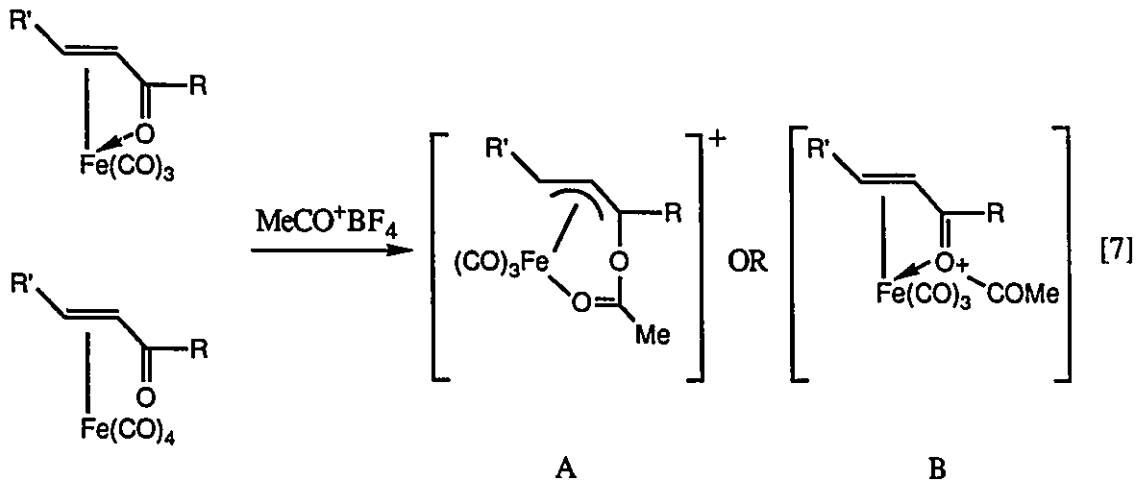

A B

The triphenylphosphine substituted complex $[Fe(CO)_2(BDA)(PPh_3)]$ has been prepared by displacement of carbon monoxide from $[Fe(CO)_3(BDA)]$ and it is capable of behaving as a source of $[Fe(CO)_2(PPh_3)]$ in exchange

reactions with polyolefins[2].

Displacement of CO has been achieved by thermal and photochemical methods as well as through the use of metal-carbonyl bond activating reagents. Among these, thermal activation is the least desirable owing to the high temperatures and extensive time periods often required to break metal-carbonyl carbon bonds. Under such conditions decomposition and subsequent reaction of initially formed products have been known to result in inseparable product mixtures. Metal-carbonyl activating reagents have proved quite successful in promoting CO substitution and require less severe thermal conditions[21].

The use of promoting agents often offers improved selectivity in the substitution pathway thereby allowing, in some cases, the synthesis of novel products not available through the usual thermal routes[21]. Trimethylamine oxide [Me_3NO] is a well established reagent in the removal of CO ligands from transition metal carbonyl derivatives. Stoichiometric amounts of [Me_3NO] oxidatively decarbonylate metal coordinated CO to produce reactive, coordinatively unsaturated intermediates which readily react with other ligands present in solution[22]. Another useful reagent is sodium benzophenone ketyl [BPK]. It promotes a radical catalyzed reaction yielding radical anions able to undergo facile CO substitution with ligands that are less π-acidic than CO. Similarly, the dinuclear complex [$Fe(CO)_2Cp]_2$ is a versatile catalyst in promoting CO substitution by a radical mechanism[21,22]. The highest yields and rates which are generally achieved using [BPK] are equally obtainable using bis(triphenylphosphine) iminium salts, [PPN^+][R^-][23]. The salts which were found to promote CO substitution with the fastest rates in the case of [$Ru_3(CO)_{12}$] are [PPN^-][$CH_3CO_2^-$] and [PPN^+][CN^-], which are easily prepared by anion exchange with readily available [PPN^+][Cl^-]. The complex [$Fe(CO)_2(PPh_3)$ (BDA)] was synthesized by thermolysis[2]. Carbon monoxide exchange in

organometallics has also been achieved by photolysis[3].

Tetracarbonyl iron complexes of α,β-unsaturated imines have been prepared in the same manner as those for the corresponding esters and amides[18]. These complexes, unlike that of the cinnamaldehyde iron complex, are coordinated through the heteroatom and not through the diene. Heating a solution of the complex gives the tricarbonyl complex XVIII.

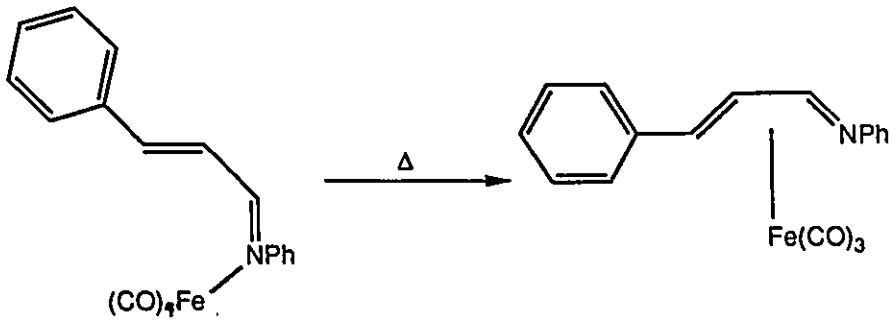

XVII XVIII

Complex XVII was unstable at temperatures >10°C. This knowledge led to a direct synthesis of [(1,4-diphenyl-2-methyl-1-azabutadiene)$Fe(CO)_3$] XIX from the aza-organic ligand and [$Fe_2(CO)_9$] in 3h at 40°C[19].

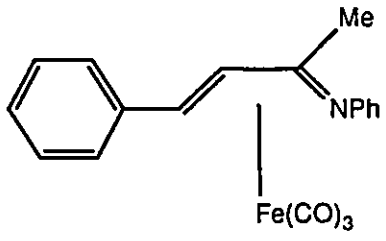

XIX

Nucleophilic addition to this complex, XIX, resulted in pyrrole production[24] and in the preparation of the first (η^4-1,3-diene)-carbene iron carbonyl complex[25].

Alkynes are known to react with conjugated heteroatom imine iron

tricarbonyl complexes. Reactions of (1,4-diaza-1,3-diene), (DAD), iron tricarbonyl complexes with alkynes such as dimethylacetylene dicarboxylate, DMAD, and methyl propynoate under a carbon monoxide atmosphere gave a bicyclic intermediate which rearranged to a (1,5-dihydropyrrol-2-one)tricarbonyl iron complex, XXII, [8][26,27,28,29].

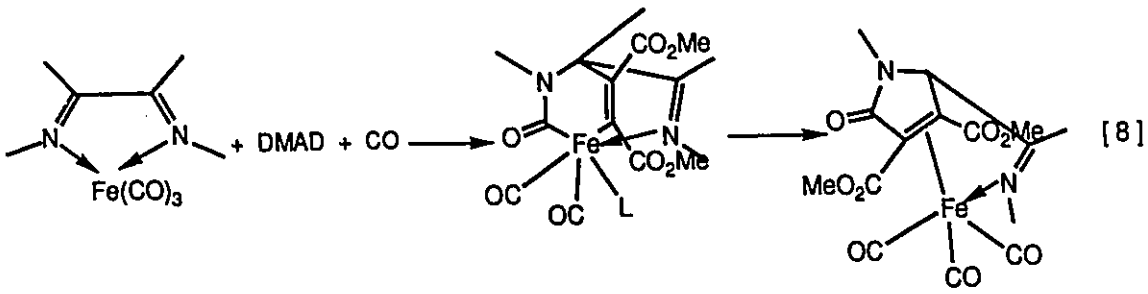

XX XXI XXII [8]

The intermediate XXI was characterized as its trimethylphosphite substituted complex, L=$P(OMe)_3$, by X-ray crystallography and product XXII was characterized as its tricarbonyl complex by X-ray crystallography. It was found that the isomerization from intermediate XXI to product XXII was fast if the C-C connected bridgehead carbon atom in XXI contained a methyl substitutent. If however there is a choice in the initial reaction to form intermediate XXI, then C-C bond formation occurred only at the unsubstituted imine carbon atom[29].

Much more forcing conditions were required upon changing the alkyne from dimethylacetylene dicarboxylate to methyl propynoate; that is, changing one of the electron withdrawing ester groups to hydrogen[29]. The reaction required 9 days at 40°C as compared to 3 hours at -20°C for the dimethylacetylene dicarboxylate reaction.

Finally, at elevated temperatures, the heterocycles could be displaced from the iron tricarbonyl fragment by adding the original ligand to regenerate the starting material, XX[26].

Ring opening of thietes using iron tricarbonyl compounds gave a

dimeric complex which was converted to the first α,β-unsaturated thioaldehyde iron carbonyl complex using triphenylphosphine to stabilize the monomer, Scheme 6[30].

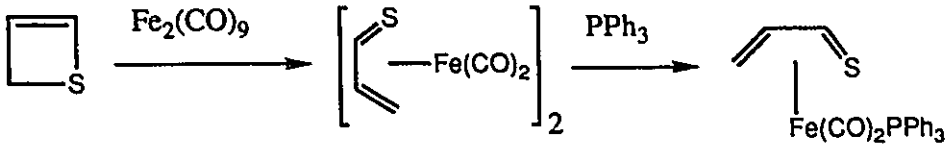

Scheme 6

This procedure was later used to generate substituted thiete complexes of iron tricarbonyl XXIII and η^5-cyclopentadienyl cobalt XXIV.

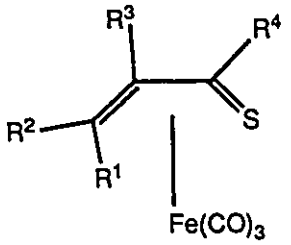

R^1=R^2=R^3=R^4=H
R^1=R^4=H; R^2=CH_3; R^3=C_2H_5
R^1=R^4=H; R^2=R^3=$(CH_2)_5$

XXIII

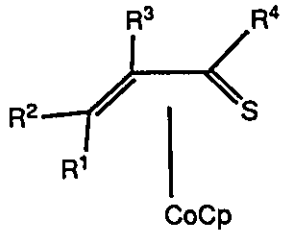

R^2=R^3=H
R^2=CH_3; R^3=CH_3

XXIV

Thiete complexes were found to undergo many reactions including electrophilic addition, hydride abstraction, and oxidation.

Iron tricarbonyl and cyclopentadienyl cobalt complexes of α,β-unsaturated thioaldehydes react with electrophiles. Treatment of the iron complexes with triphenylmethyl fluoroborates gave products resulting from hydride abstraction at the α-position, XXV, while cyclopentadienyl complexes

gave products having the proposed structures XXVI and XXVII[31].

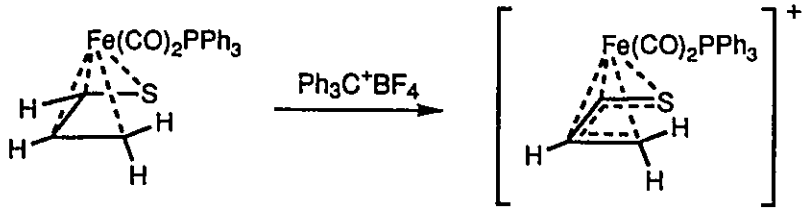

XXV

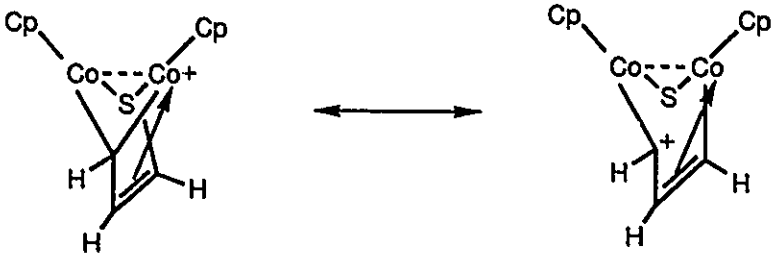

XXVI XXVII

Trimethyloxonium and triethyloxonium tetrafluoroborate, as well as mercuric chloride, reacted with α,β-unsaturated thioaldehyde iron tricarbonyl complexes and cyclopentadienyl cobalt complexes affording S-substituted complexes (Scheme 7)[32], as was found for α,β-unsaturated aldehyde and ketone substituted iron tricarbonyl and iron tetracarbonyl, [7]. With this reaction of an alkyl electrophile shown in Scheme 7, resonance structures having the positive charge centred on the sulphur and a π-allyl structure were proposed.

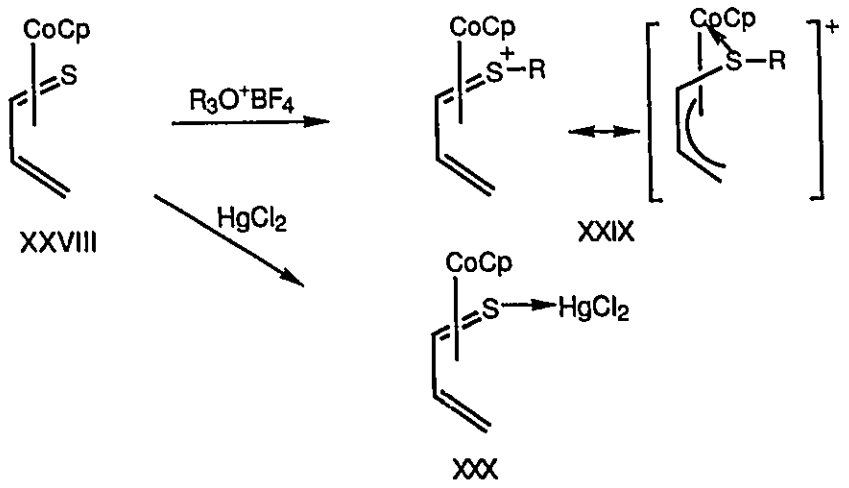

Scheme 7

The alkyl addition product, complex XXIX could also be prepared from reacting the α,β-unsaturated thioaldehyde cyclopentadienyl cobalt complex XXVIII with methyl iodide followed by anion exchange with $AgBF_4$. The S-substituted ligand of this complex, XXIX, was found to be readily displaced from the cobalt centre using tetraethylammonium cyanide providing a new route to allyl and vinyl sulphides[33].

Thioacrolein complexes of iron tricarbonyl and cyclopentadienyl cobalt are readily converted to S-oxide products (sulphines) using hydrogen peroxide in glacial acetic acid or m-chloroperbenzoic acid, [9] and [10][31].

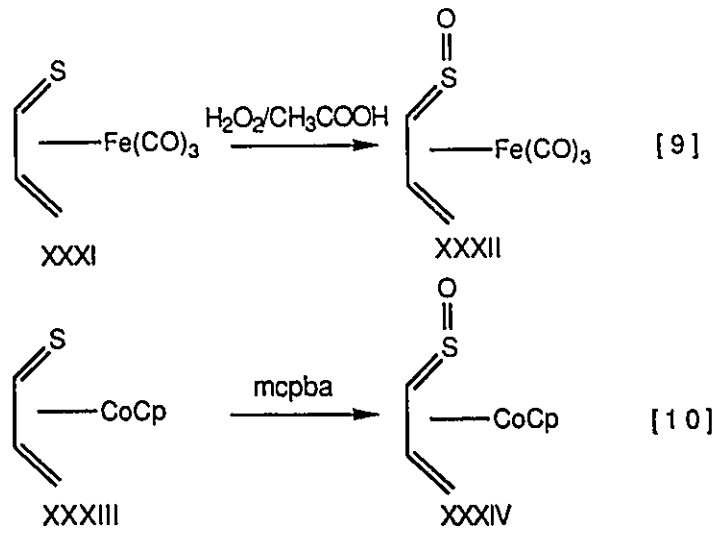

Even mild oxidizing reagents were effective, including ceric ammonium nitrate, ferric chloride, and tert-butylhypochlorite[30]. The ease of oxidation to form complexes XXXII and XXXIV was attributed to the donation of electrons from the iron or cobalt to the thioacrolein ligand. Two S-oxide forms were produced: the exo, A, and the endo, B, isomers.

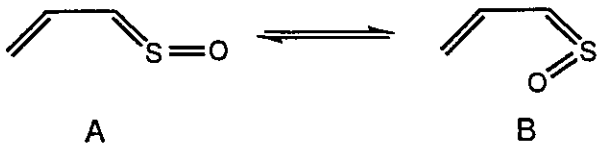

Evidence for the existence of the two isomers was based on the ^{1}H NMR spectrum which showed two signals for each proton. Low field absorptions for each proton were ascribed to isomer B because of deshielding of a sulphoxide group in proximity to an approximately co-linear proton[31]. Contrary to this, in the cis and trans isomers of non metal complexed phenyl chlorosulphine, ortho-protons were shifted downfield because of a magnetic anisotropic effect of the sulphine moiety[34].

Platinum sulphine complexes are also known but they were not

prepared from direct oxidation of a C=S group[35,36].

Only one complex of an α,β-unsaturated thioamide has been prepared. Lithium tetrachloropalladate reacted with thioamides producing complex XXXV, (Scheme 8)[37].

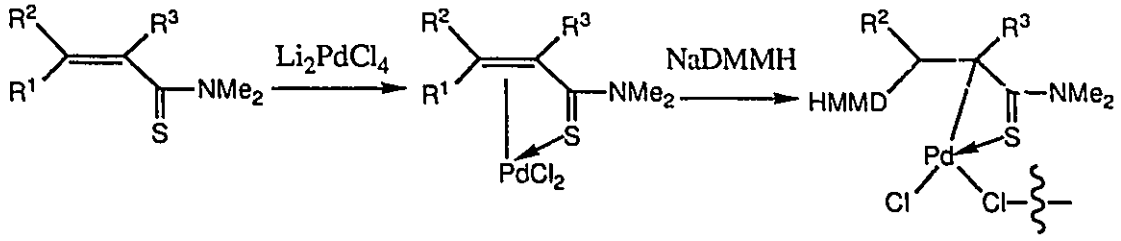

XXXV XXXVI

Scheme 8

Reactions with soft nucleophiles such as sodium dimethyl malonate, NaDMMH, were performed and gave complexes derived from Michael-type additions to the thioamide ligand, XXXVI.

1.4 Focus of the Thesis

There is a known ability of organic thio-compounds to serve as versatile starting materials for a variety of functional group transformations. Given this fact, and aware of the ability of transition metals to activate, protect, or direct reactivity of a coordinated organic compound, there was ample motive to investigate the synthesis and reactivity of transition metal complexes having thio-compounds as ligands. Iron carbonyl was an obvious choice as the transition metal centre since it is a relatively inexpensive source of a metal which has already been shown to coordinate to α,β-unsaturated heterodienes. Of equal importance, it has shown its ability to readily release the heterodiene ligand under controlled conditions.

CHAPTER 2

PREPARATION AND CHARACTERIZATION OF α,β-UNSATURATED THIOAMIDE, THIOESTER, AND THIONE IRON TRICARBONYL COMPLEXES

2.1 Ligands-Introduction

There are many methods known for the preparation of thioamides, thioesters, and thiones. Most techniques are based on the direct conversion of a C=O moiety on the amide, ester, or ketone to C=S. Thus, a diversity of thiocompounds can be prepared owing to the multitude of ketones and related compounds that are readily available.

The reactivity of thiocompounds are well documented[38,39,40,41]. These compounds have a rich chemistry which has made them valuable intermediates in a variety of industrially useful and academically interesting compounds. In particular, thioamides have established their role as vulcanization accelerators, pigments for plastics, and in the synthesis of aliphatic, aromatic, and heterocyclic compounds of pharmacological interest[40]. A few examples are shown below.

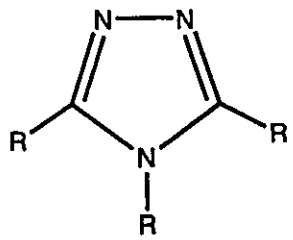

I

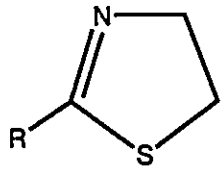

Thiazolines

II

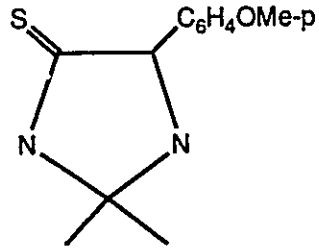

Imidazole

III

Among the many methods available for the synthesis of thiocarbonyl compounds, only a few have been applied to α,β-unsaturated systems[38,39]. Most thioamides and thioesters have been prepared by reaction with 2,4-bis-(p-methoxyphenyl)-1,3-dithiaphosphetane-2,4-disulphide, commonly referred to as Lawesson's reagent (IV)[42]. In this method, the amide or ester and Lawesson's reagent are simply refluxed in toluene or xylene, [1].

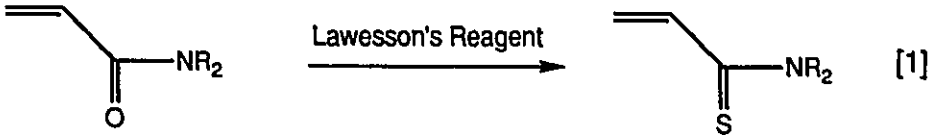

[1]

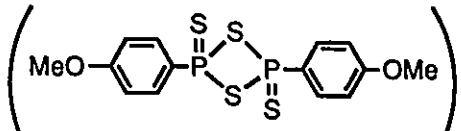

Lawesson's reagent
IV

An alternative route which was recently published involved the generation of α,β-unsaturated thioesters by condensation of (dimethoxy -phosphinyl)-thioacetate (V) with aldehydes catalyzed by aqueous potassium carbonate in a Horner-Wittig reaction, [2][43].

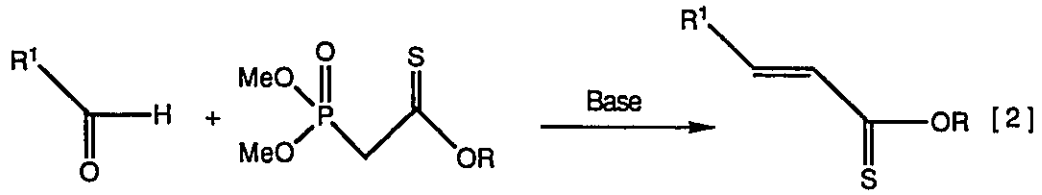

[2]

V

Alternatively, a Peterson synthesis has been used to generate thioesters, (Scheme 1)[43].

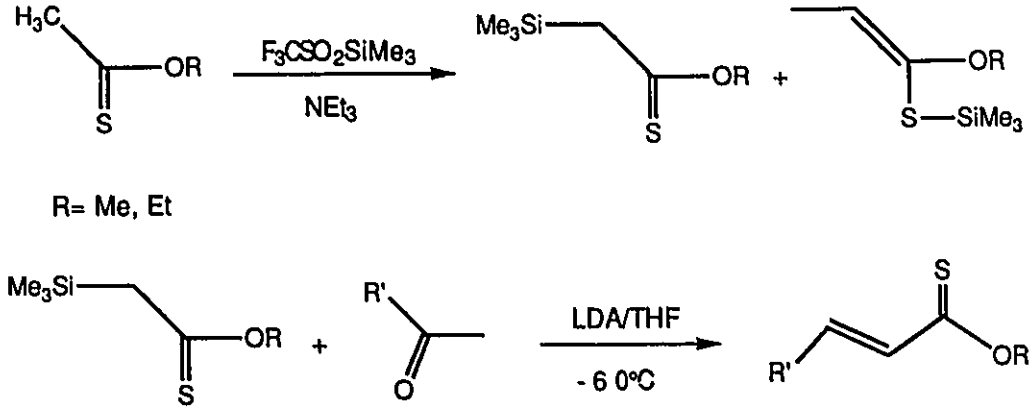

Scheme 1

The stability of α,β-unsaturated thioesters varies according to their substitution at R'.

α,β-Unsaturated thioketones are considerably more difficult to prepare than their corresponding thioesters and thioamides owing to the lack of product stability. 2,3-Diphenylcyclopropenethione has been prepared by treating the corresponding ketone with phosphorus pentasulphide at -50°C[38], but the most successful method which is applicable to a wide variety of ketones is the direct reaction of an α,β-unsaturated ketone with hydrogen sulphide and hydrogen chloride in alcohol, [3][38].

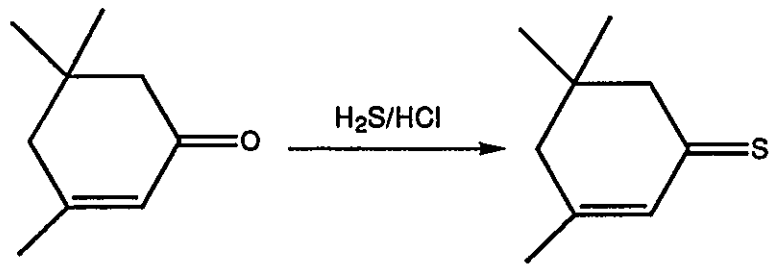

[3]

The thiocompounds which were used in the synthesis of the new thio-iron tricarbonyl complexes were all prepared from the amides, esters, and ketones using Lawesson's reagent. A discussion of their preparation and characterization is presented in the following section.

2.2 Preparation and Characterization of α,β-Unsaturated Ligands

2.2.1 Preparation of α,β-Unsaturated Compounds 1'-13'

The thiocompounds used in the preparation of the complexes throughout this thesis are illustrated below.

A. Thioamides

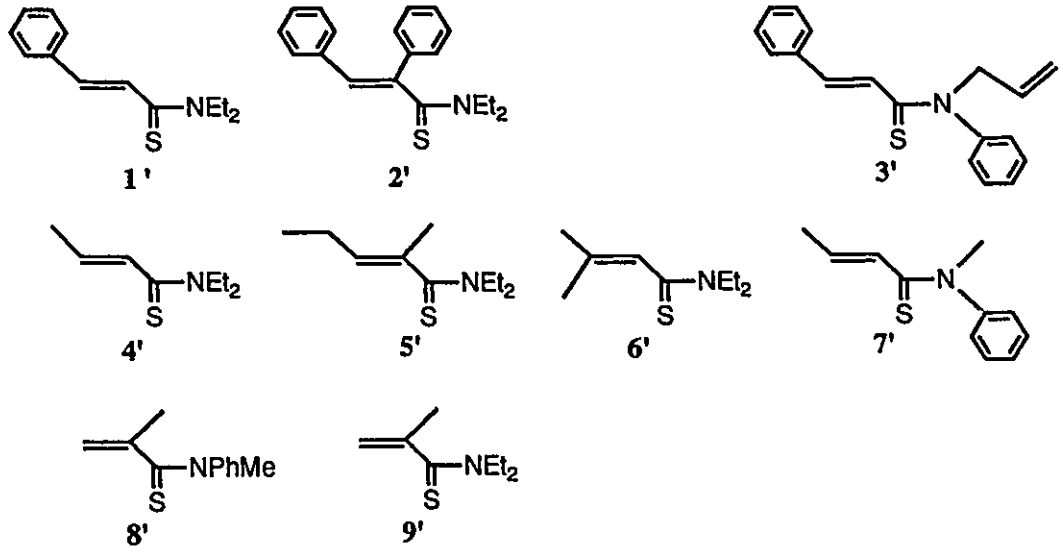

B. Thioesters

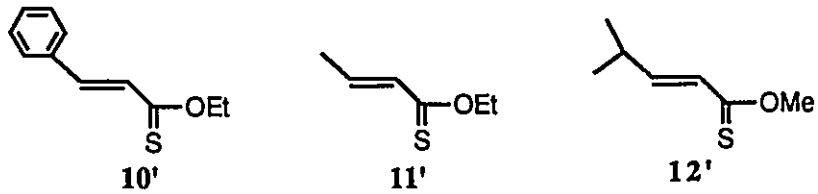

C. Thione

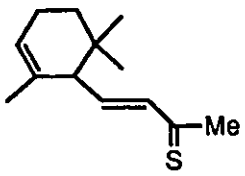

13'

All of the thioamides were prepared from their corresponding amides using Lawesson's reagent, as in reaction [1]. The amides were synthesized from their acid chlorides using the Schotten-Baumann procedure[44] and where the acid chlorides were not comercially available, the acid chloride was prepared from its carboxylic acid using thionyl chloride. Thioesters were prepared from their carboxylic esters using Lawesson's reagent. While all of the thioamides were stable towards air, thioesters were found to be sensitive to oxygen. The thione was prepared from its ketone using Lawesson's reagent or H_2S and HCl[38].

2.2.2 Spectral Characterization of α,β-Unsaturated Ligands 1'-13'

2.2.2.1 Infrared Spectra

The IR spectra were used to check for the complete conversion of the amide ester or ketone as demonstrated by the disappearance of the strong υ(CO) stretching band. The υ(CS) stretching frequency of thiocarbonyls has been reported by several researchers to be in the region between 1000-1300 cm^{-1} [38]. It is a low intensity absorption band that is generally difficult to define due to its

location in a highly absorbing region. Furthermore, the literature values are not for α,β-unsaturated thiocarbonyls which should shift to lower wavelengths and be even more difficult to characterize.

2.2.2.2 Mass Spectra

The mass spectra of all of the compounds were obtained as an aid in defining the formula weight of the C=S products. In all cases, the parent ion was observed as an intense signal. The fragmentation patterns were similar for all of the thioamides and thioesters with the exception of thioamide **7'**. The latter compound gave an initial loss of mass 15 followed by an unusual rearrangement, owing to the allylic portion of the molecule. The most dominant fragment peak, of mass 206, represents a loss of 73 mass units from the parent ion. Its origin is not obvious. For all of the other compounds there was an initial loss of 15, corresponding to a methyl group fragmentation. As well, a high intensity peak corresponding to the loss of NR_2 or OR was observed in each case.

2.2.2.3 NMR Spectra

The ^1H NMR for all of the thioamides displayed nonequivalence, geometrically and magnetically, of the nitrogen substituents, a well documented feature[45]. This effect is a consequence of the partial double bond character of the C-N bond arising from the contribution of structure VII to the resonance hybrid.

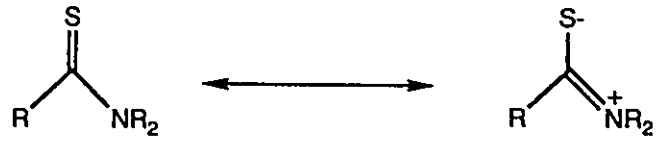

VI VII

More specifically, the occurrence of separate signal sets for each of the N-substituted proton groups in N,N-disubstituted thioamides is due to the anisotropy of the diamagnetic susceptibility of the C=S group. It has been suggested that a large shielding exists in conical regions extending above and below the plane of an amide group, while regions in the plane of the amide group are deshielded. This is illustrated by VIII[45].

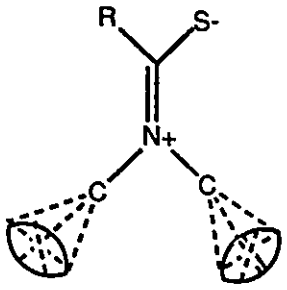

VIII

The result is that cis and trans substituents to the oxygen give well separated NMR signals whenever rotation is slow around the nitrogen-carbonyl carbon bond. Protons nearest the anisotropic group, including those α to nitrogen, will be the most magnetically non-equivalent with respect to each other.

An A_2X_3 spin system was observed for each of the ethyl groups of the N,N-diethyl-substituted thioamides and for the O-ethyl group of the ethyl thioesters. An example is shown below in the ^1H NMR of compound **4'**, figure1.

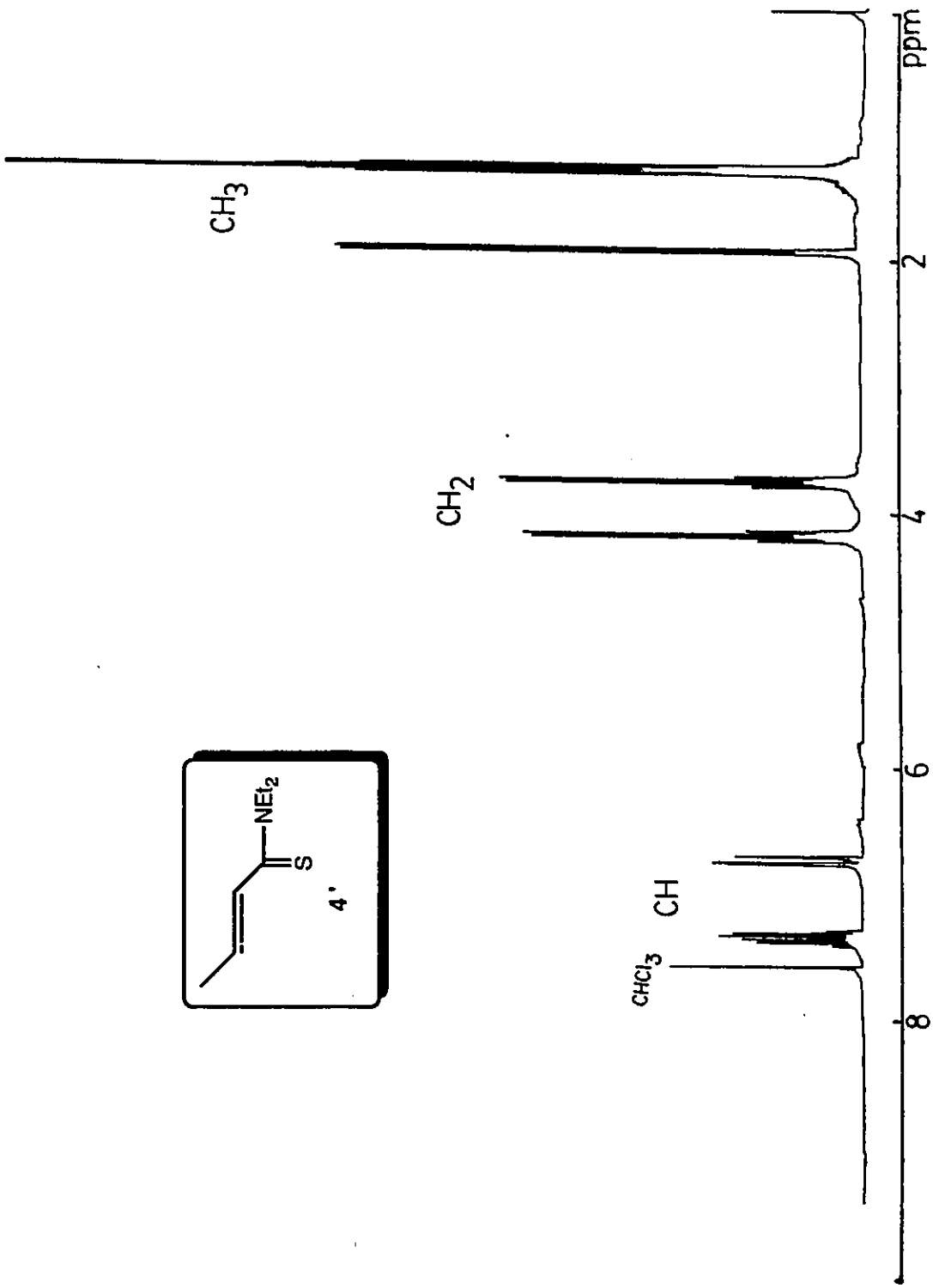

Figure 2.1: ^{1}H NMR Spectrum of Free Ligand **4'**

The addition of an alkyl or aryl substituent in the β-position changed the spin system from A_2X_3 to ABX_3. Each multiplet in the methylene region appeared to be a doublet of quartets owing to geminal coupling and coupling to the neighboring methyl group. This further inequivalence is due to the fact that the planar π-system becomes skewed due to steric influences creating a different chemical environment for each of the methylene protons of the N-ethyl groups.

A strict assignment of signals corresponding to each set of methylene protons can only be made by analogy with studies done on deuterium-decoupled methyl-deuterated N,N-diethylformamide-d_6[45]. At 40°C, N-CH_2 resonances were separated and it was found that N-CH_2 cis to oxygen resonated at lower field than the N-CH_2 group trans to oxygen. Furthermore, it was concluded in this report that the cis N-ethyl methyl group resonated at higher field than the trans methyl group.

The ^1H NMR spectrum of compound **5'**, was assigned as shown in figure 2 for its two sets of ABX_3 spin systems based on the discussion above. The ^1H NMR chemical shifts of the olefinic protons of all of the compounds were in the usual region of δ4-8 ppm. The CH's β and γ to the C=S were readily assigned on the basis of its coupling pattern when there was a γ-CH_3 substituent. By analogy with these chemical shifts, the γ-phenyl substituted compounds were characterized, with the more downfield signal assigned as the γ-CH proton. For those compounds having β and γ-CH protons, the coupling between them was greater than 15Hz, consistent with an E geometry of the double bond.

All of the ^{13}C NMR spectra were assigned using an NMR technique, DEPT-distortionless enhancement by polarization transfer, that allows for the quaternary, CH, CH_2, and CH_3 carbons to be distinguished. The C=S chemical shift ranged from δ193-201 ppm for the thioamides and at slightly higher field, δ210-211 ppm, for the thioesters. The chemical shift range of C=O of amides and

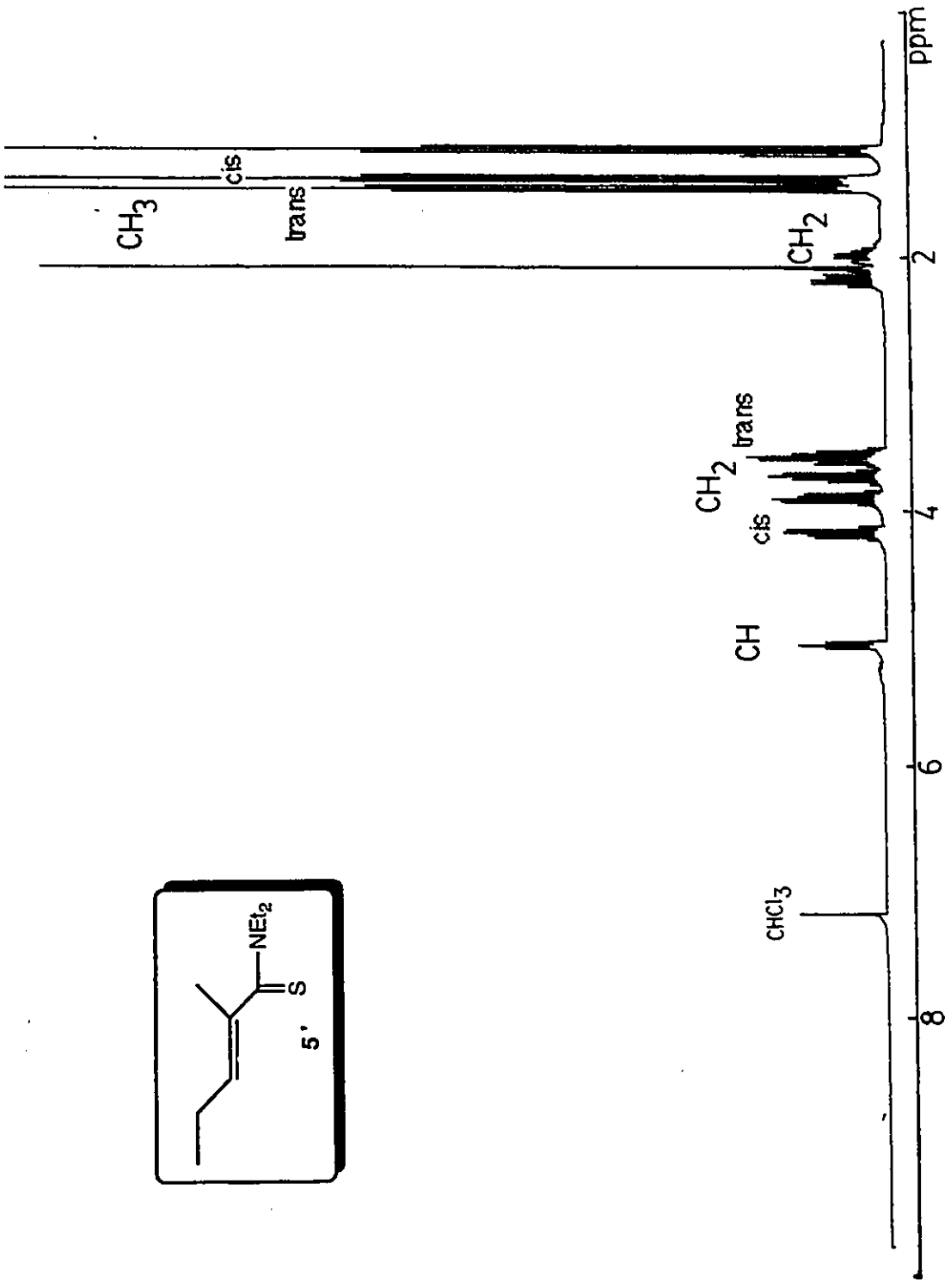

Figure 2.2: ^{1}H NMR Spectrum of Free Ligand **5'**

esters is generally δ160-180 ppm, further upfield than that for the C=S analogues.

For α,β-unsaturated C=O and the corresponding C=S compounds, the chemical shift for the olefinic γ-C in the ^{13}C NMR spectra is further downfield than that of the β-carbon[46]. Thioamide compounds **4'**, **6'**, and thioester compound **11'** are shown below with the olefinic carbon chemical shifts.

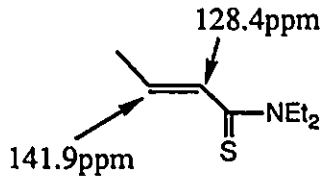

4'

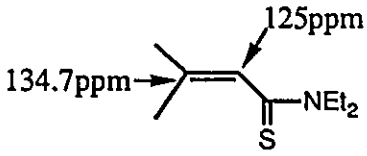

6'

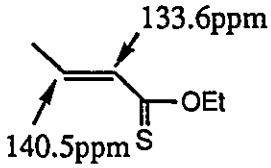

11'

This trend in the chemical shifts of β and γ-carbon chemical shifts applies when the C=O/C=S and olefinic substituents of the π-system are planar.

Of the compounds prepared, thioamide compounds **2'** and **5'** have β-substituents other than a proton and do not possess planarity .

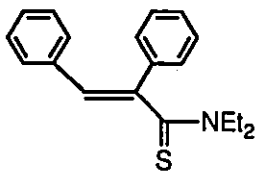

2'

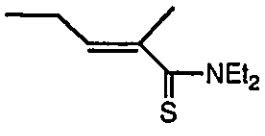

5'

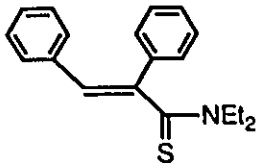

2'

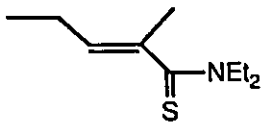

5'

2.2.2.4 X-Ray Crystal Structure

An X-ray crystal structure of compound **2'** was obtained and is shown in figure 3. The Weissenberg photographs were satisfactory and only after data collection was it found that the the structure could be refined only to R_W=0.30 owing to the presence of a crystal of the $Fe(CO)_3$-complex which was present in the solution from which the crystals were grown. The pertinent bond lengths are shown in figure 3 and the other crystal structure data is presented in Chapter 4.

The bond length of a non - conjugated thiocarbonyl C=S bond is most often quoted to be 1.61 - 1.62Å[38]. This value is inferred from CS_2 and C-S bond lengths of 1.56Å and 1.82Å respectively. The bond length of 1.58Å in thioamide compound **2'** is smaller than the 'normal' C=S bond length that might be expected for a conjugated C=S. Conjugation through the phenyl rings and the β and γ-carbons is evident in their similar bond lengths. Another bond length of note is the C-N bond, at 1.43Å, which is shorter than a 'normal' C-N single bond of 1.47Å[57]. This confirms the resonance representation in which there is some contribution from the nitrogen lone-pair to the carbon of C=S. As well, this crystal structure confirms the lack of π-system planarity associated with γ-substitution.

PAGINATION ERROR.

TEXT COMPLETE.

ERREUR DE PAGINATION.

LE TEXTE EST COMPLET.

NATIONAL LIBRARY OF CANADA.

CANADIAN THESES SERVICE.

BIBLIOTHEQUE NATIONALE DU CANADA.

SERVICE DES THESES CANADIENNES.

2.2.2.4 X-Ray Crystal Structure

An X-ray crystal structure of compound **2'** was obtained and is shown in figure 3. The Weissenberg photographs were satisfactory and only after data collection was it found that the the structure could be refined only to R_w=0.30 owing to the presence of a crystal of the $Fe(CO)_3$-complex which was present in the solution from which the crystals were grown. The pertinent bond lengths are shown in figure 3 and the other crystal structure data is presented in Chapter 4.

The bond length of a non - conjugated thiocarbonyl C=S bond is most often quoted to be 1.61 - 1.62Å[38]. This value is inferred from CS_2 and C-S bond lengths of 1.56Å and 1.82Å respectively. The bond length of 1.58Å in thioamide compound **2'** is smaller than the 'normal' C=S bond length that might be expected for a conjugated C=S. Conjugation through the phenyl rings and the β and γ-carbons is evident in their similar bond lengths. Another bond length of note is the C-N bond, at 1.43Å, which is shorter than a 'normal' C-N single bond of 1.47Å[57]. This confirms the resonance representation in which there is some contribution from the nitrogen lone-pair to the carbon of C=S. As well, this crystal structure confirms the lack of π-system planarity associated with γ-substitution.

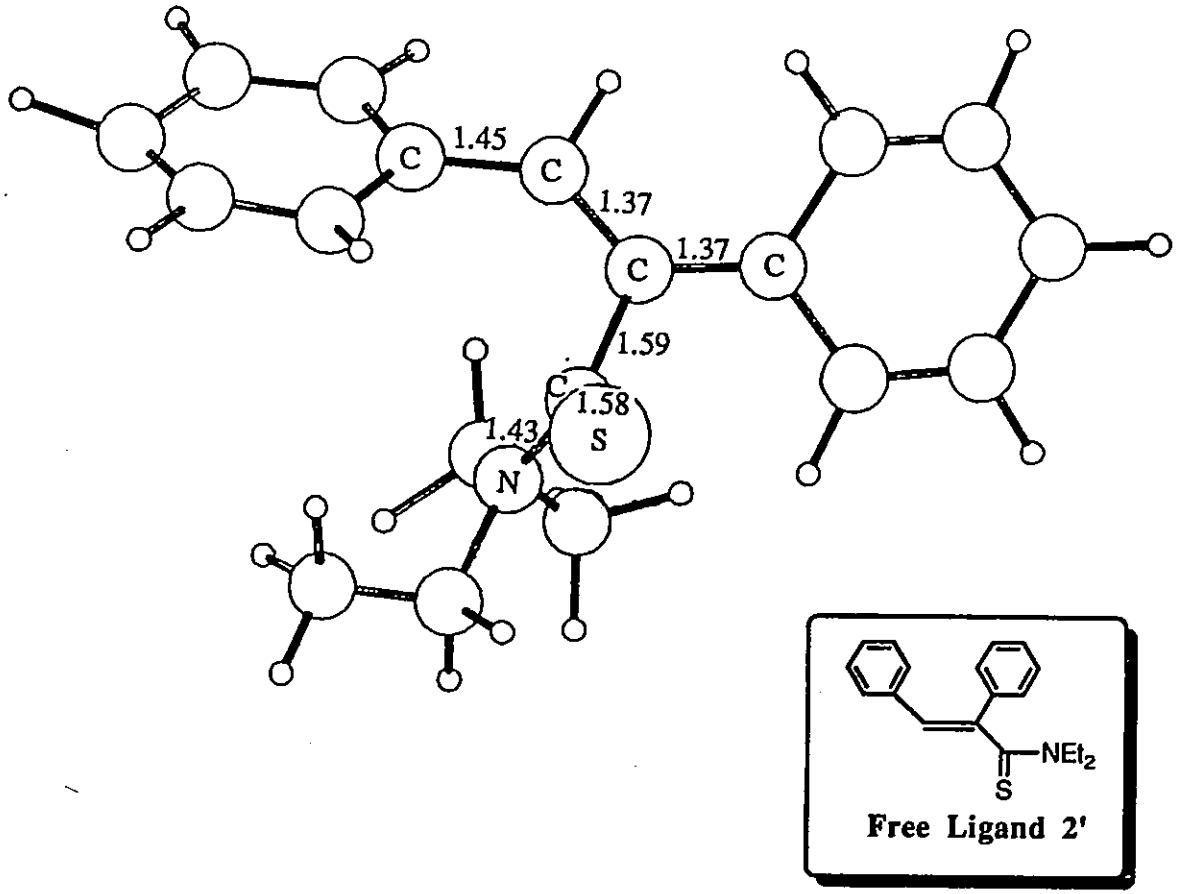

Figure 2.3: X-Ray Crystal Structure of Free Ligand **2'**

2.3 Complexes-Introduction

All of the conjugated iron tricarbonyl complexes have been prepared by one of three methods, which are illustrated in [4] and [5].

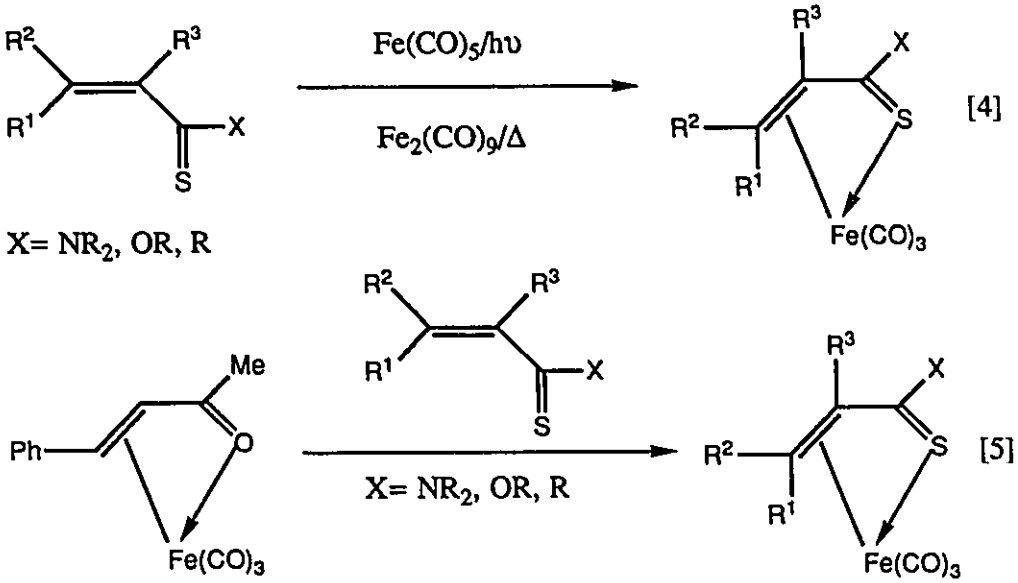

In the simplest preparation of α,β-unsaturated iron tricarbonyl complexes, the α,β-unsaturated thio-ligand is stirred in a suspension of $[Fe_2(CO)_9]$ in benzene at 40-80°C. Iron carbonyl dimer $[Fe_2(CO)_9]$ is a source of coordinatively unsaturated $[Fe(CO)_4]$ which will react with an olefinic double bond and then readily lose a CO ligand to form the desired complex.

Iron pentacarbonyl requires high temperatures to remove a CO ligand, so to circumvent this difficulty, photolysis is used and the $[Fe(CO)_4]$ fragment is generated at room temperature.

Finally, the third method of complex preparation is through ligand

exchange with α,β-unsaturated ketone iron tricarbonyl complex, [(BDA)$Fe(CO)_3$]. Heating a solution of the BDA-iron complex with the desired α,β-unsaturated thio-ligand yields the new α,β-unsaturated thio-iron complex. The initial α,β-unsaturated ketone iron tricarbonyl complex is generated by one of the first two methods mentioned above.

Two of the above methods were used in the preparation of the new thio-iron complexes. The following section discusses their preparation and characterization as well as providing some insight into the effect of substituents on the ligands in complex formation.

2.4 Preparation and Characterization of Complexes

2.4.1 Preparation of Complexes

All of the complexes were prepared by reaction of the ligand with [$Fe(CO)_4$] generated in situ by photolysis of [$Fe(CO)_5$] or by heating of [$Fe_2(CO)_9$]. The photolysis procedure was the preferred technique due to the ease of product isolation, recovery of unreacted starting ligand, and generally higher yields. As well, the reactions required less time using photolysis than by thermolysis of [$Fe_2(CO)_9$].

In the preparation of thioamide iron tricarbonyl complexes **5** and **6** there was a pronounced increase in yield when the synthesis was performed using [$Fe(CO)_5$] rather than [$Fe_2(CO)_9$]. This may be due to the sensitivity of the products towards solvents and there was less reaction time required for [$Fe(CO)_5$]/photolysis reactions. Over the course of this study it had been noted

that the complexes are solution sensitive. Their life-time in halogenated solvents was particularly short, while the complexes were more stable towards hydrocarbon solvents. Nevertheless, some decomposition was noticable within a few hours even in hydrocarbon solvents. The complexes were also more stable in aliphatic hydrocarbon solvents than in aromatic hydrocarbon solvents. The $[Fe_2(CO)_9]$/thermolysis reactions required as long as 3 days in benzene while the photolysis procedure performed in cyclohexane was usually complete within 18 hours. The prolonged period of solvent exposure to the organometallic products in the thermolysis reaction may have contributed to the lower yields observed. The most notable indication of the better suitability of photolysis was found in the purification of products by column chromatography. There was only a small amount of decomposition products formed and recovery of unreacted starting material was possible only by this synthetic method.

2.4.2 Discussion of Complexes **1-13**

A total of 13 thio-ligands were prepared in which substitution at the β and γ-positions were varied. Substituent variants were selected in order to provide a range of steric and electronic changes about the α,β-unsaturated thio-moiety. Each of these ligands was then complexed to $[Fe(CO)_3]$ by the methods discussed in section 2.4.1. All of the complexes and their yields are shown below.

A. **Thioamides**

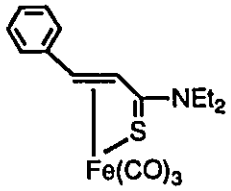

1 (41%)

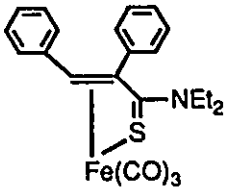

2 (22%)

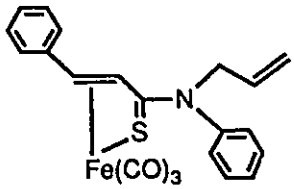

3 (66%)

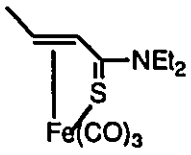

4 (29%)

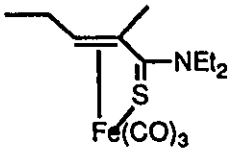

5 (6%)

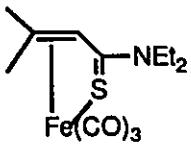

6 (2%)

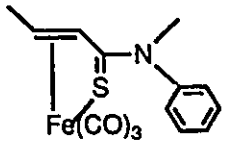

7 (60%)

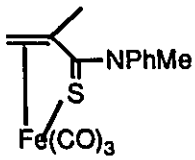

8 (59%)

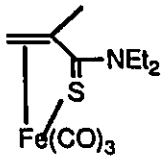

9 (32%)

B. **Thioesters**

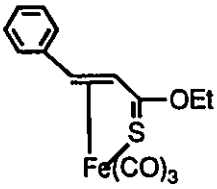

10 (51%)

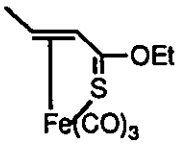

11 (37%)

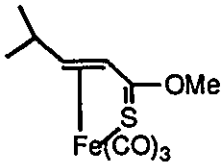

12 (NA)

C. **Thione**

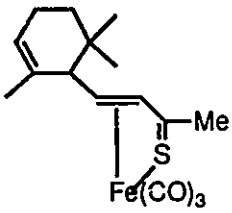

13 (NA)

2.4.2.1 Thioamides: The Effect of Substituents on Ligands in Complex Preparation

Increased substitution at the β-position, e.g. thioamide complexes 1 vs 2 or 4 vs 5 resulted in a lower isolated yield, and is likely due to a steric effect. Similarly, replacing the phenyl groups with alkyl groups results in lower yields. The phenyl groups may be providing some stabilization effect.

Thioamide iron complex 5 was formed in very low yield which may be due to its thermal instability. At temperatures above 0°C slow decomposition commences. The elemental analysis for this complex was, as a result, in poor agreement with theory.

Double γ-substitution in thioamide compound 6' was unfavourable for complex formation, assuming that yield is to be taken as a measure of ease of product formation. At temperatures below 0°C, the thioamide iron complex 6 was a deep orange solid, while at higher temperatures, it began to melt and decompose. Its elemental analysis was very low for all of the elements analyzed (C, H, N, S). It is likely that the sample decomposed prior to analysis since within two hours at room temperature under a nitrogen atmosphere, substantial decomposition was evident from formation of a brown insoluble solid. Compared to thioamide iron complex 5, which was also thermally unstable, thioamide iron complex 6 was even more susceptible to decomposition. The mass spectrum of thioamide iron complex 6, shown in figure 4, was highly unusual. The parent ion is present along with signals corresponding to successive loss of CO ligands, and there is a fragment for the free ligand. There are also higher mass peaks. This fragmentation pattern indicates that this complex may be $[Fe_2(CO)_6L]$ in which L is the α,β-unsaturated thioamide ligand. This was the only complex for which such behavior was observed.

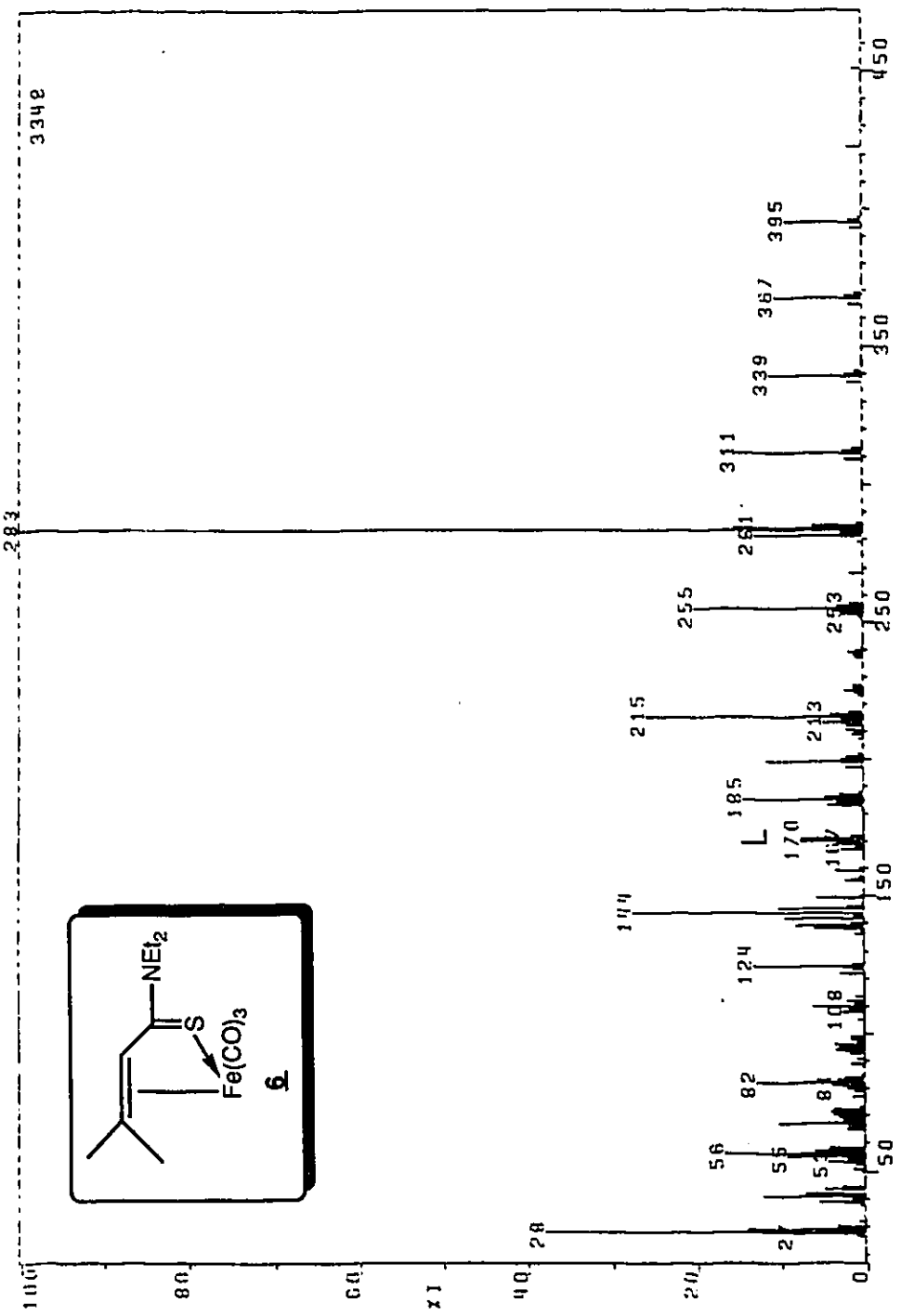

Figure 2.4: Mass Spectrum of Complex 6

A stabilizing effect, as reflected in product yield, was achieved by placing larger groups on the nitrogen, particularly phenyl groups. Evidence for this is shown by thioamide iron complexes **3** and **7** which were obtained in good yields as stable products.

2.4.2.2 Thioesters: The Effect of Ligand Substitution in Complex Preparation

Thioester complexes **10**, **11**, and **12** were prepared with improved yields relative to the corresponding thioamides but there was a dramatic decrease in the stability of complexes **10** and **12** relative to thioamide complex **4**. Thioester iron complex **12** was prepared in an effort to stabilize the alkyl substituted product by increasing the molecular weight without introducing a steric effect but it did not give the desired stabilization. The γ–phenyl thioester iron complex **10** was a low melting solid which was prepared in moderate yield. The butene thioester iron complex **11** was an unstable oil and gave an unsatisfactory elemental analysis. The mass spectrum gave the parent ion with successive loss of CO's and a mass corresponding to the free ligand.

In the preparation of thioester iron complex **12**, a yield could not be recorded owing to the impure nature of the starting material, thioester **12'**. The thioester iron complex **12** was isolated pure and had similar properties as thioester iron complex **11**. A sample was not sent for elemental analysis but the complex could be characterized by the usual spectroscopic methods. The mass spectrum for this complex gave a molecular ion followed by successive loss of CO ligands and there was a fragment in the mass spectrum corresponding to the free ligand.

2.4.2.3 Thione Complex Preparation

Only one thione complex was prepared. α,β-Unsaturated thiones are known to be unstable and the only starting ligand having potentially Z geometry at the double bond which could be prepared was thione compound **13'** (from α-ionone). Potentially Z geometry was required because rigid E geometry at the double bond was shown to not favour iron complex formation, as will be discussed in the next section. The mass spectrum of thione compound **13'** gave the parent ion; however, the ^{1}H and ^{13}C NMR clearly showed that the compound was impure. Nevertheless a pure thione iron complex, **13**, was isolated from the reaction of thione compound **13'** with $[Fe_2(CO)_9]$ under thermal conditions. The orange solid which was obtained was stable and gave a sharp melting point. The elemental analysis of thione iron complex **13** was good with respect to carbon and sulphur, but it was poor for hydrogen. The mass spectrum gave a parent ion with successive loss of CO ligands and a mass corresponding to the free ligand.

2.4.2.4 Organic Compounds Which Did Not Form Complexes With $[Fe(CO)_3]$

It is equally important to outline those organic compounds which did not afford iron carbonyl complexes. It appears that the $[Fe(CO)_3]$ fragment could not be coordinated to a C=C bond which was part of an aromatic system, thioamide compound **14'**.

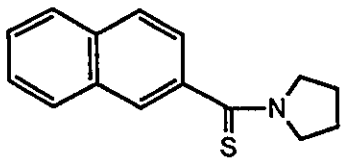

14'

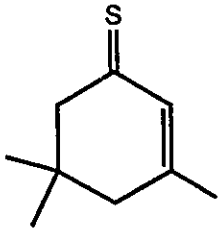

15'

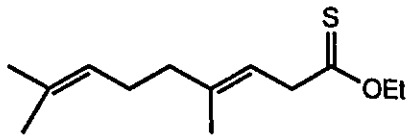

16'

As well, a rigid E orientation of the α,β-unsaturated system was not conducive to complex formation (thione compound **15'**).

Finally, it was thought that double bond migration in a α,γ-unsaturated compound might result in α,β-unsaturation and consequently complex formation. This has precedence with 1,4-dienes in their coordination to $[Fe(CO)_3]^2$. Thioester compound **16'** was prepared but it did not undergo reaction with sources of the $[Fe(CO)_3]$ fragment.

2.4.3 Spectral Characterization of Iron Complexes 1-13

2.4.3.1 Infrared Spectra

All of the complexes gave similar infrared spectra. The spectra were recorded in $CHCl_3$ and gave two strong intensity bands. The highest energy band, A'(1), was in the range of 2025 -2060cm^{-1}. The lower energy band ranging from 1950 to 1995cm^{-1} was broad and consisted of overlapping A'(2) and A". The latter could be distinguished by obtaining the spectrum in

cyclohexane.

The carbonyl stretching region contained the most information. The presence of three strong CO bands arises from distortion of the symmetry of the molecule from C_{3v}. The general appearance of the spectra are similar to that of the butadiene-iron tricarbonyl complex[48]. This suggests they have analogous solution structures, which has been described for butadiene iron tricarbonyl as having a square-based pyramidal arrangement of the diene and carbonyl groups around the iron such that the two carbonyls and the two terminal carbons of the diene form a base and the third carbonyl is at the apex[49]. This gives the $[Fe(CO)_3]$ group a local symmetry of C_S in which two carbonyls are equivalent and one unique. The symmetry of α,β-unsaturated thio-iron tricarbonyl complexes is further reduced to C_1 by the thio-organic group.

One of the iron complexes, thione iron complex **13**, gave well resolved A'(1), A'(2), and A" bands in $CHCl_3$. The M-CO vibrations of **13** are at higher energy than those of the thioamide and thioester iron tricarbonyl complexes. In iron complex **13** there is less $d\pi$-$p\pi^*$ backbonding from the metal to the carbonyls than in the thioamides and thioester iron complexes. Less backbonding corresponds to less electron density delivered to the π^*-CO orbital. This in turn enhances the CO bond order and hence increases the vibration energy. This effect of the thione ligand as compared to that of a thioamide appears to be due to a different degree of electron donation of the sulphur to the metal. In the thioamide case, the nitrogen lone-pair may contribute to the sulphur donation as illustrated by X.

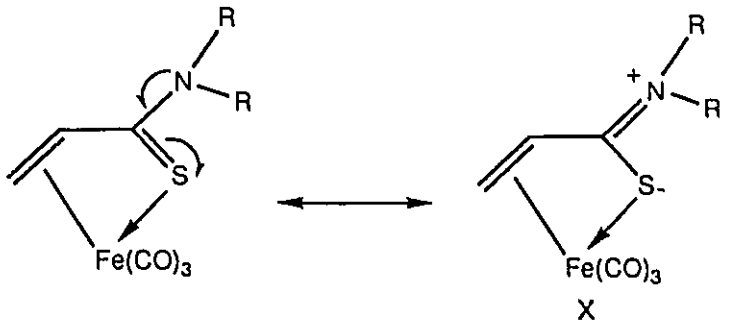

X

The structure on the right is not a real representation of the extent of nitrogen lone-pair contribution, but it illustrates the build-up of charge on the sulphur which translates into greater donation to the iron centre and thus increased backbonding resulting in lower energy CO vibrations. The thione ligand has no lone-pair contribution from another heteroatom as with the thioamides and thus less backbonding occurs.

One of the thioamide iron complexes, 6, gave an unusually complicated spectrum having five CO-stretching vibrations, suggesting that the compound might exist as a dimer $[Fe_2(CO)_6L]$ in solution. There is precedence for such a dimer in the α,β-unsaturated thioaldehyde iron tricarbonyl complex reported by Dittmer (XI)[30].

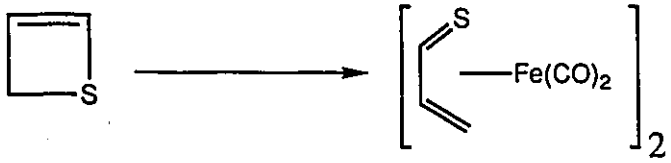

XI

2.4.3.2 NMR Spectra

2.4.3.2.1 Thioamides and Thioesters

In comparing the ^1H NMR spectra of all of the thioamide complexes to those of the free ligands, it was found that the complexes displayed the same ABX_3 patterns for each of the N-ethyl groups as were found for the free thioamide ligands **2'** and **5'** which unlike the other thioamides had β-alkyl or β-phenyl substitution. In the complexes, π-olefin coordination can be equally represented by structure XII shown below.

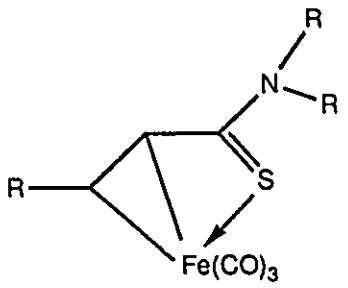

XII

This structure may also be said to have β-substitution if one considers the Fe-C bond. Coordination to the Fe disrupts the planarity of the ligand thereby creating a different environment for each of the methylene protons.

This effect was also observed for the thioester complexes. The methylene protons of ethyl thioester compounds **10'** and **11'** were chemically and magnetically equivalent, giving rise to an A_2X_3 pattern for the ethyl group. In the $[Fe(CO)_3]$-substituted thioester complexes **10** and **11**, the spin system was changed to an ABX_3 pattern. The ^1H NMR spectra of thioester compound **11'** and thioester iron complex **11** are shown in figures 5 and 6 respectively. As in the case of thioamide iron complexes, thioester iron complexes were extremely unstable in chlorinated solvents. As a result, the spectrum of the thioester iron complex **11** was recorded in benzene-d_6 and there are slight chemical shift differences from the free ligand spectrum which was recorded in $CDCl_3$.

For all of the iron complexes there was a significant upfield shift in the olefinic protons as compared to those of the free ligands. Table 1 illustrates the

olefinic proton chemical shifts and coupling for both the complexes and the free ligands (values for the free ligands are shown in parentheses).

The γ-CH proton experiences the greatest chemical shift change in that it moves upfield by as much as 5 ppm. This was also observed in the spectra of thioester iron complex **11** compared to its free ligand **11'** (above, in figures 6 and 5 respectively). The γ-olefinic CH proton of thioester iron compound **11'** occurs as a doublet of quartets at δ6.35 ppm which is the same as in the thioester iron complex except for its upfield chemical shift (δ1.45 ppm in the complex). The β-olefinic CH proton also experiences an upfield shift with coordination to the iron but it is relatively slight.

The large upfield shift of the γ-clefinic CH proton is due to its orientation with respect to the metal centre which serves to shield this proton more effectively than the β-olefinic CH proton. Based on this, a structure for thioester iron complex **11** and all other α,β-unstaurated thio-iron complexes was proposed in which an E geometry about the double bond of the organic molecule is maintained in order to reduce steric interaction.

The coupling between the β and γ-olefinic protons also changes with complex formation. The coupling constant in the free ligand was typically 14-15Hz. In iron complexes this value was significantly reduced to 7-8Hz, and is due to the decrease in π-character of the C=C bond with metal π-coordination. The β and γ-olefinic carbons approach sp^3 character, giving coupling constants that are typical of a 3-bond coupling value to neighbouring protons on sp^3

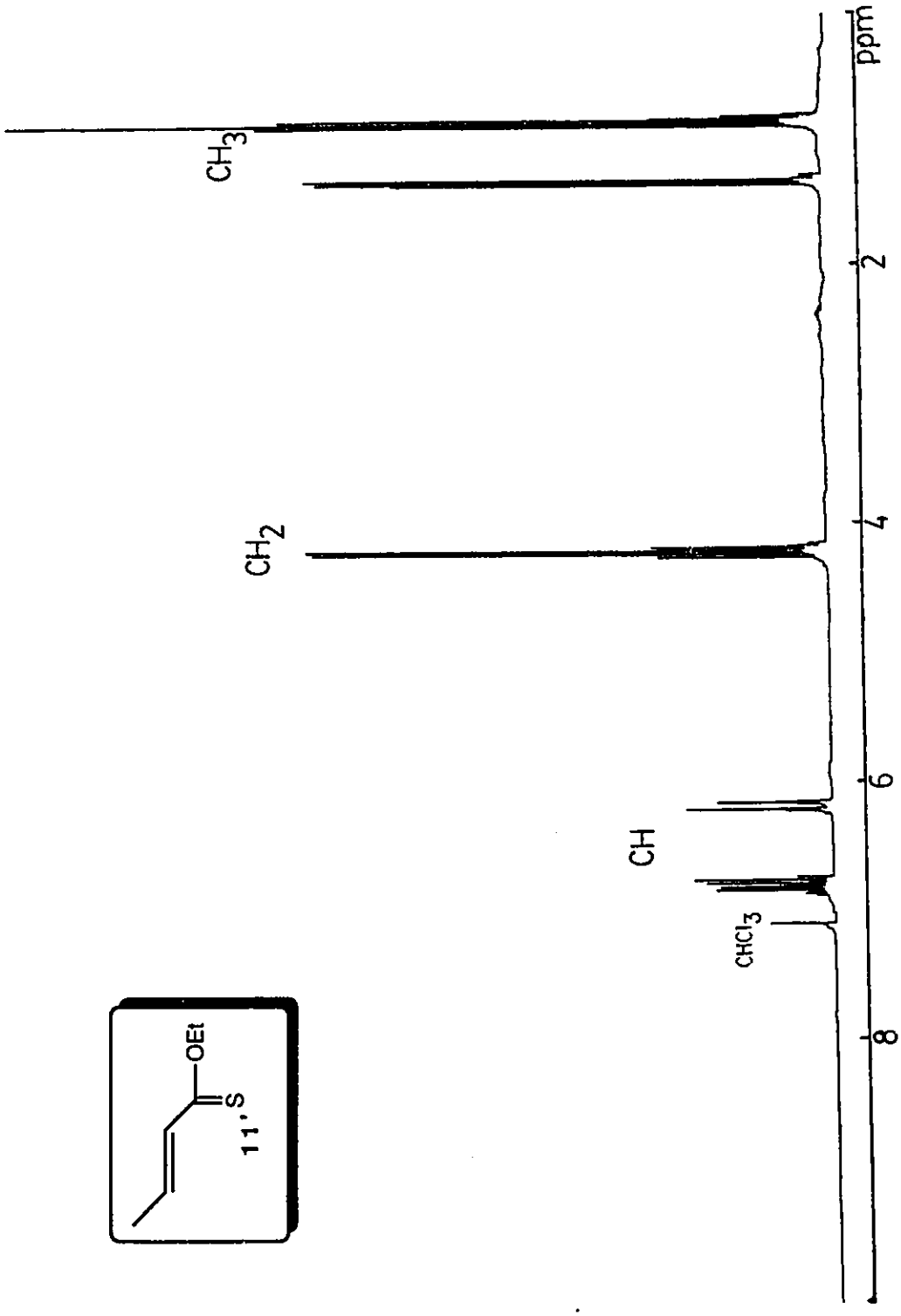

Figure 2.5: ^{1}H NMR Spectrum of Free Ligand **11'**

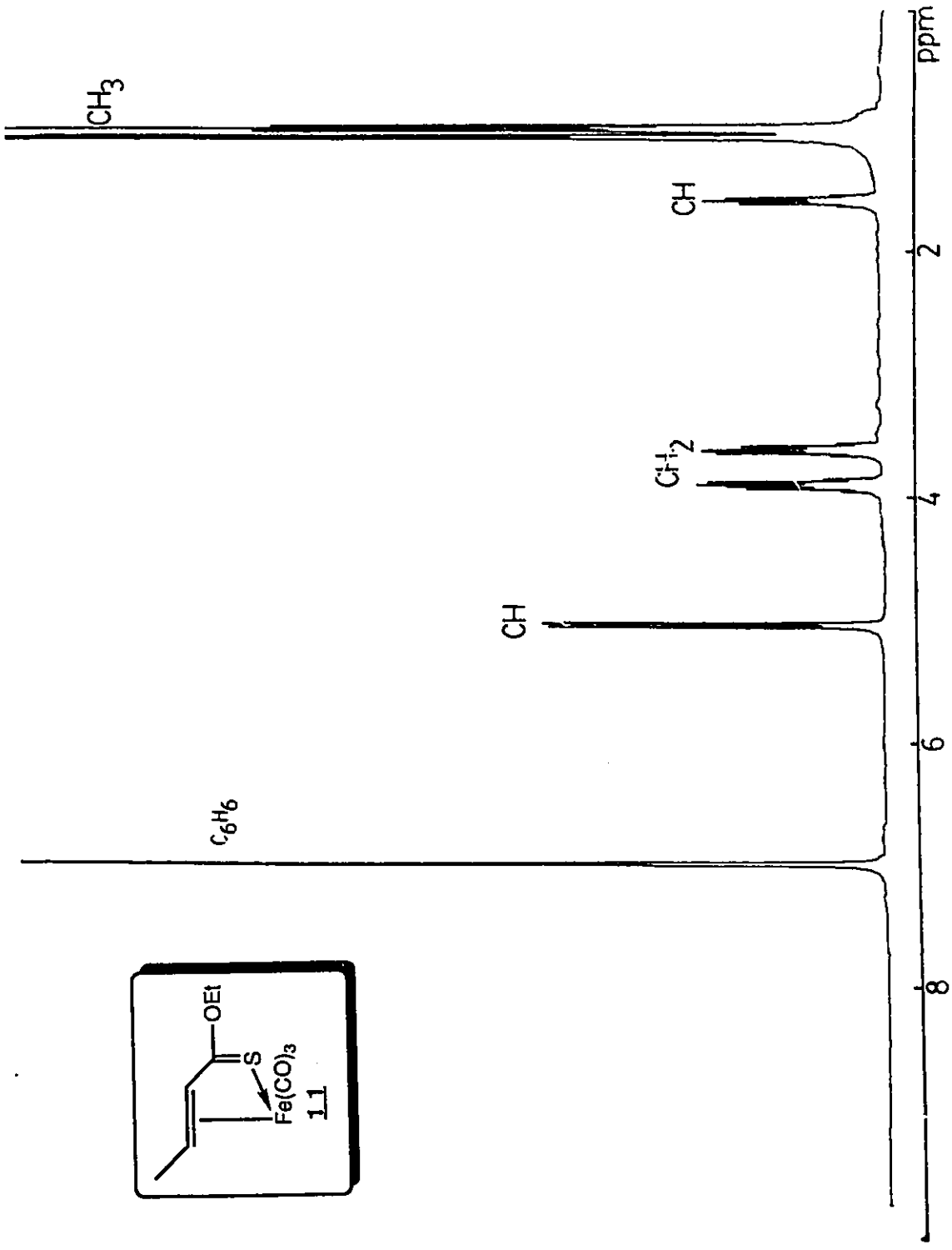

Figure 2.6: ^{1}H NMR Spectrum of Complex 11

	δC (ppm)				δH (ppm)		
	C=O	C=S	β-C	γ-C	$C_\beta H$	$C_\gamma H$	^{3}JHH(Hz)
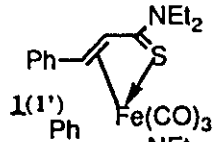 1(1')	210.5	161.69 (193.65)	63.96 (124.85)	52.42 (143.82)	5.04 (7.07)	3.47 (7.85)	7.7 (15.3)
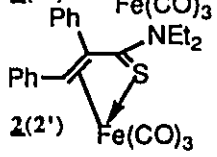 2(2')	213.43 208.35	141.20 197.62	---	66.18	–	5.17 (6.72)	
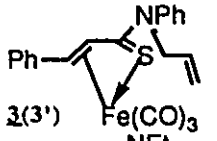 3(3')	209.98	155.85 (194.79)	63.30 (126.52)	60.16 (144.03)	5.11 (6.72)	3.63 (7.91)	8.2 (15.0)
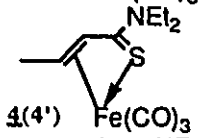 4(4')	210.39	159.69 (193.37)	58.85 (128.4)	58.78 (141.87)	4.10 (6.38)	2.53 (6.92)	7.36 (14.6)
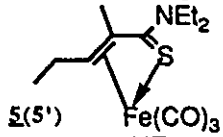 5(5')	211.4	143.01 (200.76)	92.52 (137)	46.22 (126.49)		1.13 (5.01)	
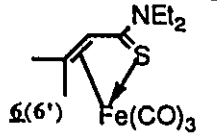 6(6')		(195.73)	49.55 (125.01)	(134.66)	2.63 (5.79)		
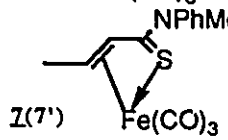 7(7')		152.95 (195.58)	67.59 (129.86)	60.85 (143.34)	4.41 (5.85)	2.28 (7.10)	7.8 (9.28)
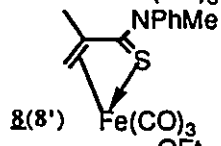 8(8')	208.2	148.96 (190.82)	92.85	51.45 (115)		1.62,1.93 (4.78,4.82)	
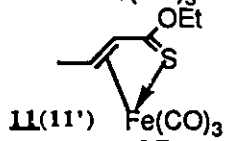 11(11')	209	155.5 (210.68)	77.8 (133.63)	59.8 (140.46)	5.16 (6.38)	1.45 (6.96)	8.3 (15.6)
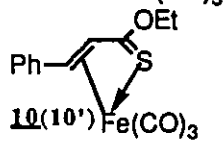 10(10')	210.7	155.5 (209.87)	71.5 (113.8)	63.3 (140.46)	6.18 (7.02)	2.70 (7.69)	8.8 (15.7)
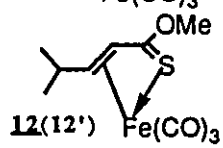 12(12')	207.95 210.72	157.15	75.88	75.12	5.25	1.57	8.4
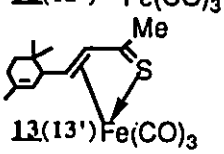 13(13')	204 209 212	134.56	122.64	78.18	5.54	1.67	9.5

Table 1

carbons. This change has also been reported for α,β-unsaturated ketones, imines, and dienes[2].

The ^{13}C spectra had equally dramatic differences in chemical shifts between free ligands and the iron complexes, (Table 1). There was the expected upfield shift for all carbons directly attached to the iron centre, the olefinic carbons shifting 70 - 80 ppm upfield relative to those of the free ligand. The spectra were assigned using DEPT and for those complexes which had CH's for both the β and γ–olefinic carbons, their assignment was based on thione iron complex **13** in which a HETCOR spectrum showed the γ–CH to be the peak further upfield. There appears to be a chemical shift trend in the ^{13}C NMR spectra of the iron complexes similar to that found in the ^{1}H NMR spectra in which the γ-olefinic carbon is shifted further upfield than the β-olefinic carbon. This change has also been observed for α,β-unsaturated ketones, imines, and dienes [2].

The carbon of C=S shifted upfield upon coordination to iron. The shift difference was not as large as that of the olefinic carbons but ranged from 30-50 ppm.

The metal carbonyls which occured as a single broad peak at room temperature in the ^{13}C NMR spectra experienced only slight chemical shift differences from one complex to another which suggests that there are only subtle differences in the electronic nature of the metal centre. This was expected owing to the equally slight differences observed in the stretching frequencies of these carbonyls in the infrared spectra. To resolve the single broad peak into its three carbonyls, a ^{13}C NMR temperature profile of thioamide iron complex **4** was conducted in which the coalescence point of the iron carbonyl ligands was found to be at approximately -13^{o}C, figure 7. At -60^{o}C, the carbonyls appear as three distinct signals at δ213.68, 213.10, and 206.17 ppm. Warming the solution to -40^{o}C gave broadening but no movement of the peaks was observed.

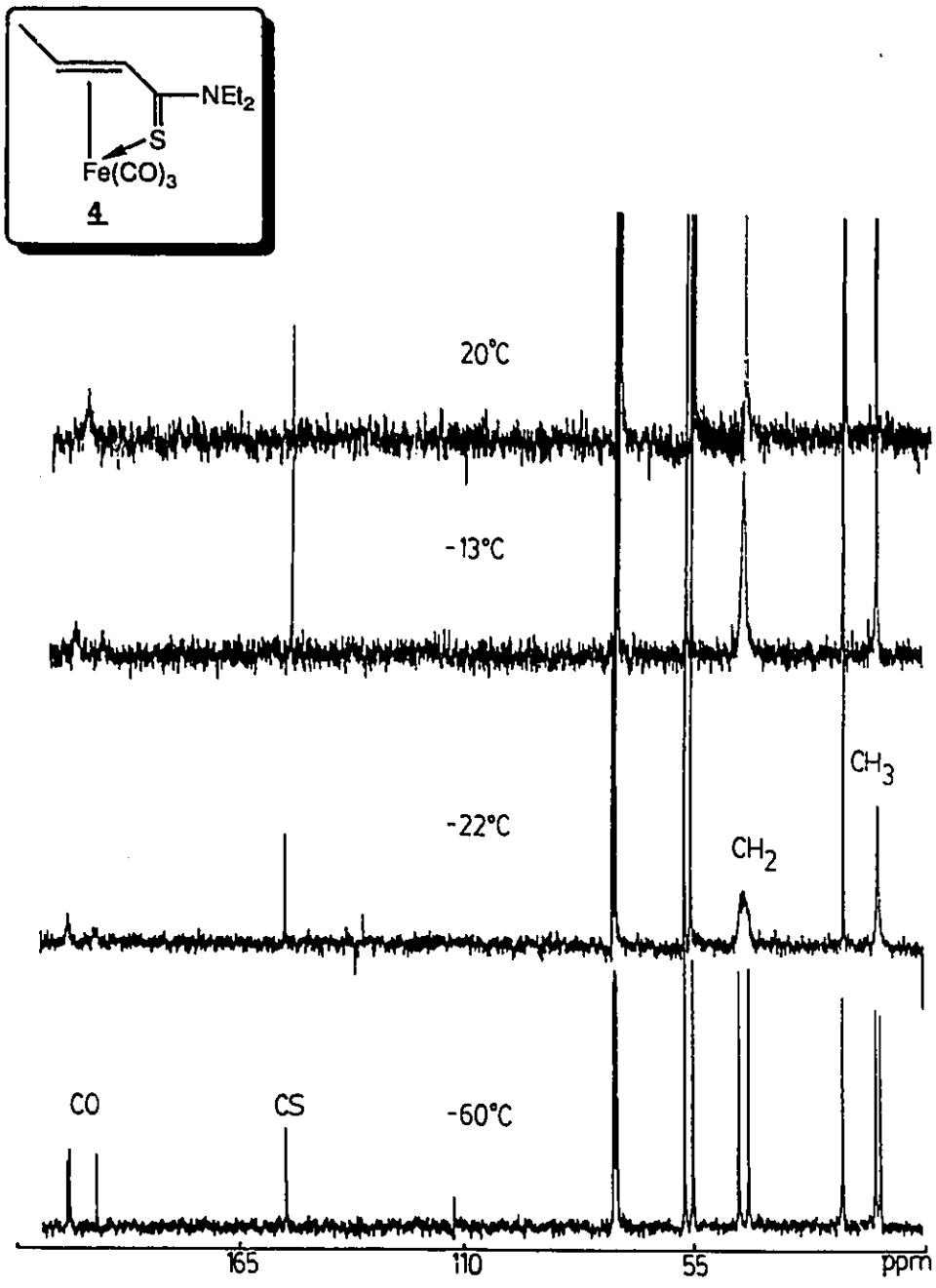

Figure 2.7: ^{13}C NMR Temperature Profile of Complex **4**

At -18°C, some movement began and at -10°C a single broad peak was observed. As well, the coalescence of N-ethyl methylene and methyl carbons could be observed. At -60°C, there are two distinct peaks for each of the two sets of ethyl groups. At -22°C, the methyl carbons had already coalesced and a single broad peak appeared for the methylene carbons.

Fluxionality in the carbonyl carbons is also observed from the ^{13}C NMR spectrum of diene iron tricarbonyl complexes[50]. Two possible explanations for this fluxionality are either dissociation followed by reassociation of one CO ligand at normal temperatures, or a process of rotation of the $[Fe(CO)_3]$ fragment which results in averaging of the magnetic environments experienced by each carbonyl. The dissociation/reassociation theory is less likely because, contrary to what might be expected, triphenylphosphine does not become incorporated at room temperature, as monitored by ^{31}P NMR, as a result of CO dissociation and coordination of PPh_3 rather than reassociation of the CO. Furthermore, stirring a solution of thioamide iron complex **4** under a ^{13}C enriched atmosphere of carbon monoxide did not indicate CO exchange by infrared spectroscopy. The other explanation, rotation of the $[Fe(CO)_3]$ fragment, is more likely but the process of apparent rotation without bond rupture is not well understood. Two processes for this rotation have been proposed which include Berry pseudorotaion and turnstile rotation. Both have been used to explain the well known nonrigidity in 5-coordinate molecules such as PF_5. Berry pseudorotation involves a pair-wise exchange of apical and equatorial ligands [6][51].

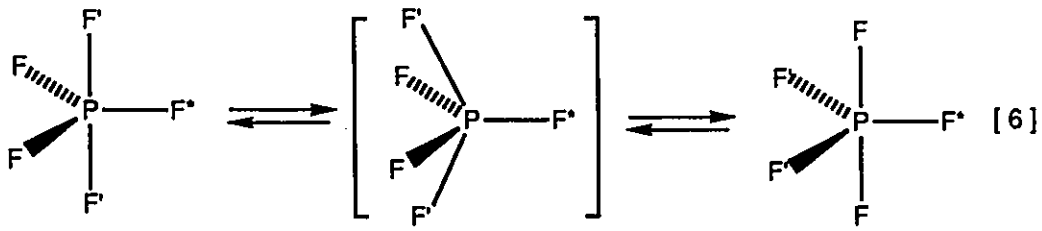

Turnstile rotation involves internal rotation of one apical and one equatorial ligand rotating as a pair vs. the opposite rotating or stationary trio of three remaining ligands [7][51].

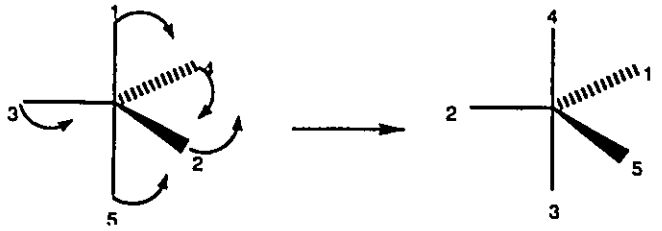

[7]

For diene iron tricarbonyl complexes as well as the thio-iron tricarbonyl complexes, the turnstile rotation is favoured because Berry pseudorotation would involve a trigonal bipyramidal intermediate with the diene ligand in one of the apical and equatorial positions which would be severely distorted due to the small bite size of the 1,3-diene moiety[52,53].

One thioamide iron complex, **2**, had ^{1}H NMR spectral information that was unusual compared to all of the other complexes. Only a small upfield chemical shift for the γ proton was observed. An X-ray crystal structure of this complex was obtained to ensure that the iron complex was similar to all of the other characterized iron complexes. The crystal structure confirmed the predicted structure and the bond lengths and bond angles were similar to those of complex **1**, so it is not at all obvious why the NMR spectra were so different. A detailed description of the crystal structure results will be discussed in a later section.

2.4.3.2.2 Thione

It has been mentioned that thione iron complex **13** was prepared from an impure ligand mixture, so there were no ^{1}H or ^{13}C NMR data for comparison

to determine the bonding site based on chemical shift changes with metal coordination. One must also consider the possibility of double bond migration to form an iron-diene complex, [8].

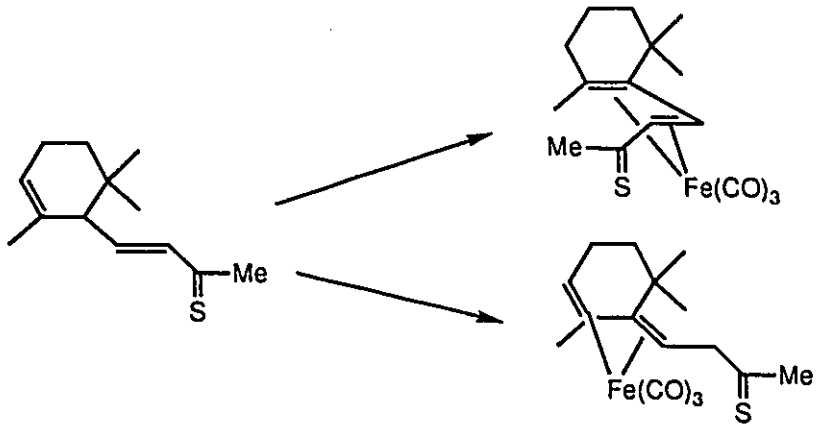

[8]

The ^{1}H NMR spectrum was readily assigned as that of a complex coordinated through the sulphur and therefore no double bond migration occurred.

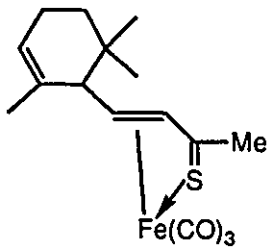

13

The signal for the β-olefinic proton was found to occur as a doublet downfield at δ5.54 ppm with 9.5Hz coupling to the γ–olefinic proton which occured as a doublet of doublets at δ1.67 ppm. The δ-proton was assigned to a doublet pattern having 10.9Hz coupling to the γ-proton. Finally, the olefinic proton in the ring was found in the usual region for non-metal complexed olefinic protons.

The ^{13}C NMR spectrum could not be assigned without the use of an

NMR HETCOR experiment which correlates carbons and protons. The HETCOR spectrum is shown in figure 8 and it allowed for the assignment of all of the CH-carbons.

2.4.3.3 X-Ray Crystallography

The nature of bonding in α,β–unsaturated heteroatom iron carbonyl complexes has been established by X-ray crystallography for cinnamaldehyde tricarbonyl iron[54], N-cinnamylideneaniline tricarbonyl iron[54], (cinnamaldehyde) (dicarbonyl)(triphenylphosphine) iron[55], and dicarbonyl(thioacrolein) triphenylphosphine iron[56] complexes. In such α,β-unsaturated heteroatom complexes there are two possible modes of coordination, π-coordination and lone pair coordination, which in the illustration below are represented by A and B.

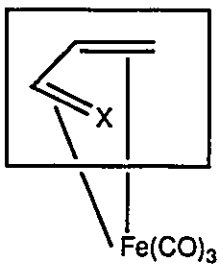

π-C=X

A

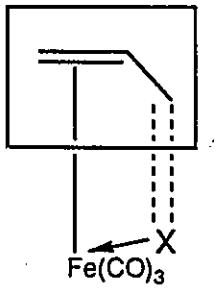

Lone-pair

B

Structure A can be considered the π-complex analogue to butadiene iron tricarbonyl in which the four atoms of the π-system lie in the same plane and in which the heteroatom lone pair does not bond directly to the iron centre.

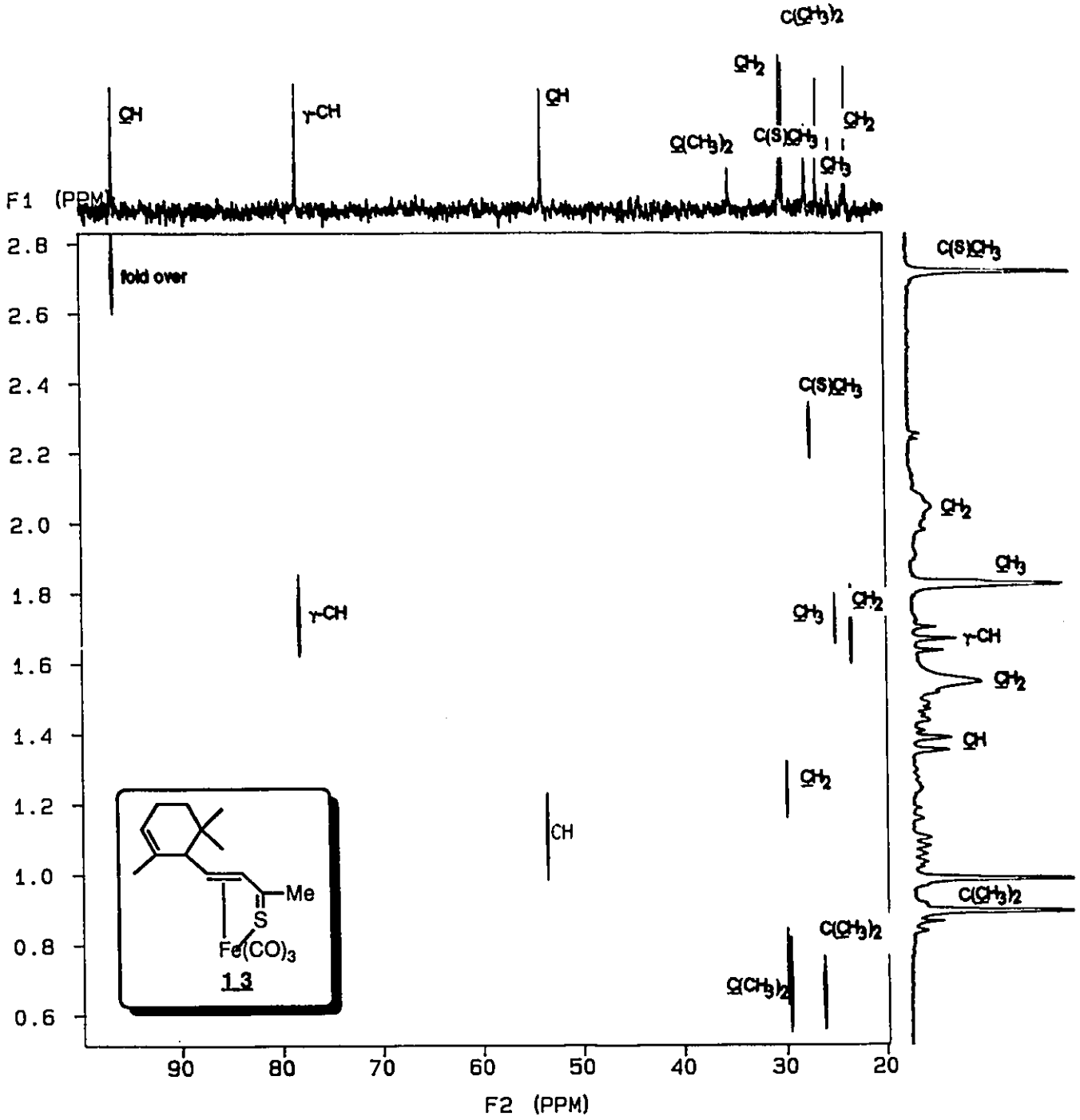

Figure 2.8: HETCOR of Complex **13**

For the complexes having nitrogen or oxygen as the heteroatom it has been suggested that they are π-complexes similar to structure A in which the oxygen and nitrogen lone pairs do not play a part in bonding with the metal[54]. The nature of bonding was described by a structural representation in which the planarity of the α,β-unsaturated heteroatom 4-atom arrangement was immediately obvious. The structure of a dicarbonyl triphenylphosphine thioacrolein iron complex had planarity of the π-system, as shown by representation A, but if it is assumed that the sulphur atom in this complex donates two electrons to the thioacrolein ligand aided by the triphenylphosphine ligand, HMO calculations on dinegative thioacrolein predict bond orders (C-S, 1.09; C_1-C_2, 1.72; C_2-C_3, 1.68) which are qualitatively in agreement with approximate bond orders derived from the bond distances (C-S, 1.1; C_1-C_2, 2.0; C_2-C_3, 1.7). This essentially predicts a full negative charge on the sulphur and a second negative charge distributed by resonance between the α and γ-carbons[30]. HMO calculations suggest a questionable degree of multiple bonding in the C-S bond, which is different from other α,β-unsaturated ketones and imines in which the C-O and C-N bonds are approximately double bonds[48].

Crystal structures of two α,β-unsaturated thioamide iron tricarbonyl complexes **1** and **2** were obtained in order to determine whether they corresponded to structures of type A or type B. All efforts to grow a good crystal of the free ligand for thioamide iron complex **1** in order to compare bond length changes upon metal complexation were unsuccessful, so the crystal structures of an alternative thioamide iron complex, **2**, and its free ligand, thioamide iron compound **2'** were obtained.

Unlike the examples of α,β-unsaturated heteroatom iron complexes which have been reported, thioamide iron tricarbonyl complexes **1** and **2** had structures in which there is significant distortion of sulphur from the plane formed

by the three carbons and there seems to be direct S-Fe bonding, illustrated by structural representation B.

The structures of complexes 1 and 2 consist of discrete molecular units having no intermolecular contacts less than the sum of van der Waals radii. The diagrams are shown in figures 9 and 10. Bond angles and bond distances are reported in Chapter 4. Pertinent bond distances are reported in Table 2. Table 2 is a compilation from the literature of some bond lengths for related η^4-heterodiene complexes of iron[48], along with the data for the crystal structures shown in figures 9 and 10.

There is a plane passing through C1, C2, and C3 of both complexes and the location of the sulphur atom deviates from this plane by 26.3° and 44.4° in thioamide iron complexes 1 and 2 respectively, and the perpendicular distance from the plane to the iron atom is 1.972Å in 1 and 1.912Å in 2.

In both complexes the bond lengths for C1-C2 and C2-C3 were approximately the same. In other words, there was little localization of double and single C-C bonds in either complex. Transition metal coordination to an olefinic bond in a π fashion usually results in bond lengthening due to π , in which complexes of metals in lower formal oxidation states have greater backbonding and therefore larger increases in the C=C bond length upon coordination[3]. A typical non-coordinated carbon-carbon double bond is approximately 1.33Å while a single bond is 1.54Å[57]. In butadiene iron complexes, simultaneous and counteracting π-donor and π-acceptor interactions between iron and the diene result in equalization of the carbon-carbon bond lengths within the coordinated 1,3-butadiene ligand. Free butadiene has a central carbon-carbon "single" bond length which is longer by 0.09Å than the formal carbon-carbon double bonds, but coordination to iron(0) makes all of the bond lengths approximately equal.

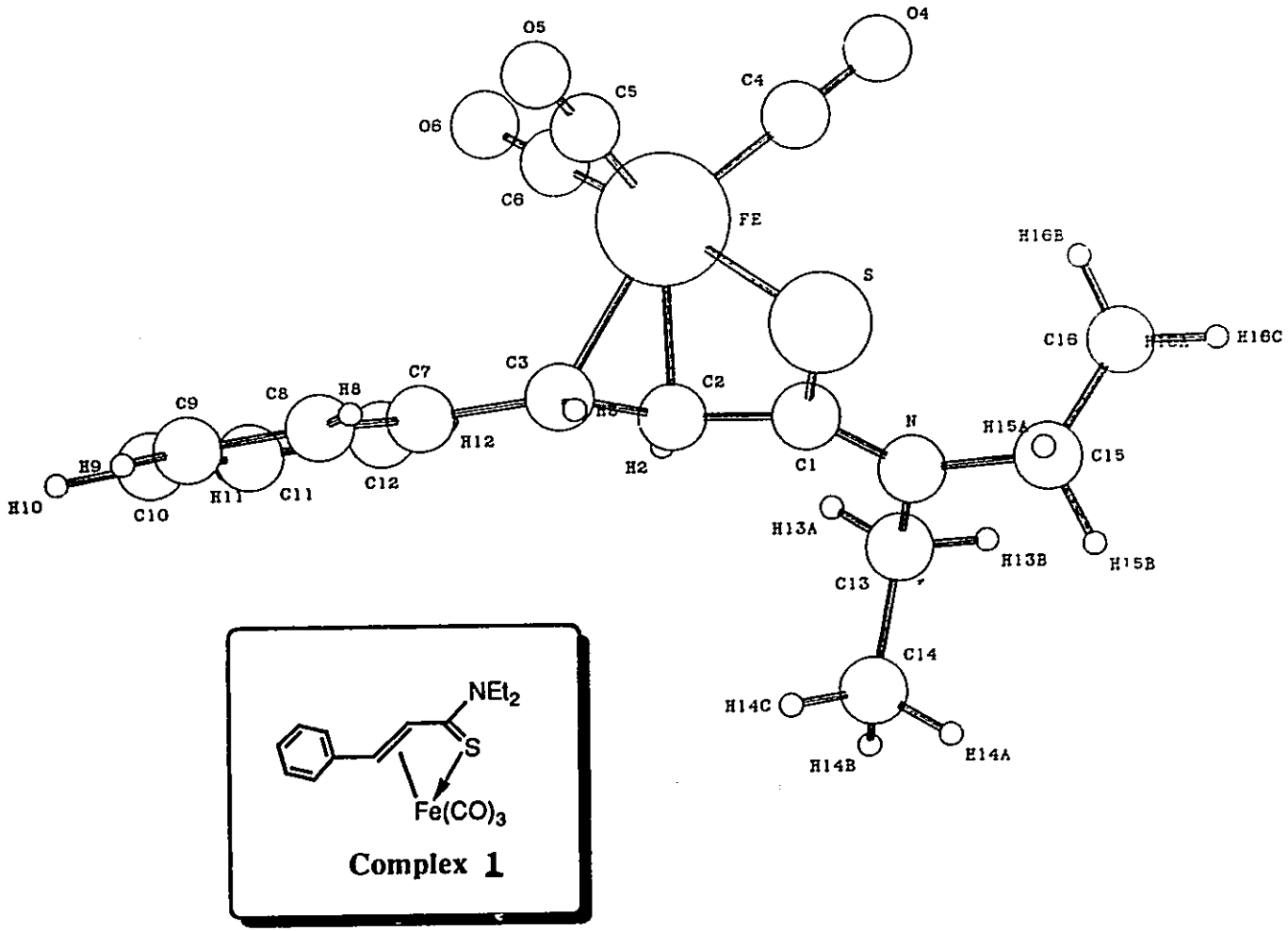

Figure 2.9: X-Ray Crystal Structure of Complex 1

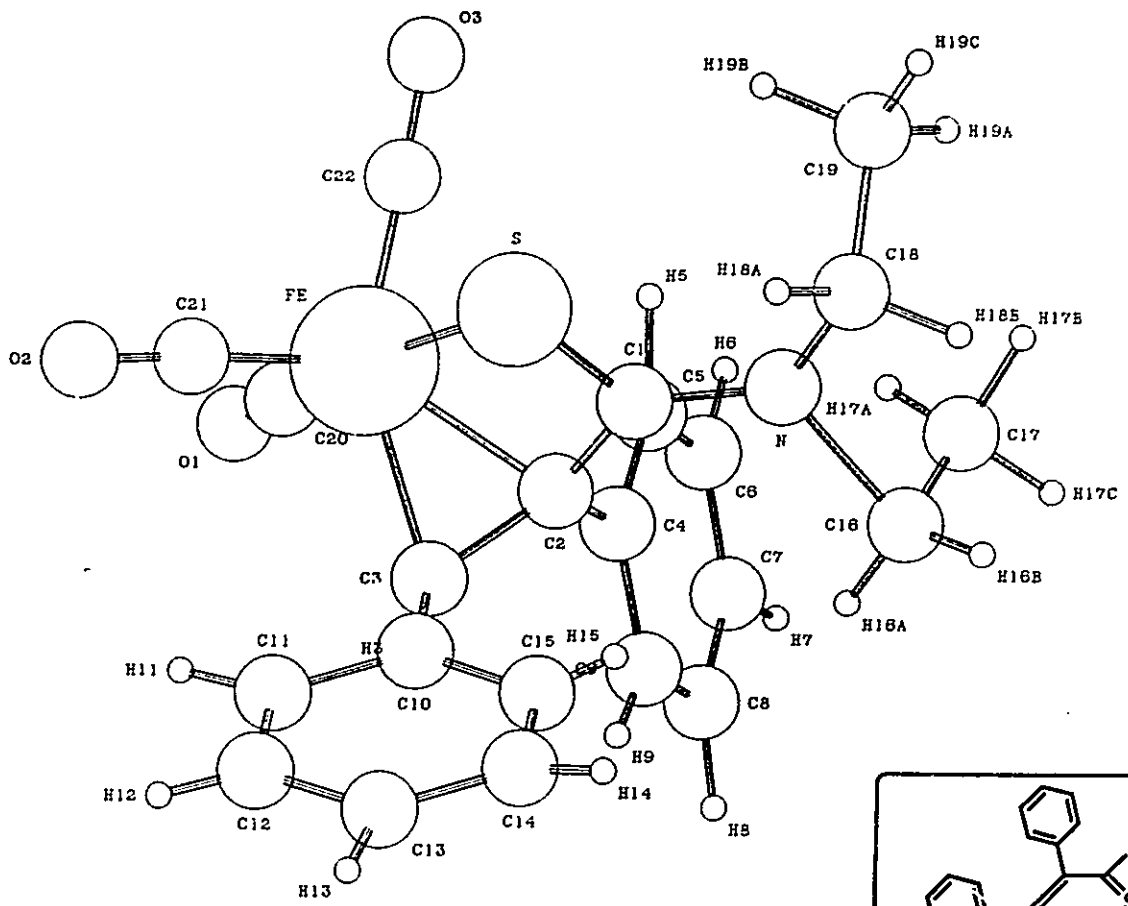

Figure 2.10: X-Ray Crystal Structure of Complex **2**

Bond Lengths (Å) for Related η^4-Heterodiene Complexes of Iron

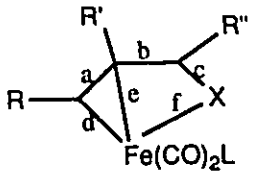

	a	b	c	d	e	f	ref.
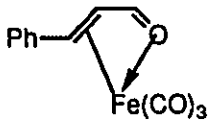	1.412	1.411	1.293	2.152	2.067	2.013	29
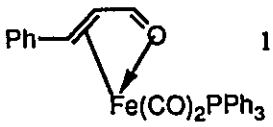	1.403	1.375	1.317	2.136	2.059	2.029	30
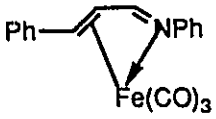	1.433	1.413	1.351	2.134	2.068	2.063	31
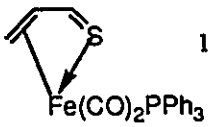	1.390	1.330	1.794	2.130	2.089	2.313	16
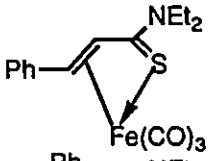	1.425	1.430	1.732	2.090	2.068	2.353	
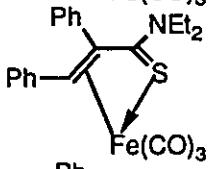	1.454	1.450	1.705	2.065	2.072	2.316	
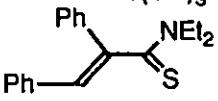	1.37	1.59	1.58				

Table 2

It was possible to compare the bond lengths of free thioamide ligand **2'** (C1-C2, 1.59Å; C2-C3, 1.37Å) to those of thioamide iron complex **2** (C1-C2, 1.45Å;

C2-C3, 1.454Å) and it is immediately obvious that the equalization of bond lengths which has been reported for butadiene iron complexes is also observed with α,β-unsaturated thioamide compound **2'**. The C1-C2 bond of thioamide compound **2'** is much longer than the C2-C3 bond by 0.22Å, which is considerably different than the 0.09Å difference found for the free ligand butadiene. The bond lengths for C1-C2 and C2-C3 of the thioamide iron complex **2** are slightly longer than those for thioamide iron complex **1** but the equalization of lengths for formal single and double bonds was also observed.

In thioamide iron complex **1** the distance from C3 to the ipso-carbon of its phenyl substituent (C3-C7) is 1.464Å, which is slightly smaller than that of a normal carbon-carbon single bond length and exactly the same value that was found for the carbon to phenyl bond length in dicarbonyl(η^4-cinnamaldehyde)-(triphenylphosphine) iron(0)[55]. As well, the value of the endocyclic C8-C7-C12 angle of 116.7° is smaller than the expected angle of 120°. This deviation of bond distance and bond angle from the norm indicates a certain degree of conjugation between the π-systems of the heterodiene and phenyl groups. The same was found for thioamide iron complex **2** and its free thioamide ligand **2'**.

The phenyl rings of each of thioamide iron complexes **1** and **2** and thioamide compound **2'** are planar with an average deviation of 0.001Å, 0.01Å, and 0.06Å respectively.

The carbon-nitrogen bond length, C1-N, is shorter than a normal C-N bond length (1.47Å[57]) and it was found that the nitrogen deviates from the plane formed by C1-C2-C3 (complex **1** ,19.8°; complex **2** , 53.8°; compound **2'**, 67.8°). The bond lengths C1-N for thioamide iron complexes **1** and **2** are 1.330Å and 1.327Å respectively, while in the free ligand **2'** this bond length was 1.43Å. A typical carbon-nitrogen double bond length is approximately 1.29Å while a typical carbon-nitrogen single bond is approximately 1.47Å[57]. The free

thioamide ligand **2'** has a C-N distance close to the normal C-N single bond length, but clearly complexation to the iron has a significant effect on this bond by shortening it to nearly that of a normal carbon-nitrogen double bond length. To illustrate the origin of this effect, one may refer to the nitrogen lone pair donation resonance structure X shown in Chapter 2. The crystal structure values showing an unusually short C-N length suggest that a significant contribution from the nitrogen lone pair into the diene π-system may explain the short bond lengths in thioamide iron complexes **1** and **2**. Although it is possible to have this contribution in the absence of coordination to the iron, the C-N bond length of the free thioamide ligand **2'**, which is an approximate single bond, suggests that the coordination of the ligand to iron significantly increases the contribution of resonance structures in which nitrogen donates electrons into the C=S carbon.

The carbon-sulphur bond lengths, C1-S, in thioamide iron complexes **1** and **2** are 1.732Å and 1.705Å respectively. The free ligand C1-S bond length is considerably shorter, being 1.58Å, which is similar to that found for CS_2 (1.56Å) and is shorter than the C=S bond length which has been adopted by several authors, 1.61-1.62Å[38] In the complexes the carbon-sulphur bond lengths approach that of a typical carbon-sulphur single bond, which is approximately 1.82Å[38]. Bond lengthening would be expected for π-coordination of the carbon-sulphur double bond to the iron, and although the deviation of sulphur from the plane formed by C1-C2-C3 is evidence for lone pair donation, π-coordination cannot be excluded from consideration. It may be that nitrogen lone pair contribution to C1 is responsible for the decrease in bond order in the C1-S double bond.

The iron tricarbonyl group linked to acyclic η^4-diene ligands have never been observed to have C_{3v} symmetry. Thioamide iron complexes **1** and **2** are no exception to this generalization. The ligand causes reduction of the

OC-Fe-CO angle cis to the carbon-carbon single bond to 89-90° for complexes **1** and **2** and to 89-93° for the η^4-diene and heterodiene complexes reported in the literature, while the other two angles remain in the range 95-107° for thioamide iron complexes **1** and **2** and 100-102° for those related complexes in the literature[54,55,56]. This reduces the symmetry of the $[Fe(CO)_3]$ group to C_S and may explain the absence of examples of C_{3V} symmetry.

In the thioamide group the bond lengths from iron to the carbon atoms in β and γ–positions to the sulphur are different. The iron-carbon bond lengths to the β-carbon (Fe-C2 is 2.068Å for thioamide iron complex **1** and 2.072Å for thioamide iron complex **2**) are shorter than that to the γ-carbon (Fe-C3 is 2.090Å for thioamide iron complex **1** and 2.065Å for thioamide iron complex **2**). This is typical of butadiene-type iron complexes, and representative bond lengths are listed in Table 2.

The iron-sulphur bond lengths were found to be 2.353(4)Å and 2.316Å for thioamide iron complexes **1** and **2**, respectively. The sulphur is bonded to the iron atom more closely in thioamide iron complex **2** than it is in the complex **1**. This is in contrast to the longer iron-olefinic carbon bond lengths observed for thioamide iron complex **2** relative to those of thioamide iron complex **1**. This presents a picture of thioamide iron complex **2** in which there is greater iron-sulphur interaction and correspondingly less π-backbonding to the olefin than is found for thioamide iron complex **1**. This is somewhat surprising in light of the fact that a shorter iron-sulphur bond would indicate enhanced electron density on the iron which would be compensated by backbonding into the π-olefin and carbonyl ligands, thus having the effect of decreasing the iron olefinic carbon bond lengths. It may be that through resonance stabilization the two phenyl groups of thioamide iron complex **2** decrease the degree of olefin-iron bonding. The crystal structure data for the thioacrolein iron complex

(Table 2) showed an iron-sulphur bond length of 2.313Å, which is similar to the iron-sulphur bond length in thioamide iron complexes **1** and **2**, while other iron-sulphur complexes having covalent bonds to the iron have been reported to have slightly shorter iron-sulphur bond lengths :

$[Fe(\eta^3\text{-}Ph_2PCH{=}C(^tBu)S\text{-}C{=}CHPh)(CO)(PMe_3)_2]BF_4$[58]: Fe-S, 2.259Å;

$[Fe((C_6H_5)CNSNC(CO_2C_2H_5)N(CH_3)_2)(CO)_3]$[12]: Fe-S, 2.301Å.

If the enhanced electron density around the iron due to the shorter iron-sulphur bond of thioamide iron complex **2** is compensated for by the iron carbonyl ligands through backbonding, then shorter iron-carbon and longer carbon-oxygen bonds of the carbonyl ligands would be anticipated. The iron-carbonyl carbon bond lengths for thioamide iron complex **2** were Fe-C20, 1.761Å; Fe-C21, 1.763Å; Fe-C22, 1.760Å and the carbon-oxygen bonds were C20-O1, 1.146Å; C21-O2, 1.174Å; C22-O3, 1.150Å. The same bonds for thioamide iron complex **1** were Fe-C4, 1.800Å; Fe-C5, 1.789Å; Fe-C6, 1.762Å and the carbon- oxygen bonds were C4-O4, 1.138Å; C5-O5, 1.139Å; C6-O6, 1.148Å. The shortest iron-carbon bonds were found for those carbonyls which were in a trans position to the sulphur. This is evidence confirming the expectation that there is greater backbonding from the metal to the carbonyls in thioamide iron complex **2** than there is in thioamide iron complex **1**. In the infrared spectra of both of these complexes the carbonyls of thioamide iron complex **2** have lower energy stretching vibrations than do those of thioamide iron complex **1**, which also suggests more backbonding in complex **2** than in complex **1**.

In summary the X-ray crystal structures of thioamide iron complexes **1** and **2** reveal a distinct difference between the α,β-unsaturated thio-group coordinated to the iron and other α,β-unsaturated heteroatom iron complexes. Only the three carbon atoms of the C=C-C=S fragment lie in the same plane,

while in other α,β-unsaturated heteroatom iron complexes the four atoms are coplanar. The sulphur atoms in complexes **1** and **2** appear to be coordinated to the iron through sulphur lone pair donation but the short carbon-nitrogen bond length indicates a degree of lone pair donation from the nitrogen to the carbon of the carbon-sulphur double bond.

Comparison of Crystal Structures for α,β-Unsaturated Heteroatom Iron Complexes

The X-ray crystal structures of a variety of α,β-unsaturated heteroatom iron complexes allows for a comparison of structural characteristics, bond lengths, and bond angles. The overall differences in the structures of the complexes have been discussed in that all of the complexes are distorted octahedrons. Furthermore, the aldehyde, imine, and thioaldehyde iron complexes all have structures in which the conjugated atoms, C=C-C=X, all lie in the same plane, as illustrated by structural representation A. As noted above, the thioamide iron complexes have only three atoms in the same plane and the structure is better represented by B in which the heteroatom, S, lies outside of this plane.

The distance of iron from the plane formed by carbons 1,2, and 3, shown below, seem to decrease with increasing electronegativity of the heteroatom.

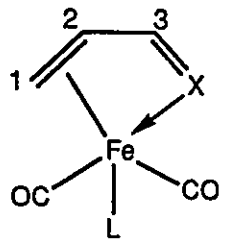

With X=oxygen, as in [C_6H_5CH=CH-CH=O] (L=CO), the C1-C2-C3 plane is 1.630Å away from the iron, while when X=nitrogen, as in [Ph-CH=CH-CH=NPh] (L=CO), this distance is 1.639Å and when X=S, for the thioaldehyde [CH_2=CH-CH=S], (L=PPh_3), this distance is 1.669Å. The corresponding distance is 1.872Å and 1.912Å for the thioamide iron complexes **1** and **2** respectively.

A feature common to all of the complexes is that the iron-C2 bond length was shorter than the iron-C1 carbon bond length. Again, the nature of the heteroatom seems to have an effect on these bond lengths but the differences are only slight and may be within the error of the measurement.

The iron-heteroatom bond distance was found to correlate with the electronegativity of the heteroatom and the degree of displacement of the heteroatom from the C1-C2-C3 plane. The bond lengths decreased with increasing electronegativity X=O, 2.013Å; X=N, 2.063Å; X=S(thioaldehyde) 2.313Å; X=S (complex **2**), 2.316Å; X=S (complex **1**), 2.353Å, and the deviations from the plane were approximately zero for X=O,N, and S(thioaldehyde), and 26.3° for X=S (complex **1**) and 44.4° for X=S (complex **2**).

The electronegativity of the heteroatom would be expected to have an influence on backbonding from the iron to the olefinic carbon-carbon bond of the heterodiene, where more electronegative atoms would be expected to decrease backbonding and less electronegative atoms would be expected to increase this backbonding. Although this might be expected to have an effect on the C1-C2 and C2-C3 bond lengths, there was no difference observed.

A comparison of mono-triphenylphosphine substituted iron complexes to their tricarbonyl complexes shows are differences in the C1-C2 bond lengths between the two types of complex. In fact, the only differences found between

such complexes are found in the C1-C2, C2-C3, and metal-carbonyl carbon bond lengths. There are no significant differences in the overall structure of the complexes or in the bond angles. The substitution of a carbon monoxide ligand by triphenylphosphine increases the charge density around the iron which is in turn reduced by increased backbonding to all of the ligands capable of behaving as π-acceptors. The result is slightly longer C1-C2 and C2-C3 bond lengths due to increased donation into the π^* orbitals of the olefin. It is not, however, possible to compare the triphenylphosphine substituted thioaldehyde iron complex to the tricarbonyl thioamide iron complexes **1** and **2**. The C1-C2 and C2-C3 bond lengths for thioamide iron complexes **1** and **2** are much longer than those for the thioaldehyde iron complex. The reverse would be true if just the triphenylphosphine substitution was influencing these bond lengths. Clearly phenyl substitution on C1 and C2 and the nitrogen on C3 was a determinant of the overall nature of the C1-C2 and C2-C3 bonds, overriding the effect of triphenyphosphine versus carbonyl substitution.

Finally, increasing electronegativity of the heteroatom favours increased backbonding to the heterodiene and decreased backbonding to the metal carbonyls. As a result, the metal-carbonyl carbon bond lengths are longer for complexes having more electronegative heteroatoms. The data suggest such a trend but the differences are only slight. Infrared spectroscopy provides a much more sensitive measure of these differences in backbonding and may give an energy difference as large as $30cm^{-1}$, depending on the heteroatom.

2.5 Conclusions

Thioamides, thioesters, and a thione were prepared from their carboxylic precursors using Lawesson's reagent. The iron tricarbonyl complexes were synthesized by photolytic or thermal methods using $[Fe(CO)_5]$ and $[Fe_2(CO)_9]$, and were characterized by the usual spectroscopic methods.

The rest of part 1 of the thesis describes the reactivity of these new α,β-unsaturated thioamide, thioester, and thione iron tricarbonyl complexes towards substitution, ligand removal, oxidation, electrophilic and nucleophilic attack, as well as alkyne addition.

CHAPTER 3

REACTIVITY

3.1 Ligand Substitution

Ligand exchange is perhaps one of the most important aspects of transition metal mediated modifications of coordinated organic compounds. For reactions to occur at the metal centre of coordinatively saturated complexes initial loss of some other ligand by a dissociative process may be required. Where carbon monoxide ligands are present, the dissociative process generally occurs with initial loss of CO, if it is labile. A way to test for the lability of such a ligand is to induce substitution for a weaker π-electron donating phosphine or phosphite ligand.

3.1.1 The Preparation and Characterization of Complexes 17-19

Several of the methods described above were used in an attempt to promote ligand exchange of the iron tricarbonyl complexes of α,β-unsaturated thioamides and thioesters. Metal-carbonyl activating agents, including $[PPN^+][CN^-]$, $[Me_3NO]$, and [BPK] were not selective towards the CO ligand. Often the α,β-unsaturated ligand was displaced or a complex mixture of products resulted. Thermal and photochemical methods were the most effective in promoting triphenylphosphine-CO exchange. Three new complexes were prepared: **17**, **18**, and **19**.

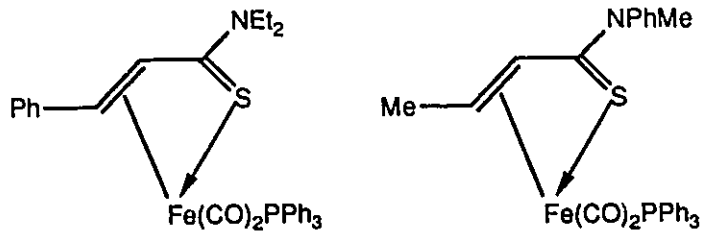

17

18

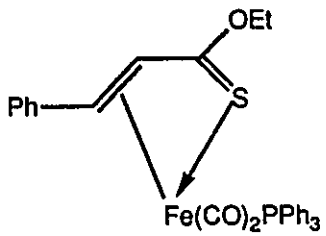

19

It was not possible to substitute more than one triphenylphosphine into the complexes.

3.1.1.1 Preparation of Complexes 17-19

Complexes 17 and 18 were prepared by refluxing a benzene solution of equimolar amounts of the tricarbonyl complex and triphenylphosphine under N_2 for 2h. The reaction was stopped when extraneous products began to appear in the reaction (as was monitored by tlc).

Complex 19 was prepared by photolysis of a cyclohexane solution of equimolar amounts of the tricarbonyl complex 10 and triphenylphosphine under N_2 for 22h. The reaction was stopped when all of the starting material had disappeared, as shown by tlc.

The isolation procedures were the same for both methods. The solutions were filtered and subsequent purification by column chromatography

gave an orange solid upon solvent removal. Complexes **17**-**19** were characterized by IR, mass spectrometry, ^{1}H, $^{13}C\{^{1}H\}$, and $^{31}P\{^{1}H\}$ NMR spectroscopy.

3.1.1.2 Spectral Characterization of Complexes 17-19

3.1.1.2.1 Mass Spectra

None of the complexes gave parent ions in the mass spectrum, using either EI or CI. The highest mass for complex **18** corresponded to $(M\text{-}PPh_3)^+$ and was followed by successive loss of CO's. Complex **18** fragmented with loss of two CO's simultaneously and a mass peak corresponding to the ligand was also present. The highest mass peak of complex **17** corresponded to $[Fe(CO)_2(PPh_3)]$, with a signal also occurring for the free ligand. The only thioester complex which was prepared, **19**, gave the highest mass peak corresponding to PPh_3 by CI and EI.

3.1.1.2.2 Infrared Spectra

The IR spectra gave two distinct metal-carbonyl υ(CO) vibrations in the region of 1975-1995 cm^{-1} and 1914-1939 cm^{-1}. Compared to the tricarbonyl analogues there was a shift of about 40 cm^{-1} to lower energy in **17**-**19**, because substitution of CO by the more basic PPh_3 ligand results in increased electron density on the metal which induces the remaining CO ligands to increase their $d\pi$-$p\pi^*$ back donation. The result is a decrease in the CO bond order, which is observed as lower energy stretching vibrations. As with the

tricarbonyl analogues, the thioester-PPh_3 complex **19** gave CO stretching vibrations approximately 20 cm^{-1} higher in energy than the thioamides. In both types of complexes, substitution by triphenylphosphine appears to have the same effect upon the infrared spectrum.

3.1.1.2.3 NMR Spectra

The ^1H NMR spectra show upfield shifts for the γ-CH in all of the complexes relative to the free ligands, which is expected since a greater charge on the metal centre would increase the shielding of that proton. Some ^1H NMR data for the complexes are shown in Table 3. The β-CH proton for all of the thio-ligands, except for complex **18** experienced a slight downfield shift upon formation of the new complex. Complex **18**, on the other hand, has a large upfield shift relative to the free ligand. In order for this to occur the proton must be aligned closer to the metal than it is in the non-phosphine substituted complex. It may be that PPh_3 is substituted at a different position than is found for the other complexes. Steric hindrance with the N-Ph group may force entry of the PPh_3 to a position remote from the N-substituents and closer to β and γ-CH. This may in turn distort the geometry of the complex to bring β-CH in closer proximity to the metal, (complex **18**).

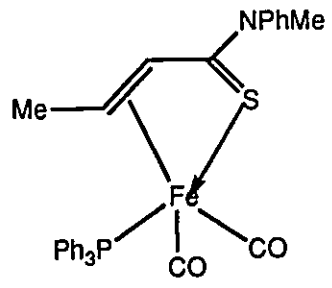

18

	δP (ppm)	δC (ppm) C=O	C=S	β-C	γ-C	δH (ppm) $C_\beta H$	$C_\gamma H$
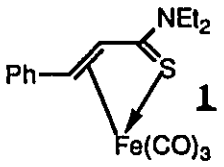 **1**		210.50	161.69	63.93	52.42	5.04	3.47
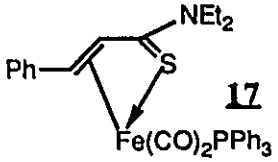 **17**	55.95	211.24 (5.6) 215.50 (12.0)	152.87	66.18	59.38	5.23	2.59
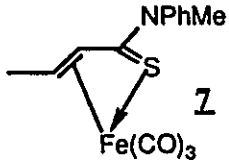 **7**		209.98	152.95	67.59	60.85	4.41	2.28
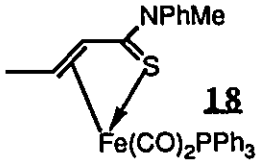 **18**	61.99	216.53 210.39	147	75.62	65.67	1.32	0.96
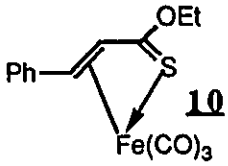 **10**		207.87	155	71.53	63.30	6.18	2.70
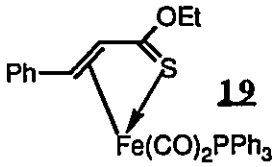 **19**	54.33	208.14 212.99	151.45	75.62	65.67	6.23	2.02

Table 3

It has been found by several researchers that ^{13}C NMR spectroscopy provides an exceedingly sensitive means of detecting relatively small electronic perturbations in organometallic systems[60,61]. The substitution of a CO ligand by a phosphine ligand should have an effect on the electron density of the metal centre which in turn can be measured by the change in chemical shifts of ligands coordinated to the metal. The extent of change with PR_3 substitution depends on

the σ-donor and π-acceptor properties of the phosphine ligand, which can be measured by the Tolman electronic parameter[62].

The effect of triphenylphosphine substitution for one of the three CO ligands in α,β-unsaturated thioamide and thicester iron tricarbonyl complexes was to dramatically increase the barrier to carbonyl rearrangement. Tricarbonyl complexes gave a broad single peak representing all three of the metal carbonyls at room temperature in the ^{13}C NMR spectrum. Dicarbonyl-triphenylphosphine complexes gave two separate signals in a 1:1 ratio at room temperature. Some of the ^{13}C NMR data are shown in Table 3. All of the phosphine substituted complexes gave slight shifts downfield for the metal carbonyls as compared to the non-phosphine substituted complexes. This is a direct result of substitution with PR_3 which, as a weaker π-acceptor than CO, expands metal d-orbitals and increases back-donation into the π*-CO orbitals. The increased electron density in the carbonyl π* orbitals serves to deshield the carbons. The same downfield shift has been observed for $[(BDA)Fe(CO)_2L]$[61] and $[(cyclic\ diene)Fe(CO)_2L]$[60] complexes. The fact that the two carbonyls have a chemical shift difference of 4-6 ppm in PPh_3 substituted complexes may be due to the effect of the heteroatom, S, in which one of the metal carbonyls may be bound more closely to the C=S fragment than is the other.

Complexes 17-19 did not show any evidence for the presence of geometric isomers in their NMR spectra. Such isomers would differ by the position of substitution of the triphenylphosphine relative to the sulphur. In 1 the triphenylphosphine is axial with respect to the sulphur and in 2 the triphenylphosphine is equatorial to the sulphur.

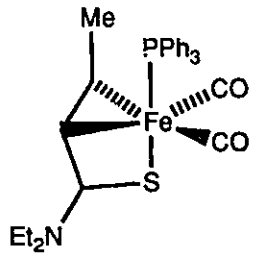

1

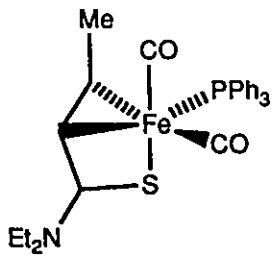

2

If it is assumed that the structures of $[(BDA)Fe(CO)_2PEt_3]$ and [(thioacrolein) $Fe(CO)_2PPh_3$] are similar to that of the α,β-unsaturated thioamide iron tricarbonyl complexes, then the phosphorus would be in an apical position[61]. The structure is represented above by 2, in which the two carbonyls are in a cis position to the phosphine where they are equally deshielded while one of the carbonyls is in a trans position relative to the sulphur where it will be further deshielded.

Coupling of the phosphorus atom to the carbonyl carbons was observed for complex 17. The largest coupling, 12Hz, was found for the carbonyl furthest downfield. Coupling constants provide a measure of the degree of s-character between the atoms experiencing the coupling. This suggests that the degree of s-character between the PPh_3 and CO in an axial position to PPh_3 is greater than that of equatorial CO which has a coupling constant of only 5.6Hz. This may be due to the orientation of axial CO also being trans to sulphur, as illustrated by complex 2 above, in which there is greater $d\pi$-$p\pi^*$ back-donation and increased s-character in the Fe-CO bond. These coupling values are lower than those found for $[(PPh_3)Fe(CO)_4]$ and $[(PPh_3)_2Fe(CO)_3]$ of 22Hz and 29.5Hz respectively[63].

Based on the strong coupling between the carbon monoxide ligands and the phosphorus, coupling of the α,β, and γ carbons to phosphorus was anticipated, but it was not observed.

The thiocarbonyl carbon was shifted slightly upfield as a result of PPh_3 substitution in complexes 17-19. Thus it appears that the interaction of the sulphur with the metal may be greater than that of the oxygen of BDA-complexes with the metal, since there is no change in the C=O chemical shift of BDA in $[(BDA)Fe(CO)_2PPh_3]$ as compared to the tricarbonyl complex. The greater the interaction of the heteroatom with Fe, the more sensitive it would be towards electronic changes at the metal centre, as measured by ^{13}C NMR shift of the carbon attatched to the heteroatom.

Molecular orbital calculations on butadiene iron tricarbonyl revealed that the iron d-orbitals which are involved in bonding to CO have an antibonding interaction with the diene. Expansion of these orbitals upon PPh_3 substitution increases the antibonding interactions so diene orbital populations show small shifts towards the uncomplexed ligand. The result was a slight shift upfield for the olefinic carbons[60]. This is not the case for the olefinic carbons β and γ to sulphur in thioamides and thioesters, which experience a downfield shift upon PPh_3 substitution. Here, olefinic backbonding into the π^* orbital must be enhanced owing to the increased electron density at the metal centre. Backbonding into the π^* orbital of the C=C double bond, similar to backbonding into the CO ligands, serves to deshield the carbons. The shift changes observed for the α,β-unsaturated thio-iron dicarbonyl triphenylphosphine complexes are different to those observed for $[(BDA)Fe(CO)_2PPh_3]$[61] in which the β and γ-carbons experienced an upfield shift relative to its corresponding $[Fe(CO)_3]$ complex much like that found for butadiene iron tricarbonyl. An explanation was offered in which the molecular orbitals of BDA which participate in bonding are polarized in such a way that the oxygen atom may be considered as a site of concentrated electron density and the γ-carbon as the major acceptor in binding to the $[Fe(CO)_2L]$ fragment. The BDA ligand is therefore seen as a "sink" for the

negative charge placed on the iron atom by the phosphorus ligand in which the BDA has a substantial contribution from structure I shown below.

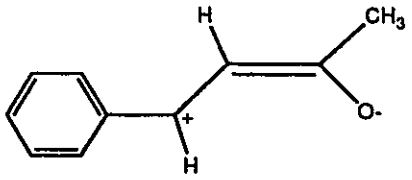

I

The result is tighter bonding of γ-C to the Fe centre, which causes greater shielding of that carbon.

A structure such as I is not likely for the thioamides and thioesters. The possible resonance structure is more like that of structure II, which retains olefinic character at the β and γ-carbons enabling π* backbonding to occur.

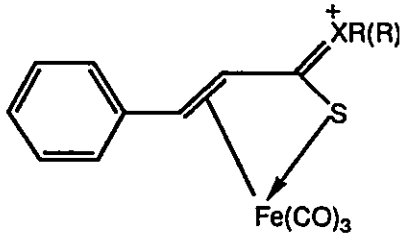

II

Complexes 17-19 gave ^{31}P chemical shifts in the range δ54.33-55.95 ppm. The dataareshown in Table 3. These shifts are all downfield from free PPh_3 (δ-5.02ppm) as would be expected with metal complexation, due to an increase in the cone angle of PPh_3 associated with such complexation[62]. As well, electron donation from the phosphine to the metal contributes to the downfield shift.

3.2 Ligand Removal

Thioamides and thioester iron tricarbonyl complexes were subjected to this ligand removal by a variety of methods. Many methods were successful; however, it was observed that conversion of C=S to C=O was a major side reaction.

3.2.1 Results and Discussion

Several methods were used to effect the removal of α,β-unsaturated thioamides from iron complexes **1** and **4**, and a thioester from iron complex **10** and the results are shown in Table 4. It was anticipated that heating a solution of the complex under nitrogen would selectively remove the organic compound. Instead, the complex decomposed resulting in moderate recovery of the thioamide ligand from iron complexes **1** and **4** as well as unidentifiable and insoluble products. Since a triphenylphosphine ligand was effectively substituted for the CO ligand in refluxing benzene, it is possible that the main route towards degradation of the complex proceeded by a path involving CO loss. To test this, a solution of the complex was refluxed in benzene under a CO atmosphere with the result being no recovery of the free ligand and only slight complex degradation, even after refluxing for 18h. The complex did therefore degrade via CO loss under thermolysis conditions.

COMPLEX	METHOD: Δ	Ce(IV) RT	Ce(IV) 0°C	Fe(III)	Me_3NO	H+	H_2O_2	hν	mcpba	PRODUCT(S) (Yield) A=amide/ester B=thioamide/thioester
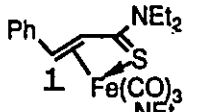 1	X									B(41%)
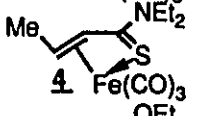 4	X									B(42%) + 4(6%)
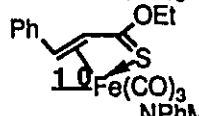 10					X(0°C)					A(84%)
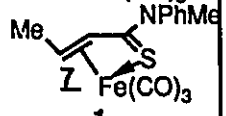 7									(0°C)	A(63%) + B(13%)
1						X				B(18%)
4						X				4(56%)
4							X			B(48%)
4							X			A(64%)
4							X			A(88%)
1								X		B(18%) + 4(48%)
4					X(RT)					A(86%)
4					X(RT)					A(89%)
1					X(0°C)					A(82%)
4									$MeCO_2H$	B(18%) + 4(35%)
4									(EtOAc)	A(38%) + B(11%)
4				X						A(57%) + B(30%)
4		X								A(49%)
1		X								A(43%) + B(51%)
4			X							B(98%)
4			X							B(94%)
1									(-30°C)	B(56%) + 4(44%)
4										

Table 4

The most effective method for α,β-unsaturated thio–ligand removal involved using oxidative cleavage. The addition of ceric ammonium nitrate to a stirring aqueous acetone mixture of the complex cooled to 0°C gave good recovery of the α,β-unsaturated thiocompound, 98% using iron complex 4 and 94% using iron complex 1. The rate of addition of ceric ammonium nitrate to the solution seemed somewhat critical in order to avoid C=S conversion to C=O as was

shown by the results obtained in the room temperature reaction using iron complex **4**, which gave 51% α,β-unsaturated thioamide and 43% α,β-unsaturated amide ligands. Also, use of iron complex **1** gave 49% recovery of just the amide ligand. The best results were obtained with the addition of small portions of the oxidizing reagent which were added only after the cessation of bubbling caused by the previous portion. Cooling the solution was necessary to avoid oxidation of the C=S to C=O. Ferric chloride was also used and the recovery of the ligand was good, but even at 0°C much of the C=S from iron complex **4** was converted to C=O (57% α,β-unsaturated amide and 30% α,β-unsaturated thioamide).

Another reagent commonly used to induce ligand removal, trimethylamine oxide, was effective for removing the organic ligand, but in all cases only C=O products were recovered and not C=S products. The room temperature reaction with thioamide iron complexes **1** and **4** gave 89% and 86% α,β-unsaturated amides respectively. Even at 0°C, only amide products were recovered, 84% from iron complex **1** and 82% from complex **4**.

The addition of a proton source, trifluoroacetic acid, gave only slight recovery of the ligand, 18% thioamide from iron complex **1**. Some insoluble and unidentifiable products were formed during acid addition. Using [HBF_4] as a proton source gave some decomposition using thioamide iron complex **4** and 56% recovery of the complex.

Other methods were found which cleaved the α,β-unsaturated ligand but ligand removal was not the intended reaction in those cases. Attempted oxidation of the C=S unit in complexes **1**-**4**, and **7** to an S-oxide complex resulted in ligand cleavage and oxidation producing a mixture of C=S and C=O products using m-chloroperbenzoic acid, and only C=C products using hydrogen peroxide, as shown in Table 4. Photolysis of a cyclohexane solution of **4**, under

nitrogen gave some decomposition along with some ligand recovery, 48% starting material and 18% thioamide ligand.

3.3 **Oxidation to a Sulphine Complex**

A high concentration of electron density on the sulphur of α,β-unsaturated iron tricarbonyl complexes would be expected to allow for facile oxidation to form an S-oxide complex. To investigate the reactivity towards oxidation of α,β-unsaturated thioamide and thioester iron tricarbonyl complexes relative to the thioacrolein complexes, oxidation reactions were performed on thio-iron complexes **1**, **4**, **7**, **10**.

3.3.1 Results and Discussion for Oxidation and Spectral Characterization of Iron Complex **20**

Thioamide iron complexes **1**, **4**, and **7** did not give S-oxide products with hydrogen peroxide in acetic acid, m-chloroperbenzioc acid, cobalt chloride and oxygen, trimethylamine oxide, ferric chloride, or ceric ammonium nitrate. In all reactions there was either recovery of starting material or some of the ligand was cleaved from the complex, accompanied by C=S to C=O conversion.

Thioester iron complex **10** was converted to S-oxide complex **20** using hydrogen peroxide in acetic acid.

It should be noted that to ensure that there was no reaction of the thioamide and thioester iron complexes with water of the hydrogen peroxide

solution, a separate experiment was carried out to show that the iron complexes are unreactive towards water.

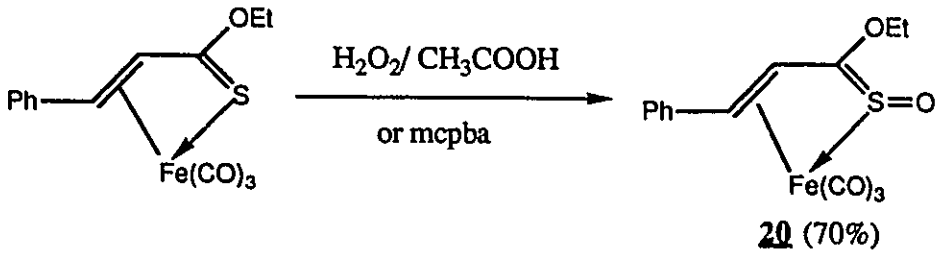

20 (70%)

The product was characterized by I.R., M.S., and ^{1}H and ^{13}C NMR spectroscopy.

3.3.1.1 Mass Spectrum

Chemical ionization was used and gave a mass spectrum corresponding to $[M-16]^{+}$. Mass peaks were also found corresponding to the free ligand S-oxide compound as well as the free ligand with loss of one oxygen. All of the S-oxide complexes of thioacrolein iron and cobalt complexes XXXII and XXXIV, Chapter 1, also gave mass spectra with a highest mass peak corresponding to the loss of one oxygen[31]. This behavior is in fact also observed for free sulfines[83].

3.3.1.2 Infrared Spectrum

Ligand vibrations in the IR spectrum of sulphine iron complex **20** were medium to weak compared to the intensity of the metal-carbonyl υ(CO) bands.

The two metal carbonyl υ(CO) bands of the S-oxide complex, 2070(s), 2015(s br) cm^{-1} were shifted to a higher energy than in the starting material, 2050(s), 1980(vs br) cm^{-1}. This results from decreased dπ-pπ* backbonding from the iron to the carbon monoxide ligands, which is in turn due to less electron donation from the sulphur lone-pair, which is involved in S=O bonding. A medium broad peak centred at 1010 cm^{-1} was assigned to S=O stretching. Cobalt and iron thioacrolein S-oxide complexes were said to have "strong" absorptions at 1020-1070 cm^{-1} [30]. Compared to the CH vibration band at 3300 cm^{-1} in the new sulphine iron complex **20**, υ(SO) was "strong".

3.3.1.3 NMR Spectra

In the ^1H NMR spectrum of sulphine iron complex **20**, O-ethyl protons are in approximately the same chemical shift region as the starting material and maintain the ABX_3 pattern of the free ligand. The olefinic β-C<u>H</u> is shifted slightly upfield while there is a dramatic downfield shift of approximately 2 ppm for the γ-C<u>H</u> proton. This indicates an endo orientation of the oxygen.

The close proximity of oxygen to the γ-C<u>H</u> proton would serve to deshield the proton and drive its resonance downfield. This seems only reasonable since an exo S=O orientation would not be expected to have as dramatic an effect on the γ-CH proton. The coupling constant between the olefinic protons remained unchanged in sulphine iron complex **20** compared to the starting material.

The ^{13}C NMR assigned by DEPT for sulphine iron complex **20** in $CDCl_3$ is shown in figure 11.

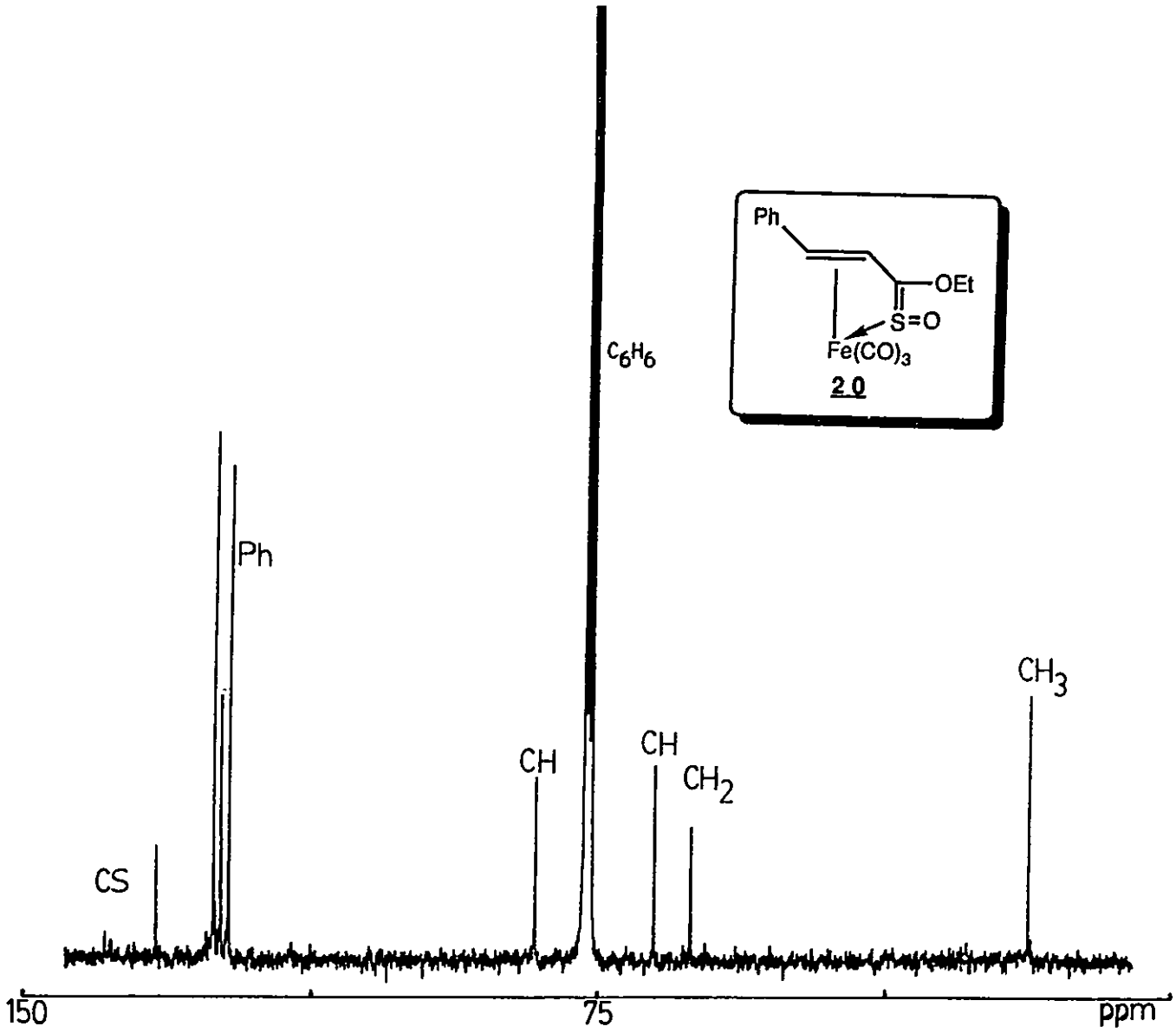

Figure 3.11: ^{13}C NMR Spectrum of Complex **20**

The metal carbonyl ligands, which are not observed in the ^{13}C NMR spectrum illustrated in figure 11, remain fluxional in the S-oxide iron complex and experience a slight upfield shift as compared to the starting material, thioester iron complex **10**.

This corresponds well with the IR data, which would predict such a shift due to the decrease in backbonding from the iron to the metal carbonyls as evidenced by the shift to higher frequency. The C=S carbon also experiences an upfield shift of carbonyl resonances in comparison to thioester iron complex **10**.

The olefinic carbons (β and γ) experienced a downfield shift relative to the starting material.

3.4 Nucleophilic Addition

Thioamide and thioester iron tricarbonyl complexes were found to react with nucleophiles producing new thioamide and thioester organic compounds. It was anticipated that similar Michael-type addition products would be obtained from α,β-unsaturated thioamide and thioester iron tricarbonyl complexes as were obtained from the α,β-unsaturated thioamide palladium complex discussed in Chapter 1. This prediction was realized but product formation was found to be temperature dependent. Similar to the observation for iron tetracarbonyl complexes of α,β-unsaturated amides and esters, it was thought that some CO insertion products would be formed with iron tricarbonyl complexes of α,β-unsaturated thioamides and thioesters. This was indeed the case and these results are discussed in the next section.

3.4.1 Results and Discussion -- Nucleophiles

The direct nucleophilic addition to α,β-unsaturated thioamide and thioester iron tricarbonyl complexes at temperatures greater than -78°C gave 1,4-Michael addition products. Anion addition to a solution of the iron complex at -78°C, followed by warming to room temperature and quenching with a proton source gave exclusively 1,4-addition to thioamide iron complexes **1** and **4** affording [C(CN)(Me)$_2$CH(Me)CH$_2$C(S)(NEt$_2$)](**25'**) and [C(CN)(Me)$_2$CH(Ph)CH$_2$C(S)(NEt$_2$)] (**26'**) in 86% and 89% yield respectively [1].

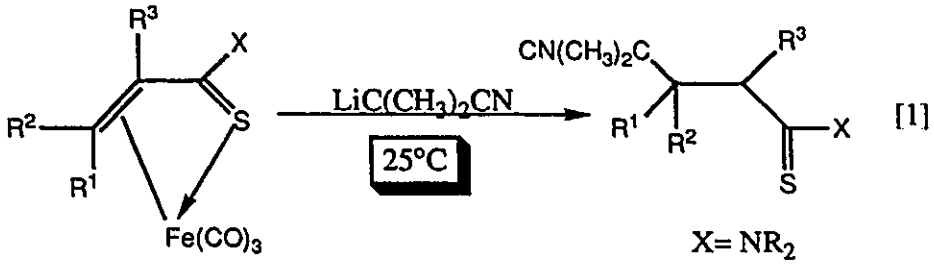

[1]

In principle, whenever there is at least one hydrogen atom next to the thiocarbonyl group, then thioketone-enethiol isomerization may be observed[38]. In practice it is only observed when the α-hydrogen atom is part of a secondary or tertiary carbon. Michael addition products of the type where R^3=H in reaction [1] would be expected to show this tautomerism. It would be readily observable by ^{1}H NMR spectroscopy in cases where the interconversion is slow and can be clearly distinguishable, as has been the case for several thione compounds.

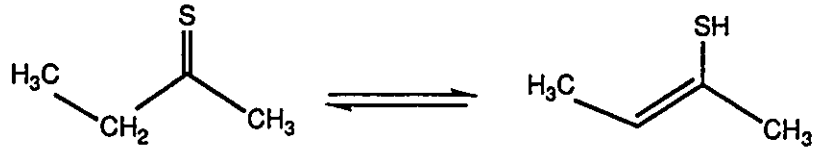

thione ene-thiol

There was no evidence for thione-enethiol tautomerism in the ^1H NMR spectra for the thioamide products even at -40°C. This absence of thione-enethiol equilibrium has also been reported for thio – esters and dithioesters[64].

If the reaction mixture was maintained at -78°C for two hours and then quenched with a proton source at that low temperature, 4-oxo-thioamides were obtained, [2], and the results are shown in Table 5.

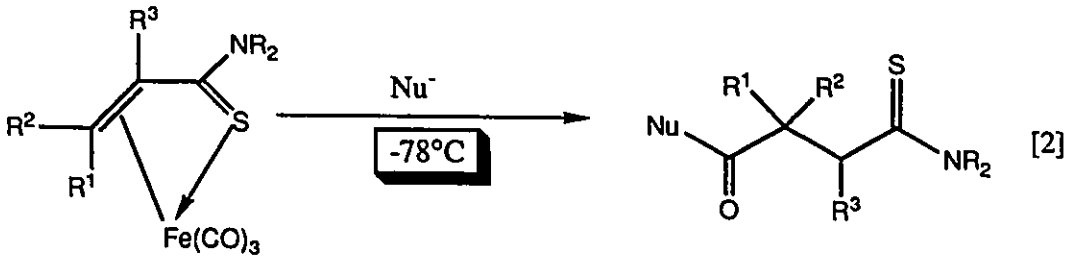

[2]

$\{Nu^- = MeLi, LiCH(CH_3)CN, LiC(CH_3)_2CN, LiC(CH_3)_2CO_2Et\}$

These 4-oxo-thioamides are potentially useful as synthetic intermediates to 4-oxo-ketoamides and 2-aminothiophenes[19,65,66,68]. Thioamides have been shown to be easily converted to a variety of types of compounds such as amides, enamines, and esters[65]. The ease of conversion of these thioamides to 4-oxo-thioamides suggests that these new 4-oxo-thioamides may provide a new route to 4-ketoamides, which are intermediates in the preparation of the 1-aryltetralin lignans, galactin and isolactin[66].

A recent investigation of the synthesis of 4-ketoamides has revealed that the addition of lithium and magnesium carbanions to α,β-unsaturated tetracarbonyl iron complexes produces 4-ketoamides in up to 82% yield [3][19].

COMPLEX	ANION	QUENCHING METHOD	PRODUCT(S) (Isolated Yield)
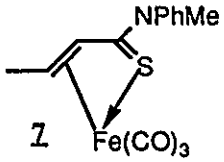 7	$LiC(CH_3)_2CN$	Ce(IV)	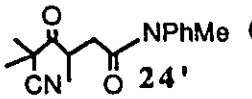 (NA) 24'
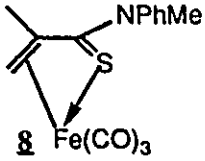 8	$LiC(CH_3)_2CN$	Ce(IV)	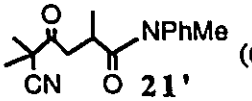 (64%) 21'
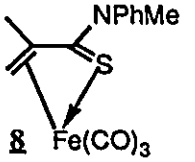 8	$LiC(CH_3)_2CN$	^tBuBr	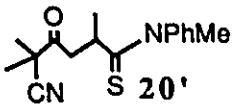 (1%) 20'
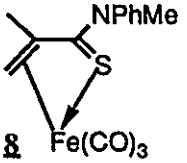 8	$LiCH_3$	^tBuBr	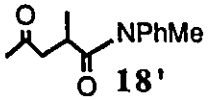 (4%) 18'
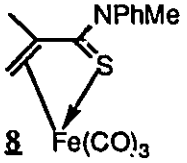 8	$LiCH(CH_3)CN$	Ce(IV)	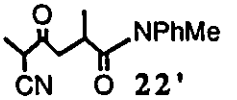 (NA) 22'
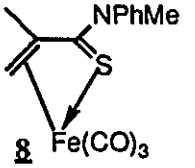 8	$LiC(CH_3)_2CO_2Et$	^tBuBr	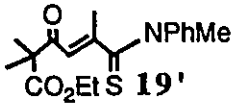 (67%) 19'
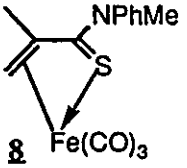 8	$LiC(CH_3)_2CO_2Et$	Ce(IV)	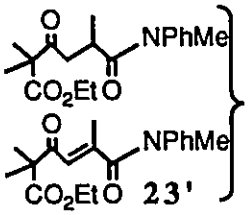 (60%) 23'
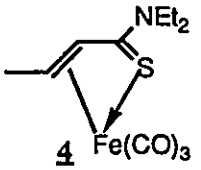 4	$LiC(CH_3)_2CN$	Ce(IV)	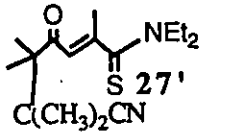 (NA%) 27'
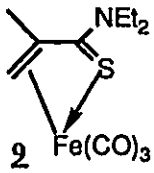 9	$LiC(CH_3)_2CN$	^tBuBr	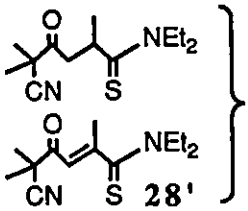 (NA%) 28'

Table 5

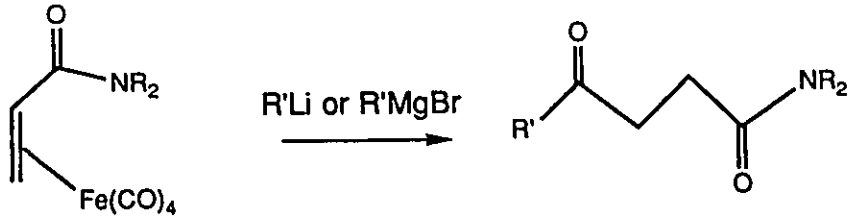

[3]

The results presented here extends the range of 4-ketoamides that can be synthesized. The 4-oxo-thioamides prepared from α,β-unsaturated thioamide iron tricarbonyl complexes could be easily converted to 4-ketoamides by using ceric ammonium nitrate. Unlike the 4-ketoamides prepared from α,β-unsaturated amide tetracarbonyl iron complexes, the 4-ketoamides prepared from α,β-unsaturated thioamide iron tricarbonyl complexes had a β-methyl substituent and, in one case, a γ-methyl substituent in the starting material. Also, the anions used in this reaction, [$LiC(CH_3)_2CN$], [$LiC(CH_3)_2CO_2Et$] and [$LiCH(CH_3)CN$], were different than those used in the reaction with α,β-unsaturated amide tetracarbonyl iron complexes (methyl, phenyl, and benzyl carbanions). In summary, the synthesis of 4-ketoamides from nucleophilic reactions with α,β-unsaturated thioamide and α,β-unsaturated amide iron carbonyl complexes together provide products which vary with the choice of nucleophile and substitution in the starting material.

The acid catalyzed reaction of 1,4-diketones with hydrogen sulphide has been used as a convenient route to thiophenes[67,68]. It was stated that the most likely route to 3-carboethoxythiophenes VII from 2-ethoxycarbonyl-1,4-diketones III was via the formation of monothionated intermediates IV and V with possibly some contribution from dithioketone VI (Scheme 1).

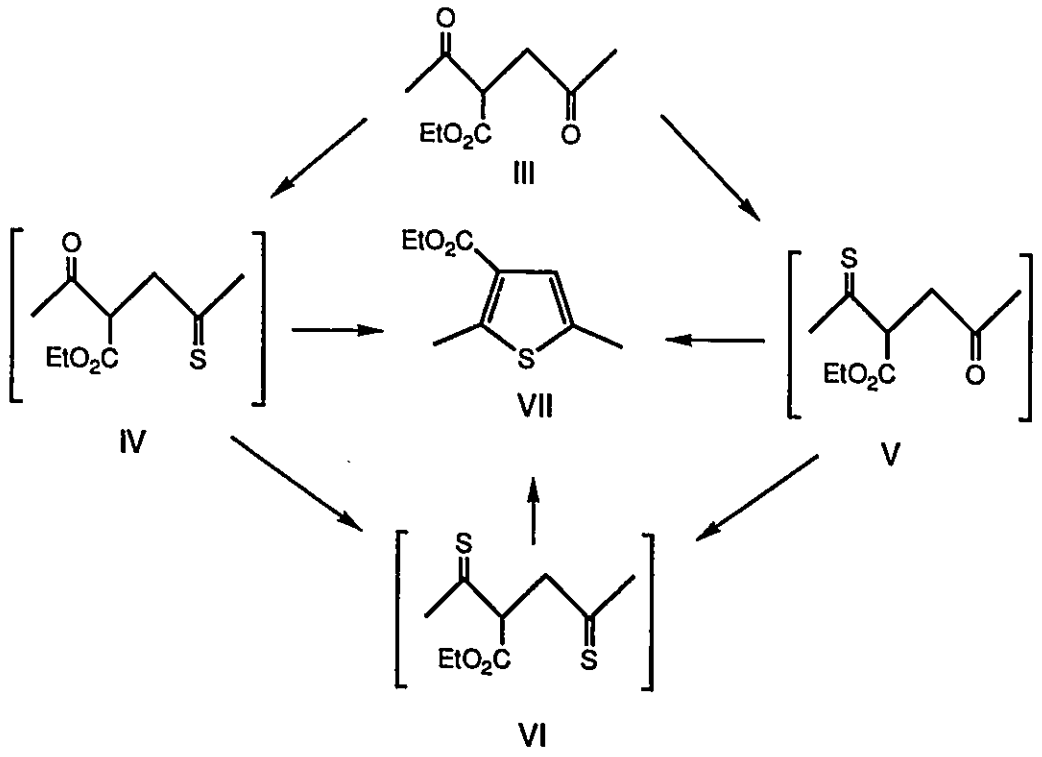

Scheme 1

The reaction conditions using hydrogen sulphide in acidic ethanol were found to be superior to the reaction of 1,4-diketones with thionation reagents such as phosphorus pentasulphide, which resulted in unpredictable yields of thiophenes and formation of non-thiophenoid and tarry products.

Given that the intermediates IV and V can form thiophenes either via VI or directly, it must be that 4-oxo-thioamides such as those prepared from nucleophilic reactions with α,β-unsaturated thioamide iron tricarbonyl complexes could be used in the synthesis of 2-aminothiophenes. Acid catalysed ring closure of 4-oxo-thioamides would probably lead to furan rather than thiophene products. On the other hand, reacting 4-oxo-thioamides with hydrogen sulphide in acidic ethanol has the potential of generating 2-aminothiophenes via dithioamides (Scheme 2).

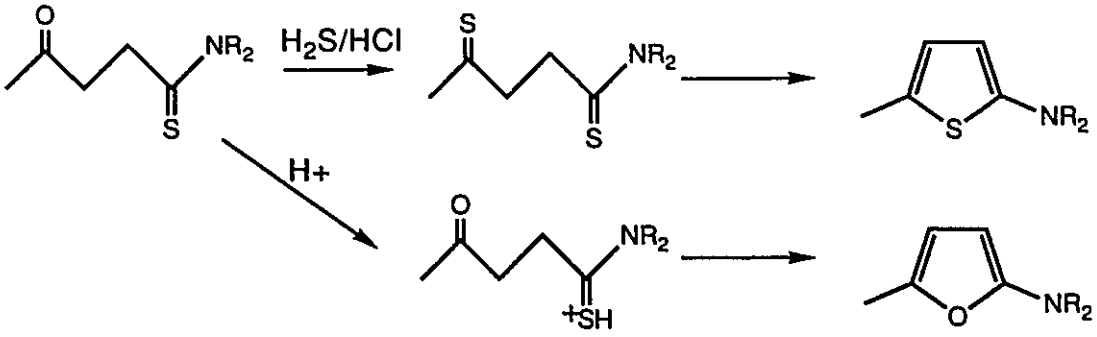

Scheme 2

Currently the Gewald synthesis provides a convenient synthetic pathway to substituted 2-aminothiophenes, specifically 2-amino-3-carbonyl substituted thiophenes which are important building blocks for the synthesis of fused thiophenes[68]. In this synthesis, α,β-unsaturated nitriles are heated to 60°C with sulphur in ethanol containing a base, usually a secondary amine, producing 3-substituted 2-amino thiophenes in 30-86% yield [4].

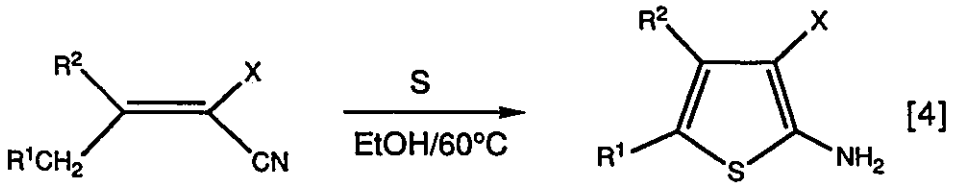

[4]

X= CN, CO_2R, $CONH_2$, COR, $PhNO_2$

VIII

A new synthetic approach to VIII could be a nucleophilic reaction with α,β-unsaturated thioamide IX producing 4-oxo-thioamide, X. Treatment of X with hydrogen sulphide in acidic ethanol could then lead to the thiophene product XI [5].

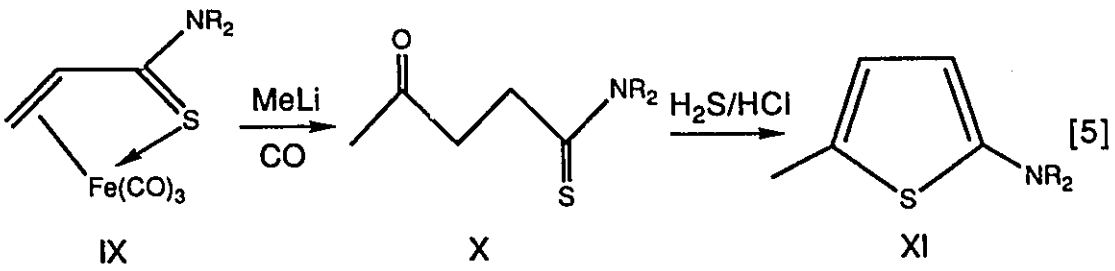

IX X XI

Modification of the nitrogen substituents in the starting material would be relatively simple and substituents in the 3-position of product XI could also be accomodated by the reaction [5]. Finally, changing the substituents at the position 4 of product XI would simply involve changing the nucleophile.

3.4.1.1 Preparation of 4-Oxo-Thioamides **18'-28'**

Temperature control was imperative and even brief warming of the solution resulted in the formation of 1,4-Michael addition products.

Steric hindrance appeared to limit the yield for the nucleophilic reactions. Only butene (thioamide iron complexes **4** and **7**) and propene (thioamide iron complexes **24** and **25**) thioamides gave CO-insertion products. The butene thioamides gave poor yields while thioamide iron complexes **1**, **2**, and **6** did not react at all. It seemed important to attempt to synthesize an α,β-unsaturated thioamide iron complex having only hydrogen substituents in the β and γ-positions. Preparation of the amide, shown below, from its acid chloride was straightforward but only one of the illustrated methods successfully produced the desired thioamide; however, its yield was very low.

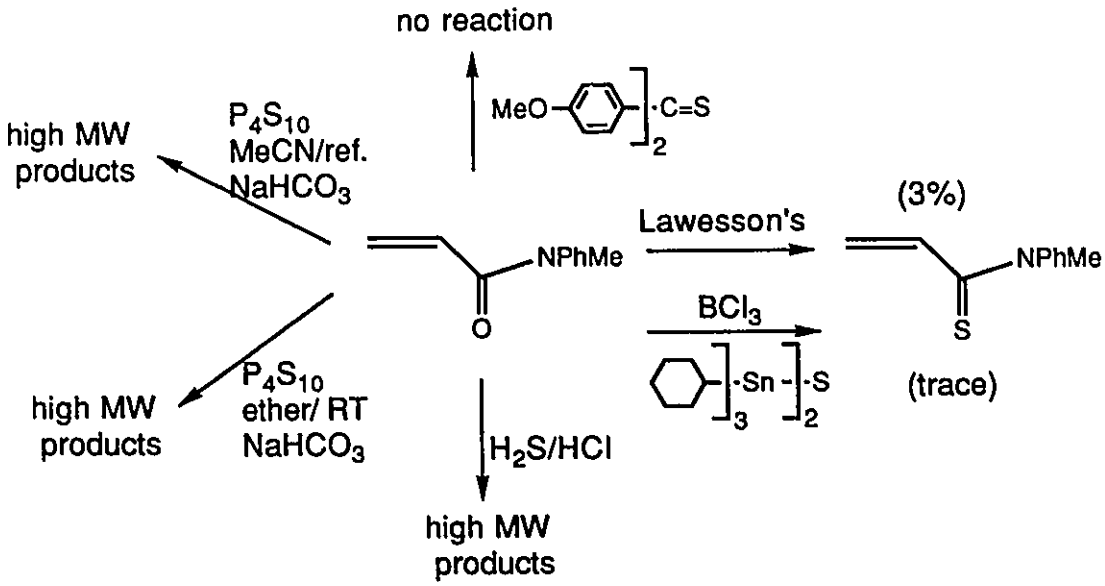

The thioamide product was used to prepare the α,β-unsaturated iron tricarbonyl complex but the yield from this reaction using photolysis was low. As a result of the lack of sufficient iron complex, an anion reaction could not be performed on a non-alkyl substituted α,β-unsaturated thioamide iron tricarbonyl complex.

The sterically hindered thioester iron complex **9** did not give a CO insertion product. A stable α,β-unsaturated thioester iron tricarbonyl complex having only hydrogen substitution in the γ-position could not be prepared. This difficulty encountered in the preparation of α,β-unsaturated thioester iron complexes was anticipated due to the overall instability of thioester iron complexes, especially γ-methyl substituted thioester iron complex **11**.

Attempts to promote addition of the nucleophile to the metal carbonyl in an effort to obtain 4-oxo-thioamide or thioester products from the more sterically hindered thioamide and thioester iron complexes proved unsuccessful. Approaches to promotion of the reaction included high CO pressure, the addition of anhydrous zinc chloride or aluminum trichloride, the addition of one equivalent of triphenylphosphine, solvent variations, and temperature variations.

An explanation for the temperature dependence of product formation

may lie in the energy of the transition states relative to the energy of the products. A proposed reaction profile for each of the nucleophilic reactions which would be consistent with the temperature dependence of the reactions is illustrated below.

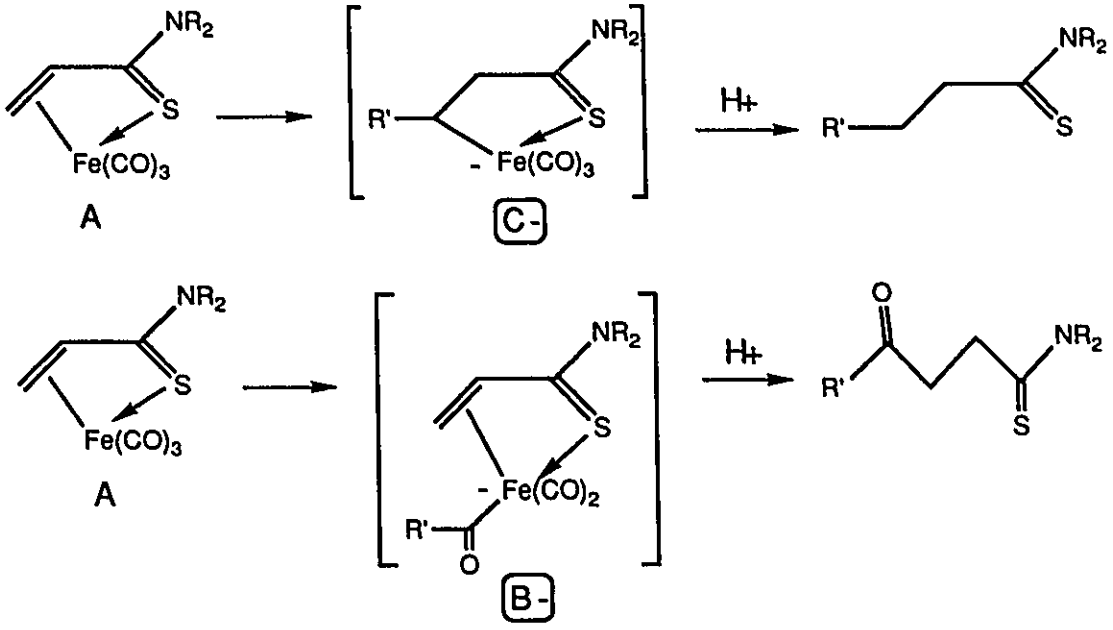

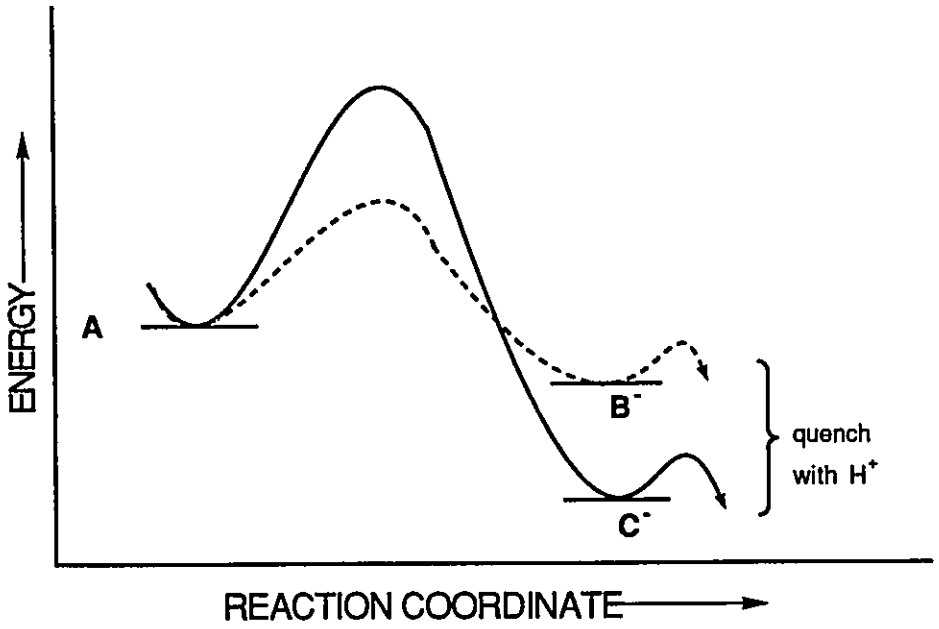

In the proposed diagram, the activation energy required to reach the lower energy anionic product [C-] is higher than that required to reach the higher energy anionic product [B-]. (The assumption is that quenching with a proton source is extremely rapid, trapping the ratio of anionic species.) At room temperature the formation of [B-] is reversible and both anions can be prepared but because anion [C-] is more stable than [B-], it dominates. At low temperature, only the transition state leading to [B-] can be surpassed and may not be reversible and only product [B-] is formed. An equilibrium between intermediate [B-] and starting material [A] was established by the fact that if the reaction was performed at low temperature and warmed to room temperature for a short period and then cooled again before quenching the reaction with a proton source, then only product from intermediate [C-] was obtained. The barriers for interconversion of [C-] and [A] are too high.

Of the nucleophiles that were used in an effort to obtain the 4-oxo-thioamide products only a few were successful. Those anions which gave the desired products were structurally parallel to the anions that Semmelhack used in his reactions with η^4-1,3-diene iron tricarbonyl complexes[11]. Other anions which did not react with α,β-unsaturated thioamide or thioester iron tricarbonyl complexes **1**, **4**, **7**, **8**, or **10** included those shown below.

a) 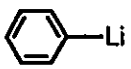

b) 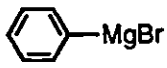

c) 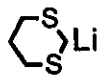

d) 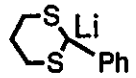

e) 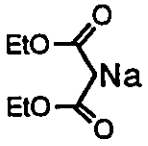

f) $LiCH_2CN$

g) HC CNa

It was surprising that no reactions were observed with compounds c and d since they were found to react with diene iron tricarbonyl complexes in high yields[11]. Likewise, phenyllithium and methyllithium were expected to react in light of the high yields of γ-ketoamides produced from the reaction of α,β-unsaturated amide iron tetracarbonyl compounds[19]. Diethylmalonate anion e was reported to react in a Michael fashion with an α,β-unsaturated palladium complex, discussed in the introduction[37], but the same results were not observed for α,β-unsaturated iron tricarbonyl complexes. The acetonitrile anion f did undergo reaction with iron complexes 4 and 7 but many unidentifiable products were obtained. The reaction with sodium acetylide and α,β-unsaturated iron complex 7 was attempted both in the presence and absence of 18-crown-6 which would coordinate to the sodium ion and enhance the reactivity, but there was no reaction in either case.

The difficulty associated with isolating compounds **18'** and **22'** in higher yield may be due to the acidity of the proton adjacent to the keto-group and subsequent decomposition.

3.4.1.2 Spectral Characterization of 4-Oxo-thioamides

3.4.1.2.1 Mass Spectra

The mass spectra of the 4-oxo-thioamides and 4-ketoamides gave parent ions, and ions corresponding to successive fragmentation of the added nucleophile and carbon monoxide. Also, fragments corresponding to $C(S)NR_2$ or $C(O)NR_2$ and NR_2 gave strong signals in the mass spectra. Some of the compounds, specifically **18'**, **22'**, and **27'**, could not be purified sufficiently to

obtain an electron impact mass spectrum. As well, products **23'** and **28'** were each a mixture of two compounds which could not be separated, so for these cases the masses were determined by GC/MS.

3.4.1.2.2 Infrared Spectra

The infrared spectrum for 4-oxo-thioamide product **20'** gave an intense carbonyl stretch at 1730 cm^{-1}. The 4-ketoamide product **21'**, analogous to compound **20'**, also gave an intense signal at 1730 cm^{-1} corresponding to the ketone carbonyl while its amide carbonyl stretch was found at 1650 cm^{-1}. All of the other 4-oxo-thioamide and 4-ketoamide products had similar IR spectra with the exception of products **19'** and **23'** which had ketone carbonyl stretching frequencies at approximately 1690 cm^{-1} and ester carbonyl stretching frequencies at approximately 1730 cm^{-1}.

3.4.1.2.3 NMR Spectra

The ^1H NMR spectra for the saturated 4-ketoamide products **18'**, **20'**, **21'**, **22'**, **23'**, and **24'** all showed chemically and magnetically inequivalent protons between the ketone (thic)amide positions. A portion of the ^1H NMR spectra of 4-ketoamides products **21'** and **24'** are shown in figure 12, illustrating this inequivalence. In the spectrum for 4-ketoamide **21'**, the methylene protons occurred as separate sets of signals having doublet of doublet patterns at δ 2.55 ppm (A) and δ 3.42 ppm (C). There was a large geminal coupling of 18.6Hz. The methylene protons for 4-ketoamide **24'** also occurred as separate sets of signals having doublet of doublet patterns at δ 2.08 ppm (A) and δ 2.65 ppm (C), but their geminal coupling was smaller (16.6Hz).

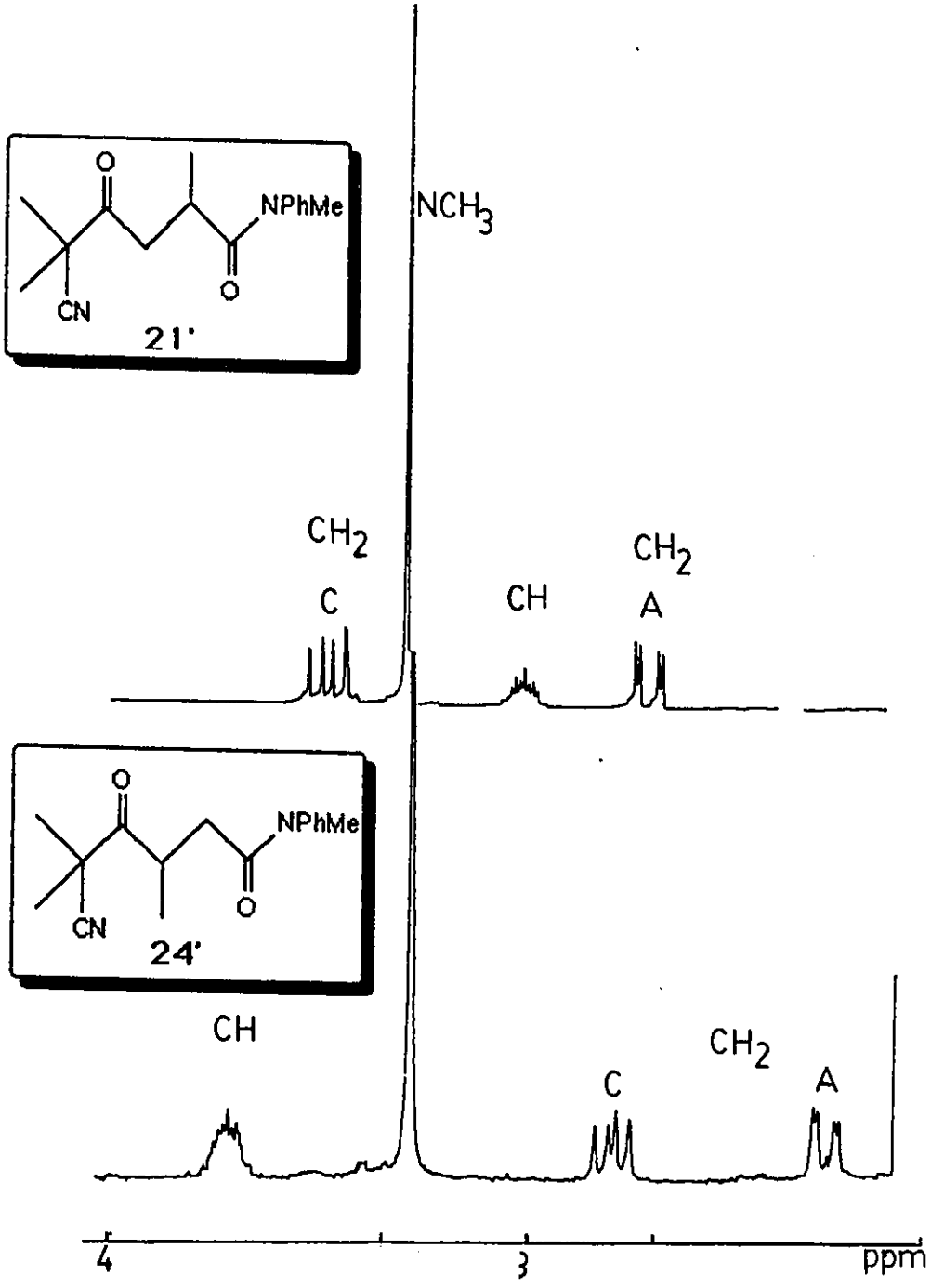

Figure 3.12: ^{1}H NMR Spectra for Compounds **21'** and **24'**

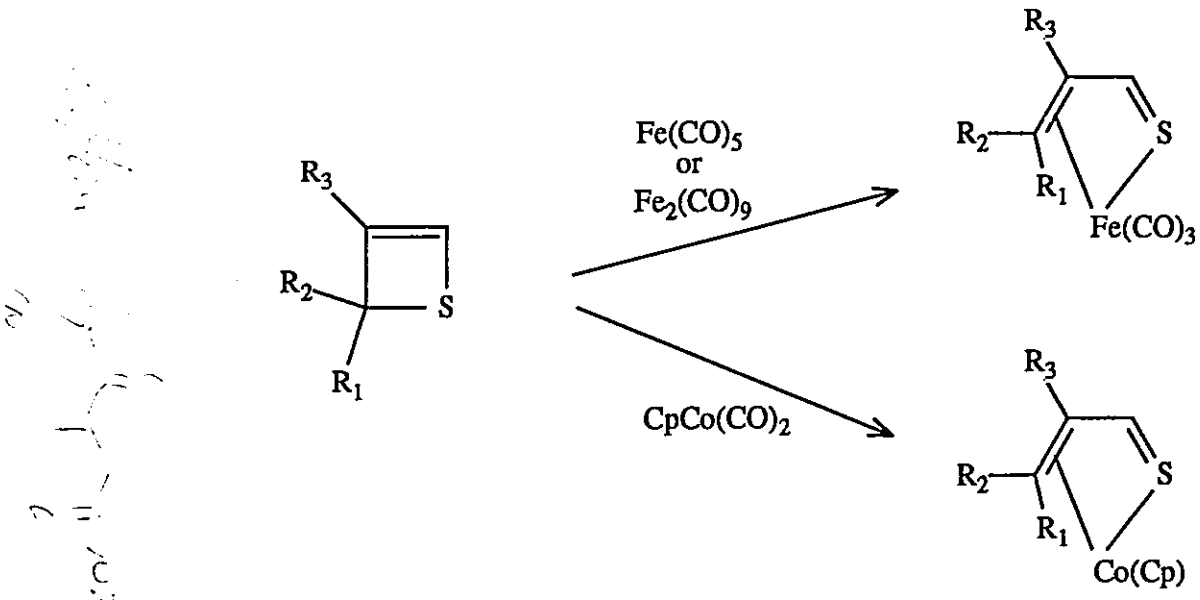
R3
R2
S
R1
Fe(CO)5
or
Fe2(CO)9
CpCo(CO)2
R3
R2
S
R1
Fe(CO)3
R3
R2
S
R1
Co(Cp)

In each spectrum the methine proton gave a broad poorly defined signal which could not be resolved by lowering the temperature to -60°C. Selective decoupling of each of the signals allowed for their assignment.

The coupling between the methylene proton corresponding to the signal at δ 3.42 ppm (C) and the methine carbon proton (B) is 10.5Hz while the coupling of the methylene proton corresponding to the signal at δ 2.55 ppm (A) and the methine proton is 3.5Hz. This leads to a structure in which the larger coupling must be due to a trans orientation of protons C and B, as shown by the Newman projection illustrated for structure **21'**. Likewise a Newman projection can be drawn for 4-ketoamide product **24'**.

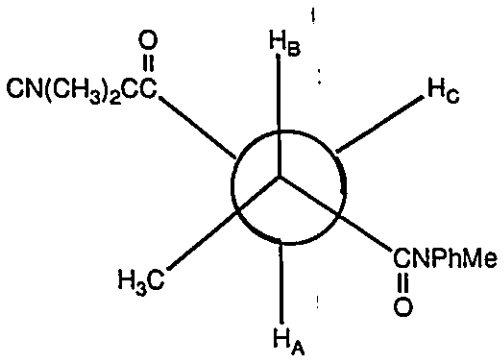

21'

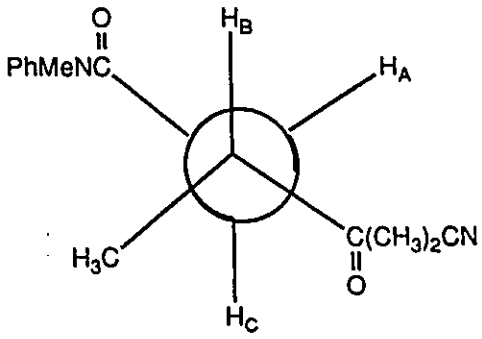

24'

The olefinic proton for the unsaturated 4-oxo-thioamide **19'** gave a broad peak in the ^{1}H NMR spectrum at δ 5.91 ppm, the usual region for olefinic protons.

3.5 Electrophilic Addition

The literature of transition metal complexes of α,β-unsaturated

heteroatoms suggests that electrophilic reaction at the heteroatom is facile and that such a reaction might occur with α,β-unsaturated thioamide and thioester iron tricarbonyl complexes. Thioamide iron complexes were found not to react with electrophiles and only one thioester iron complex gave products of electrophilic attack at the sulphur. The preparation and characterization of these new thioester iron complexes are discussed.

3.5.1 Preparation and Characterization of Complexes from Electrophilic Attack

3.5.1.1 Attempted Preparation of a Hg-complex

The addition of excess or stoichiometric amounts of $HgCl_2$ resulted in the complete decomposition of thioester iron complex **10** resulting in isolated free ligand having C=S converted to C=O. A black insoluble precipitate was also obtained, suggesting the formation of Hg_2S. It is possible that a mercuric halide or an adduct analogous to cobalt complex XXIX in Scheme 7 (Chapter 1) could have been an intermediate.

In contrast, excess mercuric acetate gave a pale orange solid which was found to be slightly soluble in DMSO and very soluble in hot ethanol. The presence of mercuric acetate, which must be used in excess, made purification of the orange product impossible. Repeated recrystallization from hot ethanol could not successfully remove the uncomplexed [$Hg(OAc)_2$]. The fact that this product was completely insoluble in hydrocarbon or chlorinated solvents eliminated the possibility that unreacted complex was adsorbed to crystals of the mercuric salt,

giving the orange colour. An ^{1}H NMR spectrum in DMSO-d_6 comfirmed the presence of protons corresponding to thioester iron complex **10**, but some excess mercuric salt made complete characterization impossible. It seemed likely from the appearance of the solid that a mercuric acetate adduct was generated, analogous to cobalt complex XXIX in Scheme 7 (Chapter 1).

3.5.1.2 Preparation of S-Alkyl Iron Complex, 21

The addition of ether to a solution of thioester iron complex **10** and a stoichiometric amount of $[(CH_3)_3OBF_4]$ in CH_2Cl_2 gave a yellow precipitate of S-methylated iron complex **21** in good yield. The complex was characterized by IR, and ^{1}H, and ^{13}C NMR.

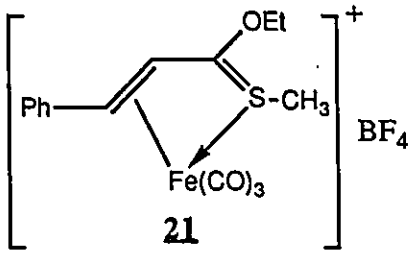

21

3.5.1.2.1 Spectral Characterization of Iron Complex 21

3.5.1.2.1.1 Infrared

Iron complex **21** was soluble only in more polar organic solvents such as acetone and acetonitrile. The infrared spectrum was obtained in acetonitrile and gave two metal carbonyl stretching bands at 2100(s) and 2045(vs) cm^{-1}, which are shifted to higher energy in comparison to the starting material (**10**).

Such a shift was anticipated with the formation of a cationic complex which should decrease the degree of $d\pi$-$p\pi^*$ backbonding, which in turn strengthens the CO bond and requires higher energy to induce CO vibrations.

3.5.1.2.1.2 NMR Spectra

The ^1H NMR spectrum of iron complex **21** is shown in figure 13. The spectrum closely resembles that of the starting material. The protons of of the methyl group at sulphur of complex **21** occur as a singlet at δ2.04 ppm. This is in a region similar to that of the resonances of the S-CH_3 group found at δ2.04 ppm for the cobalt complex XXIX, Scheme 7 (Chapter 1). The protons of non-metal complexed sulphonium salts should resonate in the range δ2.52-3.02 ppm[46]. Methylation of the iron centre is ruled out by the coordinatively saturated nature of the complex in which such a reaction would require displacement of a ligand, either CO or the thioester. Although dissociation and reassociation cannot be ruled-out, there is no evidence for loss of a CO based on the IR spectrum. Furthermore, the possibility of olefin dissociation is eliminated by the ^1H NMR spectrum in which the observed chemical shifts of the β and γ-CH protons have upfield shifts, representative of complexation. Finally, loss of iron-sulphur bonding would be evident in the ^{13}C NMR spectrum, where a non-metal coordinated C=S carbon chemical shift would be more downfield. All of this supports the structure which has S-alkylation, not metal centre alkylation.

In the ^{13}C NMR spectrum, S-CH_3 protons were assigned to the signal at δ18.49 ppm, slightly downfield from OCH_2CH_3 methyl carbon, which is in the usual region for S-CH_3 protons, δ10-20 ppm[69]. The rest of the spectrum was readily assigned using DEPT.

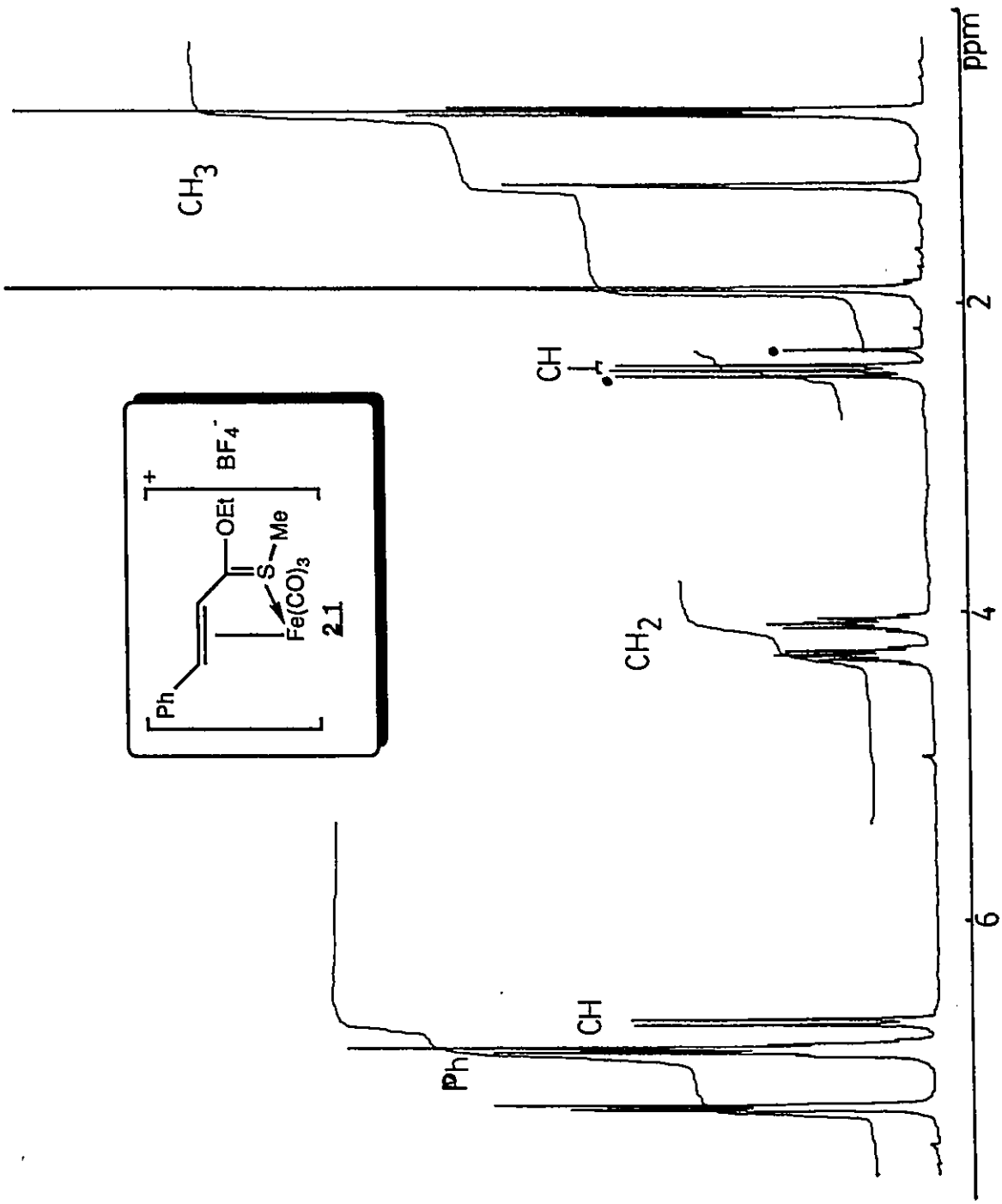

Figure 3.13: ^{1}H NMR Spectrum of Complex **21**

It is possible that the new iron complex **21** is actually oxygen alkylated as opposed to sulphur alkylated, as shown below.

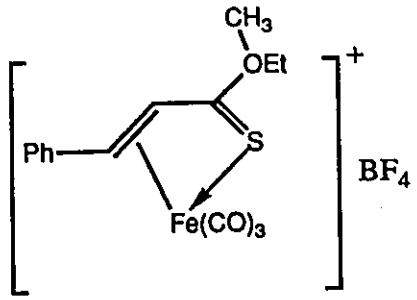

This structure is not favoured over the sulphur alkylated product because of the NMR spectra. An oxygen-methylated product would not be expected to have what appears to be two different isomers based on the γ-proton signal in the ^{1}H NMR spectrum, which has been discussed. Futhermore, since the protons of the S^+-CH_3 group in simple sulphonium salts absorb in the range δ 2.52-3.02 ppm, it is reasonable to assume sulphur alkylation. The S-methyl resonance in the ^{1}H NMR spectrum, δ 2.04 ppm, was lower than the range but S-methylated thioacrolein clclopentadienyl cobalt complex has also been reported with its methyl resonance, δ 2.40 ppm, slightly below the range[32]. The greater electronegativity of oxygen would be expected to have an O^+-CH_3 group resonate further downfield from the δ 2.52-3.02 ppm range. As well, the chemical shift for the methyl carbon in the ^{13}C NMR spectrum was further downfield 18.49 ppm, than what would be expected for an oxygen methyl carbon. A normal S-CH_3 carbon usually resonates in the range 10-20 ppm while a O-CH_3 carbon resonance would be found further upfield than the usual range, 48-60 ppm. A large shift of 30 ppm which would be required in the case of oxygen alkylated product seems unreasonable here.

On the other hand, since none of the thioamide iron complexes reacted with electrophiles, an oxygen alkylated product cannot be entirely ruled

out. The presence of the oxygen in thioester iron complex **10** is the single key feature distinguishing it from the thioamide iron complexes.

3.6 ZINDO Calculations

Theoretical calculations were performed on a few model iron complexes and their free ligands in order to predict the reactivity of the three types of iron thio-complexes; thioamides, thioesters, and thiones, and in particular to predict the site of their reactions with nucleophiles and electrophiles. Furthermore, it was hoped that the results would provide some insight into explaining the experimentally observed preference of electrophilic addition to thioester iron complexes.

All nucleophilic and electrophilic substitution reactions involve donor-acceptor interactions in which the transition state involves a formal transfer of electrons from one of the reactants to the other. The total change in energy due to the partial formation of a bond between an atom *d* of some electron acceptor molecule *D* and an atom *a* of some electron acceptor molecule *A* is given by the expression for ΔE_{total} shown below[59].

$$\Delta E_{total} = \underbrace{\frac{-q_d q_a}{R_{da}\varepsilon}}_{\text{electrostatic}} + \underbrace{2 \sum_{\substack{\text{occupied} \\ \text{orbitals in} \\ \text{donor}}} \sum_{\substack{\text{unoccupied} \\ \text{orbitals in} \\ \text{acceptor}}} \left\{ \frac{\left(C_d^m C_a^n \, \Delta\beta_{da}\right)^2}{E_m^* - E_n^*} \right\}}_{\text{covalent}}$$

The expression is essentially the sum of electrostatic and covalent terms. The electrostatic term is the product of the formal charges of the atoms *d* and *a* of the isolated molecules, represented by q_d and q_a, divided by the product of the distance the two atoms during their interaction multiplied by the dielectric constant of the solvent. The covalent term of the donor molecule D,

C^m_d, is composed of the coefficients of the atomic orbitals of each atom *d* in the various molecular orbitals *m*, and C^n_a is described similarly for the acceptor molecule A. $\Delta\beta_{ad}$ is the change in the resonance integral between interacting orbitals at a distance R_{ad}, and E_m^* and E_n^* are the energies of the various molecular orbitals *m* and *n* in the isolated molecules. If the energy difference between the two interacting orbitals is large (ie. $E_m^* - E_n^*$ is large) then the covalent term in the expression for ΔE total will become small and the interaction will be dominated by the electrostatic term. This will favour strong interactions between the two atoms having the highest positive charge density and the highest negative charge density, q_a and q_d respectively. This situation has been referred to as a charge-controlled reaction. If, on the other hand, the energy difference between the two interacting molecules is small (ie. $E_m^* - E_n^*$ is small) the covalent term becomes dominant and the reaction is controlled by orbital interactions. This situation has been referred to as an orbital-controlled reaction. The orbital-controlled reaction will proceed in such a way that the product that is formed by interactions between the two orbitals in A and D having the highest orbital coefficients, which are the LUMO (lowest unoccupied molecular orbital) in the acceptor, and the HOMO (highest occupied molecular orbital) of the donor molecule.

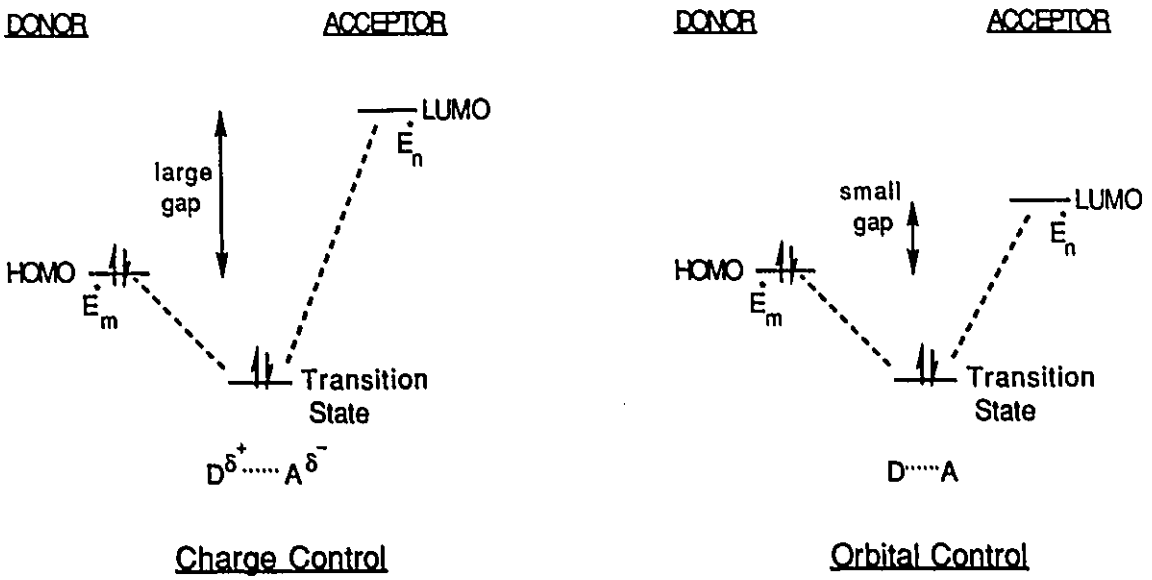

In a charge-controlled reaction the acceptor would have a LUMO of high energy, characteristic of a molecule having a low affinity for electrons, or of a highly solvated molecule having a large ionic radius. The HOMO of the donor would have a low energy, characteristic of high electronegativity or of a molecule of small ionic radius. In an orbital-controlled reaction the acceptor has a LUMO of relatively low energy and the donor has a HOMO of relatively high energy, resulting in good orbital overlap.

If the reaction between an α,β-unsaturated thio-iron complex and an electrophile or a nucleophile is charge-controlled then the pattern of reactivity would be expected to be predictable on the basis of the calculated charges at each atom of the complex. Conversely, if the reaction is orbital-controlled then the site of reaction would be predicted by the orbital coefficients of each of the atoms of the complex in either the HOMO (for reaction with an electrophile) or the LUMO (for reaction with a nucleophile) of the complex.

In order to determine the orbital and charge coefficients for some α,β-unsaturated thio-iron complexes, ZINDO calculations were performed. The

ZINDO program is a LCAO -SCF (linear combination of atomic orbitals- self--consistent field) method in which differential overlap is neglected[84]. (The acronym NDO stands for neglect of differential overlap.) This program is designed to accomodate the large basis sets required for calculations on transition metal complexes. ZINDO calculations of the charge density on each of the atoms should predict the site of reaction for charge-controlled reactions, which, when compared to the observed chemical results, would be expected to be a valuable tool for explaining and predicting reactivity patterns in other α,β-unsaturated thio-iron complexes, including those which were not easily prepared (thioesters and thiones).

The input data for the ZINDO calculations consisted of bond length and bond angle information derived from the X-ray crystal structures of iron complexes **1** and **2** and free ligand **2'**. Some bond lengths were calculated using Van der Waals radii. As well, input of dihedral angles was required; these angles were obtained from models of the complexes. The compounds for which ZINDO calculations were performed are illustrated in Table 6 which is a collection of the formal charges at selected atoms and Table 7 which is a collection of the orbital coefficients at selected atoms.

Three of the four calculated thioamide complexes were synthesized (**1**,**4**,**7**); the fourth complex was subjected to calculations for the purpose of comparison. A comparison between α,β-unsaturated thioamide-iron complexes **1** and **4** should demonstrate the effect of phenyl substitution relative to methyl substitution at the γ-position.

FORMAL CHARGE

	Fe	C=O	S(O)	β-C	γ-C	N(O)	α-C
			Complex (Free Ligand)				
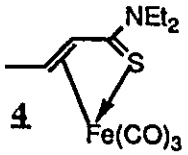 **4**	-0.181 (0.201)	-0.215 -0.089 -0.210	1.528 (-0.647)	-0.181 (0.201)	0.052 (-0.157)	-0.416	0.027 (0.254)
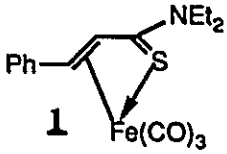 **1**	-0.494	0.384 -0.771 -0.270	1.188 (-0.585)	0.262 (-0.311)	-0.419 (-0.479)	-0.271 (-0.268)	-0.825 (-0.157)
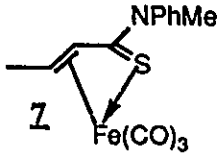 **7**	-0.297	-0.097 -0.115 -0.064	1.132 (-0.636)	0.055 (0.203)	0.112 (-0.489)	-0.425 (-0.100)	-0.071 (0.247)
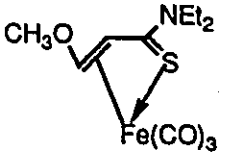	1.077	-0.198 -0.315 -1.000	1.332 (-0.584)	-0.881 (-0.270)	0.112 (-0.489)	-0.425 (-0.100)	-0.311 (-0.14)
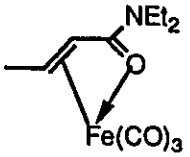	0.709	-0.073 -0.041 0.344	-0.470 (-0.748)	-0.380 (0.009)	-0.202 (-0.175)	-0.377 (-0.301)	1.00 (0.518)
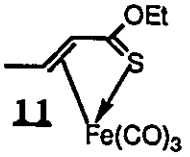 **11**	1.348	-0.093 -0.116 -0.023	1.348 (-0.550)	-0.141 (0.202)	-0.176 (-0.175)	-0.422 (-0.353)	-0.057 (0.339)
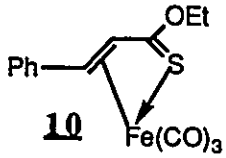 **10**	1.254	-0.059 -0.042 -0.190	0.335 (-0.479)	-0.181 (-0.282)	-0.298 (-0.442)	-0.418 (-0.360)	-0.317 (-0.104)
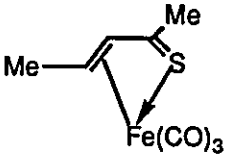	2.275	-0.972 -0.126 -0.017	-0.185 (-0.519)	-0.458 (0.132)	-0.234 (-0.084)	carbon 0.342	-0.312 (-0.025)

Table 6

A comparison between **4** and **7** should illustrate any variation in charge densities or orbital coefficients arising from the choice of different substituents on

nitrogen. A comparison between 4 and the methoxy substituted complex should allow for a prediction of the effect of methoxy substitution at the γ–position.

ORBITAL COEFFICIENTS

Complex [H=HOMO; L=LUMO]
(Free Ligand)

	Fe	C=O LUMO	S(O)	β-C	γ-C	N(O)	α-C
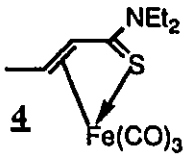 4	H .11 L .013	.025 .0080 .080	H .0069 (.90) L .48 (.055)	H .17 (.0039) L .042 (.076)	H .40 (.018) L .0086 (.40)	H .034 (.0056) L .0042 (.073)	H .0638 (.0045) L .2222 (.196)
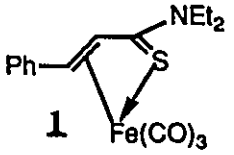 1	H .081 L .074	.15 .019 .036	H .0020 (.058) L .215 (.070)	H .031 (.014) L .075 (.14)	H .012 (.00080) L .11 (.00070)	H .069 (.00060) L .038 (.079)	H .0026 (.038) L .081 (.23)
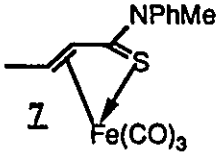 7	H .097 L .083	.15 .019 .036	H .0017 (.91) L .037 (.066)	H .00090 (.0028) L .31 (.048)	H .031 (.018) L .29 (.37)	H .099 (.0064) L .0063 (.046)	H .15 (.0048) L .056 (.22)
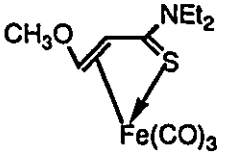	H .11 L .044	.053 .014 .10	H .11 (.29) L .30 (.10)	H .16 (.49) L .087 (.00030)	H .33 (.14) L .053 (.31)	H .015 (.00020) L .033 (.13)	H .10 (.041) L .24 (.43)
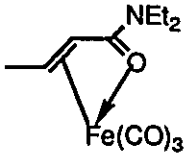	H .20 L .13	.08 .16 .16	H .0021 (.086) L .029 (.066)	H .061 (.51) L .011 (.16)	H .41 (.14) L .012 (.43)	H .0017 (.063) L .063 (.035)	H .0067 (.041) L .19 (.11)
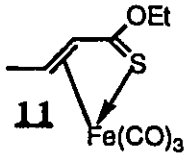 11	H .33 L .11	.014 .021 .023	H .056 (.91) L .017 (.079)	H .045 (.0080) L .20 (.039)	H .084 (.019) L .15 (.39)	H .027 (.0072) L .025 (.035)	H .23 (.11) L .13 (.25)
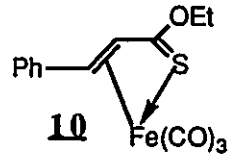 10	H .16 L .014	.040 .012 .0095	H .29 (.048) L .0028 (.090)	H .0080 (.57) L .10 (.016)	H .011 (.24) L .032 (.20)	H .0039 (.022) L .0010 (.032)	H .042 (.030) L .0010 (.25)
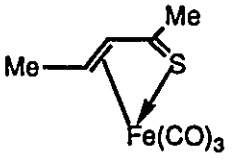	H .19 L .13	.045 .10 .054	H .067 (.40) L .054 (.22)	H .077 (.12) L .032 (.012)	H .17 (.18) L .17 (.31)	carbon H .033 (.030) L .010 (.031)	H .092 (.096) L .092 (.25)

Table 7

Only two of the three prepared α,β-unsaturated thioester-iron complexes were subjected to ZINDO calculations. These two complexes, **10** and **11**, were selected because they differed in their substitution at the γ-position, **10** having a phenyl group and **11** having a methyl group. A comparison would also be possible between the effect of changing the γ–substituent from phenyl to methyl in thioester complexes relative to the same change in thioamide complexes, which may provide insight into the role of the amide or ester group in the stability and reactivity of the complexes. Calculations were also performed on a hypothetical thione complex, which was selected as a model for the prepared complex **13**, whose input data was too complex.

Calculations were also performed on an α,β-unsaturated amide iron tricarbonyl complex in order to investigate the differences between sulphur and oxygen in these complexes.

A nucleophile is capable of attacking the metal centre itself or one of the ligands. A coordinatively saturated metal which is either neutral or negatively charged, as in the case of α,β-unsaturated thio-iron tricarbonyl complexes, does not favour nucleophilic attack at the metal centre. Nucleophilic attack at a ligand of a coordinatively saturated complex usually requires that π-acceptor spectator ligands such as carbon monoxide and olefins accomodate the increase in charge at the metal centre. Therefore, in a charge-controlled reaction, a nucleophile would be expected to react at an atom on the ligand bearing a positive charge density.

If one considers charge-controlled nucleophilic attack at the ligands of the α,β-unsaturated thioamide-iron complexes listed in Table 6, attack would be expected at sulphur, which bears a postive charge for all cases. Attack of a nucleophile at nitrogen would not be expected, however, since nitrogen was

found to have a negative charge in all of the thioamide complexes. In all of the α,β-unsaturated thioamide-iron complexes at least one of the olefinic carbons also bears positive charge. Except for the γ-phenyl substituted complex 1, this positive charge was calculated to reside on the γ-carbon, predicting nucleophilic attack at the γ-position in a charge-controlled reaction.

In the α,β-unsaturated thioester-iron complexes, a positive charge was calculated for sulphur and a negative one for the ethoxy oxygen atom, paralleling the charge distributions calculated for the thioamide complexes, but no significant positive charges were calculated for any of the olefinic carbons. Thus, for α,β-unsaturated thioester-iron complexes reaction of a nucleophile in a charge-controlled process would be expected to occur only at sulphur, and no attack would be expected at any of the olefinic carbons. Calculations of charge distributions show that α,β-unsaturated thione-iron complexes should react with a nucleophile only at the α-methyl position and that α,β-unsaturated ketone-iron complexes should react only at one of the carbon monoxide ligands in a charge-controlled reaction.

In summary, ZINDO calculations of charge distributions would predict that charge-controlled reactions of nucleophiles with α,β-unsaturated thio-iron complexes should occur preferentially at the ligand and specifically at the sulphur or γ-carbon of thioamide complexes, at the sulphur in thioester complexes, and at the α-methyl position of the thione complex.

Nucleophiles are known to attack α,β-unsaturated thioamides **1'** and **4'** at the γ-carbon, giving Michael-type products[65,85,86,87]. The ZINDO calculations of charge distribution on these free ligands predict charge-controlled nucleophilic attack at the α-carbon of ligands corresponding to complexes 1, 4, 7, 10, 11, and ketoamide complex. This discrepancy between established chemical behaviour and the predictions indicates that predictions based on a

charge-controlled reaction mechanism are unsuitable for these reactions, and that a re-evaluation of the ZINDO results in the context of orbital-control in nucleophilic attack is warranted.

An electrophile is more likely than a nucleophile to attack an electron-rich metal centre, even for coordinatively unsaturated metals. If, however, the metal centre is sterically hindered and the ligands contain heteroatoms bearing lone electron pairs, electrophilic attack would be expected at the ligand heteroatom. Charge distribution calculations predict reaction with electrophiles at those sites bearing negative charge: the nitrogen in α,β-unsaturated thioamide complexes, the sulphur atom of the thione, the ethoxy oxygen atom of α,β-unsaturated thioester complexes, and the carbon monoxide oxygen atom in all complexes. Also, a thioacrolein iron tricarbonyl complex, which is only different from the thione complex for which charges were calculated by the absence of methyl substitution at the α-position, is known to react with electrophiles at sulphur. In summary, electrophilic attack at the ligands of α,β-unsaturated thio-iron complexes is predicted by ZINDO calculations for a charge-controlled reaction to occur at the nitrogen in α,β-unsaturated thioamide complexes, the sulphur atom of the thione, the ethoxy oxygen atom of α,β-unsaturated thioester complexes, and the carbon monoxide oxygen atom in all complexes.

To this point only reactivity patterns on the basis of purely charge-controlled reactions have been considered. The assumption has therefore been made that there is a large energy difference between the the HOMO of the donor molecule and the LUMO of the acceptor molecule in both electrophilic and nucleophilic attack. This assumption may not be justified, since the energy of the LUMO of the electrophile or the HOMO of the nucleophile may not be very different from the HOMO or the LUMO of the α,β-unsaturated thio-iron

complexes, respectively. If the energy difference between the two reacting molecules is small then reaction may be controlled by orbital interactions rather than by charge distributions, and therefore orbital coefficients would be expected to provide predictive information about the site of reaction.

The orbital coefficients of the LUMOs and HOMOs are listed in Table 7 for the same selection of molecules for which charge denstities were calculated. The highest orbital coefficient for a LUMO of the complex would predict the site of nucleophilic attack, and the highest orbital coefficient for a HOMO would predict the site of electrophilic attack in a purely orbital-controlled reaction.

For nucleophilic attack, the predicted site for reaction for all of the thioamide-iron complexes was at sulphur, except for complex 7, which differed from all of the others by virtue of its substituents at nitrogen. All complexes were diethyl thioamides, except 7, which was a phenyl methyl thioamide. In complex 7 the orbital coefficients predict reaction at the β-olefinic carbons. Like complex 7, the thioester complexes 10 and 11 had the highest LUMO coefficients at the β-carbon, predicting reaction predominantly at that site. The thione complex is expected to react with nucleophiles at the γ-carbon in an orbital-controlled reaction.

In summary, an orbital-controlled nucleophilic attack on α,β-unsaturated thio-iron complexes would be predicted, on the basis of ZINDO calculations of orbital coefficients in the LUMO, to react at the sulphur of thioamide complexes and at one of the olefinic carbon atoms in thioester and thione complexes. In contrast, the free ligands corresponding to thioamide complexes 1, 7, and γ-methoxy thioamide, and thioester complex 10 would be expected to undergo nucleophilic addition at the α-carbon. On the other hand, preferred γ-carbon nucleophilic attack for the free ligands of thioamide complex 4, thioester complex 11, and the thione complex based on ZINDO calculations

are in agreement with the known reactivity of α,β-unsaturated thioamides, in which nucleophilic attack occurs at the γ-position.

For orbital-controlled electrophilic attack, the orbital coefficients for the HOMO determined by the ZINDO method suggest that reaction should occur at the metal in thioamide complex **1**, thioester complex **11**, and the thione complex. Also, reaction should occur at the γ-olefinic carbon in thioamide complex **4**, the ketoamide complex and the γ-methoxy complex; α-carbon in complex **7**, and at sulphur in thioester complex **10**. In all of the free ligands, electrophilic attack is predicted at sulphur, except for the free ligand of thioester complex **10** and the free ligand of the amide complex, where attack is predicted to occur at the β-carbon.

Based on the results of ZINDO calculations the sites for nucleophilic attack can be predicted, although care must be taken in the appropriate selection of either the charge-controlled or the orbital-controlled mechanism. The relative contributions of orbital and charge control to the course of the reaction is dependent not only on the nature of the ligand (either free or bound to iron) but also on the nature of the electrophile or nucleophile. A "harder" nucleophile, having a HOMO of even lower energy relative to the substrate, would be expected to have poorer orbital overlap in the transition state, and therefore a charge-controlled reaction may occur. Similarly, a "softer" electrophile, having a LUMO of lower energy, might be expected to result in orbital-controlled reactions with these α,β-unsaturated thio-iron complexes. Naturally, situations may arise where the relative energy of the frontier orbitals of the reacting species is at an intermediate stage where neither charge nor orbital control dominates.

3.6.1 ZINDO Calculations vs. Experimental Results

The ZINDO calculations were used to predict the reactivity of α,β–unsaturated thioamide, thioester, and thione iron tricarbonyl complexes towards electrophilic and nucleophilic addition . This section will address the success of these calculations in predicting reactivity in comparison to the chemical results.

Nucleophilic reactions at room temperature with α,β-unsaturated thioamide iron tricarbonyl complexes **1** and **4** resulted in direct addition at the γ-carbon of the thioamide ligand, but both charge and orbital controlled reactions predicted nucleophilic addition to the sulphur. (The calculations predict that thioester iron complex **10** should give sulphur substitution products in a charge-controlled reaction and β-carbon substitution of the thioester ligand in an orbital-controlled reaction. At room temperature it reacted at the γ-carbon of the ligand.) The inability to correlate the calculated and experimental results means that the difference in energy levels of the donor and acceptor molecules are not sufficiently large or small enough to completely exclude either the electrostatic or covalent expressions from the complete equation for the ΔE_{total}. As well it should be considered that the complex may be perturbed as the nucleophile approaches so that the orbitals and charge of the complex may be quite different just prior to nucleophilic addition.

Electrophiles were found to react only with thioester iron complex **10** and did so to produce sulphur substituted products while thioamide iron complexes did not react with the electrophiles leading to the formation of such products. A charge-controlled electrophilic addition reaction would have given nitrogen substituted products for the thioamide complexes and oxygen substituted products for the thioester complexes. The electrophilic addition

reaction with α,β-unsaturated thio-iron complexes appears to be an orbital-controlled reaction since it correctly predicts sulphur substitution only for thioester iron complex **10** and either iron, nitrogen, or γ-carbon substitution for thioamide iron complexes. While it cannot be firmly established that the new alkylated product **21** is sulphur rather than oxygen substituted, the spectroscopic evidence for the complex supports sulphur substitution. Furthermore, the prediction of nitrogen substitution products from the reaction of electrophiles with thioamide iron complexes should have been observed if in fact the products from these electrophilic reactions are entirely charge-controlled. Either way, the ZINDO calculations were successful in predicting a site for reactivity; oxygen in a charge-controlled reaction and sulphur in an orbital-controlled reaction.

The computational results could not be used with confidence for predicting nucleophilic addition products but an orbital-controlled electrophilic addition correlated the chemical observations which allows for a prediction of the site of substitution for complexes on which reactions and calculations were not attempted including thione iron complex **13** and thioester iron complex **11**. If it is assumed that the orbitals and energy levels for thione complex **13** are not significantly different from those of the thione complex used in the calculation, then direct addition to the metal centre would be the initial site for electrophilic attack and likewise for thioester complex **11**.

Finally, it can be said that based on the calculations and the experimental observations that a general trend in reactivity for all of the thio-iron complexes cannot be established, particularily for electrophilic and nucleophilic addition reactions.

In conclusion, the ZINDO calculations were highly successful in predicting the site of reactivity for electrophilic reactions based on an orbital-control model. On the other hand, there seem to be too many

assumptions to allow for a successful prediction for the nucleophilic addition site of these α,β-unsaturated thio-iron complexes with the nucleophiles that were used experimentally. The good correlation between calculated and experimental results for electrophilic reactions suggests that the nucleophilic reactions could have been equally successfully correllated if the nucleophiles had been chosen so that their energy levels were such that the reactions would be either purely charge or orbital controlled.

3.7 Alkyne Addition

Alkynes are known to react with rhodium, cobalt, and iron carbonyl complexes generating alkyne carbon monoxide coupled cyclopentadienone complexes[70,71,72]. When reacted with manganese and iron complexes containing both carbonyl and thio-ligands, the alkynes usually react with the thio-ligand[73,74,76]. Therefore it was anticipated that α,β-unsaturated thioamide and thioester iron tricarbonyl complexes would react with the C=S fragment of the thio-ligand, but instead alkynes were found to react with these complexes producing iron complexes derived from coupling of the alkyne, carbon monoxide and the coordinated olefin.

3.7.1 The Preparation and Characterization of Iron Complexes **22-26**

3.7.1.1 The Preparation of Iron Complexes **22-26**

α,β-Unsaturated thioamide iron tricarbonyl complexes **1**, **4**, and **7** reacted with dimethylacetylene dicarboxylate, methyl propynoate, and n-butyl propynoate under a carbon monoxide atmosphere in refluxing THF or by photolysis in cyclohexane producing the new iron tricarbonyl complexes **22-26**, (Table 8). If the reaction was performed under a nitrogen atmosphere instead of carbon monoxide then alkyne addition products were obtained, but in much lower yield.

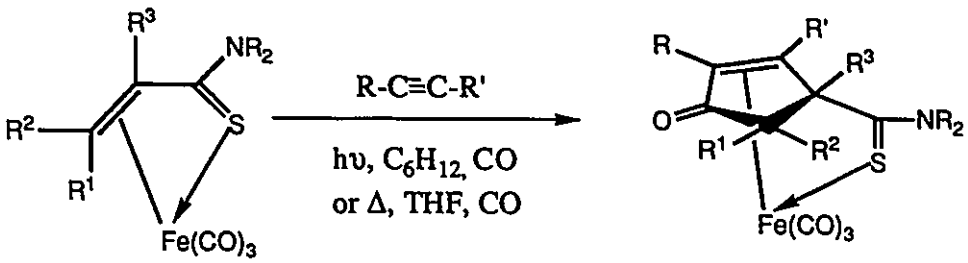

Various attempts were made to improve the product yield. Increasing the CO pressure to 400 psi or refluxing in a higher boiling solvent was unsuccessful in this regard.

Among the alkynes that were used, dimethylacetylene dicarboxylate and methyl propynoate gave the highest product yields while n-butyl propynoate gave a significantly lower yield than the other two alkynes. There was no reaction with the following alkynes: [$CH_3C_2CO_2Et$], [$F_3CC_2CF_3$], [$HC_2C(O)CH_3$], [$HC_2C(O_2Me)(CH_3)C_2H_5$], [HC_2Ph], [$HC_2C(CH_3)CCH_2$], and [HC_2SiMe_3].

COMPLEX	ALKYNE	CONDITIONS	PRODUCT(S) (Isolated Yield)
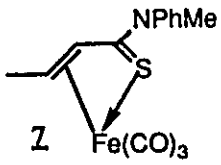	$MeO_2CC_2CO_2Me$	THF ref 2h	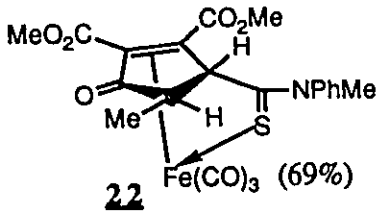
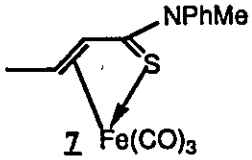	$HCC_2CO_2{}^nBu$	THF ref 1h40min	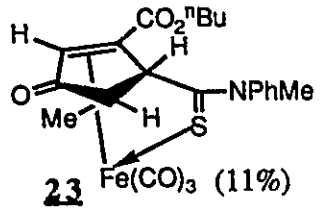
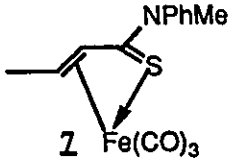	HC_2CO_2Me	THF ref 15h	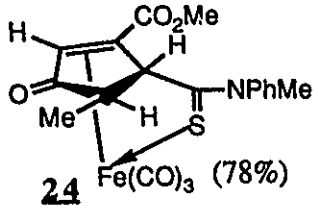
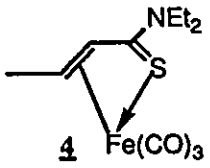	$MeO_2CC_2CO_2Me$	THF ref 6h	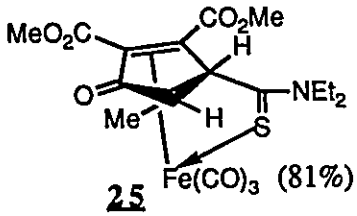
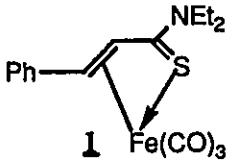	$MeO_2CC_2CO_2Me$	hυ 3h	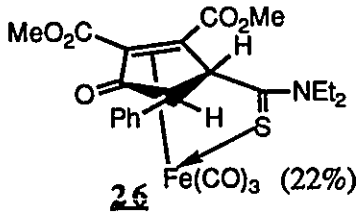

Table 8

The nature of the starting complex also had an effect on the product. Thioamide iron complex 7 was used in all of the reactions designed to investigate the reactivity of various alkynes, as well as the effect of varying the

reaction conditions. Reaction of thioamide iron complex 7 with dimethylacetylene dicarboxylate (DMAD) gave a much higher yield than phenyl substituted thioamide iron complex 1 but an even higher yield was obtained with thioamide iron complex 4. β-Methyl substituted thioamide iron complex 8 did react with DMAD but an inseparable mixture of products resulted. Thioester iron complex 10 also reacted with DMAD but an uncharacterizable mixture of products were formed.

Efforts were made to remove the resulting thioamide-cyclopentadienone ligand from the iron tricarbonyl fragment. Unlike the DAD-iron tricarbonyl complex system discussed earlier, the addition of excess free thioamide or even ligands such as triphenylphosphine, diphenylphosphinoethane, dimethylphosphinoethane, or bipyridine did not result in selective cleavage of the thioamide-cyclopentenone ligand. High carbon monoxide pressure (1200 psi) was equally ineffective. Photolysis in ethanol or the use of ceric ammonium nitrate, potassium cyanide, or trimethylamine oxide, all of which have the potential to free the ligand, gave decomposition of the complexes to unidentifiable products. One oxidizing agent, m-chloroperbenzoic acid, did give the free ligand based on the GC/MS but further characterization was impossible due to recovery of less than one milligram which was a mixture of products. Modifying the reaction conditions did not improve the recovery of free ligand and repeating the original reaction with a larger amount of starting material gave even less of the free ligand and more of other products.

In summary, α,β-unsaturated thioamide tricarbonyl complexes reacted with alkynes and carbon monoxide generating novel iron tricarbonyl complexes 22-26 which were characterized by infrared, mass spectrometry, elemental analysis, ^{1}H and $^{13}C\{^{1}H\}$ NMR spectroscopy, and in one case by X-ray crystallography.

3.7.1.2 Spectral Characterization of Iron Complexes 22-26

3.7.1.2.1 Mass Spectra and Elemental Analysis

Iron complexes **24**-**26** gave CI mass spectra having mass peaks corresponding to the parent ion, $[M+1]^+$, followed by successive loss of carbon monoxide ligands, and a signal was also present representing the free thioamide-cyclopentenone ligand. Iron complexes **22** and **23** gave mass fragments corresponding to the free thioamide-cyclopentenone ligand as well as higher mass peaks.

The elemental analyses for all of the complexes were consistent with their formulas.

3.7.1.2.2 Infrared Spectra

The infrared spectra gave three intense metal carbonyl stretching bands at approximately 2060, 2000, and 1980 cm^{-1} for each of the complexes. Dimethylacetylene dicarboxylate reaction products **22** and **26** gave a single strong absorption at approximately 1690 cm^{-1} for the ketone and ester carbonyls while products **23**-**25** gave distinct bands for these carbonyls at approximately 1720 cm^{-1} for the ketone carbonyl and 1695 cm^{-1} for the ester carbonyls.

3.7.1.2.3 NMR Spectra

The ^1H NMR spectrum of iron complex **23** is shown in figure 14. As was found for all of the iron complexes **22**-**26**, there was no coupling observed

between the proton in a β-position to C=S and its neighboring proton on the carbon in a β-position to C=O. The X-ray crystal structure of complex **22** shows the dihedral angle between these protons to be 100.2°. The Karplus relation predicts coupling constants for neighboring protons based on their dihedral angle but it does not account for a zero coupling constant[77]. The Karplus relationship between dihedral angles and the magnitudes of coupling constants is, however, a poor model for these couplings, since the relationship is based on calculations with ethane and substitution can cause substantial changes in coupling[77]. A dihedral angle of 90° would result in the smallest coupling and thus an angle of 100.2° would be expected to have a small coupling. It may be that the protons do have a very small coupling, but selective decoupling of the neighbouring protons gave no change in the linewidth of the signals. It is not evident why there is an apparent absence of coupling between these neighboring protons.

The olefinic protons for iron complexes **23** and **24** experienced a shift upfield to approximately δ4.60 ppm, which would be anticipated with metal coordination.

The ^{13}C NMR spectrum of iron complex **23** is shown in figure 15. The five signals furthest downfield in the ^{13}C NMR spectrum, in the region of δ200-210 ppm, could not be specifically assigned, but as a group were assigned to the three metal carbonyls, the ketone carbonyl, and the C=S carbon. The large downfield chemical shift of the C=S carbon gave the first indication that the C=S was no longer conjugated with the olefin, since the starting material, thioamide iron complex **7**, gave a C=S chemical shift of δ152.95 ppm. This region, near δ150 ppm, was typical of the chemical shifts of C=S carbons in α,β-unsaturated thioamide iron tricarbonyl complexes.

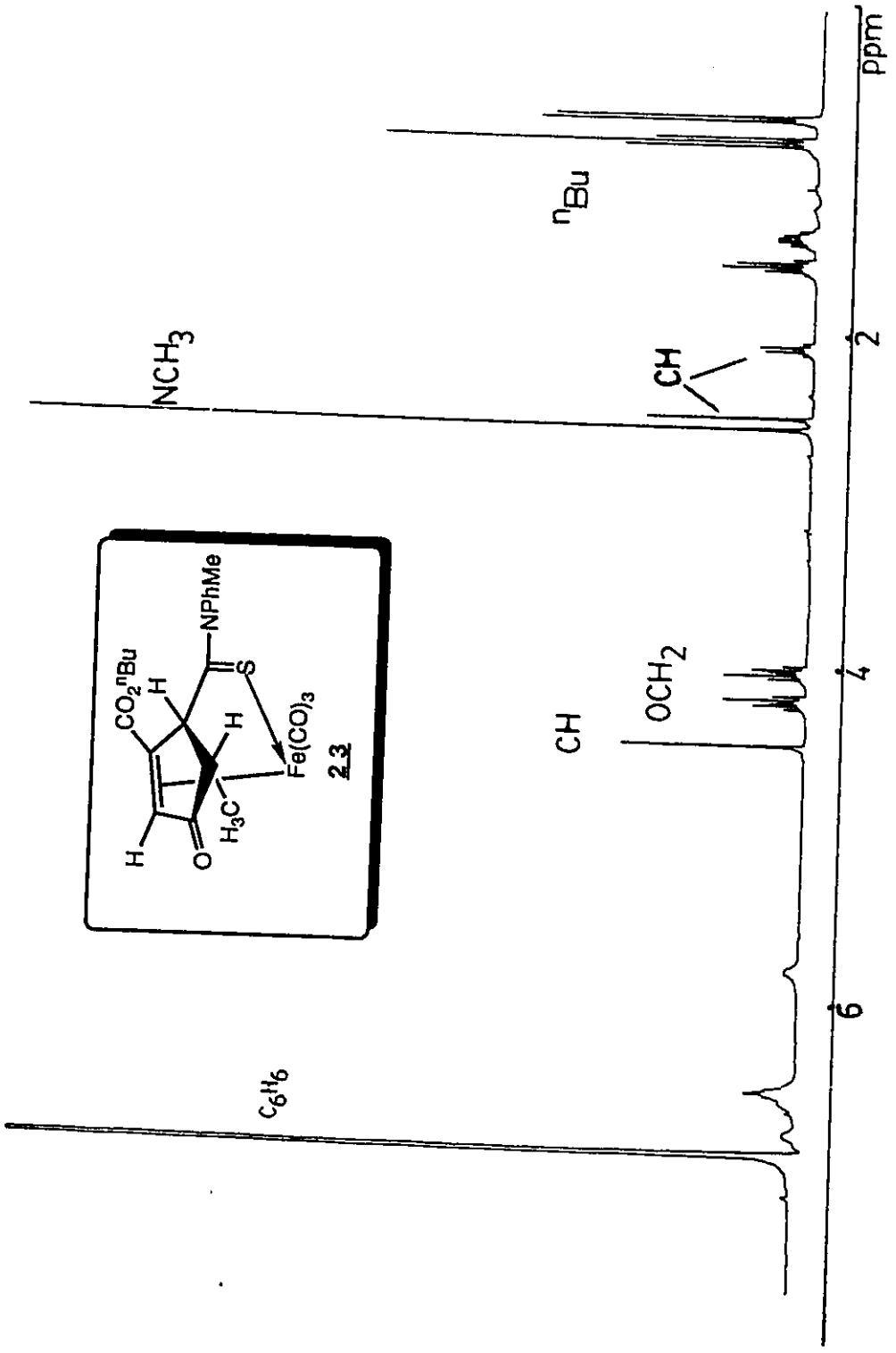

Figure 3.14: ^{1}H NMR Spectrum of Complex 23

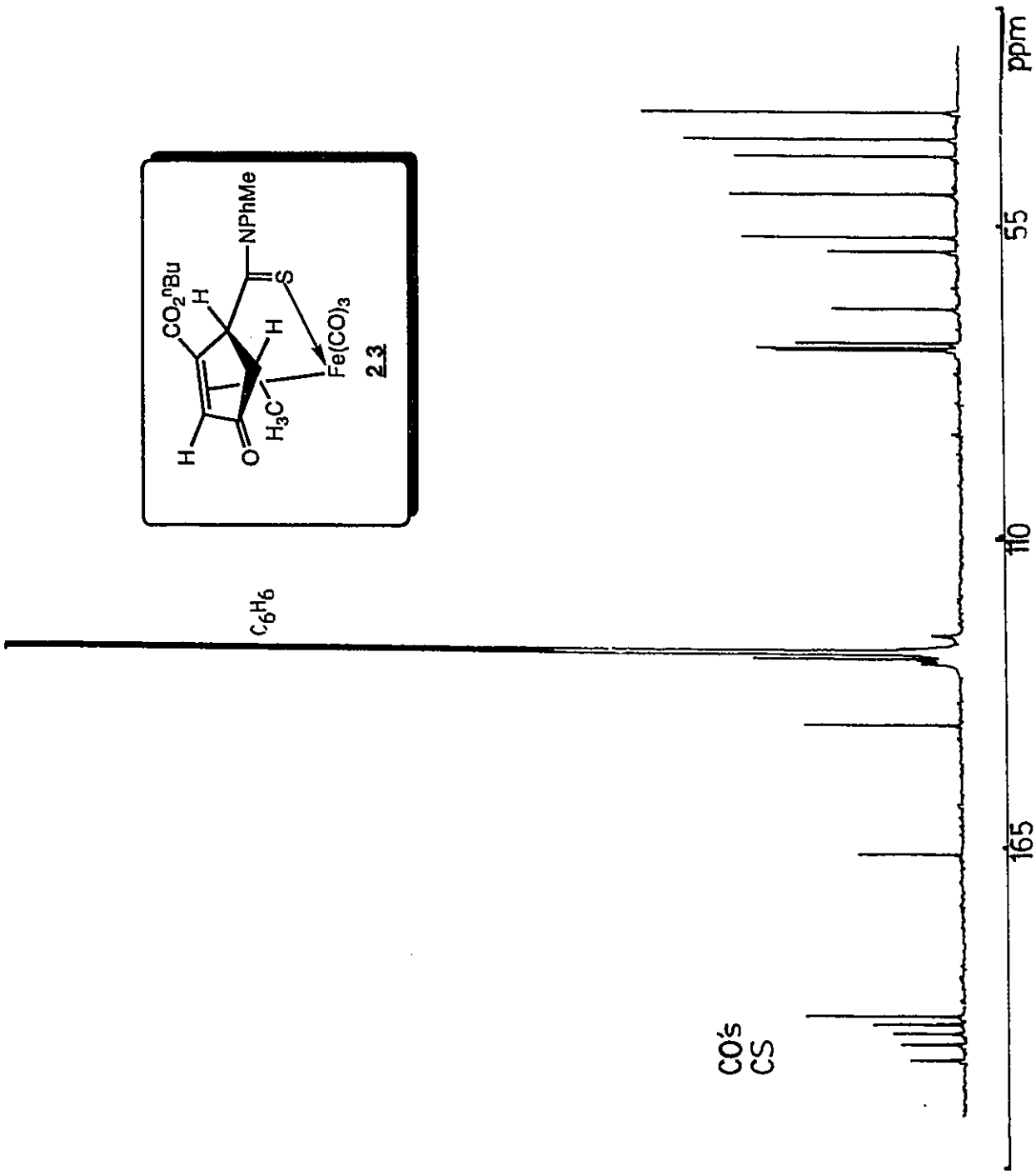

Figure 3.15: ^{13}C NMR Spectrum of Complex **23**

3.7.1.2.4 X-Ray Crystal Structure

The X-ray crystal structure of iron complex **22** was obtained and was found to consist of discrete molecular units having no intermolecular contacts less than the sum of van der Waal s' radii. An ORTEP diagram of this complex is shown in figure 16 along with pertinent bond lengths. Two alternate perspectives of the complex are shown in figure 17. Bond angles and bond distances are reported in Chapter 4 along with the crystallographic details.

The structure can be described as being a distorted octahedron about the iron in which the iron is π-bonded to the olefinic carbons of the cyclopentenone fragment and bonded to the sulphur through a lone pair on the sulphur, forming a six-member metallocycle. The three carbonyls are oriented about the iron such that they are staggered relative to the other three iron ligand bonds and one of the carbonyls lies in a plane normal to the midpoint of the cyclopentenone double bond. This carbonyl has an unusually small Fe-C2-O2 angle of 172.6° compared to the other Fe-C-O angles, which come much closer to the expected 180° angle: Fe-C1-O1, 178.7° and Fe-C3-O3, 177.3°. It appears that the ester oxygen atoms are in close proximity to the iron carbonyl oxygen O2 and there may be electrostatic repulsive interactions between the two types of oxygen which result in this deviation of the Fe-C-O angle from 180°.

Much like the tricarbonyl fragment of thioamide iron complexes **1** and **2**, that of iron complex **22** does not have local C_{3v} symmetry. Two of the OC-Fe-CO angles in complex **22** are very small, (C1-Fe-C2 is 88.7° and C2-Fe-C3 is 88.0°), while the remaining OC-Fe-CO angle is quite large (C1-Fe-C3 is 110.1°). The largest angle found is for the OC-Fe-CO trans to that carbon-carbon double bond which itself has a tight C-Fe-C angle (40.9°).

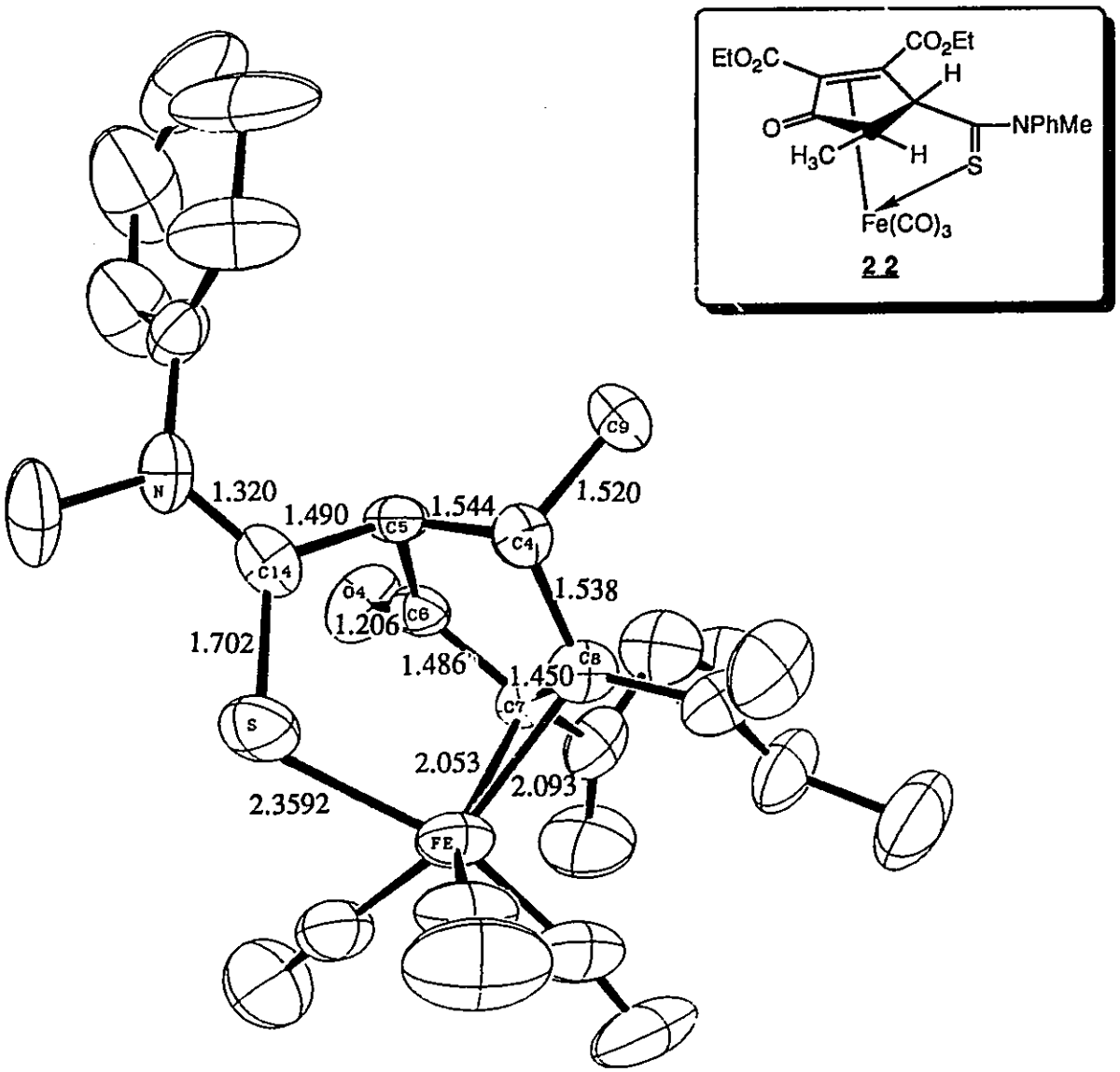

Figure 3.16: X-Ray Crystal Structure of Complex **22**

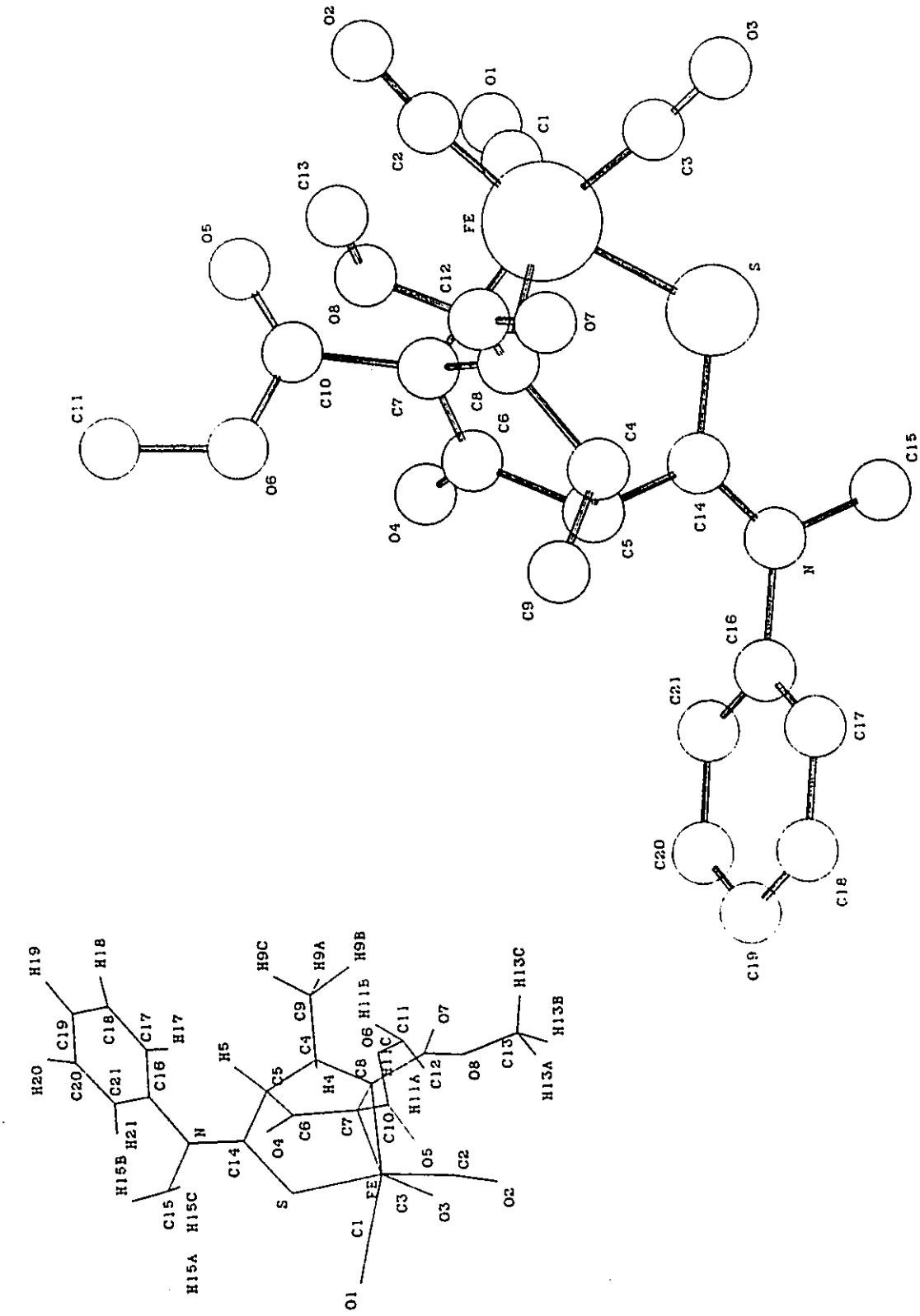

Figure 3.17: X-Ray Crystal Structure of Complex 22

The iron tricarbonyl fragment of iron complex **22** is much more distorted than that of thioamide iron complex **1** in which there was only one small OC-Fe-CO angle, while the other OC-Fe-CO angles did not have as large distortions compared to iron complex **22**. The local symmetry of the $Fe(CO)_3$ for both iron complexes **1** and **22** was C_S.

The iron-carbon bond lengths for bonding to the carbonyl groups in iron complex **22** were slightly longer than those of thioamide iron tricarbonyl complexes **1** and **2** (discussed in Chapter 2). This difference would be expected based on the infrared spectra, in which the carbon monoxide stretching frequencies are slightly higher in energy for iron complex **22** than for either thioamide iron complexes **1** or **2**, indicating stronger C≡O bonds in the iron complex **22** and therefore a lesser degree of backbonding from the metal. The carbonyl trans to the sulphur has the shortest C-Fe bond length, while the carbonyl closest and cis to the sulphur has the longest C-Fe bond.

The iron-sulphur bond for complex **22** is 2.3595Å, which is very similar to that of thioamide iron complex **1**. As well, the carbon-sulphur double bond for complex **22** is 1.702Å, which was similar to that of thioamide iron complex **2** but shorter than that found for thioamide iron complex **1**. This suggests that the carbon-sulphur and the iron-sulphur bonding in the thioamide iron complexes **1** and **2** are not significantly altered by reaction with alkynes. The alkyne products also appear to be bound to iron via the sulphur lone pair.

The length of the carbon-nitrogen bond (C14-N) of iron complex **22** is considerably shorter, at 1.320Å, than a normal carbon-nitrogen single bond, 1.47Å, and is found to be longer than a normal carbon-nitrogen double bond, 1.29Å[57]. There appears therefore to be some nitrogen interaction with the C=S carbon, similar to that found for the thioamide iron complexes **1** and **2**.

The amine bound phenyl ring of iron complex **22** is planar, with an

average deviation from planarity of 0.02Å.

In iron complex **22** the cyclopentenone ring carbons are not coplanar. Carbon atom C4 of the ring is 0.125Å above the best-fit plane and carbon C5 sits 0.104Å below the plane, giving the cyclopentenone portion an overall puckered envelope shape. The bond length between the olefinic carbons is 1.450Å, which is between that of a normal double bond (1.33Å) and single bond (1.54Å)[57]. This bond lengthening relative to a typical C=C double bond is due to coordination to the iron but resonance into the electron withdrawing ester groups must be a contributing factor in this increase. This bond length is very close to that of the diphenyl-substituted iron complex **2** (1.454Å), which has the combined effect of both iron coordination and electron withdrawing groups on each of the olefinic carbons.

The ketone carbon-oxygen bond length in iron complex **22** of 1.206Å was similar to the ester carbon-oxygen double bond lengths, C10-O5 1.197Å and C12-O7 1.193Å, found in this complex and slightly shorter than a normal ketone carbon oxygen double bond length, 1.22Å[57]. The differences between the ketone, ester, and normal ketone C=O double bond lengths are so small that they cannot be attributed to any effects due to iron coordination or complex orientation.

The olefinic carbon-iron bond lengths in iron complex **22** are not equivalent (Fe-C7 is 2.053Å and Fe-C8 is 2.093Å). The Fe-C8 bond may be longer because its ester group is in close proximity to the iron carbonyl ligands which, through electron repulsion, may force the C8 carbon further away from the iron than is the C7 carbon. The Fe-C8 and Fe-C7 bond lengths are similar to those of thioamide iron complexes **1** and **2**.

The angles and lengths observed for the bonding of atoms to the iron in complex **22** was not very different from those observed for the other

α,β-unsaturated heterodiene iron complexes discussed in Chapter 2, but it is important to note that the carbon-sulphur and the carbon-carbon double bonds are not conjugated to each other in iron complex **22**. The result is a puckered metallocycle in which C14 is at a 112.12° angle to the plane formed by the cyclopentenone.

In summary, the X-ray crystal structure of iron complex **22** revealed a distorted octahedral geometry about the iron centre. The sulphur ligand contained a cyclopentenone fragment which had a puckered shape. The iron complex cannot attain a planar orientation of the thio-ligand atoms directly bonded to the iron since the carbon-sulphur and carbon-carbon double bonds of the thio-ligand are not conjugated as they were with the iron complexes discussed in Chapter 2.

3.7.2 Route to Product Formation

A possible pathway for the formation of the alkyne addition products is outlined in Scheme 4. The α,β-unsaturated iron tricarbonyl complex could have a resonance structure XVIII in which the sulphur atom is coordinated to the iron through a covalent rather than a lone pair donor bond. This complex could then undergo intramolecular CO-insertion to generate complex XIX which now has a vacant coordination site available for alkyne addition, producing complex XX. Alkyne insertion would give intermediate complex XXI which would then ring close and the iron would recoordinate at the olefin forming the π-bonded product XXII.

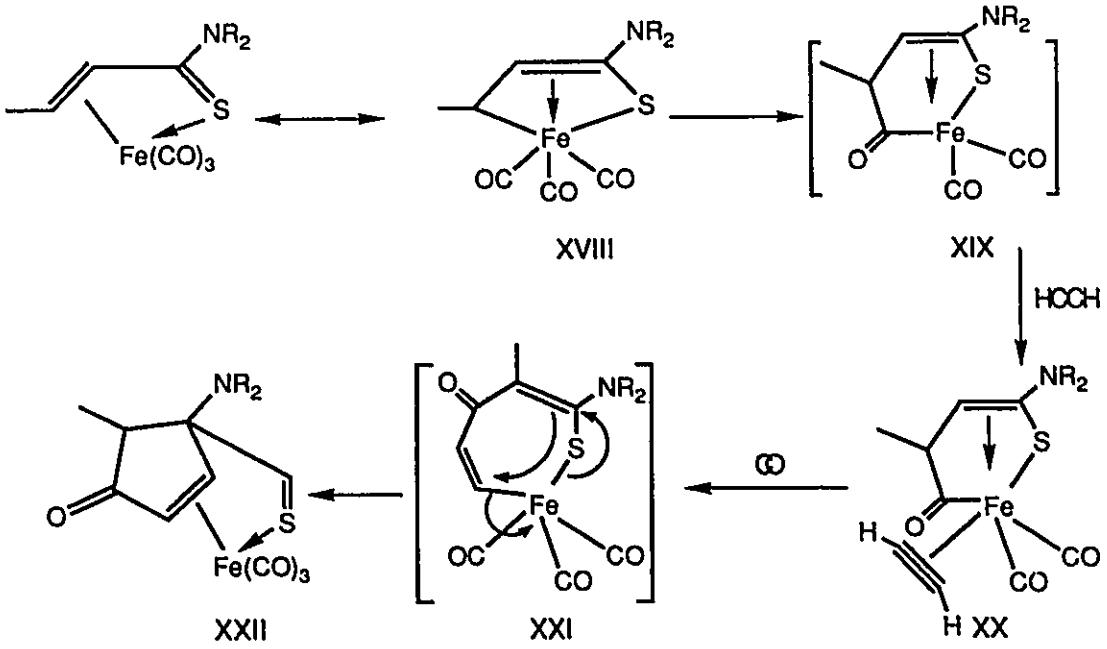

Scheme 4

There is ample literature support for the second-fourth steps in the above scheme. Carbon monoxide insertion into an iron alkyl bond is a fundamental process in the formation of iron mediated CO-insertion products[3]. One example is the route postulated for the formation of cyclopentenones from nucleophilic reactions with a diene iron tricarbonyl complex[78] (Scheme 5).

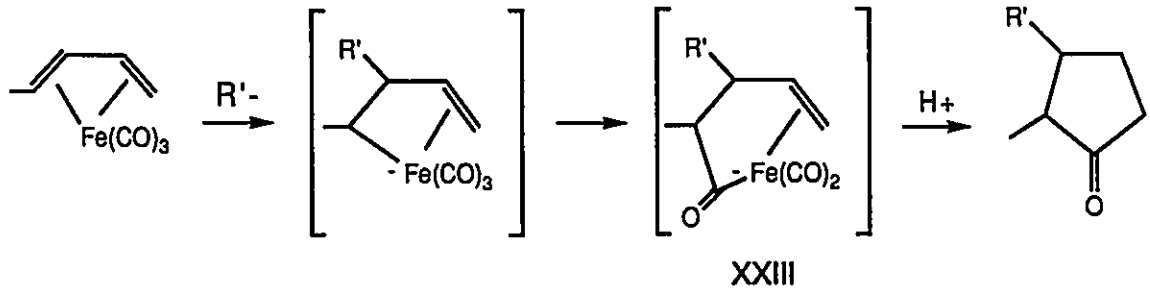

XXIII

Scheme 5

Carbon monoxide insertion in the formation of XXIII is analogous to that

suggested for intermediate XIX in Scheme 4. Alkyne addition to an available coordination site in 16-electron complexes such as XIX is a typical route for the formation of π-alkyne coordinated products, such as XX[3]. Acetylene insertion into a metal acyl bond is known and Scheme 6 indicates in one case that the reaction proceeds via a four coordinate metal intermediate, XXIV, having an alkyne ligand similar to complex XX in Scheme 4[75].

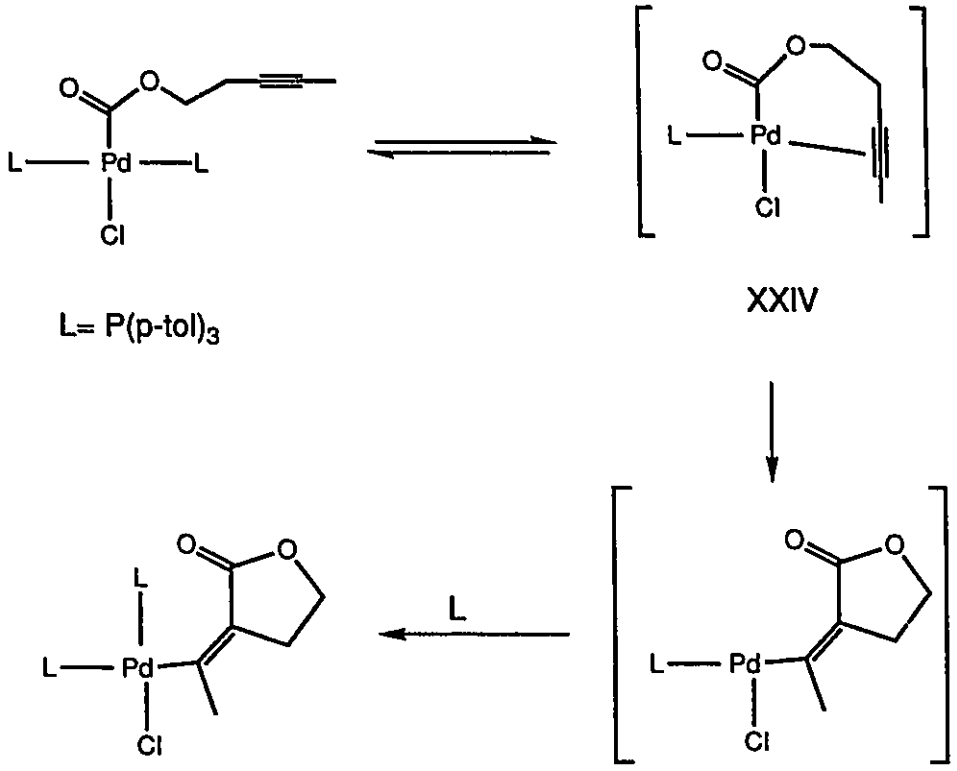

Scheme 6

3.8 Reactions with Miscellaneous Reagents

Many reactions were performed to investigate the scope of reagents that might undergo a reaction with the thio-iron complexes leading to the formation of new products. All of the reactions which will be discussed in this section gave either recovery of the pure starting material, products similar to the reaction

performed on the free ligand, or inconclusive results. This section is included to give the reader an appreciation of the range of reactions that were tested on these α,β-unsaturated thioamide and thioester iron tricarbonyl complexes.

3.8.1 Dienes and Miscellaneous Reagents

The ease of carbon monoxide ligand exchange by photolysis or thermolysis presented the possibility of reaction by any reagent capable of occupying the available coordination site of the metal centre. Thermolysis and photolysis of α,β-unsaturated thioamide iron tricarbonyl complex 7 with 2,3-dimethyl-1,3-butadiene under a carbon monoxide atmosphere gave recovery of iron complex 7, with yields of 93% and 84% for thermolysis and photolysis respectively. Likewise, thermolysis of 2,3-dimethoxy-1,3-butadiene gave no reaction with thioamide iron complex 7 (90% recovery). Phenyl isocyanide (Ph-N=C=O), 3-phenyl-1,2-propadiene (Ph-HC=C=CH_2), and ethyl diazoacetate ($N_2CHCO_2C_2H_5$), all gave very high recovery of the starting material, thioamide iron complex 7, in their reactions by thermolysis and photolysis both in the presence and absence of carbon monoxide.

3.8.2 Hydride Abstraction

As discussed in Chapter 1, α,β-unsaturated thioaldehyde iron tricarbonyl and cobalt cyclopentadienyl complexes reacted with triphenylmethylfluoroborate, which abstracted the hydride from the position α to the C=S. Although there are no α-protons in the α,β-unsaturated thio-iron complexes, it may have been possible to remove a hydride from the γ-methyl group of thioamide iron complexes 4 or 7 [6].

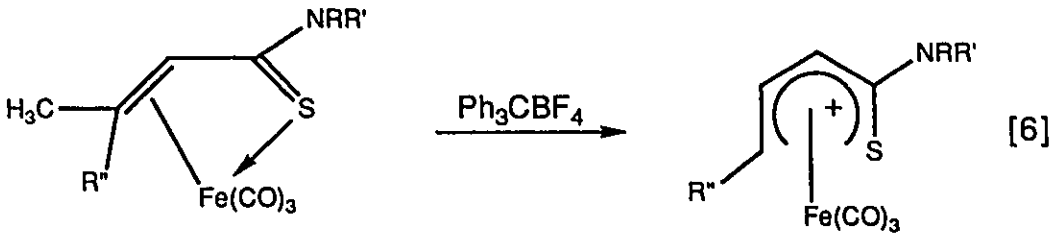

[6]

4 R=R'=Et, R"=H
7 R=CH_3, R'=Ph, R"=H

XXV

There was some reaction of complexes **4** and **7** with the hydride abstacting agent but the products were unidentifiable (other than recovery of starting material). In previous reactions with dienes it was stated that if the complex could be made to have a rigid orientation such as XXVI, then hydride abstraction would be expected to occur[79].

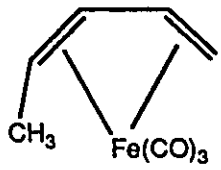

XXVI

To test this, hydride abstraction reaction [6] was repeated using thioamide iron complex **6** (R=R'=Et, R"=CH_3) which having two γ-methyl substituents should have a hydride suitable for abstraction, but in fact only starting material was recovered in 91% yield.

3.8.3 Reduction

The addition of a hydride source such as sodium borohydride or lithium aluminum hydride to α,β-unsaturated thioamide iron complex **4** gave the saturated free ligand, XXVII [7].

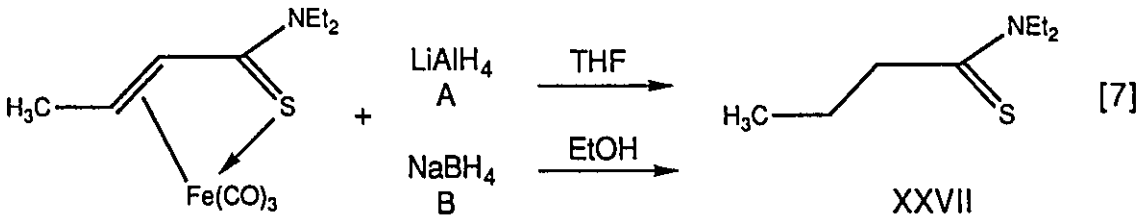

[7]

XXVII

A= 57%

B= 50%

4

The same reactions with the free thioamide ligand also gave the saturated thioamide product XXVII, but in a lower yield using sodium borohydride (28%) and a higher yield using lithium aluminum hydride (72%) relative to the reactions with the complex. Another hydride source, potassium-Selectride, gave only insoluble by-products and a low recovery of the starting material (18%).

Iron tricarbonyl fragments are able to protect conjugated dienes, allowing for selective hydrogenation of other C=C double bonds on the molecule[3]. Thioamide iron complex 1 was reacted with hydrogen and a heterogeneous catalyst, Pd/C (5% and 10%) or PtO_2 and as was anticipated, only the unsaturated starting material was recovered illustrating the protecting role of the $[Fe(CO)_3]$ fragment. There was no hydrogenation of the free thioamide ligand under the same reaction conditions which may have been due to sulphur poisoning of the catalyst. Thioamide iron complex 3 was prepared in order to investigate hydrogenation at the free olefin but the outcome was disappointing, resulting in 14% reduction of iron complex 3 compared to 25% reduction of its free ligand.

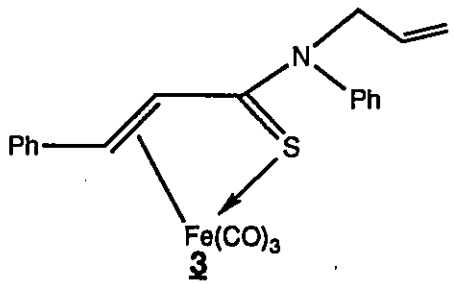

3

3.9 Conclusions

Of all of the α,β-unsaturated thio-iron tricarbonyl complexes that were prepared, an investigation into their reactivity towards thermolysis, photolysis, and a variety of reagents could only be done on thioamide iron complexes, **1**, **3**, **4**, **7**, **8**, and **9**, and one thioester iron complex, **10**. The other thioester complexes, **11** and **12**, and thione complex, **13**, were either too unstable or they were prepared in such low yields that a sufficient amount of material was not available for investigation of their reactivity. The choice of starting material throughout the investigation was primarily guided by its availability or by the variation of substitution necessary to develop an overall picture of their susceptibility towards reaction with specific reagents.

Removal of the thio-ligand, which is an important aspect in organic synthesis using organometallics by stoichiometric methods, was achieved by using ceric ammonium nitrate at 0°C. Oxidation of the C=S fragment to C=O resulted at higher temperatures. Thermolysis and photolysis were used to promote thio-ligand removal but the recovery of the free thio-ligand was poor and the reactions were detrimental to the starting materials in that much decomposition was observed. Reagents which are known to induce ligand removal by oxidation of the metal centre were very effective for selectively removing the thio-ligand but in all cases there was a large amount of oxidation of the C=S fragment.

Careful control of the oxidizing conditions resulted in the formation of α,β-unsaturated thioester iron tricarbonyl sulphine complex **20**. A thioamide iron sulphine complex could not be isolated from the reaction of oxidants with

α,β-unsaturated thioamide iron complexes. This reaction with thioamide iron complexes and hydrogen peroxide or m-chloroperbenzoic acid always resulted in ligand removal and oxidation to the free amide ligand.

Carbon monoxide ligands could also be selectively removed from α,β-unsaturated thioamide and thioester iron tricarbonyl complexes. This was achieved using thermolysis or photolysis. To ensure loss of carbon monoxide, triphenylphosphine was added to these reactions and as a result three new mono-phosphine substituted complexes were prepared in good yields: thioamide complexes **17** and **18** and thioester complex **19**. In no reaction could more than one triphenylphosphine be incorporated into the complex.

The addition of alkynes instead of triphenylphosphine under photolysis or thermolysis produced new iron complexes **22**-**26** resulting from coupling of the alkyne, carbon monoxide, and the coordinated olefin of α,β-unsaturated thioamide iron complexes **1**, **4**, and **7**. An X-ray crystal structure of **22** revealed a distorted octahedral geometry about the iron centre and coordination of the iron to the organic compound through a lone pair from the sulphur and π-coordinated to the olefin of a cyclopentenone ring in which the C=S and olefinic fragments are not conjugated. A similar non-conjugated C=S and C=C complex could not be directly prepared in the reaction of (O-methyl)-(4,8-dimethyl)-non-3,7-diene-thioate, **16'** with $[Fe(CO)_5]$ or $[Fe_2(CO)_9]$. Attempts at removing the thio-ligand were successful but decomposition of the products under the reaction conditions prevented isolation of the free ligand.

Electrophilic addition gave sulphur-substituted complexes. Mercuric acetate reacted with α,β-unsaturated thioester iron tricarbonyl complex **10** yielding a new complex which could not be purified sufficiently for absolute characterization. Methyl cation, $[(CH_3)_3OBF_4]$, reacted with thioester iron complex **10** producing what is believed to be a new S-methylated iron complex

21. The location of electrophilic substitution is based on the ^{1}H and ^{13}C NMR spectra.

Thioamide and thioester iron tricarbonyl complexes were reacted with nucleophiles and the nature of the products was dependent on the temperature at which the reaction was performed. At room temperature, simple 1,4-addition products were obtained, which is not unusual since the free ligand reacts in the same fashion. At -78°C, 4-oxo-thioamides were obtained in moderate yields from the nucleophilic addition reaction. The reaction at -78°C was very sensitive to the degree of substitution in the γ–position of the metal-coordinated thiocompound, and because of the difficulties associated with preparing thioesters with various substituents, only thioamide iron complexes were used as starting materials. These new 4-oxo-thioamides are potentially useful as synthetic intermediates to 4-ketoamides and 2-aminothiophenes.

Many other reactions were performed in order to investigate the reactivity with various types of reagents having the potential of forming novel products, but the iron complexes were either unreactive or they gave products similar to those obtained from the same reactions with the free thio-ligand, or they gave inconclusive results. The reactions investigated included reduction, hydride abstraction, alkene addition, and the use of an isocyanide, ketene, or diazo-compound.

CHAPTER 4

EXPERIMENTAL DETAILS FOR CHAPTERS 2 AND 3

4.O Solvents and Reagents

Reagents were purchased from Aldrich Chemical Company, Farchan Laboratories, and Fluka. Most were used without further purification.

Tetrahydrofuran, benzene, and ether were dried over sodium prior to each reaction. Hexane was dried over calcium hydride. All of the other solvents were used without further purification. All solvents were purchased from BDH Chemicals or Aldrich Chemical Company.

Columns were packed with silica gel 60 (70-200 mesh ASTU) purchased from J.T.Baker Chemical Company and neutral activated alumina, Brockmann I, and Florisil (60-100 mesh) purchased from Aldrich Chemical Company. Preparatory TLC plates (0.25mm and 1.20mm silica gel and aluminum oxide 60 with fluorescent indicator UV_{254}) were purchased from Chromatographic Specialties Inc.

All of the deuterated solvents were purchased from MSD Isotopes.

Elemental analyses were performed by M-H-W Laboratories in Phoenix, Arizona and Guelph Chemical Laboratories in Guelph, Ontario.

4.1 Instrumentation

4.1.1 Nuclear Magnetic Resonance Spectroscopy

The ^{1}H, $^{13}C\{^{1}H\}$, and $^{31}P\{^{1}H\}$ NMR spectra were recorded on a Varian XL-300 spectrometer. Chemical shifts were reported relative to the solvent peak

for ^{1}H and $^{13}C\{^{1}H\}$ and relative to external 85% H_3PO_4 in water for $^{31}P\{^{1}H\}$.

4.1.2 Infrared Spectroscopy

Infrared spectra were recorded on a Perkin-Elmer 783 Infrared spectrometer using NaCl solution cells.

4.1.3 Gas Chromatography

GC spectra were obtained from a Varian 3400 gas chromatograph using a 2m column packed with 3% OV-100 on chromosorb W and from a Varian 3300 gas chromatograph using a 10m DB-1 column.

4.1.4 Mass Spectrometry

Mass spectra were obtained from a VG7070E mass spectrometer using a PDP8A data system.

4.1.5 Pressure Reactor

High pressure reactions were performed in a Parr 40ml glass lined stainless steel pressure reactor.

4.1.6 Mass Balance

Mass determinations were obtained using a Mettler EA100 analytical balance.

4.1.7 Melting Point Determination

Melting point determinations were performed using a Gallenkamp melting point apparatus.

4.1.8 X-Ray Crystal Strucures

The intensity data for the X-ray crystal structures were collected on an Enraf-Nonius CAD4 diffractometer using the theta/2theta scan mode in the laboratory of Dr. Eric J. Gabe at the National Research Council, Ottawa.

4.2 Experimental Details for Chapter 2

4.2.1 Preparation of α,β-Unsaturated Thiocarbonyls

4.2.1.1 (N,N-Diethyl)-3-phenylpropenethioamide, 1'

3-Phenylpropenoyl-chloride (60mmol) was added dropwise to a stirred solution of N,N-diethylamine (240mmol) in 5% KOH (150ml) at 0°C [44]. After the acid chloride was added, the solution was allowed to warm to room temperature and was stirred overnight. The solution was then extracted with ether (4 × 100ml) and the combined organic fractions were washed with distilled water (3 × 100ml). The organic layer was dried over Na_2SO_4, filtered, and the solvent was removed leaving 11.33g (93%) of a white solid, N,N-diethyl-(3-phenyl)-propenamide. The amide was characterized by IR and ^1H NMR.

The amide (20mmol) was converted to the thioamide using 2,4-bis-(p-methoxyphenyl)-1,3-dithiaphosphetane-2,4-disulphide (Lawesson's reagent) (12mmol) by refluxing in toluene under N_2 for 1h[42]. After cooling the solution to room temperature, sufficient silica (~15g) was added to give a dry powder after removal of the solvent by rotary evaporation. The solid was added to the top of a dry-packed silica column and was eluted with hexanes:ether (9:1). The first band which was orange in colour was collected and the solvent was removed by

rotary evaporation leaving an orange solid which was recrystallized from ethanol. Yield from amide: 95%. M.p. 47-49°C [Lit. 48-50°C[23]]. M.S.: 239(M)$^+$ (m/e). ^{1}H NMR ($CDCl_3$): δ 1.32 [t, 3H, ^{3}J=7.4Hz, $CH_2\underline{C}H_3$]; 1.33 [t, 3H, ^{3}J=7.4Hz, $CH_2\underline{C}H_3$]; 3.70 [q, 1H, ^{3}J=7.4Hz, $\underline{C}H_2CH_3$]; 4.09 [q, 1H, ^{3}J=7.4Hz, $\underline{C}H_2CH_3$]; 7.07 [d, 1H, ^{3}J=15.3Hz, β-$\underline{C}H$]; 7.33 , 7.49 [m, 1H, aromatics]; 7.85 [d, 1H, ^{3}J=15.3Hz, γ-$\underline{C}H$] ppm. ^{13}C NMR ($CDCl_3$): δ 11.54 [$CH_2\underline{C}H_3$]; 13.83 [$CH_2\underline{C}H_3$]; 46.46 [$\underline{C}H_2CH_3$]; 48.55 [$\underline{C}H_2CH_3$]; 124.85 [β-$\underline{C}H$]; 127.85 [aromatic $\underline{C}H$]; 128.80 [aromatic $\underline{C}H$]; 129.44 [aromatic $\underline{C}H$]; 135.61 [quaternary aromatic C]; 143.82 ppm [γ-$\underline{C}H$]; 193.65 [1C, C=S] ppm.

4.2.1.2 (N,N-Diethyl)-2,3-diphenylpropenethioamide, **2'**

2,3-Diphenylpropenoic acid (70mmol) was refluxed in a benzene solution of thionyl chloride (270mmol) for 1h. The solvent was removed by rotary evaporation, leaving a yellow oil (93% yield). IR confirmed the absence of the starting material and the acid chloride was used without further purification.

The acid chloride was converted to the amide (96% yield) as in 4.2.1.1 and was characterized by IR and ^{1}H NMR.

The thioamide was prepared from the amide (20mmol) by refluxing in toluene with Lawesson's reagent (12mmol) for 40min. Purification on a dry-packed silica column using hexanes:ether (1:1) gave a yellow solid after solvent removal. Yield from amide: 89%. M.p. 56-58°C. M.S.:295(M)$^+$ (m/e). ^{1}H NMR ($CDCl_3$): δ 0.82 [t, 3H, ^{3}J=7.2Hz, $CH_2\underline{C}H_3$]; 1.37 [t, 3H, ^{3}J=7.1Hz, $CH_2\underline{C}H_3$]; 3.53 [overlapping dq, 2H, $\underline{C}H_2CH_3$]; 4.02 [dq, 1H, ^{3}J=7.2Hz, ^{2}J=7.1Hz, $\underline{C}H_2CH_3$]; 4.23 [dq, 1, ^{3}J=7.2Hz, ^{2}J=7.1Hz, $\underline{C}H_2CH_3$]; 6.72 [s, 1, γ-$\underline{C}H$]; 7.35, 7.60 [m, 10H, aromatics] ppm. ^{13}C NMR ($CDCl_3$): δ 10.42 [$CH_2\underline{C}H_3$]; 12.82 [$CH_2\underline{C}H_3$]; 44.94 [$\underline{C}H_2CH_3$]; 47.59 [$\underline{C}H_2CH_3$]; 123.59, 125.92, 126.29, 127.66, 127.93, 128.17, 128.49, 128.93 [aromatic CH]; 135.46,

138.19, 141.07 [quaternary aromatic C]; 197.62 [C=S] ppm.

4.2.1.3 (N-phenyl,N-(2-propenyl))-3-phenylpropenethioamide, **3'**

The amide was prepared (94% yield) as in 4.2.1.1 and was characterized by IR and ^{1}H NMR.

The thioamide was prepared from the amide (20mmol) by refluxing in toluene with Lawesson's reagent (12mmol) for 17h. Purification on a dry-packed silica column using hexanes:ether (3:7) gave an orange solid which was spectroscopically pure but gave a broad m.p. range. Yield from amide: 81%. M.p. 56-77°C. M.S.: 279(M)$^+$ (m/e). ^{1}H NMR ($CDCl_3$): δ 5.03 [d, 2H, ^{3}J=6.3Hz, $N\underline{C}H_2CHCH_2$]; 5.15 [dd, 1H, ^{3}J=20.0Hz, ^{2}J=1.4Hz, $NCH_2CH\underline{C}H_2$]; 5.20 [dd, 1H, ^{3}J=10.3Hz, ^{2}J=1.4Hz, $NCH_2CH\underline{C}H_2$]; 6.04 [ddt, 1H, ^{3}J=20.0, 10.3, 6.3Hz, $NCH_2\underline{C}HCH_2$]; 6.56 [d, 1H, ^{3}J=15.0Hz , β-CH]; 7.17 [m, 2H, aromaticS]; 7.24 [s, 5H, aromatics]; 7.42 [m, 3H, aromatics]; 7.91 [d, 1,H γ-CH] ppm. ^{13}C NMR ($CDCl_3$): δ 59.19 [$N\underline{C}H_2CHCH_2$]; 118.7 [$NCH_2CH\underline{C}H_2$]; 125.94, 126.94 [β-CH and $NCH_2\underline{C}HCH_2$]; 127.43, 128.02, 129.10, 129.25, 130.66 [aromatics CH]; 134.99, 143.30 [quaternary aromatic C]; 144.03 [γ-CH]; 194.79 ppm [C=S] ppm.

4.2.1.4 (N,N-Diethyl)but-2-ene-thioamide, **4'**

The amide was prepared from crotyl chloride (97% yield) as in 4.2.1.1 and was characterized by IR and ^{1}H NMR.

The thioamide was prepared from the amide (20mmol) by refluxing in toluene with Lawesson's reagent (12mmol) for 2h. Purification on a dry-packed silica column using hexanes:ether (9:1) gave a yellow oil. Yield from amide: 45%. B.p.192-194°C. M.S.: 157(M)$^+$ (m/e). ^{1}H NMR ($CDCl_3$): δ 1.79 [2

overlapping t, 6H, ^{3}J=7.1Hz, $CH_2\underline{C}H_3$]; 1.80 [dd, 3H, ^{3}J=6.9Hz, ^{4}J=1.6Hz, $\underline{C}H_3$]; 3.53 [q, 2H, ^{3}J=7.1Hz, $\underline{C}H_2CH_3$]; 3.93 [q, 2H, ^{3}J=7.1Hz, $\underline{C}H_2CH_3$]; 6.38 [d, 1H, ^{3}J=14.6Hz, β-$\underline{C}$H]; 6.92 [dq, 1H, ^{3}J=14.6Hz, ^{3}J=6.9Hz, γ-$\underline{C}$H] ppm. ^{13}C NMR ($CDCl_3$): δ 10.94 [$CH_2\underline{C}H_3$]; 13.11 [$CH_2\underline{C}H_3$]; 18.02 [$\underline{C}H_3$]; 45.69 [$\underline{C}H_2CH_3$]; 47.55 [$\underline{C}H_2CH_3$]; 128.40 [β-$\underline{C}$H]; 141.97 [γ-$\underline{C}$H]; 193.37 [C=S] ppm.

5.2.1.4 (N,N-Diethyl)-2-methylpent-2-ene-thioamide, **5'**

The acid chloride was prepared in 89% yield from 2-methyl-hexenoic acid (70mmol) in refluxing benzene with thionyl chloride (270mmol) for 1h.

The amide was prepared (90% yield) as in 4.2.1.1 and was characterized by IR and ^{1}H NMR.

The thioamide was prepared from the amide (20mmol) by refluxing in toluene with Lawesson's reagent (12mmol) for 40min. Purification on a dry-packed silica column using hexanes:ether (9:1) gave a yellow oil. Yield from amide: 65%. B.p. 170°C/10mmHg. M.S.: 185$(M)^+$ (m/e). ^{1}H NMR ($CDCl_3$): δ 0.91 [t, 3H, ^{3}J=7.5Hz, $CH_2\underline{C}H_3$]; 1.16 [t, 3H, ^{3}J=7.2Hz, $CH_2\underline{C}H_3$]; 1.24 [t, 3H, ^{3}J=7.1Hz, $\underline{C}H_3$]; 1.90 [d, 3H, ^{4}J=1.3Hz, $\underline{C}H_3$]; 3.46 [dq, 1H, ^{3}J=7.1Hz, ^{2}J=7.0Hz, $\underline{C}H_2CH_3$]; 3.62 [dq, 1H, ^{3}J=7.1Hz, ^{2}J=7.0Hz, $\underline{C}H_2CH_3$]; 3.81 [dq, 1H, ^{3}J=7.1Hz, ^{2}J=7.0Hz, $\underline{C}H_2CH_3$]; 4.09 [dq, 1H, ^{3}J=7.1Hz, ^{2}J=7.0Hz, $\underline{C}H_2CH_3$]; 5.01 [m, 1H, γ-$\underline{C}$H] ppm. ^{13}C NMR ($CDCl_3$): δ 11.11 [$\underline{C}H_3$]; 13.03 [$\underline{C}H_3$]; 22.51 [$\underline{C}H_3$]; 13.76 [$\underline{C}H_3$]; 44.54 [$\underline{C}H_2CH_3$]; 46.53 [$\underline{C}H_2CH_3$]; 137.00 [β-$\underline{C}$]; 126.49 [γ-$\underline{C}$H]; 200.76 [C=S] ppm.

4.2.1.6 (N,N-Diethyl)-3-methylbut-2-ene-thioamide, **6'**

The acid chloride was prepared in 86% yield from 3-methylbutenoic acid (70mmol) in refluxing benzene with thionyl chloride (270mmol) for 1h.

The amide was prepared from the acid chloride (89% yield) as in 4.2.1.1 and was characterized by IR and ^{1}H NMR.

The thioamide was prepared from the amide (20mmol) by refluxing in toluene with Lawesson's reagent (12mmol) for 5h. Purification on a dry-packed silica column using hexanes:ether (9:1) gave a yellow oil. Yield from amide: 80.5%. B.p. 130°C/12mmHg [Lit.B.p.105-108°C/2mmHg][80]. M.S.: 171(M)$^+$ (m/e). ^{1}H NMR ($CDCl_3$): δ 1.04 [t, 3H, ^{3}J=7.2Hz, $CH_2\underline{C}H_3$]; 1.15 [t, 3H, ^{3}J=7.1Hz, $CH_2\underline{C}H_3$]; 1.59 [s, 3H, $\underline{C}H_3$]; 1.66 [s, 3H, $\underline{C}H_3$]; 3.46 [q, 2H, ^{3}J=7.2Hz, $\underline{C}H_2CH_3$]; 3.87 [q, 2H, ^{3}J=7.2Hz, $\underline{C}H_2CH_3$]; 5.79 [s, 1H, β-$\underline{C}$H] ppm. ^{13}C NMR ($CDCl_3$): δ 10.61 [$CH_2\underline{C}H_3$]; 12.66 [$CH_2\underline{C}H_3$]; 18.66 [$\underline{C}H_3$]; 24.41 [$\underline{C}H_3$]; 44.95 [$\underline{C}H_2CH_3$]; 46.17 [$\underline{C}H_2CH_3$]; 125.01 [β-$\underline{C}$H]; 134.66 [γ-$\underline{C}$]; 195.73 [C=S] ppm.

4.2.1.7 (N-Methyl,N-phenyl)but-2-ene-thioamide, **7'**

The amide was prepared from crotonyl chloride (96% yield) as in 4.2.1.1 and was characterized by IR and ^{1}H NMR.

The thioamide was prepared from the amide (20mmol) by refluxing in toluene with Lawesson's reagent (12mmol) for 23h. Purification on a dry-packed silica column using hexanes:ether (9:1) gave an orange solid. Yield from amide: 73%. M.p. 82-83°C. M.S.: 191(M)$^+$ (m/e). ^{1}H NMR ($CDCl_3$): δ 1.62 [dd, 3H, ^{3}J=7.0Hz, ^{4}J=1.6Hz, $\underline{C}H_3$]; 3.71 [s, 3H, N-$\underline{C}H_3$]; 5.85 [d, 1H, ^{3}J=15.0Hz, β-$\underline{C}$H]; 7.10 ppm [m, 3H, γ-$\underline{C}$H and aromatics]; 7.40 [m, 3H, aromatics] ppm. ^{13}C NMR ($CDCl_3$): δ 18.28 [$\underline{C}H_3$]; 45.46 [N-$\underline{C}H_3$]; 125.71 [aromatic $\underline{C}$H]; 127.88 [aromatic $\underline{C}$H]; 129.42 [aromatic $\underline{C}$H]; 129.86 [β-$\underline{C}$H]; 143.34 [γ-$\underline{C}$H]; 195.58 [C=S] ppm.

4.2.1.8 (N-Methyl,N-phenyl)-2-methylprop-2-ene-thioamide, **8'**

The amide was prepared from acryloyl chloride (85% yield) as in 4.2.1.1 and was characterized by IR and ^{1}H NMR.

The thioamide was prepared from the amide (20mmol) by refluxing in toluene with Lawesson's reagent (12mmol) for 23h. Purification on a dry-packed silica column using hexanes:ether (9:1) gave an orange oil. Yield from amide: 58%. B.p. 238°C [Lit.B.p.70°C/0.7mmHg][81]. M.S.: 191(M)$^+$ (m/e). ^{1}H NMR ($CDCl_3$): δ 1.82 [s, 3H, $\underline{C}H_3$]; 3.74 [s, 3H, N-$\underline{C}H_3$]; 4.78 [s, 1H, $\underline{C}H_2$]; 7.11-7.38 [m, 5H, aromatics] ppm. ^{13}C NMR ($CDCl_3$): δ 22.60 [$\underline{C}H_3$]; 44.98 [N-$\underline{C}H_3$]; 115.00 [$\underline{C}H_2$]; 125.00 [aromatic $\underline{C}$H]; 127.60 [aromatic $\underline{C}$H]; 129.60 [aromatic $\underline{C}$H]; 145.94, 146.82 [quaternary $\underline{C}$]; 190.82 [C=S] ppm.

4.2.1.9 (N,N-Diethyl)-3-methylprop-2-ene-thioamide, **9'**

The amide was prepared from acryloyl chloride (83% yield) as in 4.2.1.1 and was characterized by IR and ^{1}H NMR.

The thioamide was prepared from the amide (20mmol) by refluxing in toluene with Lawesson's reagent (12mmol) for 2h. Purification on a dry-packed silica column using hexanes:ether (9:1) gave a yellow oil. Yield from amide: 27%. B.p.218-220°C. M.S.: 157(M)$^+$ (m/e). ^{1}H NMR ($CDCl_3$): δ 1.19 [t, 3H, ^{3}J=7.2Hz, $NCH_2\underline{C}H_3$]; 1.24 [t, 3,H ^{3}J=7.2Hz, $NCH_2\underline{C}H_3$]; 2.01 [dd, 3H, ^{4}J=1.6,1.0Hz, $\underline{C}H_3$]; 3.55 [q, 2H, ^{3}J=7.2Hz, $N\underline{C}H_2CH_3$]; 3.93 [q, 2H, ^{3}J=7.2Hz, $N\underline{C}H_2CH_3$]; 4.81 [m, 1H, γ-$\underline{C}H_2$]; 4.86 [m, 1H, γ-$\underline{C}H_2$] ppm. ^{13}C NMR ($CDCl_3$): δ 11.03 [$NCH_2\underline{C}H_3$]; 14.10 [$NCH_2\underline{C}H_3$]; 45.02 [$N\underline{C}H_2CH_3$]; 47.10 [$N\underline{C}H_2CH_3$]; 111.09 [γ-$\underline{C}H_2$]; 146.79 [β-$\underline{C}$]; 201.45 [C=S] ppm.

4.2.1.10 (O-Ethyl)but-2-ene-thioate, **11'**

Ethyl crotonate (44mmol) was refluxed for 2h in a solution of Lawesson's reagent (44mmol) in p-xylene (40ml). The sample was cooled and placed directly on a dry-packed silica column and eluted with hexanes:ether (9:1). The volatile solvents were removed by rotary evaporation with no heating. Distillation of the remaining liquid gave an impure yellow oil. The oil was cleaned on a dry-packed silica column using hexanes:ether (9:1) and distilled to give a pure yellow oil. Yield from ester: 50%. B.p. 130°C/0.25mmHg [Lit. 60°C/10mmHg[42]]. M.S.: 130$(M)^+$ + higher mass peaks (m/e). ^{1}H NMR ($CDCl_3$): δ 1.39 [t, 6H, ^{3}J=7.1Hz, $CH_2\underline{C}H_3$]; 1.82 [dd, 3H, ^{3}J=6.9Hz, ^{3}J=1.7Hz, $\underline{C}H_3$]; 4.51 [q, 2H, ^{3}J=7.1Hz, $\underline{C}H_2CH_3$]; 6.38 [d, 1H, ^{3}J=15.6Hz, β-$\underline{C}$H]; 6.96 [dq, 1H, ^{3}J=15.6Hz, ^{4}J=6.6Hz, γ-$\underline{C}$H] ppm. ^{13}C NMR ($CDCl_3$): δ 13.78 [$CH_2\underline{C}H_3$]; 18.02 [$\underline{C}H_3$]; 67.55 [$\underline{C}H_2CH_3$]; 133.63 [β-$\underline{C}$H]; 140.46 [β-$\underline{C}$H]; 210.68 [C=S] ppm.

4.2.1.11 (O-Ethyl)-3-phenylpropenethioate, **10'**

Ethyl cinnamate (50mmol) was refluxed for 16h in a solution of Lawesson's reagent (30mmol) in toluene (150ml). After cooling the solution to room temperature, sufficient silica (~15g) was added to give a dry powder after removal of the solvent by rotary evaporation. The solid was added to the top of a dry-packed silica column and was eluted with hexanes:ether (9:1). The first band which was yellow in colour was collected and the solvent was removed by rotary evaporation leaving a yellow oil. Yield: from ester 70%. B.p. 135°C/10mmHg [Lit. 140°C/12mmHg[42]]. M.S.: 192$(M)^+$ (m/e). ^{1}H NMR ($CDCl_3$): δ 1.50 [t, 3H, ^{3}J=7.1Hz, $CH_2\underline{C}H_3$]; 4.63 [q, 2H, ^{3}J=7.1Hz, $\underline{C}H_2CH_3$]; 7.02 [d, 1H, ^{3}J=15.7Hz, γ-$\underline{C}$H]; 7.38 [m, 5H, aromatics]; 7.69 [d, 1H, ^{3}J=15.7Hz, β-$\underline{C}$H] ppm. ^{13}C NMR ($CDCl_3$): δ 13.79 [$CH_2\underline{C}H_3$]; 67.71 [$\underline{C}H_2CH_3$]; 113.80 [β-$\underline{C}$H]; 128.10 [

aromatic CH]; 128.69 [aromatic CH]; 129.99 [aromatic CH]; 140.09 [γ-CH]; 163.85 [quaternary aromatic C]; 209.87 [1C, C=S] ppm.

4.2.1.12 (O- Methyl)-4-methylpent-2-ene-thioate, **12'**

The ester was prepared by a Wittig reaction (79% yield) using $Ph_3P{=}CHC(O)OCH_3$ (123mmol) and methyl propanal (123mmol) in refluxing THF (300ml) for 22h.

The thioester (56mmol) was refluxed in a p-xylene solution of Lawesson's reagent (34mmol) for 22h. The sample was cooled and placed directly on a dry-packed silica column and eluted with hexanes:ether (9:1). The volatile solvents were removed by rotary evaporation with no heating. Distillation of the remaining liquid gave an impure orange oil. The oil was cleaned on a dry-packed silica column using hexanes:ether (9:1) and distilled to give an orange impure oil (0.8936g). B.p. 195-198°C. M.S.: 144$(M)^+$ + higher mass peaks (m/e). ^1H and ^{13}C NMR were impure.

4.2.1.13 (2',6',6'-trimethyl-cyclohex-2'-enyl)but-3-ene-2-thione **13'**

(2,6,6-trimethyl-cyclohex-2-enyl)but-3-en-2-one (24mmol) was refluxed for 1.5h in a toluene solution of Lawesson's reagent (15mmol). The solvent volume was reduced by rotary evaporation and the sample was cleaned on a dry-packed Florisil column using hexanes:ether (9:1). Solvent removal left a pale yellow oil which was distilled, B.p. 110°/2mmHg. The compound was spectroscopically impure and was used without further purification in preparing the organometallic complex.

4.2.1.14 Tetrahydropyrrole-(2-naphthyl)-thione **14'**

2-Naphthoyl chloride (26mmol) was stirred overnight in a solution of

tetrahydropyrrole (53mmol) in 5%KOH (150ml). The aqueous solution was extracted with ether (4×100ml) and the combined organic fraction was washed with distilled water (3×100ml). The organic layer was then dried over Na_2SO_4, filtered, and the solvent was removed by rotary evaporation leaving a yellow viscous oil 5.7330g (98% yield). The amide was characterized by IR and ^1H NMR.

The thioamide was prepared from the amide (20mmol) by refluxing in toluene with Lawesson's reagent (12mmol) for 21h. Purification on a dry-packed silica column using hexanes:ether (1:1) gave a pale yellow solid. Yield from amide: 14%. M.p. 173-175°C. M.S. 241$(M)^+$ (m/e). ^1H NMR ($CDCl_3$): δ 1.96 [m, 2H, $\underline{CH_2}$]; 2.10 [m, 2H, $\underline{CH_2}$]; 3.51 [t, 2H, ^3J=6.7Hz, N-$\underline{CH_2}$]; 4.02 [t, 2H, ^3J=6.5Hz, N-$\underline{CH_2}$]; 7.49 [m, 3H, aromatics]; 7.80 [m, 4H, aromatics] ppm.

4.2.1.15 <u>3,5,5-Trimethyl-2-cyclohexenethione</u> **15'**

Through a solution of 3,5,5-trimethyl-2-cyclohexen-1-one (6.7mmol) in ethanol cooled to 0°C was bubbled H_2S and HCl for 6h[82]. Ether (150ml) was added and the solution was transferred to a separatory funnel and more ether (200ml) was added. The ether layer was washed with distilled water (3×100ml) and was then dried over Na_2SO_4, filtered, and the solvent was removed leaving a red-purple oil. The oil was distilled and a purple oil was collected. Yield: 49%. B.p. 83°/5mmHg (lit. 103-106°C/20mmHg[96]). M.S.: 154$(M)^+$ (m/e). ^1H NMR (benzene-d_6): δ 0.73 [s, 6H, $\underline{CH_3}$]; 1.44 [d, 3H, ^4J=1.4Hz, γ-$\underline{CH_3}$]; 1.59 [s, 2H, $\underline{CH_2}$]; 1.99 [s, 2H, $\underline{CH_2}$]; 5.82 [q, 1H, ^4J=1.4Hz, β-$\underline{CH}$] ppm.

4.2.1.16 <u>(O-Methyl)-4,8-dimethylnon-3,7-diene-thioate</u>, **16'**

Linalyl acetate (40mmol), diisopropylethylamine (40mmol), sodium iodide (8mmol), triphenylphosphine (3.2mmol), $Pd_2(dba)_3$ (1.6mmol), and

ethanol were added to a stainless steel autoclave. The autoclave was charged with 430psi CO and heated to 60°C with stirring for 40h[88]. Purification by column chromatography on silica using hexanes:ether (1:1) and distillation gave the ester of compound **16'**. Yield: 24%.

The thioester was prepared from the ester by refluxing in toluene with Lawesson's reagent for 48h. Purification on a dry-packed silica column using hexanes:ether (1:1) gave a deep orange coloured oil. Yield: 7%. B.p.258°C. M.S: 226$(M)^+$ (m/e). ^{1}H NMR ($CDCl_3$): δ 1.24 [t, 3H, ^{3}J=7.0Hz, $OCH_2\underline{CH_3}$]; 1.54 [s, 3H, $\underline{CH_3}$]; 1.58 [s, 3H, $\underline{CH_3}$]; 1.62 [s, 3H, $\underline{CH_3}$]; 2.03 [m, 4H, $\underline{CH_2}$]; 3.00 [d, 2H, ^{3}J= 6.8Hz, β–$\underline{CH_2}$]; 4.50 [q, 2H, ^{3}J=7.0Hz, $O\underline{CH_2}CH_3$]; 5.07 [m, 1H, γ-$\underline{CH}$]; 5.30 [t, 1H, ^{3}J= 6.8Hz, $\underline{CH}$] ppm.

4.2.1.17 1-Piperoylpiperidine-thioamide, **17'**

The thioamide was prepared from its amide (20mmol) in refluxing toluene with Lawesson's reagent (12mmol) for 2h. Purification on a dry-packed silica column eluted with hexanes:ether (1:1) gave an orange solid which was recystallized from CH_2Cl_2/ether. Yield: 2.5%. M.p. 138-141°C. M.S.: 301$(M)^+$ (m/e). ^{1}H NMR (benzene-d_6): δ 0.6-1.4 [broad peaks, 8H]; 3.09 [m, 2H]; 4.16 [m, 2H]; 6.33-6.66 [6H, overlapping aromatics and olefinic CH]; 7.90 [dd, 1H, β or γ-$\underline{CH}$] ppm.

4.2.2 General Preparation Methods for Complexes **1**-**13**

Method A: To a stirred suspension of $[Fe_2(CO)_9]$ (1.5 eqv.) in freshly distilled benzene under flowing N_2 was added dropwise a solution of the

α,β–unsaturated thiocarbonyl (1 eqv.) in benzene. The mixture was stirred for 48h or until the formation of extraneous products as indicated by tlc. (Reactions which were carried out at 40°C generally required less time.) The solution was then filtered and the solvent was reduced by rotary evaporation. Column chromatography on silica using 9:1 hexanes:ether or on neutral alumina using hexane as eluent gave two fractions. The first fraction which was deep red in colour was characterized as $[S_2Fe_2(CO)_6]$ by IR and ^{13}C NMR. The second fraction which was orange in colour corresponded to the desired organometallic complex.

Method B: To a stirred solution of $[Fe(CO)_5]$ (1.2 eqv.) in degassed cyclohexane was added a cyclohexane solution of the α,β–unsaturated thiocarbonyl (1 eqv.). The solution was photolyzed and the reaction was followed by IR and tlc. Generally the reaction required 18h. The solution was then filtered and the solvent was reduced by rotary evaporation. Column chromatography on Florisil using hexane as eluent gave two fractions. The first fraction was orange in colour and corresponded to the desired organometallic complex. A second fraction was collected and identified as unreacted thiocarbonyl.

4.2.2.1 $[Fe(PhCH{=}CHC(S)NEt_2)(CO)_3]$, **1**

Complex **1** was isolated in 44% yield by method A.

Complex **1** was isolated in 22% yield by method B.

Purification on a silica column using hexanes as eluent gave an orange oily solid. Dissolving the latter in pentane and cooling to -78°C afforded an orange powder. Recrystallization from pentane at -30°C gave needle-like crystals. M.p. 67-70°C. Anal. calcd. for $C_{16}H_{17}NO_3SFe$: C, 53.48; H, 4.74; N, 3.90; S, 8.91%. Found: C, 53.80; H, 4.89; N, 3.94; S, 9.33%. M.S.:

303(M-2CO)$^+$, 275(M-3CO)$^+$, 219(Ligand)$^+$ (m/e). IR ($CHCl_3$) υ(CO): 2030(s), 1965(vs br) cm^{-1}. ^1H NMR ($CDCl_3$): δ 1.30 [t, 6H, ^3J=6.9Hz, $CH_2\underline{C}H_3$]; 3.47 [d, 1H, ^3J=7.7Hz, γ-$\underline{C}H$]; 3.55 [dq, 2H, ^3J=6.9Hz, ^2J=6.9Hz, $\underline{C}H_2CH_3$]; 3.77 [dq, 2H, ^3J=6.9Hz, ^2J=6.9Hz, $\underline{C}H_2CH_3$]; 5.04 [d, 1H, ^3J=7.7Hz, β-$\underline{C}H$]; 7.25 [m, 5H, aromatics] ppm. ^{13}C NMR ($CDCl_3$): δ 11.59 [$CH_2\underline{C}H_3$]; 45.76 [$\underline{C}H_2CH_3$]; 52.42 [γ-$\underline{C}H$]; 63.93 [β-$\underline{C}H$]; 125.74 [aromatic $\underline{C}H$]; 126.20 [aromatic $\underline{C}H$]; 128.51 [aromatic $\underline{C}H$]; 142.30 [quaternary aromatic C]; 161.69 [C=S]; 210.5 [C=O] ppm.

4.2.2.2 $\underline{[Fe(PhCH{=}C(Ph)C(S)NEt_2)(CO)_3]}$, **2**

Complex **2** was isolated in 22% yield using method A at 40°C.

Purification on a silica column using hexanes:ether (9:1) gave an orange oily solid. An orange powder was obtained from pentane at -78°C. Recrystallization from pentane at -30°C gave needle-like crystals. M.p. 105-108°C. Anal. calcd. for $C_{22}H_{21}NO_3SFe$: C, 60.69; H, 4.83; N, 3.22; S, 7.36%. Found: C, 61.12; H, 5.20; N, 3.34; S, 7.17%. M.S.: 295(Ligand)$^+$ (m/e). IR ($CHCl_3$) υ(CO): 2020(s), 1950(vs br) cm^{-1}. ^1H NMR (Benzene-d_6): δ 0.36 [t, 3H, ^3J=7.2Hz, $CH_2\underline{C}H_3$]; 1.11 [t, 3H, ^3J=7.1Hz, $CH_2\underline{C}H_3$]; 3.02 [m, 2H, $\underline{C}H_2CH_3$]; 3.66 [dq, 1H, ^3J=7.2Hz, ^2J=7.1Hz, $\underline{C}H_2CH_3$]; 3.94 [dq, 1H, ^3J=7.2Hz, ^2J=7.1Hz, $\underline{C}H_2CH_3$]; 5.17 [s, 1H, γ-$\underline{C}H$]; 7.14 and 7.64 [m, 10H, aromatics] ppm. ^{13}C NMR ($CDCl_3$): δ 10.51 [$CH_2\underline{C}H_3$]; 12.91 [$CH_2\underline{C}H_3$]; 45.02 [$\underline{C}H_2CH_3$]; 47.66 [$\underline{C}H_2CH_3$]; 123.72, 126.02, 127.75, 128.02, 128.27, 128.58, 129.03, 129.55 [aromatic $\underline{C}H$]; 135.57, 138.31, 141.20 [quaternary aromatic C]; 141.20 [C=S]; 210.0 [C=O] ppm.

4.2.2.3 [Fe(PhCH=CHC(S)N(Ph)(CH_2CHCH_2))($CO)_3$], **3**

Complex **3** was isolated in 66% yield using method B.

Purification on a neutral alumina column using hexanes:ether (8:2) afforded an orange solid. Recrystallization from pentane at -30°C resulted in needle-like crystals. M.p. 85°C (dec.). Anal. calcd. for $C_{21}H_{21}NO_3SFe$: C, 60.14; H, 4.06; N, 3.34; S, 7.64%. Found: C, 60.57; H, 4.14; N, 3.21; S, 7.13%. M.S.: 362(M-2CO)$^+$, 334(M-3CO)$^+$, 278(Ligand)$^+$ (m/e). IR ($CHCl_3$) υ(CO): 2045(s), 1983(vs br) cm^{-1}. ^{1}H NMR (Benzene-d_6): δ 3.63 [d 6H, ^{3}J=8.2Hz, γ-CH]; 3.96 [dd, 1H, ^{3}J=15.4Hz, ^{2}J=6.1Hz, NCH_2CHCH_2]; 4.57 [dd, 1H, ^{3}J=15.4Hz, ^{2}J=6.1Hz, NCH_2CHCH_2]; 4.90 [m, 2H, NCH_2CHCH_2]; 5.11 [d, 1H, ^{3}J=8.2Hz, β-CH]; 5.69 [ddt, 1H, ^{3}J=15.4Hz, ^{3}J=6.0Hz, NCH_2CHCH_2]; 6.88 [m, 2H, aromatics]; 7.03 [s, 5, aromatics] ppm. ^{13}C NMR (Benzene-d_6): δ 57.28 [NCH_2CHCH_2]; 60.16 [γ-CH]; 65.30 [β-CH]; 118.79 [NCH_2CHCH_2]; 126.51, 127.25, 128.03, 128.33, 128.94, 130.39, 131.86 [aromatic CH]; 141.30, 143.61 [quaternary aromatic C]; 155.85 [C=S]; 209.43 [C=O] ppm.

4.2.2.4 [Fe(MeCH=CHC(S)NEt_2)($CO)_3$], **4**

Complex **4** was isolated in 29% yield using method A.

Complex **4** was isolated in 22% yield using method B.

Purification by column chromatography on neutral alumina using hexanes afforded an orange oil. An orange solid precipitated from pentane at -78°C. Crystal growth was unsuccessful. M.p. 36-39°C. Anal. calcd. for $C_{11}H_{15}NO_3SFe$: C, 44.44; H, 5.05; N, 4.71; S, 10.71%. Found: C, 44.31; H, 5.20; N, 4.75; S, 10.72%. M.S.: 297(M)$^+$, 269(M-1CO)$^+$, 241(M-2CO)$^+$, 213(M-3CO)$^+$, 157(Ligand)$^+$ (m/e). IR ($CHCl_3$) υ(CO): 2025(s), 1955(vs br) cm^{-1}. ^{1}H NMR (Benzene-d_6): δ 0.74 [t, 6H, ^{3}J=7.1Hz, CH_2CH_3]; 1.44 [d, 3H, ^{4}J=6.3Hz, CH_3]; 2.53 [dq, 1H, ^{3}J=7.3Hz, ^{4}J=6.3Hz, γ-CH]; 2.70 [2 overlapping

q, 2H, ^3J=7.1Hz, $\underline{C}H_2CH_3$]; 3.04 [2 overlapping q, 2H, ^3J=7.1Hz, $\underline{C}H_2CH_3$]; 4.10 [d, 1H, ^3J=7.3Hz, β-$\underline{C}H$] ppm. ^{13}C NMR ($CDCl_3$): δ 11.48 [$CH_2\underline{C}H_3$]; 19.99 [$\underline{C}H_3$]; 45.46 [$\underline{C}H_2CH_3$]; 58.78 [γ-$\underline{C}H$]; 59.85 [β-$\underline{C}H$]; 159.69 [C=S]; 210.4 [C=O] ppm.

4.2.2.5 $\underline{[Fe(C_2H_5)\overline{C}H=C(CH_3)C(S)NEt_2)(CO)_3]}$, **5**

Complex **5** was isolated in 5.5% yield using method A.

Complex **5** was isolated in 49% yield using method B.

Purification by column chromatography on neutral alumina using hexanes resulted in isolation of an orange oil. Orange thermally-sensitive crystals were obtained at 0°C. When warmed to room temperature the solid melted and decomposed. M.S.: 297$(M-1CO)^+$, 269$(M-2CO)^+$, 241$(M-3CO)^+$, 185$(Ligand)^+$ (m/e). IR ($CHCl_3$) υ(CO): 2050(s), 2020(s sh), 2010(s), 1980(s sh), 1960(vs) cm^{-1}. ^1H NMR (Benzene-d_6): δ 0.74 [m, 9H, $CH_2\underline{C}H_3$, β-$\underline{C}H_3$]; 1.13 [m, 1H, β-$\underline{C}H$]; 1.48 [s, 1H, γ-$\underline{C}H_3$]; 2.81 [m, 3H, $\underline{C}H_2CH_3$]; 2.95 [dq, 1H, ^3J=7.1Hz, ^2J=6.7Hz, $\underline{C}H_2CH_3$] ppm. ^{13}C NMR (Benzene-d_6): δ 11.75 [$CH_2\underline{C}H_3$]; 14.72 [$CH_2\underline{C}H_3$]; 27.00 [$\underline{C}H_3$]; 27.00 [$\underline{C}H_3$]; 44.32 [$\underline{C}H_3$]; 44.95 [$\underline{C}H_2CH_3$]; 46.22 [γ-$\underline{C}H$]; 92.52 [β-$\underline{C}$]; 143.01 [C=S]; 211.4 [C=O] ppm.

4.2.2.6 $\underline{[Fe_2(Me_2\overline{C}=CHC(S)NEt_2)(CO)_6]}$, **6**

Preparation by method A at room temperature gave **6** in only 2% yield.

Preparation by method B afforded **6** in 67% yield.

Purification by column chromatography on neutral alumina using hexanes:ether (7:3) gave an orange oil. The oil could be crystallized at 0°C forming a thermally-sensitive orange solid. When warmed to room temperature the solid melted and decomposed. M.S.: 451$(M)^+$, 423 $(M-1CO)^+$, 395 $(M-2CO)^+$, 367 $(M-3CO)^+$, 339 $(M-4CO)^+$, 171$(Ligand)^+$ (m/e). IR ($CHCl_3$) υ(CO):

υ(CO): 2050(m), 2010(s), 1985(s), 1960(s sh), 1940(sh m) cm^{-1}. ^1H NMR (Benzene-d_6): δ 0.47 [t, 3H, ^3J=7.2Hz, $CH_2\underline{C}H_3$]; 0.70 [s, 3H, $\underline{C}H_3$]; 0.96 [t, 3H, ^3J=7.2Hz, $CH_2\underline{C}H_3$]; 1.73 [s, 3H, $\underline{C}H_3$]; 2.41 [m, 2H, $\underline{C}H_2CH_3$]; 2.63 [s, 1H, β-$\underline{C}H$]; 3.33 [dq, 1H, ^3J=6.8Hz, ^2J=6.7Hz, $\underline{C}H_2CH_3$]; 3.65 [dq, 1H, ^3J=6.8Hz, ^2J=6.7Hz, $\underline{C}H_2CH_3$] ppm. ^{13}C NMR (Benzene-d_6): δ 12.94 [$CH_2\underline{C}H_3$]; 13.01 [$CH_2\underline{C}H_3$]; 30.98 [$\underline{C}H_3$]; 40.32 [$\underline{C}H_3$]; 46.02 [$\underline{C}H_2CH_3$]; 49.55 [β-$\underline{C}H$]; 46.02 [$\underline{C}H_2CH_3$]; 54.45 [$\underline{C}H_2CH_3$] ppm.

4.2.2.7 [Fe(Me)CH=CHC(S)N(Ph)(Me))$(CO)_3$], **7**

Complex **7** was isolated in 60% yield using method B.

Purification by column chromatography on neutral alumina using hexanes:ether (8:2) gave an orange oil. An orange solid precipitated from pentane at -78°C. M.p. 39-41°C. Anal. calcd. for $C_{14}H_{13}NO_3SFe$: C, 50.57; H, 3.93; N, 4.23%. Found: C, 50.35; H, 4.18; N, 4.28%. M.S.: 331$(M)^+$, 303$(M-1CO)^+$, 275$(M-2CO)^+$, 247$(M-3CO)^+$, 191$(Ligand)^+$ (m/e). IR ($CHCl_3$) υ(CO): 2025(s), 1975(vs br) cm^{-1}. ^1H NMR (Benzene-d_6): δ 1.11 [d, 3H, ^3J=6.1Hz, γ-$\underline{C}H_3$]; 2.28 [dq, 1H, ^3J=7.8Hz, ^3J=6.1Hz, γ-$\underline{C}H$]; 2.98 [s, 3H, N-$\underline{C}H_3$]; 4.41 [d, 1H, ^3J=7.8Hz, β-$\underline{C}H$]; 7.02 [m, 5H, aromatics] ppm. ^{13}C NMR(Benzene-d_6): δ 19.24 [$\underline{C}H_3$]; 42.21 [N-$\underline{C}H_3$]; 60.85 [β-$\underline{C}H$]; 67.59 [γ-$\underline{C}H$]; 125.93 [aromatic-$\underline{C}H$]; 127.34 [aromatic-$\underline{C}H$]; 130.24 [aromatic-$\underline{C}H$]; 145.37 [aromatic quaternary $\underline{C}$]; 152.95 [C=S]; 209.98 [C=O] ppm.

4.2.2.8 [Fe(CH_2=C(Me)C(S)N(Ph)(Me))$(CO)_3$], **8**

Complex **8** was isolated in 58% yield using method B.

Purification by column chromatography on neutral alumina using hexanes:ether (8:2) gave an orange oil. An orange solid precipitated from pentane at -78°C. M.p. 74-76°C. Anal. calcd. for $C_{14}H_{13}NO_3SFe$: C, 50.76; H,

3.93; N, 4.23; S,9.67%. Found: C, 50.71; H, 4.13; N, 3.91; S,9.79. M.S. CI: 332(M+1)$^+$, 276(M+1-2CO)$^+$, 248(M+1-3CO)$^+$, 192(Ligand+1)$^+$ (m/e) . IR ($CHCl_3$) υ(CO): 2060(s), 1990(vs br) cm^{-1}. ^1H NMR (Benzene-d_6): δ 1.44 [s, 3H, $\underline{C}H_3$]; 1.62 [s, 1H, $\underline{C}H_2$]; 1.93 [s, 1H, $\underline{C}H_2$]; 3.12 [s, 3H, N-$\underline{C}H_3$]; 6.72-6.96 [m, 5H, aromatics] ppm. ^{13}C NMR(Benzene-d_6): δ 23.98 [$\underline{C}H_3$]; 43.22 [N-$\underline{C}H_3$]; 51.45 [$\underline{C}H_2$]; 92.85 [β-$\underline{C}$]; 123.04 [aromatic-$\underline{C}$H]; 123.90 [aromatic-$\underline{C}$H]; 129.54 [aromatic-$\underline{C}$H]; 148.96 [C=S]; 208.20 [3C, C=O] ppm.

4.2.2.9 $\underline{[Fe(CH_2=C(Me)C(S)NEt_2)(CO)_3]}$, **9**

Complex **9** was isolated in 30% yield using method B.

Purification by column chromatography on neutral alumina using hexanes:ether (8:2) afforded an orange oil which was crystallized from pentane at -78°C. M.p. 23°C. M.S.:297(M)$^+$, 269(M-1CO)$^+$, 241(M-2CO)$^+$, 213(M-3CO)$^+$, 157(Ligand)$^+$ (m/e). IR ($CHCl_3$) υ(CO): 2040(s), 1965(vs br) cm^{-1}. ^1H NMR (Benzene-d_6): δ 0.74 [t, 6H, ^3J=7.1Hz,$NCH_2\underline{C}H_3$]; 1.75 [s, 3H, $\underline{C}H_3$]; 2.21 [s, 1H, γ-$\underline{C}H_2$]; 2.28 [s, 1H, γ-$\underline{C}H_2$]; 2.91 [dq, 2H, ^3J=7.1Hz, ^2J=7.1Hz, $N\underline{C}H_2CH_3$]; 3.01 [dq, 2H, ^3J=7.1Hz, ^2J=7.1Hz, $N\underline{C}H_2CH_3$] ppm. ^{13}C NMR(Benzene-d_6): δ 12.85 [$NCH_2\underline{C}H_3$]; 26.11 [$\underline{C}H_3$]; 46.47 [$N\underline{C}H_2CH_3$]; 54.07 [γ-$\underline{C}H_2$]; 67.30 [β-$\underline{C}$]; 178.07 [$\underline{C}$=S]; 218.77 [3C, C=O] ppm.

4.2.2.10 $\underline{[Fe(PhCH=CHC(S)OEt)(CO)_3]}$, **10**

Complex **10** was isolated in 51% yield using method A.

Purification by column chromatography on Florisil using hexanes:ether (9:1) gave an orange oil which crystallized from pentane at -78°C. M.S.: 332(M)$^+$, 304(M-1CO)$^+$, 276(M-2CO)$^+$, 248(M-3CO)$^+$, 192(Ligand)$^+$ (m/e). Anal. calcd. for $C_{14}H_{12}NO_4SFe$: C, 50.60; H, 3.61; N, 9.64%. Found: C, 50.84; H,

3.67; N, 9.94%.IR ($CHCl_3$) υ(CO): 2050(s), 1980(vs br) cm^{-1}. ^1H NMR ($CDCl_3$): δ 1.40 [overlapping dd, 3H, ^3J=7.1Hz, $CH_2\underline{C}H_3$]; 2.70 ppm [d, 1H, ^3J=8.8Hz, γ-$\underline{C}H$]; 3.95 [dq, 1H, ^3J=7.1Hz, ^2J=3.4Hz, $\underline{C}H_2CH_3$]; 6.18 [d, 1H, ^3J=8.8Hz, β-$\underline{C}H$]; 7.27 [m, 5H, aromatics] ppm. ^{13}C NMR ($CDCl_3$): δ 14.36 [$CH_2\underline{C}H_3$]; 63.30 [γ-$\underline{C}H$]; 67.24 [$\underline{C}H_2CH_3$]; 71.53 [β-$\underline{C}H$]; 126.55 [aromatic $\underline{C}H$]; 126.77 [quaternary aromatic $\underline{C}$]; 128.71 [aromatic $\underline{C}H$]; 139.08 [aromatic $\underline{C}H$]; 155.00 [C=S]; 207.87 [C=O] ppm.

4.2.2.11 $\underline{[Fe(Me)CH{=}CHC(S)OEt)(CO)_3]}$, **11**

Complex **11** was isolated in 36.5% yield using method A.

Purification by column chromatography on silica using hexanes:ether (9:1) resulted in an orange oil which could not be solidified. M.S.: $270(M)^+$, $242(M\text{-}1CO)^+$, $214(M\text{-}2CO)^+$, $186(M\text{-}3CO)^+$,$130(Ligand)^+$ (m/e). IR ($CHCl_3$) υ(CO): 2025(s), 1993(vs br) cm^{-1}. ^1H NMR (Benzene-d_6): δ 0.99 [t, 3H, ^3J=7.1Hz, $CH_2\underline{C}H_3$]; 1.06 [d, 3H, ^3J=6.4Hz, γ-$\underline{C}H_3$]; 1.45 [dq, 1H, ^3J=8.3Hz, ^3J=6.4Hz, β-$\underline{C}H$]; 3.68 [dq, 1H, ^3J=7.1Hz, ^3J=7.0Hz, $\underline{C}H_2CH_3$]; 3.97 [dq, 1H, ^3J=7.1Hz, ^3J=7.0Hz, $\underline{C}H_2CH_3$]; 5.16 [d, 1H, ^3J=8.3Hz, α-$\underline{C}H$] ppm. ^{13}C NMR (Benzene-d_6): δ 14.45 [$CH_2\underline{C}H_3$]; 18.49 [γ-$\underline{C}H_3$]; 59.84 [γ-$\underline{C}H$]; 67.22 [$\underline{C}H_2CH_3$]; 77.79 [γ-$\underline{C}H$]; 155.52 [C=S]; 209.00 [C=O] ppm.

4.2.2.12 $\underline{[Fe(Me)_2CHCH{=}CHC(S)OMe)(CO)_3]}$, **12**

Complex **12** was isolated in 5.5% yield using method B.

Purification by column chromatography on neutral alumina using hexanes afforded an orange oil which could not be solidified. M.S.: $284(M)^+$, $256(M\text{-}1CO)^+$, $228(M\text{-}2CO)^+$, $200(M\text{-}3CO)^+$, $144(Ligand)^+$ (m/e). IR ($CHCl_3$) υ(CO): 2060(s), 2040(m sh), 1995(vs br) cm^{-1}. ^1H NMR (Benzene-d_6): δ 0.81 [d, 3H, ^3J=6.1Hz, $CH(\underline{C}H_3)_2$]; 0.93 [d, 3H, ^3J=6.1Hz, $CH(\underline{C}H_3)_2$]; 1.30 [m, 1H,

^{3}J=8.3Hz, C<u>H</u>(CH$_3$)$_2$]; 1.57 [overlapping dd, 1H, ^{3}J=8.4Hz, γ-C<u>H</u>]; 3.36 [s, 3H, OC<u>H</u>$_3$]; 5.25 [d, 1H, ^{3}J=8.4Hz, β-C<u>H</u>] ppm. ^{13}C NMR (Benzene-d$_6$): δ 24.93 [CH(C<u>H</u>$_3$)$_2$]; 26.29 [CH(C<u>H</u>$_3$)$_2$]; 33.92 [C<u>H</u>(CH$_3$)$_2$]; 57.64 [OC<u>H</u>$_3$]; 75.12 [γ-C<u>H</u>]; 75.88 [β-C<u>H</u>]; 157.15 [C=S]; 207.95, 210.72 [C=O] ppm.

4.2.2.13 Complex **13**

Preparation was by method B using impure thioamide.

Purification on alumina using hexanes afforded an orange powder. This powder could not be recrystallized to give a crystalline solid. M.p. 92-94°C. Anal. calcd. for $C_{16}H_{20}O_3SFe$: C, 55.17; H, 5.75; S, 9.20%. Found: C, 55.55; H, 56.35; S, 8.90%. M.S.: 348(M)$^+$, 320(M-1CO)$^+$, 292(M-2CO)$^+$, 264(M-3CO)$^+$, 208(Ligand)$^+$ (m/e). IR ($CHCl_3$) υ(CO): 2060(s), 2005(s), 1983(s) cm^{-1}. ^{1}H NMR ($CDCl_3$): δ 0.89 [s, 3H, C(C<u>H</u>$_3$)$_2$]; 0.98 [s, 3H, C(C<u>H</u>$_3$)$_2$]; 1.37 [d, 1H, ^{3}J=10.9Hz, C<u>H</u>]; 1.54 [s, 2H, C<u>H</u>$_2$]; 1.67 [dd, 1H, ^{3}J=9.6Hz, γ-C<u>H</u>]; 2.05 [m 2H, C<u>H</u>$_2$]; 2.72 [s, 3H, CSC<u>H</u>$_3$]; 5.39 [s, 1H, olefinC<u>H</u>]; 5.54 [d, 1H, ^{3}J=9.6Hz, β-C<u>H</u>] ppm. ^{13}C NMR ($CDCl_3$): δ 23.60 [C<u>H</u>$_2$]; 25.23 [C<u>H</u>$_3$]; 26.45 [C(C<u>H</u>$_3$)$_2$]; 27.57 [CSC<u>H</u>$_3$]; 29.78 [C(C<u>H</u>$_3$)$_2$]; 30.05 [C<u>H</u>$_2$]; 35.08 [C(CH$_3$)$_2$]; 53.61 [C<u>H</u>]; 78.18 [γ-C<u>H</u>]; 96.32 [olefinic C<u>H</u>]; 22.64 [β-C<u>H</u>]; 113.78 [C<u>H</u>]; 134.56 [C=S]; 204.29, 209.47, 212.43 [C=O] ppm.

4.3 Experimental Details for Chapter 3

4.3.1 [Fe(PhCH=CHC(S)NEt$_2$)(CO)$_2$(PPh$_3$)] 17

Triphenylphosphine (0.84mmol) was added to a stirred solution of complex **1** (0.84mmol) in dry benzene (50ml). The solution was refluxed under

N_2 for 2h, cooled the solution to room temperature, and the solvent was reduced by rotary evaporation. The sample was purified on a neutral alumina column using hexanes:ether (8:2) and afforded an orange solid after solvent removal. Yield 26%. M.p. 95°C decomp. Anal. calcd. for $C_{33}H_{32}NO_2PSFe$: C, 66.78; H, 5.40; S, 2.36%. Found: C, 66.67; H, 5.47; S, 2.27%. M.S.: CI only $Fe(CO)_2(PPh_3)$ fragment and free ligand. EI gave only PPh_3 (m/e). IR ($CHCl_3$) υ(CO): 1977(vs br), 1917(s br) cm^{-1}. ^1H NMR (Benzene-d_6): δ 0.99 [t, 6H, ^3J=7.1Hz, $CH_2\underline{CH_3}$]; 2.59 [apparent t, 1H, ^3J=8.1Hz, γ-$\underline{CH}$]; 2.94 [dq, 1H, ^3J=7.1Hz, ^2J=7.0Hz, $\underline{CH_2}CH_3$]; 3.48 [dq, 1H, ^3J=7.1Hz, ^2J=7.0Hz, $\underline{CH_2}CH_3$]; 5.23 [dd, 1H, ^3J=8.1Hz, ^3J(HP)=2.7Hz, β-$\underline{CH}$]; 6.81-7.58 [m, 20H, aromatics] ppm. ^{13}C NMR (Benzene-d_6): δ 11.89 [$CH_2\underline{C}H_3$]; 45.56 [$\underline{C}H_2CH_3$]; 59.38 [γ-$\underline{C}$H]; 66.18 [β-$\underline{C}$H]; 124.79, 126.12, 127.86, 128.53, 128.73, 128.82, 129.55, 133.49, 133.63, 133.99, 134.25 [aromatic CH]; 136.33, 136.82, 144.92 [quaternary aromatic C]; 152.87 [C=S]; 211.24 [^2J(PC)=5.6Hz, C=O]; 215.50 [^2J(PC)=12.0Hz, C=O] ppm. ^{31}P NMR (Benzene-d_6): δ 55.95 ppm [s] major species; 25.27 [s] minor species.

4.3.2 $\underline{[Fe(PhCH{=}CHC(S)N(Ph)(Me))(CO)_2(PPh_3)]}$, **18**

A solution of PPh_3 (0.90mmol) in THF (4ml) was added to a stirred degassed solution of complex **7** (0.90mmol) in C_6H_{12} (16ml). The solution was photolyzed for 22h. The solvent was reduced by rotary evaporation and the solution was chromatographed on neutral alumina using hexanes:ether (6:4). Recrystallization from ether/hexanes at -10°C resulted in the formation of deep orange coloured crystals. Yield 85%. M.p. 134-137°C. M.S.: 537$(M\text{-}PPh_3)^+$, 481$(M\text{-}PPh_3\text{-}2CO)^+$, 191$(Ligand)^+$ (m/e). IR ($CHCl_3$) υ(CO): 1975(s), 1914(s) cm^{-1}. ^1H NMR (Benzene-d_6): δ 0.96 [d, 3H, ^3J=6.1Hz, γ-$\underline{CH_3}$]; 1.32 [m, 1H, ^3J=6.6, 6.1Hz, β-$\underline{CH}$]; 3.33 [s, 3H, N-$\underline{CH_3}$]; 4.75 [d, 1H, ^3J=6.6Hz, β-$\underline{CH}$]; 7.04 [

m, 13H, aromatics]; 7.30 [m, 2H, aromatics]; 7.79 [m, 5H, N-aromatics] ppm. ^{13}C NMR (Benzene-d_6): δ 18.44 ppm [$\underline{C}H_3$]; 42.22 [N-$\underline{C}H_3$]; 61.92 [γ-$\underline{C}H$]; 72.86 [β-$\underline{C}H$]; 126.34, 126.70, 126.96, 129.64, 130.02, 131.53, 132.33, 132.45, 132.69, 132.85, 133.36, 133.50 [aromatic-$\underline{C}H$]; 136.80, 137.29 [aromatic quaternary $\underline{C}$]; 147.02 or 147.54 [C=S]; 216.53, 210.39 [C=O] ppm. ^{31}P NMR (Benzene-d_6): δ 61.99 ppm [s] major species; 25.55 [s] minor species.

4.3.3 [Fe(PhCH=CHC(S)OEt)$(CO)_2$$(PPh_3)$], **19**

Triphenylphosphine (1.60mmol) was added to a stirred solution of complex **10** (1.60mmol) in dry benzene (50ml). The solution was refluxed under N_2 for 2h. After cooling the solution to room temperature, the solvent was reduced by rotary evaporation. The sample was purified on a neutral alumina column using hexanes:ether (8:2) affording an orange solid after solvent removal. Yield 76%. M.p. 143-146°C. M.S.: 262$(PPh_3)^+$ (m/e). IR ($CHCl_3$) υ(CO): 1995(s), 1939(s) cm^{-1}. ^1H NMR (Benzene-d_6): δ 1.17 [t, 3H, ^3J=7.1Hz, $CH_2\underline{C}H_3$]; 2.02 [m, 1H, γ-$\underline{C}H$]; 4.08 [m, 1H, $\underline{C}H_2CH_3$]; 4.31 [m, 1H, $\underline{C}H_2CH_3$]; 6.23 [d, 1H, ^3J=9.0Hz , β-$\underline{C}H$]; 6.96 [s, 13H, aromatics]; 6.54 [s, 2H, aromatics]; 7.46 [m, 5H, aromatics] ppm. ^{13}C NMR (Benzene-d_6): δ 14.80 [$CH_2\underline{C}H_3$]; 65.67 [γ-$\underline{C}H$]; 66.76 [$\underline{C}H_2CH_3$]; 75.62 [β-$\underline{C}H$]; 125.51, 126.52, 128.56, 129.90, 133.40, 133.53 [aromatic $\underline{C}H$]; 135.95, 142.00 [quaternary aromatic $\underline{C}$]; 151.45 [C=S]; 208.14, 212.99 [C=O] ppm. ^{31}P NMR (Benzene-d_6): δ 54.33 ppm [s].

Ligand removal

4.3.4 Using H_2O_2 on complexes **1**, **4**, **10**

To a stirred solution of the complex (0.3mmol) in CH_3COOH (5ml)

cooled to 5-10°C was added dropwise a 30% aqueous solution of H_2O_2 (0.5ml). The solution was stirred for 10min followed by the addition of CH_2Cl_2 (30ml). The mixture was washed with distilled water (3x50ml). The organic layer was dried over $MgSO_4$, filtered, and the solvent was removed by rotary evaporation. Purification on an alumina column using ether gave the α,β-unsaturated amide or ester in nearly quantitative yield.

4.3.5 Using mcpba on complexes **1, 4**

To a stirred solution of the complex (0.3mmol) in ethyl acetate (5ml) cooled to -30°C was added dropwise a solution of mcpba (0.6mmol) in ethyl acetate. The solution was warmed to room temperature and was stirred for 1h. The solvent was reduced by rotary evaporation and purification on an alumina column using ethyl acetate gave α,β-unsaturated thioamide.

4.3.6 Using $[Me_3NO]$ on complexes **1, 4, 10**

To a stirred solution of the complex (0.5mmol) in THF (10ml) was added a solution of $[Me_3NO]$ (0.5mmol) in $CHCl_3$ (3ml). The solution was heated to 50°C under N_2 for 24h. The solvent was then reduced and purification on an alumina column using ether resulted in a mixture of thioamide and amide.

4.3.7 Using $[Ce(NH_4)_2(NO_3)_6]$ on complexes **1, 4, 10**

To a stirred aqueous acetone solution of the complex cooled to 0°C was added $[Ce(NH_4)_2(NO_3)_6]$ in small portions until bubbling ceased. The solution was then extracted with ether (3x100ml) and the combined organic layers were washed with water (3x100ml). After drying the organic layer over $MgSO_4$, the solution was filtered and the solvent was removed leaving a yellow oil of thioamide or thioester. NOTE: At temperatures >0°C, during the addition of

$[Ce(NH_4)_2(NO_3)_6]$, a substantial amount of thioamide or thioester was converted to the amide or ester.

Sulphine Complex Formation

4.3.8 [Fe(PhCH=CHC(S=O)OEt)(CO)$_3$] **20**

A 30% solution of H_2O_2 (0.5ml) was added dropwise to a stirred solution of thioester **10** (0.6mmol) in CH_3COOH (3ml) cooled to 5-10°C. After stirring for 1h, $CHCl_3$ (50ml) was added and the organic layer was washed with H_2O (1x50ml), saturated $NaHCO_3$ (2x30ml), 5% $Na_2S_2O_3$ (1x30ml), and again with H_2O (1x30ml). The organic layer was dried over $MgSO_4$, filtered, and the solvent was removed by rotary evaporation leaving a yellow oil. Crystals were obtained from ethyl acetate/pentane at 0°C. Yield 69.5%. M.p. 50°C decomp. M.S.: EI highest mass 306. CI 333(M-16+1)$^+$, 193(Ligand)$^+$, 177(ligand-O)$^+$ (m/e). IR ($CHCl_3$) υ(CO): 2070(s), 2015(s), 1998(sh). υ(SO):1010(m br) cm^{-1}. ^1H NMR (Acetone-d_6): δ 1.39 [t, 3H, ^3J=7.0Hz, $OCH_2\underline{C}H_3$]; 3.96 [dq, 1H, ^3J=7.0Hz, ^2J=6.8Hz, $O\underline{C}H_2CH_3$]; 4.19 [dq, 1H, ^3J=7.0Hz, ^2J=6.8Hz, $O\underline{C}H_2CH_3$]; 4.40 [d, 1H, ^3J=9.5Hz, β-<u>C</u>H]; 7.09 [d, 1H, ^3J=9.5Hz, γ-<u>C</u>H]; 7.30-7.62 [m, 5H, aromatics] ppm. ^{13}C NMR (Benzene-d_6): δ 14.84 [$OCH_2\underline{C}H_3$]; 62.65 [$OCH_2\underline{C}H_3$]; 67.79 [γ-<u>C</u>H]; 84.17 [β-<u>C</u>H]; 126.90 [aromatic <u>C</u>H]; 127.98 [aromatic <u>C</u>H]; 129.03 [aromatic <u>C</u>H]; 137.23 [quaternary aromatic <u>C</u>]; 144.39 [C=S]; 205.43 [C=O] ppm.

Nucleophilic Substitution

4.3.9 General anion reactions:

Method A: LDA was prepared at -78°C under nitrogen by adding ^{n}butyllithium (0.20mL; 0.50mmol) to a solution of diisopropylamine (0.07mL; 0.50mmol) in freshly distilled THF (5mL). To the solution was added the various carbon acids (0.045mL; 0.50mmol) and the mixture was stirred for 10 minutes before adding dropwise a solution of organometallic complex (0.45mmol) in THF (2mL). The solution was stirred for 2h at -78°C under a flow of nitrogen.

Method B: LDA was generated as in method A. After addition of the organometallic complex to the solution, the solution was warmed to room temperature and was stirred for 2h under flowing nitrogen.

4.3.10 General quenching methods:

Method A: After 2h of stirring, the solution was cooled to -78°C and excess trifluoroacetic acid (0.17mL; 5eqv) was added. The solution was allowed to warm to room temperature and it was then added to an aqueous acetone mixture (1:1) which was cooled to 0°C. Solid ceric ammonium nitrate was added in small portions, allowing sufficient time in between additions to allow the bubbling to cease. After there was no further bubbling observed, the aqueous acetone solution was extracted with ether (3X100mL). The combined ether layer was washed with water (3X100mL), dried over $MgSO_4$, filtered, and solvent was removed by rotary evaporation. Products were purified by preparatory tlc on alumina using hexanes/ether (1:1) as eluent.

Method B: After 2h of stirring, the solution was cooled to -78°C and excess tert-butyl bromide (0.07mL; 1.5eqv) was added and the solution was left to warm to room temperature. The solvent was reduced by rotary evaporation and the remaining solution was purified by column chromatography on neutral alumina using hexanes to remove any unreacted complex followed by ethyl

acetate to remove the product organic compounds. Further purification was performed by preparatory tlc on alumina using hexanes/ether (1:1) as eluent.

4.3.11 [MeC(O)CH_2CH(Me)C(O)N(Ph)(Me)] **18'**

Anion reaction method A.

Quenching procedure B.

A yellow oil was obtained after purification on a silica tlc plate using hexanes/ether (1:1). Yield 4%. M.S.: 235$(M)^+$, 220$(M\text{-}CH_3)^+$, 192$(M\text{-}CO)^+$ (m/e). IR ($CHCl_3$) υ(CO): 1715(s) cm^{-1}. ^1H NMR ($CDCl_3$): δ 1.01 [d, 3H, ^3J=6.8Hz, $CHCH_3$]; 2.09 [s, 3H, CH_3]; 2.34 [dd, 1H, ^3J=3.7Hz, ^2J=18.0Hz, CH_2]; 3.21 [m, 1H, $CHCH_3$]; 3.52 [dd, 1H, ^3J=10Hz, ^2J=18.0Hz, CH_2]; 3.69 [s, 3H, NCH_3]; 7.38-7.59 [m, 5H, N-aromatics] ppm.

4.3.12 [C(CO_2Et)$(Me)_2$C(O)CHC(Me)C(S)N(Ph)(Me)] **19'**

Anion reaction method A.

Quenching procedure B.

A yellow oil was obtained after purification on a silica tlc plate using hexanes/ether (1:1). Yield 67%. M.S.: 333$(M)^+$, 218$(M\text{-}C(CH_3)_2CO_2Et)^+$, 190$(M\text{-}C(CH_3)_2CO_2Et\text{-}CO)^+$ (m/e). IR ($CHCl_3$) υ(CO): 1732(s), 1690(s) cm^{-1}. ^1H NMR ($CDCl_3$): δ 1.12 [s, 6H, CH_3]; 1.19 [t, 3H, ^3J=7.1Hz, OCH_2CH_3]; 2.17 [d, 3H, ^3J=1.4Hz, CH_3]; 3.75 [s, 3H, NCH_3]; 4.09 [q, 2H, ^3J=7.1Hz, OCH_2CH_3]; 5.91 [s, 2H, γ-CH]; 7.08-7.38 [m, 5H, N-aromatics] ppm. ^{13}C NMR ($CDCl_3$): δ 14.17 [CH_3]; 20.23 [CH_3]; 21.64 [CH_3]; 44.61 [NCH_3]; 55.50 [quaternary C]; 61.34 [OCH_2CH_3]; 118.06 [β-C]; 120.91 [γ-CH]; 125.45 [aromatic CH]; 128.19 [aromatic CH]; 129.54 [aromatic CH]; 145.40 [quaternary aromatic C]; 156.61 [CO_2Et]; 196.71 [C=S]; 202.15 [C=O] ppm.

4.3.13 [C(CN)(Me)$_2$C(O)CH$_2$CH(Me)C(S)N(Ph)(Me)] **20'**

Anion reaction method A.

Quenching procedure B.

A colourless oil was obtained after purification on a silica tlc plate using hexanes/ether (1:1). Crystals were obtained from ether/hexanes at 0°C. Yield 1%. M.S.: 288(M)$^+$, 220(M-C(CH$_3$)$_2$CN)$^+$, 192(M-C(CH$_3$)$_2$CN-CO)$^+$ (m/e). IR ($CHCl_3$) υ(CO): 1730(s) cm^{-1}. ^{1}H NMR ($CDCl_3$): δ 1.03 [d, 3H, ^{3}J=6.8Hz, CH$_3$]; 1.45 [s, 3H, CH$_3$]; 1.55 [s, 3H, CH$_3$]; 2.65 [dd, 1H, ^{3}J=3.4Hz, ^{2}J=18.6Hz, CH$_2$]; 3.30 [m, 1H, CH]; 3.69 [s, 3H, NCH$_3$]; 3.90 [dd, 1H, ^{3}J=10.0Hz, ^{2}J=18.6Hz, CH$_2$]; 7.40-7.43 [m, 5H, N-aromatics] ppm. ^{13}C NMR ($CDCl_3$): δ 21.12 [CH$_3$]; 23.42 [CH$_3$]; 24.62 [CH$_3$]; 38.96 [CH or NCH$_3$]; 43.46 [CH or NCH$_3$]; 46.91 [CH$_2$]; 127.64 [aromatic CH]; 128.54 [aromatic CH]; 129.51 [aromatic CH] ppm.

4.3.14 [C(CN)(Me)$_2$C(O)CH$_2$CH(Me)C(O)N(Ph)(Me)] **21'**

Anion reaction method A.

Quenching procedure B.

A yellow oil was obtained after purification on a silica tlc plate using hexanes/ether (1:1). Yield 64%. M.S.: 272(M)$^+$, 204(M-C(CH$_3$)$_2$CN)$^+$, 176(M-C(CH$_3$)$_2$CN-CO)$^+$ (m/e). IR ($CHCl_3$) υ(CO): 1730(s), 1650(s) cm^{-1}. ^{1}H NMR ($CDCl_3$): δ 0.97 [d, 3H, ^{3}J=7.1Hz, CH$_3$]; 1.46 [s, 3H, CH$_3$]; 1.54 [s, 3H, CH$_3$]; 2.55 [dd, 1H, ^{3}J=3.5Hz, ^{2}J=18.6Hz, CH$_2$]; 2.89 [m, 1H, CH]; 3.21 [s, 3H, CH$_3$]; 3.43 [dd, 1H, ^{3}J=10.5Hz, ^{2}J=18.6Hz, CH$_2$]; 7.41 [m, 5H, N-aromatics] ppm. ^{13}C NMR ($CDCl_3$): δ 17.61 [CH$_3$]; 23.38 [CH$_3$]; 24.51 [CH$_3$]; 32.27 [CH or NCH$_3$]; 37.73 [CH or NCH$_3$]; 43.00 [CH$_2$]; 43.54 [quaternary C]; 121.86 [CN]; 127.64 [aromatic CH]; 127.82 [aromatic CH]; 129.64 [aromatic CH]; 143.69 [quaternary aromatic C]; 174.81 [C=O]; 203.50 [C=O] ppm.

4.3.15 [CH(CN)(Me)C(O)CH_2CH(Me)C(O)N(Ph)(Me)] **22'**

Anion reaction method A.

Quenching procedure A.

A yellow oil was obtained after purification on a silica tlc plate using hexanes/ether (1:1). GC/M.S: 204(M-$CH(CH_3)CN)^+$, 176(M-$CH(CH_3)CN$-CO)$^+$. IR ($CHCl_3$) υ(CO): 1718(s), 1650(s) cm^{-1}.

4.3.16 [$C(CO_2Et)(Me)_2$C(O)CH_2CH(Me)C(O)N(Ph)(Me)] and [$C(CO_2Et)(Me)_2$C(O)CHC(Me)C(O)N(Ph)(Me)] **23'** (mixture of two products)

Anion reaction method A.

Quenching procedure B.

A yellow oil was obtained after purification on a silica tlc plate using hexanes/ether (1:1). GC/M.S: 317, 319 $(M)^+$, 202, 204 (M-$CH(CH_3)CO_2Et)^+$. IR ($CHCl_3$) υ(CO): 1733(s), 1710(s), 1694(s), 1650(vs br), 1645(sh), 1598(s) cm^{-1}.

4.3.17 [C(CN)$(Me)_2$C(O)CH(Me)CH_2C(O)N(Ph)(Me)] **24'**

Anion reaction method A.

Quenching procedure A.

A yellow oil was obtained after purification on a silica tlc plate using hexanes/ether (1:1). M.S.: 272$(M)^+$, 204(M-$C(CH_3)_2CN)^+$, 176(M-$C(CH_3)_2CN$ -CO)$^+$ (m/e). IR ($CHCl_3$) υ(CO): 1723(s), 1650(vs) cm^{-1}. ^1H NMR ($CDCl_3$): δ 1.07 [d, 3H, ^3J=7.1Hz, $\underline{C}H_3$]; 1.50 [s, 3H, $\underline{C}H_3$]; 1.65 [s, 3H, $\underline{C}H_3$]; 2.08 [dd, 1H, ^3J=2.6Hz, ^2J=16.1Hz, $\underline{C}H_2$]; 2.65 [dd, 1H, ^3J=10.5Hz, ^2J=16.6Hz, $\underline{C}H_2$]; 3.10 [s, 3H, N$\underline{C}H_3$]; 3.66 [m, 1H, $\underline{C}H$]; 7.21-7.45 [m, 5H, N-aromatics] ppm. ^{13}C NMR ($CDCl_3$): δ 17.78 [$\underline{C}H_3$]; 25.01, 25.36 [$\underline{C}H_3$]; 29.79 [quarternary $\underline{C}$]; 37.44 [$\underline{C}H$]; 39.35 [$\underline{C}H_2$]; 39.75 [N$\underline{C}H_3$]; 127.29 [aromatic $\underline{C}H$]; 127.95 [

aromatic CH]; 129.85 [aromatic CH]; 133.87 [CN]; 143.58 [quaternary aromatic C]; 170.30 [C=O]; 208.04 [1C, C=O] ppm.

4.3.18 $[C(CN)(Me)_2CH(Me)CH_2C(S)NEt_2]$ **25'**

Anion reaction method B.

Quenching procedure A.

A yellow oil was obtained after purification on a silica tlc plate using hexanes/ether (1:1). Yield 86%. M.S.: 226$(M)^+$, 158$(M\text{-}C(CH_3)_2CN)^+$ (m/e). ^1H NMR ($CDCl_3$): δ 1.04 [d, 3H, ^3J=7.1Hz, CH_3]; 1.25 [t, 3H, ^3J=7.0Hz, NCH_2CH_3]; 1.26 [t, 3H, ^3J=7.0Hz, NCH_2CH_3]; 1.34 [s, 3H, CH_3]; 1.38 [s, 3H, CH_3]; 2.53 [m, 1H, CH]; 2.79 [m, 2,H CH_2]; 3.60 [dq, 1H, ^3J=7.0Hz, ^2J=7.0Hz, NCH_2CH_3]; 3.70 [dq, 1H, ^3J=7.0Hz, ^2J=7.0Hz, NCH_2CH_3]; 3.91 [dq, 1H, ^3J=7.0Hz, ^2J=7.0Hz, NCH_2CH_3]; 4.12 [dq, H1, ^3J=7.0Hz, ^2J=7.0Hz, NCH_2CH_3] ppm.

4.3.19 $[C(CN)(Me)_2CH(Ph)CH_2C(S)NEt_2]$ **26'**

Anion reaction method B.

Quenching procedure A.

A yellow oil was obtained after purification on a silica tlc plate using hexanes/ether (1:1). Yield 89%. M.S.: 288$(M)^+$, 220$(M\text{-}C(CH_3)_2CN)^+$ (m/e). ^1H NMR ($CDCl_3$): δ 0.91 [t, 3H, ^3J=7.1Hz, NCH_2CH_3]; 1.08 [t, 3H, ^3J=7.1Hz, NCH_2CH_3]; 1.13 [s, 3H, CH_3]; 1.60 [s, 3H, CH_3]; 3.11 [m, 2H, CH_2]; 3.40 [m, 3H, NCH_2CH_3]; 3.62 [dd, 1H, ^3J=10.4, 3.3Hz, CH]; 7.23-7.41 [m, 5H, aromatics] ppm.

Electrophilic Substitution

4.3.20 [Fe(PhCH=CHC(S$^+$=Me)OEt)(CO)$_3$][BF$_4^-$] **21**

Thioester iron complex **10** (0.3mmol) was dissolved in dry CH_2Cl_2 (5ml) and $[(CH_3)_3OBF_4]$ (0.3mmol) was added. The solution was stirred for 17h under N_2 at room temperature. Addition of anhydrous ether resulted in the precipitation of a yellow solid. The solid was filtered and washed with ether. Yield 76%. M.p. 150°C sublimes. IR (CH_3CN) υ(CO): 2100(s), 2045(s) cm^{-1}. ^1H NMR (Acetone-d_6): δ 1.59 [t, 3H, ^3J=7.0Hz, $OCH_2\underline{C}H_3$]; 2.68 [s, 3H, $S\underline{C}H_3$]; 3.17 [d, 1H, ^3J=9.7Hz, γ-$\underline{C}H$]; 4.73 [dq, 1H, ^3J=7.0Hz, ^2J=2.5Hz, $O\underline{C}H_2CH_3$]; 4.92 [dq, 1H, ^3J=7.0Hz, ^2J=2.5Hz, $O\underline{C}H_2CH_3$]; 7.26 [d, 1H, ^3J=9.7Hz, β-$\underline{C}H$]; 7.34 [m, 3H, aromatics]; 7.70 [d, 2H, ^3J=6.8Hz, aromatics] ppm. ^{13}C NMR (Acetone-d_6): δ 14.28 [$OCH_2\underline{C}H_3$]; 18.49 [$S\underline{C}H_3$]; 58.71 [γ-$\underline{C}H$]; 70.97 [$O\underline{C}H_2CH_3$]; 73.36 [β-$\underline{C}H$]; 127.82 [aromatic $\underline{C}H$]; 128.98 [aromatic $\underline{C}H$]; 129.51 [aromatic $\underline{C}H$]; 134.77 [quaternary aromatic $\underline{C}$]; 134.77 [C=S] ppm.

4.3.21 Thioester iron complex **10** adduct with $[Hg(OAc)_2]$

Thioester iron complex **10** (0.3mmol) was dissolved in dry methanol (15ml) and $[Hg(OAc)_2]$ (1.8mmol, 6eqv) was added. The initial orange colour of the thioester solution immediately turned pale pink. The suspension was stirred for 18h under N_2. The solution was filtered and the solid was washed with anhydrous ether. The solid was repeatedly recrystallized from hot ethanol in an effort to separate out the excess $[Hg(OAc)_2]$. ^1H NMR in DMSO-d_6 was inconclusive owing to the presence of excess $[Hg(OAc)_2]$. The complex could not be sufficiently purified to allow for complete characterization. All attempts to use less $[Hg(OAc)_2]$ or other Hg-salts gave only $[Hg_2S]$ or other insoluble products.

Alkyne Addition

4.3.22 Complex **22**

This complex was prepared by 5 different procedures. Each gave complex **22** but in different yields.

Method A: To a stirred solution of thioamide iron complex **7** (0.67mmol) dissolved in THF (6ml) under a CO atmosphere and cooled to 0°C was added dropwise a solution of dimethylacetylene dicarboxylate, DMAD, (0.67mmol) dissolved in THF (12ml). The solution was allowed to warm to room temperature and was stirred for 2h. The solvent was reduced by rotary evaporation and the sample was purified on a neutral alumina column. Eluting with $CHCl_3$:ether (1:1) gave two fractions. The first fraction, which was orange in colour, corresponded to unreacted complex **7** and the second fraction which was yellow in colour corresponded to the desired product. The resulting yellow oil was crystallized from $CHCl_3$/ether at 0°C. Yield 14%. M.p. 130°C. Anal. calcd. for $C_{21}H_{19}NO_8SFe$: C, 50.30; H, 3.79; N, 2.79; S, 6.39%. Found: C, 50.52; H, 3.99; N, 2.90; S, 6.06%. M.S.: 445(Highest mass)$^+$, 361(Ligand)$^+$ (m/e). IR ($CHCl_3$) υ(CO): 2060(s), 1998(s sh), 1985(s), 1690(s) cm^{-1}. ^1H NMR ($CDCl_3$): δ 1.12 [d, 3H, ^3J=7.0Hz, CH$\underline{CH_3}$]; 2.59 [q, 1H, ^3J=7.0Hz, CH$\underline{CH_3}$]; 2.82 [s, 1H, $\underline{CH}$]; 3.63 [s, 3H, N-$\underline{CH_3}$]; 3.73 [s, 3H, O$\underline{CH_3}$]; 3.74 [s, 3H, O$\underline{CH_3}$]; 7.45 [m, 5H, aromatics] ppm. ^{13}C NMR (Benzene-d_6): δ 20.98 [CH$\underline{CH_3}$]; 42.34 [$\underline{CH}CH_3$]; 43.58 [N-$\underline{CH_3}$]; 50.94 [O$\underline{CH_3}$]; 53.07 [O$\underline{CH_3}$]; 63.46 [$\underline{CH}$]; 66.52 [β or γ-$\underline{CH}$]; 67.06 [β or γ-$\underline{CH}$]; 127-129 [aromatic $\underline{CH}$]; 143.19 [C=S]; 169.23, 173.85 [CO_2CH_3]; 205.32, 206.47, 208.86, 210.38 [C=O and M-CO's] ppm.

Method B: A solution of DMAD (0.67mmol) in THF (12ml) was added dropwise to a stirring solution of thioamide iron complex **7** (0.67mmol) in THF (6ml) in a stainless steel autoclave cooled to -32°C under a CO atmosphere. The

autoclave was then charged with 400psi CO after warming to room temperature. It was stirred for 3d at 55°C. A 14% yield of the product was isolated by column chromatography.

Method C: To a stirred solution of thioamide iron complex 7 (0.67mmol) dissolved in THF (6ml) under a N_2 atmosphere and cooled to 0°C was added dropwise a solution of dimethylacetylene dicarboxylate, DMAD, (0.67mmol) dissolved in THF (12ml). The solution was allowed to warm to room temperature and was stirred for 2h. A 2.8% yield of the product was isolated by column chromatography.

Method D: To a stirred solution of thioamide iron complex 7 (0.67mmol) dissolved in THF (6ml) under a flowing CO atmosphere and cooled to 0°C was added dropwise a solution of dimethylacetylene dicarboxylate, DMAD, (0.67mmol) dissolved in THF (12ml). The solution was allowed to warm to room temperature and was stirred for 2h with flowing CO. A 39% yield of the product was isolated by column chromatography.

Method E: A solution of DMAD (0.45mmol) in C_6H_{12} (4ml) was added dropwise to a stirred solution of thioamide iron complex 7 (0.45mmol) in C_6H_{12} (16ml) at room temperature with CO bubbling into the solution through a needle. The sample was photolyzed for 2h. A 63% yield of the product was isolated by column chromatography.

4.3.23 Complex **23**

To a solution of thioamide iron complex 7 (0.67mmol) in THF (5ml) was

added dropwise a solution of n-butylpropynoate (0.67mmol) in THF (10ml) at room temperature with flowing CO. The solution was refluxed for 1h40min. The solvent was reduced by rotary evaporation. Purification on a neutral column eluted with $CHCl_3$:ether (1:1) gave unreacted starting material followed by the yellow product. Solvent removal left a yellow oil. Crystals were obtained from $CHCl_3$/ether at 0°C. Yield 10.7%. M.p. 130°C. Anal. calcd. for $C_{22}H_{24}NO_6SFe$: C, 54.43; H, 4.95; N, 2.89; S, 6.60%. Found: C, 54.62; H, 5.07; N, 2.96; S, 6.53%. M.S.: 401(Highest mass)$^+$, 329(Ligand)$^+$ (m/e). IR ($CHCl_3$) υ(CO): 2085(w), 2050(s), 1985(s), 1970(s), 1720(m), 1690(m br) cm^{-1}. ^1H NMR (Benzene-d_6): δ 0.68 [d, 3H, ^3J=7.0Hz, $CH\underline{C}H_3$]; 0.82 [t, 3H, ^3J=7.3Hz, $O(CH_2)_3\underline{C}H_3$]; 1.42 [tq, 2H, ^3J=7.3Hz, ^3J=6.5Hz, $O(CH_2)_2\underline{C}H_2CH_3$]; 1.58 [m, 2H, $OCH_2\underline{C}H_2CH_2CH_3$]; 2.11 [q, 1H, ^3J=7.1Hz, $\underline{C}HCH_3$]; 2.55 [s, 1H, $\underline{C}H$]; 2.62 [s, 3H, N-$\underline{C}H_3$]; 4.15 [dt, 1H, ^2J=10.9Hz, $O\underline{C}H_2(CH_2)_2CH_3$]; 4.3 [dt, 1H, $O\underline{C}H_2(CH_2)_2CH_3$]; 4.60 [s, 1H, β-$\underline{C}H$]; 6.73-6.78 [m, 5H, aromatics] ppm. ^{13}C NMR (Benzene-d_6): δ 20.98 [$CH\underline{C}H_3$]; 42.34 [$\underline{C}HCH_3$]; 43.58 [N-$\underline{C}H_3$]; 50.94 [$O\underline{C}H_3$]; 53.07 [$O\underline{C}H_3$]; 63.46 [$\underline{C}H$]; 66.52 [β or γ-$\underline{C}H$]; 67.06 [β or γ-$\underline{C}H$]; 127-129 [aromatic $\underline{C}H$]; 143.19 [C=S]; 169.23, 173.85 [CO_2CH_3]; 205.32, 206.47, 208.86, 210.38 [C=O and M-CO's] ppm.

4.3.24 Complex **24**

To a stirred solution of thioamide iron complex **7** (0.30mmol) in ether (30ml) at room temperature was added methyl propynoate (0.60mmol). Carbon monoxide was bubbled through the solution which was heated to reflux for 15h. The solvent was reduced by rotary evaporation. Purification by column chromatography on neutral alumina eluted with $CHCl_3$ gave a yellow band. The solvent was reduced by rotary evaporation and crystals were obtained from ether/hexanes at 0°C. Yield 78%. M.p. 135°C decomp. Anal. calcd. for

$C_{19}H_{17}NO_6SFe$: C, 51.47; H, 3.84; N, 3.16%. Found: C, 51.21; H, 4.04; N, 2.95%. M.S. CI: 444(M+1)$^+$, 416(M+1-CO)$^+$, 388(M+1-2CO)$^+$, 360(M+1-3CO)$^+$, 304 (Ligand+1)$^+$ (m/e). IR ($CHCl_3$) υ(CO): 2060(s), 1990(s), 1975(s), 1725(m), 1695(m) cm^{-1}. ^{1}H NMR (Benzene-d_6): δ 0.67 [d, 3H, ^{3}J=7.0Hz, $\underline{C}H_3$]; 2.10 [q, 1H, ^{3}J=7.0Hz, $\underline{C}H$]; 2.54 [s, 1H, $\underline{C}H$]; 2.60 [s, 1H, N-$\underline{C}H_3$]; 3.54 [s, 3H, O$\underline{C}H_3$]; 4.57 [s, 1H, $\underline{C}H$]; 6.75 [m, 5H, aromatics] ppm. ^{13}C NMR (Benzene-d_6): δ 23.22 [$\underline{C}H_3$]; 40.37 [$\underline{C}H$]; 43.24 [N-$\underline{C}H_3$]; 51.22 [O$\underline{C}H_3$]; 54.86 [quaternary olefinic $\underline{C}$]; 62.72 [$\underline{C}H$]; 63.37 [$\underline{C}H$]; 143.08 [quaternary $\underline{C}$]; 170.43 [$\underline{C}(=O)OCH_3$]; 203.93, 205.87, 207.57, 208.38, 209.67, 213.39 [ketone C=O, 3 M-CO's, C=S] ppm.

4.3.25 Complex **25**

To a stirred solution of thioamide iron complex **4** (0.67mmol) in THF (30ml) at room temperature was added dimethylacetylene dicarboxylate, DMAD, (1.35mmol). Carbon monoxide was bubbled through the solution which was heated to reflux for 6h. The solvent was reduced by rotary evaporation. Purification by column chromatography on neutral alumina eluted with $CHCl_3$/ether (1:1) gave a yellow band. The solvent was removed by rotary evaporation and crystals were obtained with the addition of ether. Yield 81%. M.p. 120°C decomp. Anal. calcd. for $C_{18}H_{21}NO_8SFe$: C, 46.25; H, 4.50; N, 3.00%. Found: C, 46.37; H, 4.75; N, 2.86%. M.S. CI: 468(M+1)$^+$, 412(M+1-2CO)$^+$, 384(M+1-3CO)$^+$, 328(Ligand+1)$^+$ (m/e). IR ($CHCl_3$) υ(CO): 2065(s), 2000(s sh), 1988(s), 1728(m), 1695(s) cm^{-1}. ^{1}H NMR ($CDCl_3$): δ 1.25 [m, 3H, N-$CH_2\underline{C}H_3$]; 1.33 [m, 3H, N-$CH_2\underline{C}H_3$]; 1.42 [d, 3H, ^{3}J=6.0Hz, $\underline{C}H_3$]; 2.56 [q, 1H, ^{3}J=6.0Hz, $\underline{C}H$]; 3.05 [s, 1H, $\underline{C}H$]; 3.61 [m, 3H, N-$\underline{C}H_2CH_3$]; 3.74 [s, 3H, O$\underline{C}H_3$]; 3.92 [m, 1H, N-$\underline{C}H_2CH_3$] ppm. ^{13}C NMR ($CDCl_3$): δ 11.61 [$\underline{C}H_3$]; 15.11 [$\underline{C}H_3$]; 21.67 [$\underline{C}H_3$]; 41.90 [$\underline{C}H$]; 48.59 [N-$\underline{C}H_2CH_3$]; 48.74 [

N-$\underline{C}H_2CH_3$]; 51.17 [$CO_2\underline{C}H_3$]; 61.85 [$\underline{C}H$]; 65.59 [olefinic quaternary $\underline{C}$]; 169.23 [$\underline{C}O_2CH_3$]; 173.95 [$\underline{C}O_2CH_3$]; 203.77, 205.13, 206.98, 207.17, 208.84 [ketone C=O, 3 M-CO's, C=S] ppm.

4.3.26 Complex **26**

To a stirred solution of thioamide iron complex **1** (0.28mmol) in cyclohexane (20ml) at room temperature was added dimethylacetylene dicarboxylate, DMAD, (0.28mmol). Carbon monoxide was bubbled through the solution which was photolyzed for 3h. The solution was filtered and the solvent was reduced by rotary evaporation. Purification by column chromatography on neutral alumina eluted with $CHCl_3$/ether (1:1) gave a yellow band. The solvent was removed by rotary evaporation and crystals were obtained from $CHCl_3$/ether at 0°C. Yield 22%. M.p. 130°C decomp. Anal. calcd. for $C_{23}H_{23}NO_8SFe$: C, 52.17; H, 4.35; N, 2.65%. Found: C, 52.09; H, 4.48; N, 2.69%. M.S. CI: 530$(M+1)^+$, 474$(M+1-2CO)^+$, 446$(M+1-3CO)^+$, 390$(Ligand+1)^+$ (m/e). IR ($CHCl_3$) υ(CO): 2065(s), 1998(br s), 1695(m br) cm^{-1}. ^1H NMR ($CDCl_3$): δ 1.15 [t, 3H, ^3J=7.0Hz, $CH_2\underline{CH_3}$]; 1.28 [t, 3H, ^3J=7.0Hz, $CH_2\underline{CH_3}$]; 3.29 [s, 1H, $\underline{CH}$]; 3.40 [m, 1H, $\underline{CH_2}CH_3$]; 3.42 [s, 3H, $CO_2\underline{CH_3}$]; 3.50 [m, 1H, $\underline{CH_2}CH_3$]; 3.63 [s, 1H, $\underline{CH}$]; 3.68 [m, 1H, $\underline{CH_2}CH_3$]; 3.87 [s and overlapping m, 4H, $CO_2\underline{CH_3}$ and $\underline{CH_2}CH_3$]; 7.22-7.42 [m, 5H, aromatics] ppm.

4.4 X-Ray Crystal Structure Data

4.4.1 Thioamide Compound 2'

```
   Space Group and Cell Dimensions    Monoclinic,   P 21/n
a  11.9484(14)   b   9.6957(10)   c  15.4629(13)
beta 111.661(8)
        Volume  1664.8(3)A**3

Empirical formula : S N C19 H21


Cell dimensions were obtained from  30 reflections with 2Theta angle
in the range  40.00 -  50.00 degrees.

Crystal dimensions :  0.20  X  0.20  X  0.20  mm

FW =    295.44     Z =    4     F(000) =     631.91

Dcalc  1.179Mg.m-3, mu   0.18mm-1, lambda 0.70930A, 2Theta(max)  45.0

The intensity data were collected on a Nonius diffractometer,
using the theta/2theta scan mode.
The h,k,l ranges are :--     -12  11,     0   9,     0  16
No. of reflections measured                      6302
No. of unique reflections                        2145
No. of reflections with Inet > 2.5sigma(Inet)    1405
No correction was made for absorption


The last least squares cycle was calculated with
 44 atoms, 207 parameters and 1405 out of 2145 reflections.
Unit weights were used.

The residuals are as follows :--
For significant reflections,  RF 0.283, Rw 0.314 GoF  2.34
For all reflections,          RF 0.283, Rw 0.314.
where RF = Sum(Fo-Fc)/Sum(Fo),
      Rw = Sqrt[Sum(w(Fo-Fc)**2)/Sum(wFo**2)] and
     GoF = Sqrt[Sum(w(Fo-Fc)**2)/(No. of reflns - No. of params.)]
The maximum shift/sigma ratio was  4.708.

The last map type is not given. D-map is assumed
In the last D-map, the deepest hole was  -1.350e/A**3,
and the highest peak   1.740e/A**3.
```

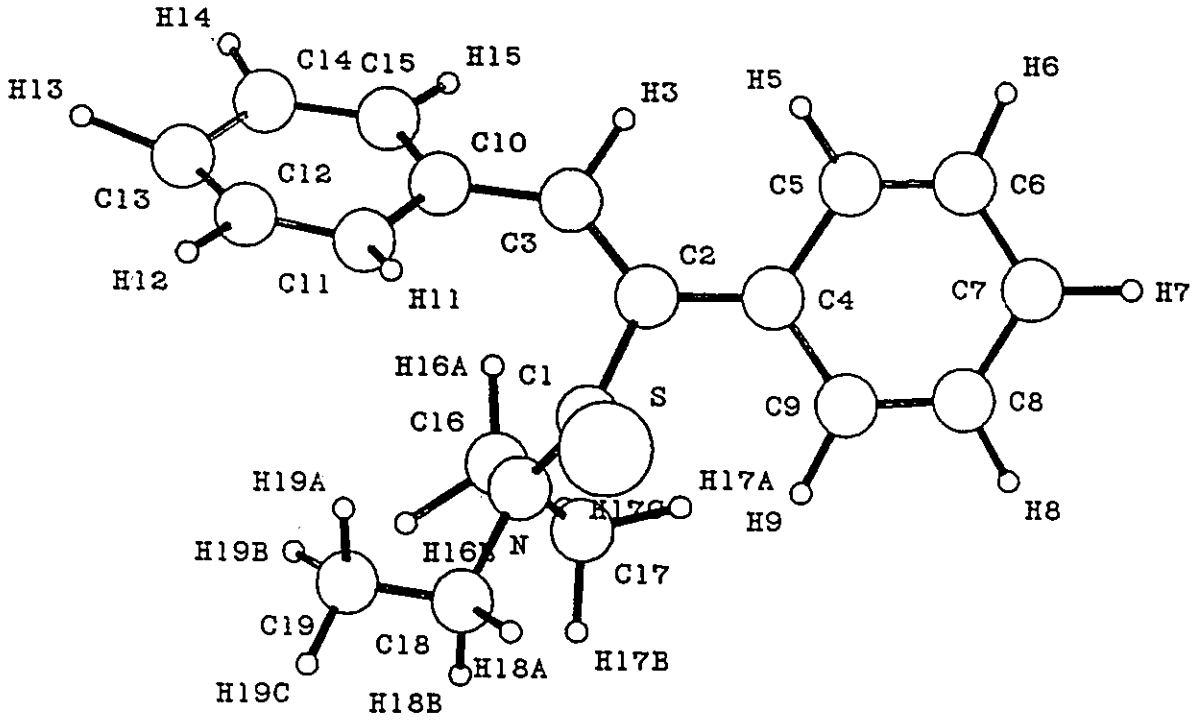

X-Ray Crystal Structure of Free Ligand **2'**

Table of Bond Distances in Angstroms

S-C(1)	1.58(3)	C(11)-C(12)	1.36(6)
N-C(1)	1.43(4)	C(11)-H(11)	1.21(22)
N-C(16)	1.40(4)	C(12)-C(13)	1.30(6)
N-C(18)	1.49(4)	C(12)-H(12)	1.13(4)
C(1)-C(2)	1.59(4)	C(13)-C(14)	1.43(7)
C(2)-C(3)	1.37(4)	C(13)-H(13)	1.21(17)
C(2)-C(4)	1.37(4)	C(14)-C(15)	1.38(6)
C(3)-C(10)	1.45(5)	C(14)-H(14)	1.10(4)
C(3)-H(3)	1.12(3)	C(15)-H(15)	1.12(4)
C(4)-C(5)	1.52(5)	C(16)-C(17)	1.53(5)
C(4)-C(9)	1.43(4)	C(16)-H(16B)	1.22(16)
C(5)-C(6)	1.27(6)	C(16)-H(16A)	1.09(3)
C(5)-H(5)	1.10(3)	C(17)-H(17C)	1.09(4)
C(6)-C(7)	1.40(6)	C(17)-H(17A)	1.11(4)
C(6)-H(6)	1.09(3)	C(17)-H(17B)	1.10(4)
C(7)-C(8)	1.44(5)	C(18)-C(19)	1.35(6)
C(7)-H(7)	1.12(4)	C(18)-H(18A)	1.08(4)
C(8)-C(9)	1.32(5)	C(18)-H(18B)	1.08(3)
C(8)-H(8)	1.10(3)	C(19)-H(19C)	1.07(4)
C(9)-H(9)	1.08(3)	C(19)-H(19A)	1.10(4)
C(10)-C(11)	1.38(5)	C(19)-H(19B)	1.09(5)
C(10)-C(15)	1.39(5)		

Table of Bond Angles in Degrees

C(1)-N-C(16)	128(3)	C(11)-C(12)-C(13)	133(4)
C(1)-N-C(18)	114.9(24)	C(11)-C(12)-H(12)	113(4)
C(16)-N-C(18)	116(3)	C(13)-C(12)-H(12)	112(4)
S-C(1)-N	125.7(21)	C(12)-C(13)-C(14)	108(3)
S-C(1)-C(2)	120.6(24)	C(12)-C(13)-H(13)	143(7)
N-C(1)-C(2)	113.7(24)	C(14)-C(13)-H(13)	106(7)
C(1)-C(2)-C(3)	117(3)	C(13)-C(14)-C(15)	124(3)
C(1)-C(2)-C(4)	114(3)	C(13)-C(14)-H(14)	119(4)
C(3)-C(2)-C(4)	127(3)	C(15)-C(14)-H(14)	115(4)
C(2)-C(3)-C(10)	133(3)	C(10)-C(15)-C(14)	118(4)
C(2)-C(3)-H(3)	110(3)	C(10)-C(15)-H(15)	117(4)
C(10)-C(3)-H(3)	115(3)	C(14)-C(15)-H(15)	123(4)
C(2)-C(4)-C(5)	123(3)	N-C(16)-C(17)	114(3)
C(2)-C(4)-C(9)	125(3)	N-C(16)-H(16B)	84(7)
C(5)-C(4)-C(9)	110(3)	N-C(16)-H(16A)	113(3)
C(4)-C(5)-C(6)	124(3)	C(17)-C(16)-H(16B)	111(7)
C(4)-C(5)-H(5)	113(3)	C(17)-C(16)-H(16A)	109(3)
C(6)-C(5)-H(5)	120(3)	H(16B)-C(16)-H(16A)	121(8)
C(5)-C(6)-C(7)	122(3)	C(16)-C(17)-H(17C)	113(3)
C(5)-C(6)-H(6)	115(4)	C(16)-C(17)-H(17A)	111(3)
C(7)-C(6)-H(6)	121(3)	C(16)-C(17)-H(17B)	111(4)
C(6)-C(7)-C(8)	115(3)	H(17C)-C(17)-H(17A)	106(4)
C(6)-C(7)-H(7)	122(3)	H(17C)-C(17)-H(17B)	107(3)
C(8)-C(7)-H(7)	122(4)	H(17A)-C(17)-H(17B)	105(3)
C(7)-C(8)-C(9)	123(3)	N-C(18)-C(19)	112(3)
C(7)-C(8)-H(8)	118(3)	N-C(18)-H(18A)	110(3)
C(9)-C(8)-H(8)	117(3)	N-C(18)-H(18B)	111(3)
C(4)-C(9)-C(8)	122(3)	C(19)-C(18)-H(18A)	106(3)
C(4)-C(9)-H(9)	117(3)	C(19)-C(18)-H(18B)	106(3)
C(8)-C(9)-H(9)	119(3)	H(18A)-C(18)-H(18B)	109(3)
C(3)-C(10)-C(11)	123(3)	C(18)-C(19)-H(19C)	112(4)
C(3)-C(10)-C(15)	117(3)	C(18)-C(19)-H(19A)	109(3)
C(11)-C(10)-C(15)	118(3)	C(18)-C(19)-H(19B)	109(4)
C(10)-C(11)-C(12)	115(3)	H(19C)-C(19)-H(19A)	108(4)
C(10)-C(11)-H(11)	125(10)	H(19C)-C(19)-H(19B)	109(4)
C(12)-C(11)-H(11)	112(10)	H(19A)-C(19)-H(19B)	107(4)

Table of Atomic Parameters x,y,z and Biso.
E.S.Ds. refer to the last digit printed.

	x	y	z	Biso
S	0.7561(7)	0.5339(9)	0.1028(7)	4.5(4)
N	0.5970(20)	0.718 (3)	-0.0046(17)	4.0(13)
C 1	0.706 (3)	0.640 (3)	0.0195(18)	3.3(16)
C 2	0.780 (3)	0.671 (3)	-0.0454(22)	3.3(15)
C 3	0.8377(25)	0.795 (3)	-0.035 (3)	4.3(19)
C 4	0.7856(24)	0.563 (4)	-0.1005(23)	4.6(17)
C 5	0.895 (3)	0.531 (5)	-0.125 (3)	7.1(22)
C 6	0.902 (3)	0.432 (5)	-0.1763(25)	7.2(25)
C 7	0.808 (3)	0.338 (5)	-0.216 (3)	7.7(27)
C 8	0.701 (3)	0.365 (5)	-0.196 (3)	9.6(27)
C 9	0.696 (3)	0.459 (4)	-0.136 (3)	5.8(20)
C10	0.8417(23)	0.918 (3)	0.0193(22)	3.8(15)
C11	0.834 (3)	0.916 (4)	0.1061(23)	3.8(17)
C12	0.839 (3)	1.040 (5)	0.147 (3)	5.7(21)
C13	0.838 (3)	1.166 (4)	0.119 (3)	4.5(19)
C14	0.845 (3)	1.164 (3)	0.029 (4)	7.7(24)
C15	0.840 (3)	1.045 (4)	-0.022 (3)	5.6(21)
C16	0.550 (3)	0.816 (4)	-0.0747(25)	4.7(18)
C17	0.455 (3)	0.761 (4)	-0.164 (3)	7.0(24)
C18	0.527 (3)	0.693 (4)	0.0562(24)	4.[illegible](8)
C19	0.552 (4)	0.785 (5)	0.126 (3)	7.[illegible](29)
H 3	0.891	0.801	-0.081	5.3
H11	0.866 (17)	0.822 (22)	0.161 (14)	-0.9(45)
H 7	0.817	0.247	-0.257	8.1
H 8	0.617	0.312	-0.237	8.0
H13	0.850 (12)	1.285 (17)	0.144 (9)	-1.4(26)
H16B	0.503 (13)	0.864 (15)	-0.023 (10)	-1.6(29)
H 9	0.616	0.467	-0.119	6.0
H 6	0.982	0.431	-0.194	7.2
H 5	0.976	0.587	-0.081	6.6
H14	0.848	1.262	-0.007	5.8
H15	0.835	1.046	-0.096	6.1
H12	0.844	1.034	0.222	6.6
H16A	0.618	0.873	-0.091	5.5
H18A	0.549	0.592	0.088	5.7
H18B	0.432	0.700	0.017	5.7
H19C	0.503	0.765	0.170	9.2
H19A	0.649	0.782	0.169	9.2
H19B	0.532	0.889	0.098	9.2
H17C	0.420	0.838	-0.219	7.6
H17A	0.491	0.675	-0.194	7.6
H17B	0.377	0.717	-0.152	7.6

Biso is the Mean of the Principal Axes of the Thermal Ellipsoid

4.4.2 Thioamide Iron Tricarbonyl Complex 1

Space Group and Cell Dimensions Monoclinic, P 21/n
a 13.620(3) b 7.6598(16) c 15.979(4)
beta 96.296(22)
Volume 1657.0(6)A**3

Empirical formula : Fe S O3 N C16 H17

Cell dimensions were obtained from 15 reflections with 2Theta angle in the range 35.00 - 38.00 degrees.

Crystal dimensions : 0.20 X 0.30 X 0.40 mm

FW = 359.22 Z = 4 F(000) = 743.88

Dcalc 1.440Mg.m-3, mu 1.04mm-1, lambda 0.70930A, 2Theta(max) 45.0

The intensity data were collected on a Nonius diffractometer, using the theta/2theta scan mode.
The h,k,l ranges are :-- -14 14, 0 7, 0 17
No. of reflections measured 5157
No. of unique reflections 2140
No. of reflections with Inet > 2.5sigma(Inet) 1580
No correction was made for absorption

The last least squares cycle was calculated with
39 atoms, 267 parameters and 1580 out of 2140 reflections.
Unit weights were used.

The residuals are as follows :--
For significant reflections, RF 0.028, Rw 0.029 GoF 0.29
For all reflections, RF 0.051, Rw 0.051.
where RF = Sum(Fo-Fc)/Sum(Fo),
Rw = Sqrt[Sum(w(Fo-Fc)**2)/Sum(wFo**2)] and
GoF = Sqrt[Sum(w(Fo-Fc)**2)/(No. of refIns - No. of params.)]
The maximum shift/sigma ratio was 0.201.

In the last D-map, the deepest hole was -0.180e/A**3,
and the highest peak 0.250e/A**3.

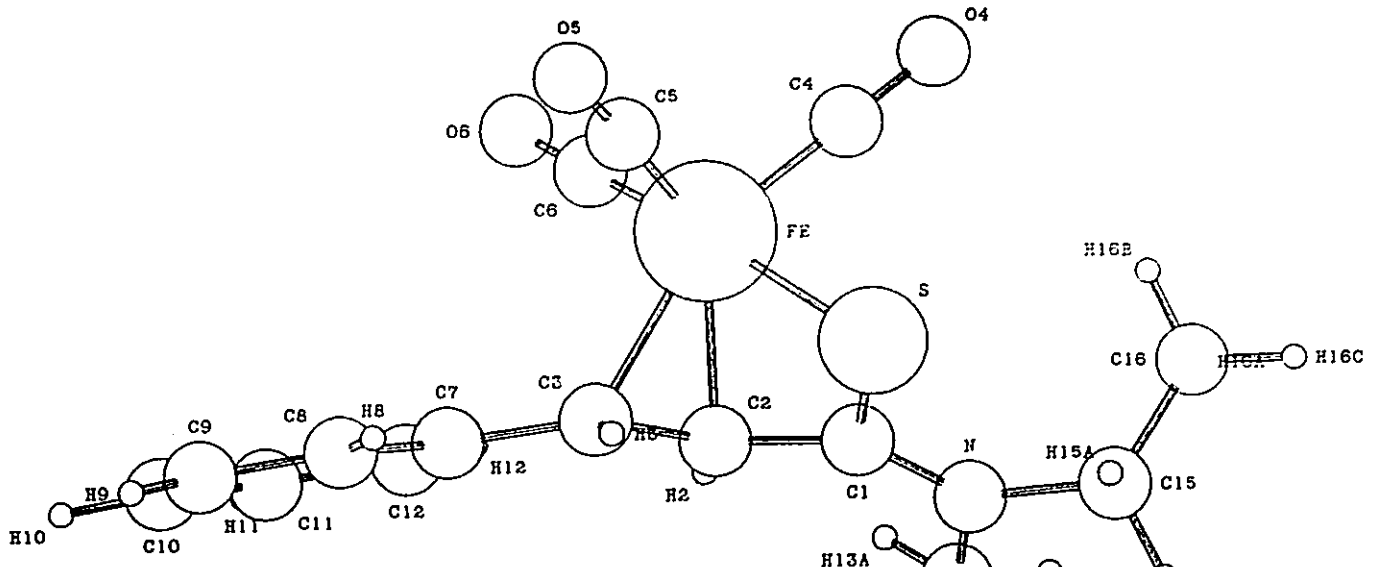

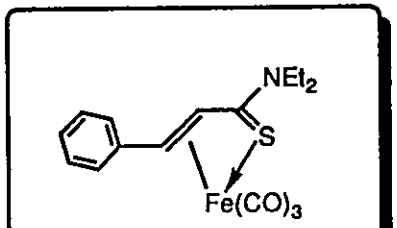

Complex 1

X-Ray Crystal Structure of Complex 1

Table of Bond Distances in Angstroms

Fe-S	2.3534(12)	C(9)-C(10)	1.369(10)
Fe-C(2)	2.068(4)	C(9)-H(9)	0.94(5)
Fe-C(3)	2.090(4)	C(10)-C(11)	1.376(9)
Fe-C(4)	1.800(5)	C(10)-H(10)	1.00(5)
Fe-C(5)	1.789(5)	C(11)-C(12)	1.376(7)
Fe-C(6)	1.762(4)	C(11)-H(11)	0.92(5)
S-C(1)	1.732(4)	C(12)-H(12)	0.93(4)
N-C(1)	1.330(5)	C(13)-C(14)	1.484(7)
N-C(13)	1.473(5)	C(13)-H(13A)	0.93(4)
N-C(15)	1.469(5)	C(13)-H(13B)	1.01(4)
C(1)-C(2)	1.430(5)	C(14)-H(14A)	1.01(5)
C(2)-C(3)	1.425(6)	C(14)-H(14B)	0.99(6)
C(2)-H(2)	0.87(3)	C(14)-H(14C)	0.98(5)
C(3)-C(7)	1.464(5)	C(15)-C(16)	1.505(7)
C(3)-H(3)	0.93(4)	C(15)-H(15A)	0.92(4)
C(4)-O(4)	1.138(6)	C(15)-H(15B)	1.01(4)
C(5)-O(5)	1.139(6)	C(16)-H(16A)	0.96(5)
C(6)-O(6)	1.148(5)	C(16)-H(16B)	0.97(5)
C(7)-C(8)	1.385(6)	C(16)-H(16C)	1.02(5)
C(7)-C(12)	1.399(6)		
C(8)-C(9)	1.379(7)		
C(8)-H(8)	1.01(4)		

Table of u(i,j) or U values *100.
E.S.Ds. refer to the last digit printed

	u11(U)	u22	u33	u12	u13	u23
FE	4.26(3)	3.89(3)	3.53(3)	0.18(3)	0.499(23)	0.43(3)
S	4.95(6)	5.42(7)	4.01(6)	-0.04(5)	1.22 (5)	0.80(5)
N	3.69(18)	4.64(20)	4.35(19)	-0.35(16)	0.29 (15)	0.71(16)
C 1	4.35(23)	3.32(23)	4.11(22)	0.43(18)	0.82 (19)	-0.06(18)
C 2	4.42(24)	4.1 (3)	3.30(24)	0.20(19)	0.48 (19)	1.00(20)
C 3	4.45(24)	4.28(24)	3.41(24)	-0.06(20)	0.59 (20)	0.05(19)
C 4	5.0 (3)	5.1 (3)	6.3 (3)	-0.01(23)	1.27 (22)	0.43(25)
O 4	8.05(24)	5.24(23)	10.9 (3)	-0.71(19)	0.73 (21)	-1.87(21)
C 5	5.2 (3)	6.6 (3)	5.6 (3)	0.41(23)	0.87 (22)	0.94(25)
O 5	8.74(25)	13.4 (3)	5.58(21)	1.2 (3)	-1.42 (19)	2.68(23)
C 6	5.2 (3)	4.8 (3)	5.1 (3)	-0.07(22)	0.44 (21)	0.36(22)
O 6	6.46(20)	7.57(24)	8.12(22)	0.33(18)	3.38 (18)	0.48(19)
C 7	3.96(22)	3.58(24)	4.84(25)	0.44(18)	0.12 (19)	-0.14(19)
C 8	4.3 (3)	7.2 (4)	6.3 (3)	-0.49(24)	-0.08 (22)	-0.8 (3)
C 9	5.6 (3)	8.6 (4)	8.9 (4)	-1.1 (3)	-1.2 (3)	-2.5 (4)
C10	4.4 (3)	6.2 (3)	12.1 (5)	-1.0 (3)	0.5 (3)	-0.4 (3)
C11	6.1 (3)	6.0 (3)	8.8 (4)	-0.8 (3)	1.8 (3)	1.4 (3)
C12	5.7 (3)	5.5 (3)	5.2 (3)	-1.2 (3)	0.29 (22)	-0.06(25)
C13	4.4 (3)	5.4 (3)	4.9 (3)	-0.20(23)	-0.20 (22)	-0.06(22)
C14	7.6 (4)	5.8 (3)	6.9 (4)	0.5 (3)	-0.8 (3)	1.0 (3)
C15	4.1 (3)	6.1 (3)	5.8 (3)	-0.20(22)	0.63 (22)	0.48(24)
C16	6.5 (3)	5.4 (3)	6.7 (4)	-1.0 (3)	0.4 (3)	-0.1 (3)

Anisotropic Temperature Factors are of the form
Temp=-2*Pi*Pi*(h*h*u11*astar*astar+---+2*h*k*u12*astar*bstar+---)

Table of Bond Angles in Degrees

S-Fe-C(2)	72.87(12)
S-Fe-C(3)	82.07(11)
S-Fe-C(4)	89.16(14)
S-Fe-C(5)	93.72(14)
S-Fe-C(6)	169.81(14)
C(2)-Fe-C(3)	40.07(15)
C(2)-Fe-C(4)	115.56(18)
C(2)-Fe-C(5)	135.00(19)
C(2)-Fe-C(6)	98.39(18)
C(3)-Fe-C(4)	155.61(18)
C(3)-Fe-C(5)	96.58(19)
C(3)-Fe-C(6)	94.62(18)
C(4)-Fe-C(5)	106.71(21)
C(4)-Fe-C(6)	90.04(20)
C(5)-Fe-C(6)	96.23(19)
Fe-S-C(1)	71.53(12)
C(1)-N-C(13)	122.3(3)
C(1)-N-C(15)	122.2(3)
C(13)-N-C(15)	115.4(3)
S-C(1)-N	122.5(3)
S-C(1)-C(2)	112.6(3)
N-C(1)-C(2)	124.5(3)
Fe-C(2)-C(1)	86.43(24)
Fe-C(2)-C(3)	70.79(23)
Fe-C(2)-H(2)	124.8(20)
C(1)-C(2)-C(3)	120.9(4)
C(1)-C(2)-H(2)	116.8(20)
C(3)-C(2)-H(2)	121.0(20)
Fe-C(3)-C(2)	69.14(22)
Fe-C(3)-C(7)	123.5(3)
Fe-C(3)-H(3)	100.4(23)
C(2)-C(3)-C(7)	123.3(4)
C(2)-C(3)-H(3)	115.9(22)
C(7)-C(3)-H(3)	114.8(22)
Fe-C(4)-O(4)	178.9(4)
Fe-C(5)-O(5)	177.4(4)
Fe-C(6)-O(6)	179.4(4)
C(3)-C(7)-C(8)	119.5(4)
C(3)-C(7)-C(12)	123.8(4)
C(8)-C(7)-C(12)	116.7(4)
C(7)-C(8)-C(9)	121.5(5)
C(7)-C(8)-H(8)	115.2(25)
C(9)-C(8)-H(8)	123.2(25)
C(8)-C(9)-C(10)	121.1(5)
C(8)-C(9)-H(9)	119(3)
C(10)-C(9)-H(9)	119(3)
C(9)-C(10)-C(11)	118.4(5)
C(9)-C(10)-H(10)	124(3)
C(11)-C(10)-H(10)	117(3)
C(10)-C(11)-C(12)	121.0(5)
C(10)-C(11)-H(11)	119(3)
C(12)-C(11)-H(11)	119(3)
C(7)-C(12)-C(11)	121.2(5)
C(7)-C(12)-H(12)	117.9(21)
C(11)-C(12)-H(12)	120.7(22)
N-C(13)-C(14)	112.0(4)
N-C(13)-H(13A)	107.0(23)
N-C(13)-H(13B)	107.5(22)
C(14)-C(13)-H(13A)	112.3(24)
C(14)-C(13)-H(13B)	108.2(22)
H(13A)-C(13)-H(13B)	109(3)
C(13)-C(14)-H(14A)	111(3)
C(13)-C(14)-H(14B)	113(3)
C(13)-C(14)-H(14C)	112(3)
H(14A)-C(14)-H(14B)	100(4)
H(14A)-C(14)-H(14C)	109(4)
H(14B)-C(14)-H(14C)	108(4)
N-C(15)-C(16)	112.3(4)
N-C(15)-H(15A)	108.7(24)
N-C(15)-H(15B)	105.7(21)
C(16)-C(15)-H(15A)	109(3)
C(16)-C(15)-H(15B)	112.2(21)
H(15A)-C(15)-H(15B)	107(3)
C(15)-C(16)-H(16A)	113(3)
C(15)-C(16)-H(16B)	112(3)
C(15)-C(16)-H(16C)	110(3)
H(16A)-C(16)-H(16B)	104(4)
H(16A)-C(16)-H(16C)	106(4)
H(16B)-C(16)-H(16C)	107(4)

Table . Atomic Parameters x,y,z and Biso.
E.S.Ds. refer to the last digit printed.

	x	y	z	Biso
FE	0.44565(4)	0.28861(8)	0.18205(3)	3.071(24)
S	0.29487(8)	0.32433(15)	0.23922(6)	3.74 (5)
N	0.20813(22)	0.4349 (4)	0.08915(19)	3.35 (14)
C 1	0.2883 (3)	0.4367 (5)	0.14473(23)	3.08 (17)
C 2	0.3806 (3)	0.5134 (5)	0.1301 (3)	3.10 (18)
C 3	0.4520 (3)	0.5592 (5)	0.19845(24)	3.19 (19)
C 4	0.3998 (3)	0.0871 (6)	0.1347 (3)	4.28 (22)
O 4	0.3722 (3)	-0.0414 (5)	0.10522(24)	6.39 (20)
C 5	0.5125 (3)	0.2331 (6)	0.2812 (3)	4.54 (21)
O 5	0.5530 (3)	0.2024 (6)	0.34566(21)	7.42 (21)
C 6	0.5477 (3)	0.2798 (6)	0.1232 (3)	3.99 (19)
O 6	0.61397(23)	0.2724 (4)	0.08481(21)	5.68 (17)
C 7	0.5400 (3)	0.6638 (5)	0.18843(24)	3.28 (17)
C 8	0.5929 (3)	0.7370 (7)	0.2588 (3)	4.75 (23)
C 9	0.6751 (4)	0.8391 (8)	0.2522 (4)	6.2 (3)
C10	0.7071 (4)	0.8733 (7)	0.1757 (4)	6.0 (3)
C11	0.6556 (4)	0.8022 (7)	0.1049 (4)	5.4 (3)
C12	0.5738 (3)	0.6992 (6)	0.1106 (3)	4.34 (21)
C13	0.2036 (3)	0.5279 (6)	0.0081 (3)	3.89 (20)
C14	0.1713 (4)	0.7118 (7)	0.0153 (4)	5.4 (3)
C15	0.1177 (3)	0.3414 (6)	0.1048 (3)	4.20 (22)
C16	0.1144 (4)	0.1592 (7)	0.0695 (4)	4.9 (3)
H 2	0.3859 (22)	0.551 (4)	0.0794 (20)	1.7 (7)
H 3	0.429 (3)	0.569 (5)	0.2505 (24)	3.7 (9)
H 8	0.568 (3)	0.707 (6)	0.314 (3)	6.0 (11)
H 9	0.705 (3)	0.896 (6)	0.301 (3)	5.6 (11)
H10	0.765 (4)	0.949 (7)	0.168 (3)	7.2 (13)
H11	0.675 (4)	0.825 (7)	0.053 (3)	7.4 (15)
H12	0.543 (3)	0.643 (5)	0.0635 (22)	3.2 (9)
H13A	0.266 (3)	0.519 (5)	-0.0104 (23)	3.9 (9)
H13B	0.154 (3)	0.466 (5)	-0.033 (3)	4.7 (10)
H14A	0.101 (4)	0.719 (6)	0.030 (3)	6.4 (13)
H14B	0.164 (4)	0.774 (8)	-0.039 (4)	9.5 (17)
H14C	0.215 (4)	0.780 (7)	0.056 (3)	7.2 (14)
H15A	0.114 (3)	0.337 (5)	0.162 (3)	4.4 (10)
H15B	0.061 (3)	0.416 (5)	0.0786 (23)	3.9 (9)
H16A	0.122 (3)	0.155 (6)	0.010 (3)	5.8 (12)
H16B	0.167 (3)	0.085 (6)	0.096 (3)	6.3 (13)
H16C	0.049 (4)	0.100 (7)	0.077 (3)	7.5 (14)

Biso is the Mean of the Principal Axes of the Thermal Ellipsoid

4.4.3 Thioamide Iron Tricarbonyl Complex 2

Space Group and Cell Dimensions Monoclinic, P 21/n
a 12.991(4) b 12.9207(14) c 14.636(3)
beta 111.401(19)
Volume 2287.4(8)A**3

Empirical formula : Fe S N O8 C21 H19

Cell dimensions were obtained from 24 reflections with 2Theta angle in the range 26.00 - 34.00 degrees.

Crystal dimensions : 0.30 X 0.20 X 0.20 mm

FW = 501.29 Z = 4 F(000) = 1007.85

Dcalc 1.456Mg.m-3, mu 0.79mm-1, lambda 0.70930A, 2Theta(max) 44.8

The intensity data were collected on a Nonius diffractometer, using the theta/2theta scan mode.
The h,k,l ranges are :-- -13 12, 0 13, 0 15
No. of reflections measured 3292
No. of unique reflections 2967
No. of reflections with Inet > 2.5sigma(Inet) 1714
No correction was made for absorption

The last least squares cycle was calculated with
51 atoms, 340 parameters and 1714 out of 2967 reflections.
Weights based on counting-statistics were used.

The residuals are as follows :--
For significant reflections, RF 0.050, Rw 0.030 GoF 2.11
For all reflections, RF 0.050, Rw 0.030.
where RF = Sum(Fo-Fc)/Sum(Fo),
Rw = Sqrt[Sum(w(Fo-Fc)**2)/Sum(wFo**2)] and
GoF = Sqrt[Sum(w(Fo-Fc)**2)/(No. of reflns - No. of params.)]
The maximum shift/sigma ratio was 1.034.

In the last D-map, the deepest hole was -0.360e/A**3,
and the highest peak 0.320e/A**3.

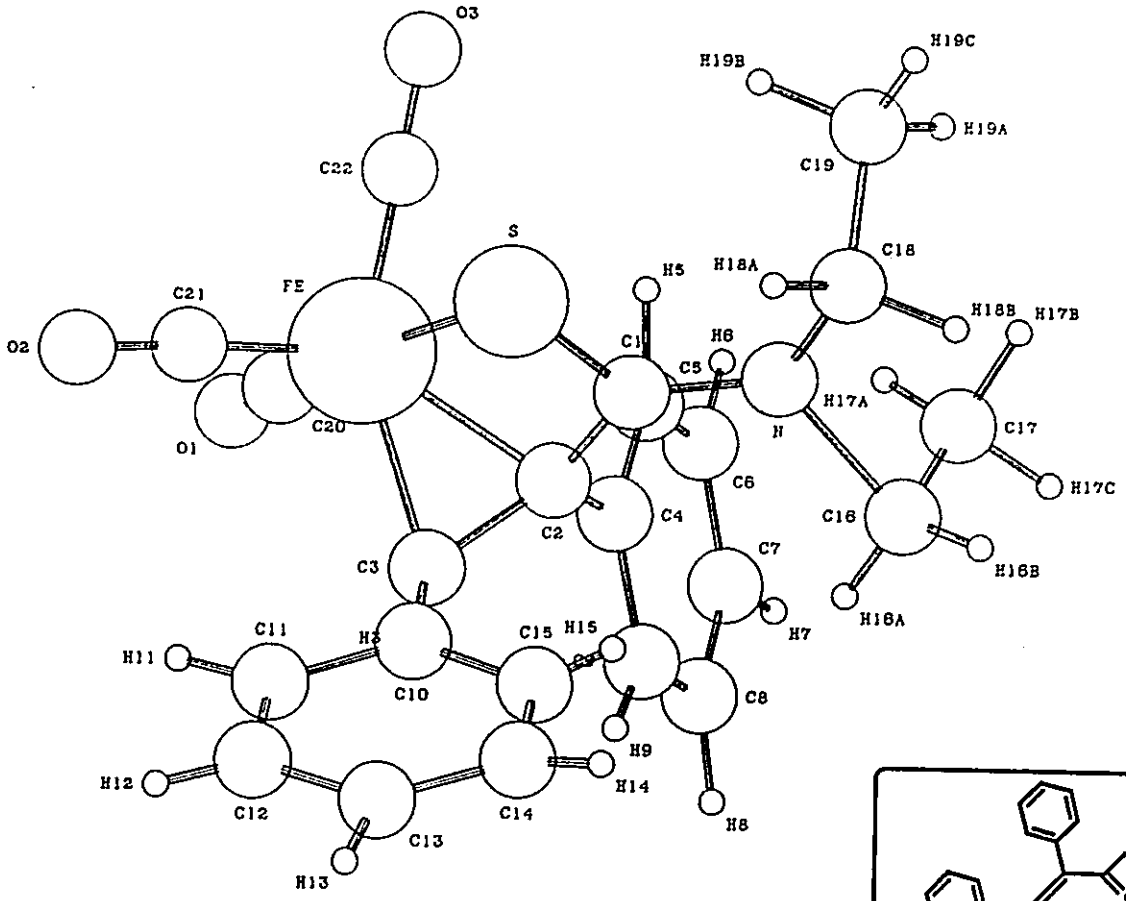

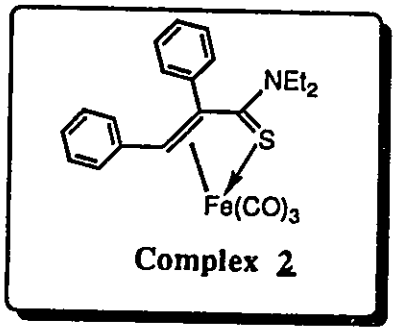

Complex 2

X-Ray Crystal Structure of Complex 2

Table of Bond Distances in Angstroms

Fe-S	2.3592(25)	C(8)-C(12)	1.455(11)
Fe-C(1)	1.849(8)	C(9)-H(9A)	0.99(6)
Fe-C(2)	1.779(9)	C(9)-H(9B)	1.16(7)
Fe-C(3)	1.801(9)	C(9)-H(9C)	1.01(6)
Fe-C(7)	2.053(7)	C(11)-H(11A)	0.82(8)
Fe-C(8)	2.093(7)	C(11)-H(11B)	0.94(7)
S-C(14)	1.702(7)	C(11)-H(11C)	1.57(7)
O(1)-C(1)	1.100(10)	C(13)-H(13A)	1.04(6)
O(2)-C(2)	1.131(11)	C(13)-H(13B)	0.98(7)
O(3)-C(3)	1.139(10)	C(13)-H(13C)	0.91(7)
O(4)-C(6)	1.206(9)	C(15)-H(15A)	1.38(7)
O(5)-C(10)	1.197(10)	C(15)-H(15B)	0.91(6)
O(6)-C(10)	1.333(11)	C(15)-H(15C)	0.73(7)
O(6)-C(11)	1.449(12)	C(16)-C(17)	1.354(13)
O(7)-C(12)	1.193(11)	C(16)-C(21)	1.362(12)
O(8)-C(12)	1.347(11)	C(17)-C(18)	1.371(14)
O(8)-C(13)	1.431(12)	C(17)-H(17)	1.02(6)
N-C(14)	1.320(10)	C(18)-C(19)	1.395(19)
N-C(15)	1.476(12)	C(18)-H(18)	1.01(7)
N-C(16)	1.465(9)	C(19)-C(20)	1.391(20)
C(4)-C(5)	1.544(10)	C(19)-H(19)	1.010(10)
C(4)-C(8)	1.538(10)	C(20)-C(21)	1.346(15)
C(4)-C(9)	1.520(11)	C(20)-H(20)	0.944(10)
C(4)-H(4)	1.08(5)	C(21)-H(21)	0.98(7)
C(5)-C(6)	1.559(10)	H(9A)-H(9B)	1.47(9)
C(5)-C(14)	1.490(11)	H(11A)-H(11C)	1.46(12)
C(5)-H(5)	0.94(6)	H(11B)-H(11C)	1.46(11)
C(6)-C(7)	1.486(10)	H(13A)-H(13B)	1.51(10)
C(7)-C(8)	1.450(10)	H(13B)-H(13C)	1.30(10)
C(7)-C(10)	1.518(11)	H(15B)-H(15C)	1.50(9)

Table of Bond Angles in Degrees

S-Fe-C(1)	83.9(3)	O(5)-C(10)-C(7)	126.7(8)
S-Fe-C(2)	166.8(3)	O(6)-C(10)-C(7)	109.6(7)
S-Fe-C(3)	84.2(3)	O(6)-C(11)-H(11A)	108(6)
S-Fe-C(7)	100.75(20)	O(6)-C(11)-H(11B)	109(5)
S-Fe-C(8)	96.07(21)	O(6)-C(11)-H(11C)	110.2(25)
C(1)-Fe-C(2)	88.7(4)	H(11A)-C(11)-H(11B)	127(9)
C(1)-Fe-C(3)	110.1(4)	H(11A)-C(11)-H(11C)	66(7)
C(1)-Fe-C(7)	105.1(3)	H(11B)-C(11)-H(11C)	65(6)
C(1)-Fe-C(8)	145.7(3)	O(7)-C(12)-O(8)	122.5(8)
C(2)-Fe-C(3)	88.0(4)	O(7)-C(12)-C(8)	125.4(8)
C(2)-Fe-C(7)	91.8(3)	O(8)-C(12)-C(8)	112.1(7)
C(2)-Fe-C(8)	96.2(4)	O(8)-C(13)-H(13A)	112(4)
C(3)-Fe-C(7)	144.7(4)	O(8)-C(13)-H(13B)	114(5)
C(3)-Fe-C(8)	104.0(3)	O(8)-C(13)-H(13C)	108(5)
C(7)-Fe-C(8)	40.9(3)	H(13A)-C(13)-H(13B)	96(6)
Fe-S-C(14)	109.3(3)	H(13A)-C(13)-H(13C)	134(6)
C(10)-O(6)-C(11)	116.3(7)	H(13B)-C(13)-H(13C)	86(7)
C(12)-O(8)-C(13)	114.9(7)	S-C(14)-N	123.1(6)
C(14)-N-C(15)	120.4(7)	S-C(14)-C(5)	116.2(6)
C(14)-N-C(16)	122.5(6)	N-C(14)-C(5)	120.7(6)
C(15)-N-C(16)	116.9(7)	N-C(15)-H(15A)	121(3)
Fe-C(1)-O(1)	178.7(9)	N-C(15)-H(15B)	110(4)
Fe-C(2)-O(2)	172.6(8)	N-C(15)-H(15C)	104(7)
Fe-C(3)-O(3)	177.3(8)	H(15A)-C(15)-H(15B)	84(5)
C(5)-C(4)-C(8)	104.1(6)	H(15A)-C(15)-H(15C)	104(7)
C(5)-C(4)-C(9)	109.8(6)	H(15B)-C(15)-H(15C)	131(8)
C(5)-C(4)-H(4)	113(3)	N-C(16)-C(17)	118.4(7)
C(8)-C(4)-C(9)	111.0(6)	N-C(16)-C(21)	117.6(8)
C(8)-C(4)-H(4)	109(3)	C(17)-C(16)-C(21)	124.0(8)
C(9)-C(4)-H(4)	109(4)	C(16)-C(17)-C(18)	119.2(9)
C(4)-C(5)-C(6)	106.3(6)	C(16)-C(17)-H(17)	121(4)
C(4)-C(5)-C(14)	111.7(6)	C(18)-C(17)-H(17)	119(4)
C(4)-C(5)-H(5)	111(4)	C(17)-C(18)-C(19)	117.0(10)
C(6)-C(5)-C(14)	109.0(6)	C(17)-C(18)-H(18)	119(4)
C(6)-C(5)-H(5)	112(4)	C(19)-C(18)-H(18)	122(4)
C(14)-C(5)-H(5)	106(4)	C(18)-C(19)-C(20)	122.5(9)
O(4)-C(6)-C(5)	125.2(6)	C(18)-C(19)-H(19)	116.8(14)
O(4)-C(6)-C(7)	128.4(7)	C(20)-C(19)-H(19)	120.7(13)
C(5)-C(6)-C(7)	106.4(6)	C(19)-C(20)-C(21)	118.6(9)
Fe-C(7)-C(6)	106.9(5)	C(19)-C(20)-H(20)	107.8(11)
Fe-C(7)-C(8)	71.0(4)	C(21)-C(20)-H(20)	133.6(12)
Fe-C(7)-C(10)	120.0(5)	C(16)-C(21)-C(20)	118.7(9)
C(6)-C(7)-C(8)	110.2(6)	C(16)-C(21)-H(21)	128(4)
C(6)-C(7)-C(10)	112.7(6)	C(20)-C(21)-H(21)	112(4)
C(8)-C(7)-C(10)	128.4(6)		
Fe-C(8)-C(4)	115.9(5)	C(4)-C(8)-C(7)	109.4(6)
Fe-C(8)-C(7)	68.0(4)	C(4)-C(8)-C(12)	115.4(6)
Fe-C(8)-C(12)	112.0(5)	C(7)-C(8)-C(12)	127.5(7)
C(4)-C(9)-H(9A)	119(4)	H(9A)-C(9)-H(9B)	86(5)
C(4)-C(9)-H(9B)	115(3)	H(9A)-C(9)-H(9C)	107(5)
C(4)-C(9)-H(9C)	116(4)	H(9B)-C(9)-H(9C)	106(5)
O(5)-C(10)-O(6)	123.7(8)		

Table of Atomic Parameters x,y,z and Biso.
E.S.Ds. refer to the last digit printed.

	x	y	z	Biso
Fe	0.23474(9)	0.63971(10)	0.00983(8)	3.81(6)
S	0.26697(17)	0.46857(16)	0.06976(15)	4.57(12)
O 1	0.0342 (5)	0.6249 (6)	0.0588 (4)	7.7 (4)
O 2	0.1365 (5)	0.8254 (5)	-0.0989 (4)	8.2 (4)
O 3	0.1945 (6)	0.5462 (6)	-0.1832 (4)	9.3 (5)
O 4	0.3515 (4)	0.6595 (4)	0.2834 (3)	4.6 (3)
O 5	0.2333 (5)	0.8692 (5)	0.1223 (4)	6.7 (4)
O 6	0.4160 (5)	0.8758 (4)	0.2017 (4)	5.3 (3)
O 7	0.4768 (5)	0.7139 (4)	-0.0618 (4)	5.7 (4)
O 8	0.3886 (4)	0.8422 (4)	-0.0193 (3)	5.2 (3)
N	0.4194 (5)	0.3813 (5)	0.2254 (4)	3.5 (4)
C 1	0.1092 (7)	0.6293 (7)	0.0408 (5)	4.7 (5)
C 2	0.1810 (7)	0.7567 (7)	-0.0538 (6)	5.6 (6)
C 3	0.2113 (7)	0.5803 (7)	-0.1073 (6)	5.5 (5)
C 4	0.4855 (6)	0.5991 (5)	0.1110 (5)	2.8 (4)
C 5	0.4504 (6)	0.5628 (6)	0.1959 (5)	2.8 (4)
C 6	0.3763 (5)	0.6504 (6)	0.2121 (5)	2.8 (4)
C 7	0.3469 (6)	0.7190 (5)	0.1248 (5)	3.1 (4)
C 8	0.4011 (6)	0.6839 (6)	0.0596 (5)	3.1 (4)
C 9	0.6021 (6)	0.6428 (7)	0.1521 (6)	4.3 (5)
C10	0.3223 (8)	0.8292 (7)	0.1466 (6)	4.0 (5)
C11	0.4058 (10)	0.9805 (9)	0.2327 (9)	8.1 (9)
C12	0.4267 (7)	0.7445 (7)	-0.0132 (6)	4.0 (5)
C13	0.3975 (10)	0.9018 (8)	-0.0985 (8)	7.9 (8)
C14	0.3852 (6)	0.4650 (6)	0.1710 (5)	3.3 (4)
C15	0.3566 (10)	0.2837 (8)	0.1983 (6)	5.6 (7)
C16	0.5236 (7)	0.3781 (6)	0.3102 (5)	3.5 (5)
C17	0.6181 (8)	0.3586 (8)	0.2943 (6)	6.7 (6)
C18	0.7164 (9)	0.3550 (9)	0.3727 (10)	9.6 (8)
C19	0.7117 (11)	0.3689 (10)	0.4656 (8)	10.2 (8)
C20	0.6129 (10)	0.3857 (11)	0.4799 (8)	10.4 (10)
C21	0.5188 (8)	0.3925 (8)	0.4007 (7)	6.7 (7)
H4	0.482 (5)	0.539 (5)	0.059 (4)	6.3
H5	0.512 (5)	0.549 (5)	0.253 (4)	6.3
H9A	0.615 (6)	0.710 (5)	0.187 (5)	6.3
H9B	0.633 (5)	0.682 (5)	0.096 (4)	6.3
H9C	0.662 (5)	0.593 (5)	0.191 (5)	6.3
H11A	0.342 (7)	0.999 (7)	0.204 (7)	6.3
H11B	0.448 (6)	0.987 (6)	0.300 (5)	6.3
H11C	0.336 (5)	0.981 (5)	0.300 (5)	6.3
H13A	0.356 (6)	0.867 (6)	-0.166 (4)	6.3
H13B	0.355 (6)	0.966 (5)	-0.112 (5)	6.3
H13C	0.459 (6)	0.943 (6)	-0.074 (5)	6.3
H15A	0.243 (5)	0.281 (5)	0.174 (4)	6.3
H15B	0.359 (6)	0.248 (5)	0.253 (5)	6.3
H15C	0.365 (7)	0.266 (7)	0.154 (5)	6.3
H17	0.617 (5)	0.338 (5)	0.227 (4)	6.3
H18	0.784 (5)	0.326 (5)	0.363 (5)	6.3
H19	0.784	0.369	0.523	8.6
H20	0.629	0.391	0.548	8.2
H21	0.455 (5)	0.414 (6)	0.418 (5)	6.3

Biso is the Mean of the Principal Axes of the Thermal Ellipsoid

Table of u(i,j) or U values *100.
E.S.Ds. refer to the last digit printed

	u11(U)	u22	u33	u12	u13	u23
FE	4.06(7)	6.45(9)	3.30(6)	0.62(8)	0.53(5)	0.00(7)
S	4.85(15)	5.42(16)	5.50(15)	-0.78(13)	-0.03(12)	-1.06(12)
O 1	6.7 (5)	13.0 (6)	11.3 (5)	0.8 (5)	5.5 (4)	2.0 (5)
O 2	9.6 (6)	11.6 (6)	7.8 (5)	4.2 (5)	0.5 (4)	4.1 (4)
O 3	10.9 (6)	16.8 (7)	5.4 (4)	2.5 (5)	0.6 (5)	-3.7 (5)
O 4	8.1 (4)	6.4 (4)	4.1 (3)	2.0 (3)	3.7 (3)	0.6 (3)
O 5	6.8 (4)	7.5 (5)	10.5 (5)	3.1 (4)	2.7 (4)	-0.4 (4)
O 6	7.0 (4)	5.0 (4)	7.7 (4)	0.8 (4)	2.0 (4)	-1.7 (3)
O 7	9.4 (5)	8.9 (5)	5.6 (4)	1.6 (4)	5.3 (4)	0.7 (4)
O 8	8.6 (5)	6.9 (4)	5.4 (4)	1.0 (4)	4.0 (3)	2.5 (3)
N	6.0 (5)	3.1 (5)	4.9 (4)	-1.0 (4)	2.8 (4)	-0.4 (4)
C 1	5.2 (6)	7.1 (7)	4.7 (5)	0.4 (6)	0.9 (5)	0.5 (5)
C 2	5.4 (7)	9.7 (9)	4.8 (6)	1.0 (6)	0.3 (5)	0.0 (6)
C 3	4.4 (6)	9.3 (8)	6.2 (6)	2.0 (5)	0.6 (6)	0.0 (6)
C 4	3.7 (5)	3.8 (5)	3.7 (5)	0.1 (4)	1.9 (4)	-0.3 (4)
C 5	2.7 (5)	3.4 (5)	3.8 (5)	0.4 (4)	0.1 (4)	-0.1 (4)
C 6	2.9 (5)	3.3 (5)	3.9 (5)	-0.1 (4)	0.3 (4)	-0.6 (5)
C 7	3.8 (5)	4.0 (5)	3.6 (5)	0.6 (4)	0.8 (4)	0.3 (4)
C 8	4.1 (5)	5.1 (6)	2.8 (4)	0.6 (4)	1.6 (4)	-0.7 (4)
C 9	3.5 (5)	6.4 (7)	6.2 (6)	-1.2 (6)	1.6 (5)	0.7 (5)
C10	6.8 (7)	5.8 (7)	3.8 (5)	1.1 (6)	3.5 (6)	0.8 (5)
C11	11.6 (14)	6.9 (8)	11.2 (11)	2.2 (8)	2.6 (10)	-4.6 (9)
C12	5.5 (6)	5.3 (7)	4.0 (5)	0.9 (5)	1.3 (5)	0.7 (5)
C13	13.0 (13)	9.3 (11)	7.0 (8)	-1.0 (8)	2.8 (9)	3.8 (8)
C14	4.1 (5)	4.3 (6)	4.7 (5)	-0.8 (5)	2.3 (5)	-1.6 (5)
C15	10.2 (8)	4.6 (7)	7.1 (8)	-3.6 (6)	3.7 (8)	-0.5 (6)
C16	5.3 (6)	3.8 (6)	3.4 (5)	-0.2 (5)	0.7 (5)	0.7 (4)
C17	7.4 (7)	11.5 (9)	5.6 (6)	4.5 (8)	1.1 (6)	-2.9 (7)
C18	7.9 (9)	10.9 (9)	12.4 (10)	6.5 (8)	-2.4 (9)	-3.8 (9)
C19	15.2 (12)	9.2 (9)	6.1 (7)	-2.2 (11)	-6.0 (9)	2.1 (8)
C20	12.5 (11)	20.7 (15)	4.3 (7)	-7.9 (12)	0.6 (8)	2.4 (8)
C21	8.7 (8)	13.1 (10)	3.8 (6)	-3.4 (8)	2.6 (6)	-0.7 (6)

Anisotropic Temperature Factors are of the form
Temp=-2*Pi*Pi*(h*h*u11*astar*astar+---+2*h*k*u12*astar*bstar+---)

4.4.4 Complex 22

Space Group and Cell Dimensions Orthorhombic P 212121
a 8.9127(11) b 12.2595(16) c 19.6009(17)
Volume 2141.7(4)A**3

Empirical formula : Fe C22 O3 N S H21

Cell dimensions were obtained from 21 reflections with 2Theta angle in the range 25.00 - 29.00 degrees.

Crystal dimensions : 0.44 X 0.14 X 0.14 mm

FW = 435.32 Z = 4 F(000) = 903.86

Dcalc 1.350Mg.m-3, mu 0.82mm-1, lambda 0.70930A, 2Theta(max) 44.8

The intensity data were collected on a Nonius diffractometer, using the theta/2theta scan mode.

The h,k,l ranges are :--	0 9, 0 12, 0 20
No. of reflections measured	6131
No. of unique reflections	2775
No. of reflections with Inet > 2.5sigma(Inet)	1930

No correction was made for absorption

The last least squares cycle was calculated with
49 atoms, 253 parameters and 1134 out of 1611 reflections.
Unit weights were used.

The residuals are as follows :--
For significant reflections, RF 0.048, Rw 0.051 GoF 0.35
For all reflections, RF 0.048, Rw 0.051.
where RF = Sum(Fo-Fc)/Sum(Fo),
Rw = Sqrt[Sum(w(Fo-Fc)**2)/Sum(wFo**2)] and
GoF = Sqrt[Sum(w(Fo-Fc)**2)/(No. of reflns - No. of params.)]
The maximum shift/sigma ratio was 0.067.

In the last D-map, the deepest hole was -0.250e/A**3,
and the highest peak 0.290e/A**3.

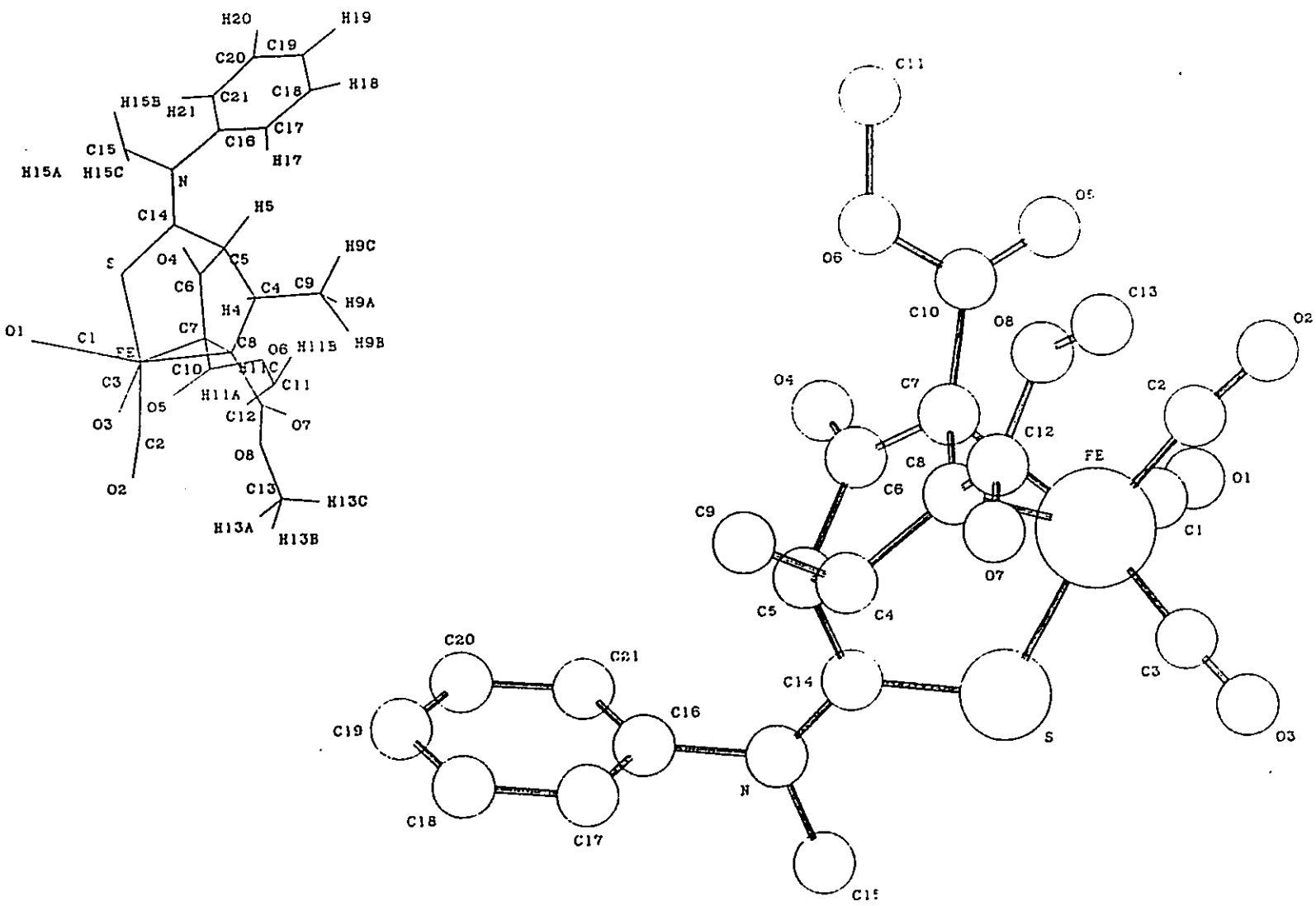

X-Ray Crystal Structure of Complex **22**

Table of Bond Distances in Angstroms

Fe-S	2.316(3)	C(8)-C(9)	1.367(20)
Fe-C(2)	2.072(11)	C(8)-H(8)	1.103(15)
Fe-C(3)	2.065(12)	C(9)-H(9)	1.126(15)
Fe-C(20)	1.761(13)	C(10)-C(11)	1.405(18)
Fe-C(22)	1.763(16)	C(10)-C(15)	1.377(18)
Fe-C(21)	1.760(17)	C(11)-C(12)	1.393(19)
S-C(1)	1.705(11)	C(11)-H(11)	1.111(12)
O(1)-C(20)	1.146(16)	C(12)-C(13)	1.38(3)
O(2)-C(21)	1.174(20)	C(12)-H(12)	1.089(13)
O(3)-C(22)	1.150(20)	C(13)-C(14)	1.38(3)
N-C(1)	1.327(17)	C(13)-H(13)	1.082(14)
N-C(16)	1.78(4)	C(14)-C(15)	1.373(21)
N-C(18)	1.478(17)	C(14)-H(14)	1.111(16)
C(1)-C(2)	1.450(16)	C(15)-H(15)	1.121(14)
C(2)-C(3)	1.454(19)	C(16)-C(17)	1.24(4)
C(2)-C(4)	1.506(16)	C(16)-H(17A)	1.074(22)
C(3)-C(10)	1.506(18)	C(16)-H(17B)	1.06(3)
C(3)-H(3)	1.106(11)	C(17)-H(16A)	1.099(23)
C(4)-C(5)	1.385(19)	C(17)-H(16B)	1.135(24)
C(4)-C(9)	1.388(19)	C(17)-H(16C)	1.13(3)
C(5)-C(6)	1.385(19)	C(18)-C(19)	1.509(23)
C(5)-H(5)	1.106(13)	C(18)-H(18A)	1.091(13)
C(6)-C(7)	1.34(3)	C(18)-H(18B)	1.083(13)
C(6)-H(6)	1.150(14)	C(19)-H(19A)	1.128(17)
C(7)-C(8)	1.38(3)	C(19)-H(19B)	1.109(17)
C(7)-H(7)	1.097(13)	C(19)-H(19C)	1.044(15)

Table of Bond Angles in Degrees

S-Fe-C(2)	73.1(3)	C(4)-C(9)-C(8)	119.4(14)
S-Fe-C(3)	84.5(3)	C(4)-C(9)-H(9)	120.6(12)
S-Fe-C(20)	169.1(5)	C(8)-C(9)-H(9)	120.0(14)
S-Fe-C(22)	87.0(5)	C(3)-C(10)-C(11)	118.3(11)
S-Fe-C(21)	95.8(5)	C(3)-C(10)-C(15)	123.2(12)
C(2)-Fe-C(3)	41.2(5)	C(11)-C(10)-C(15)	118.2(12)
C(2)-Fe-C(20)	98.7(6)	C(10)-C(11)-C(12)	120.2(12)
C(2)-Fe-C(22)	110.1(7)	C(10)-C(11)-H(11)	120.5(11)
C(2)-Fe-C(21)	140.7(6)	C(12)-C(11)-H(11)	119.3(12)
C(3)-Fe-C(20)	94.1(5)	C(11)-C(12)-C(13)	120.6(13)
C(3)-Fe-C(22)	151.3(7)	C(11)-C(12)-H(12)	122.1(14)
C(3)-Fe-C(21)	101.5(6)	C(13)-C(12)-H(12)	117.3(13)
C(20)-Fe-C(22)	89.1(6)	C(12)-C(13)-C(14)	118.8(13)
C(20)-Fe-C(21)	95.1(7)	C(12)-C(13)-H(13)	123.2(17)
C(22)-Fe-C(21)	106.6(7)	C(14)-C(13)-H(13)	118.0(17)
Fe-S-C(1)	77.4(4)	C(13)-C(14)-C(15)	121.2(14)
C(1)-N-C(16)	121.1(11)	C(13)-C(14)-H(14)	118.3(14)
C(1)-N-C(18)	121.9(11)	C(15)-C(14)-H(14)	120.5(16)
C(16)-N-C(18)	113.0(11)	C(10)-C(15)-C(14)	121.1(14)
S-C(1)-N	121.3(9)	C(10)-C(15)-H(15)	121.8(13)
S-C(1)-C(2)	112.1(8)	C(14)-C(15)-H(15)	117.0(13)
N-C(1)-C(2)	126.5(10)	N-C(16)-C(17)	89.3(24)
Fe-C(2)-C(1)	91.4(7)	N-C(16)-H(17A)	114.0(21)
Fe-C(2)-C(3)	69.2(6)	N-C(16)-H(17B)	114.1(18)
Fe-C(2)-C(4)	119.5(8)	C(17)-C(16)-H(17A)	111.8(19)
C(1)-C(2)-C(3)	116.1(10)	C(17)-C(16)-H(17B)	114.6(22)
C(1)-C(2)-C(4)	123.6(11)	H(17A)-C(16)-H(17B)	111(3)
C(3)-C(2)-C(4)	118.6(10)	C(16)-C(17)-H(16A)	116(3)
Fe-C(3)-C(2)	69.7(6)	C(16)-C(17)-H(16B)	113.7(23)
Fe-C(3)-C(10)	121.2(8)	C(16)-C(17)-H(16C)	113(3)
Fe-C(3)-H(3)	106.2(7)	H(16A)-C(17)-H(16B)	104.3(21)
C(2)-C(3)-C(10)	126.8(10)	H(16A)-C(17)-H(16C)	104.5(22)
C(2)-C(3)-H(3)	112.6(10)	H(16B)-C(17)-H(16C)	102.2(24)
C(10)-C(3)-H(3)	112.5(10)	N-C(18)-C(19)	112.9(11)
C(2)-C(4)-C(5)	122.3(11)	N-C(18)-H(18A)	112.1(12)
C(2)-C(4)-C(9)	118.6(11)	N-C(18)-H(18B)	110.8(11)
C(5)-C(4)-C(9)	119.1(11)	C(19)-C(18)-H(18A)	106.2(11)
C(4)-C(5)-C(6)	119.4(13)	C(19)-C(18)-H(18B)	105.9(12)
C(4)-C(5)-H(5)	118.4(12)	H(18A)-C(18)-H(18B)	108.4(11)
C(6)-C(5)-H(5)	122.2(13)	C(18)-C(19)-H(19A)	108.7(14)
C(5)-C(6)-C(7)	121.4(13)	C(18)-C(19)-H(19B)	109.5(12)
C(5)-C(6)-H(6)	117.7(15)	C(18)-C(19)-H(19C)	115.6(14)
C(7)-C(6)-H(6)	120.9(13)	H(19A)-C(19)-H(19B)	104.0(14)
C(6)-C(7)-C(8)	119.4(12)	H(19A)-C(19)-H(19C)	108.5(14)
C(6)-C(7)-H(7)	118.4(16)	H(19B)-C(19)-H(19C)	109.9(15)
C(8)-C(7)-H(7)	122.2(16)	Fe-C(20)-O(1)	177.5(14)
C(7)-C(8)-C(9)	121.2(14)	Fe-C(22)-O(3)	179.3(15)
C(7)-C(8)-H(8)	118.6(14)	Fe-C(21)-O(2)	176.1(12)
C(9)-C(8)-H(8)	120.1(16)		

Table of Atomic Parameters x,y,z and Biso.
E.S.Ds. refer to the last digit printed.

	x	y	z	Biso
Fe	0.45851(20)	0.20334(15)	0.18707(9)	4.38(8)
S	0.4184 (4)	0.2678 (3)	0.07753(15)	4.82(14)
O 1	0.4579 (16)	0.1523 (10)	0.3319 (5)	9.5 (7)
O 2	0.7155 (12)	0.0653 (10)	0.1512 (6)	8.3 (6)
O 3	0.5721 (16)	0.4198 (10)	0.2201 (6)	10.9 (8)
N	0.1425 (14)	0.3462 (10)	0.0886 (5)	5.7 (6)
C 1	0.2451 (13)	0.2787 (10)	0.1136 (5)	4.1 (6)
C 2	0.2284 (12)	0.2082 (11)	0.1725 (5)	4.4 (6)
C 3	0.2848 (13)	0.0976 (10)	0.1651 (5)	4.0 (5)
C 4	0.1272 (13)	0.2337 (10)	0.2320 (6)	4.4 (6)
C 5	0.1468 (16)	0.3254 (11)	0.2723 (7)	5.5 (7)
C 6	0.0509 (20)	0.3433 (12)	0.3268 (7)	6.9 (8)
C 7	-0.0612 (20)	0.2746 (14)	0.3409 (7)	7.4 (9)
C 8	-0.0840 (16)	0.1853 (14)	0.2997 (8)	7.2 (8)
C 9	0.0103 (17)	0.1627 (12)	0.2466 (7)	6.3 (7)
C10	0.2854 (13)	0.0300 (10)	0.1009 (6)	4.3 (6)
C11	0.3829 (14)	-0.0599 (10)	0.0975 (6)	4.8 (6)
C12	0.3787 (16)	-0.1296 (11)	0.0414 (8)	5.9 (7)
C13	0.2781 (22)	-0.1122 (13)	-0.0109 (8)	7.3 (9)
C14	0.1826 (21)	-0.0236 (14)	-0.0069 (7)	7.0 (9)
C15	0.1847 (16)	0.0450 (11)	0.0485 (7)	5.4 (7)
C16	-0.052 (4)	0.3243 (17)	0.1036 (9)	12.4 (18)
C17	-0.057 (3)	0.4123 (24)	0.1348 (11)	14.6 (20)
C18	0.1719 (15)	0.4146 (11)	0.0279 (6)	5.2 (7)
C19	0.2416 (20)	0.5232 (13)	0.0455 (8)	7.3 (9)
C20	0.4608 (17)	0.1710 (11)	0.2746 (7)	5.8 (7)
C22	0.5264 (20)	0.3346 (13)	0.2071 (7)	7.2 (8)
C21	0.6161 (17)	0.1232 (13)	0.1665 (7)	6.3 (8)
H 3	0.267	0.048	0.211	4.7
H 5	0.241	0.381	0.260	6.2
H 6	0.072	0.419	0.360	7.8
H 7	-0.135	0.294	0.384	8.4
H 8	-0.178	0.130	0.312	7.7
H 9	-0.008	0.087	0.215	7.0
H11	0.461	-0.078	0.140	5.5
H12	0.457	-0.197	0.036	6.7
H13	0.267	-0.166	-0.054	7.7
H14	0.107	-0.007	-0.051	7.7
H15	0.100	0.113	0.049	6.5
H16A	0.015	0.420	0.180	13.1
H16B	-0.028	0.486	0.102	13.1
H16C	-0.174	0.434	0.154	13.1
H17A	-0.075	0.256	0.136	10.0
H17B	-0.118	0.322	0.059	10.0
H18A	0.070	0.433	0.000	6.5
H18B	0.250	0.375	-0.006	6.5
H19A	0.165	0.568	0.082	7.7
H19B	0.345	0.510	0.076	7.7
H19C	0.265	0.574	0.004	7.7

Biso is the Mean of the Principal Axes of the Thermal Ellipsoid

Table of u(i,j) or U values *100.
E.S.Ds. refer to the last digit printed

	u11(U)	u22	u33	u12	u13	u23
FE	5.27(9)	6.01(10)	5.35(9)	-0.30(11)	-0.27(10)	-0.17(10)
S	5.99(20)	6.82(22)	5.50(17)	0.10(17)	1.37(16)	0.62(16)
O 1	14.9 (10)	15.3 (10)	6.1 (6)	0.3 (10)	-2.1 (7)	1.6 (6)
O 2	6.8 (7)	11.8 (10)	13.1 (9)	3.0 (7)	-0.9 (7)	-2.6 (8)
O 3	16.4 (13)	10.8 (9)	14.2 (10)	-5.5 (10)	0.1 (10)	-4.1 (8)
N	6.9 (8)	9.6 (9)	5.0 (7)	1.1 (7)	0.9 (6)	1.7 (6)
C 1	6.3 (8)	5.6 (8)	3.7 (6)	1.3 (8)	0.5 (6)	0.0 (6)
C 2	4.5 (6)	6.3 (8)	5.9 (8)	0.0 (7)	-0.4 (6)	-0.2 (7)
C 3	5.6 (8)	5.7 (8)	3.9 (7)	-1.9 (7)	-0.4 (6)	0.6 (6)
C 4	5.2 (8)	6.5 (9)	4.9 (7)	1.2 (7)	0.9 (6)	1.2 (7)
C 5	8.3 (10)	6.0 (9)	6.6 (8)	-0.1 (8)	1.8 (8)	0.5 (7)
C 6	10.7 (12)	8.9 (10)	6.7 (9)	2.6 (11)	2.9 (11)	-0.1 (8)
C 7	10.1 (13)	11.2 (14)	6.6 (9)	1.6 (13)	4.3 (10)	1.9 (10)
C 8	6.5 (9)	11.6 (13)	9.1 (11)	0.2 (10)	2.4 (9)	1.6 (11)
C 9	7.2 (9)	10.6 (11)	6.1 (8)	-0.2 (9)	1.6 (7)	1.0 (8)
C10	4.5 (7)	5.1 (8)	6.7 (8)	-1.2 (7)	-0.2 (7)	1.7 (7)
C11	6.4 (9)	4.8 (7)	6.9 (8)	-0.1 (7)	0.5 (7)	0.2 (7)
C12	8.0 (10)	6.1 (9)	8.4 (10)	0.6 (8)	2.3 (9)	-1.2 (8)
C13	13.1 (16)	6.9 (11)	7.9 (11)	-2.6 (11)	1.9 (11)	-2.7 (9)
C14	12.0 (15)	8.4 (11)	6.1 (9)	-1.9 (12)	-1.9 (10)	-1.5 (9)
C15	6.4 (9)	7.2 (10)	7.0 (9)	0.6 (8)	-1.7 (9)	0.5 (8)
C16	27.3 (35)	13.2 (20)	6.8 (12)	9.8 (26)	2.7 (18)	3.9 (12)
C17	17.6 (26)	24.7 (31)	13.2 (20)	-8.9 (28)	-6.7 (21)	9.9 (19)
C18	5.8 (8)	7.9 (9)	6.3 (8)	2.0 (9)	-0.3 (8)	0.9 (7)
C19	10.2 (13)	8.4 (12)	9.2 (11)	0.2 (11)	1.0 (11)	1.7 (10)
C20	5.8 (8)	9.2 (11)	7.1 (9)	-2.3 (9)	-0.6 (9)	-0.2 (8)
C22	10.4 (12)	9.1 (11)	7.8 (10)	0.9 (11)	1.9 (10)	-2.1 (8)
C21	7.7 (11)	8.4 (11)	7.8 (11)	-0.4 (9)	-1.6 (8)	-2.4 (8)

Anisotropic Temperature Factors are of the form
Temp=-2*Pi*Pi*(h*h*u11*astar*astar+---+2*h*k*u12*astar*bstar+---)

4.5.1 Reactions with dienes and miscellaneous reagents

Iron complex 7 (0.3mmol) was dissolved in THF (10mL) and 2,3-dimethyl-1,3-butadiene (0.3mmol) was added dropwise. Carbon monoxide was bubbled through the solution. The solution was refluxed for 38 hours but there was no reaction and 7 was recovered by column chromatography on alumina using hexanes in 93% yield. Photolysis of the same reaction mixture for 48 hours gave no reaction and 84% recovery of iron complex 7. The same procedures were followed using phenylisocyanide, 3-phenyl-1,2-propadiene, and ethyldiazoacetate instead of the butadiene but there was no reaction and the iron complex was recovered in 96%/92%, 94%/90%, 95%/94% yields respectively (photolysis/thermolysis).

4.5.2 Hydride abstraction

Iron complex 4 (0.3mmol) was dissolved in CH_2Cl_2 (5mL) and Ph_3CBF_4 (0.3mmol) was added. After 3 hours ether was added to the stirring solution. Column chromatography on alumina using hexanes gave 90% recovery of the iron complex 4. Using iron complex 7 and 6 in the same procedure gave recovery of the complexes in 89% and 91%.

4.5.3 Reduction

Iron complex 7 (0.3mmol) was dissolved in THF (10mL) and $LiAlH_4$ (1.2mmol) was added. The solution was stirred for 1 hour. Column chromatography on alumina using ether gave compound XXVII in 57% yield.

Iron complex 7 (0.3mmol) was dissolved in THF (10mL) and $NaBH_4$ (1.2mmol) was added. The solution was stirred for 1 hour. Column chromatography on alumina using ether gave compound XXVII in 50% yield.

Iron complex 7 (0.3mmol) was dissolved in THF (10mL) and K-Selectride (1.2mmol) was added. The solution was stirred for 1 hour. Column chromatography on alumina using ether gave 18% recovery of the iron complex 4.

The reactions with $LiAlH_4$ and $NaBH_4$ were repeated using thioamide compound 4' resulting in isolation of compound XXVII in 72% and 28% yield respectively. Compound 4': M.S.: 159$(M)^+$ (m/e). ^1H NMR ($CDCl_3$): δ 1.79 [2 overlapping t, 6H, ^3J=7.1Hz, $CH_2\underline{CH_3}$]; 1.20 [t, 3H, ^3J=7.0 Hz, $\underline{CH_3}$]; 1.96 [m, 2H, $C\underline{H_2}$]; 2.10 [m, 2H, $C\underline{H_2}$]; 3.53 [q, 2H, ^3J=7.1Hz, $\underline{CH_2}CH_3$]; 3.93 [q, 2H, ^3J=7.1Hz, $\underline{CH_2}CH_3$] ppm.

Iron complex 1 (0.3mmol) was dissolved in THF (10mL) and Pd/C 5% (0.3mmol) or Pd/C 10% (0.3mmol) or PtO_2 (0.3mmol) was added. The reaction vessel was charged with 40 psi H_2 and it was stirred for two days. Column chromatography on alumina gave 75%, 68%, and 70% recovery of 1 respectively.

Iron complex 3 was reacted with PtO_2 and 40 psi H_2 as above. Purification by column chromatography on alumina gave mostly complex 3 and NMR showed 14% reduction of the allylic double bond.

REFERENCES FOR PART I

1) Advanced Inorganic Chemistry- A Comprehensive Text, Fourth Edition, F.A.Cotton and G.Wilkinson, John Wiley and Sons (1980), N.Y, USA.

2) Comprehensive Organometallic Chemistry, Volume **8**, Editor-G.Wilkinson, Pergamon Press (1982), Oxford, England, 940.

3) Principles and Applications of Organotransition Metal Chemistry, J.P.Collman, L.S.Hegedus, J.R.Norton, and R.G.Finke, University Science Books (1987), Mill Valley, CA., USA.

4) G.W.Daub, *Prog.Inorg.Chem.*, **22**, 409 (1977).

5) A.J.Birch and L.F.Kelly, *J. Organometall.Chem.*, **285**, 267 (1985).

6) L.deMontarby, P.Mosset, and R.Grée, *Tetrahedron Lett.*, **29**, 3937 (1988).

7) A.J.Pearson and V.Khetani, *J.Org.Chem.*, **53**, 3395 (1988).

8) A.J.Pearson and C.Ong, *J.Am.Chem.Soc.*, **103**, 6686 (1981).

9) A.J.Pearson and Y.Chem, *J.Org.Chem.*, **51**, 1939 (1986).

10) A.J.Pearson and M.O'Brien, *J.Chem.Soc.,Chem.Comm.*, 1445 (1987).

11) M.F.Semmelhack and H.Le, *J.Am.Chem.Soc.*, **106**, 2715 (1984).

12) M.Bouzid, J.P.Pradére, P.Palvadreau, J.Vénien, and L.Toupet, *J. Organometall. Chem.*, **369**, 205 (1989).

13) J.Howell, B.Johnson, P.Josty, and J.Lewis, *J. Organometall.Chem.*, **39**, 329 (1972).

14) K.Stark, J.Lancaster, H.Murdoch, and E.Weiss, *Z.Naturforsch B*, **19**, 284 (1964).

15) C.Graham, G.Scholes, and M.Brookhart, *J.Am.Chem.Soc.*, **99**, 1180 (1977).

16) A.Birch, W.Raverty, and G.R.Stephenson, *Organometallics*, **3**, 1075

(1984).

17) W.Zhang, D.Jakiela, A.Maul, C.Knors, J.Lauher, P.Helquist, and D.Enders, *J.Am.Chem.Soc.*, **110**, 4652 (1988).

18) E.Weiss, K.Stark, J.E.Lancaster, and H.D.Murdoch, *Helv.Chim.Acta.*, **46**, 288 (1963).

19) A.Pouilhés and S.E.Thomas, *Tetrahedron Lett.*, **30**, 2285 (1989).

20) A.Nesmeyanov, L.Rybin, N.Gubenko, M.Rybinskaya, and P.Petrovskii, *J. Organometall. Chem.*, **71**, 271 (1974).

21) S.Aime, M.Botta, R.Gobetto, and D.Osella, *Inorg. Chim. Acta*, **115**, 129 (1986).

22) S.Aime, M.Botta, R.Gobetto, and D.Osella, *Organometallics*, **4**, 1475 (1985).

23) H.D.Kaesz and G.Lavigne, *J.Am.Chem.Soc.*, **106**, 4647 (1984).

24) T.N.Danks and S.E.Thomas, *Tetrahedron Lett.*, **29**, 1425 (1988).

25) J.Yin, J.Chen, W.Xu, Z.Zang, and T.Tang, *Organometallics*, **7**, 21 (1988).

26) H.Frühauf, F.Seils, M.Romao, and G.Goddard, *Angew.Chem.Int.Ed.Engl.*, **22**, 992 (1983).

27) H.Frühauf, F.Seils, M.Romao, and G.Goddard, *Organometallics*, **4**, 948 (1985).

28) H.Frühauf and F.Seils, *J. Organometall.Chem.*, **302**, 59 (1986).

29) H.Frühauf and F.Seils, *J. Organometall.Chem.*, **323**, 67 (1987).

30) D.C.Dittmer, P.Chang, R.L.Harlow, L.E.Harris, J.E.McCaskie, M.Iwanami, A.Tsai, C.Pfluger, I.Stamos, and K.Takahashi, *J.Am.Chem.Soc.*, **95**, 6113 (1973).

31) D.C.Dittmer, P.Chang, M.Iwanami, A.Tsai, I.Stamos, B.Blidner, and K.Takahashi, *J.Am.Chem.Soc.*, **98**, 2795 (1976).

32) E.J.Parker, J.R.Bodwell, T.C.Sedergran, and D.C.Dittmer,

Organometallics, 1, 517 (1982).

33) E.J.Parker and D.C.Dittmer, *Organometallics*, 1, 522 (1982).

34) B.Zwanenburg and J.Strating, *Quarterly Reports on Sulfur Chemistry*, 5, 79 (1970).

35) F.Götzfried and W.Beck, *J. Organometall.Chem.*, 191, 329 (1980).

36) J.Gosselink, F.Paap, and G.Vankoten, *Inorg. Chim. Acta.*, 59, 155 (1982).

37) Z.Yoshida, Y.Tamaru, and M.Kagotani, *J.Org.Chem.*, 44, 2816 (1979).

38) D.Paquer, *Int.J.Sulfur Chem., B*, 7, 269 (1972).

39) R.N.Hurd and G.DeLaMater, *Chem.Rev.*, 6, 45 (1961).

40) R.Mayer, J.Morgenstern, and J.Fabian, *Angew.Chem.Int.Ed.Engl.*, 3, 277 (1964).

41) H.Viola, H.Hartenhauer, and R.Mayer, *Zeit. f.Chem.*, 8, 269 (1988).

42) S.Scheibye, S.O.Lawesson, and C.Rømming, *Acta.Chem., Scand. B*, 35, 239 (1981).

43) K.Hartke and O.Kunze, *Ann.*, 321-330 (1989).

44) Advanced Organic Chemistry: Reactions, Mechanisms, and Structure- 3rd Edition, J.March, Wiley (1985), New York, USA.

45) W.Stewart and T.Siddall III, *Chem.Rev.*, 70, 517 (1970).

46) Carbon-13 NMR Spectral Problems, R.B.Bates, Humana Press (1981), Clifton, N.J., USA.

47) D.Rakshit and S.E.Tomas, *J. Organometall.Chem.*, 333, C3 (1987).

48) Comprehensive Organometallic Chemistry, Volume 4, Editor-G.Wilkinson, Pergamon Press (1982), Oxford, England.

49) M.Büsch and R.J.Clark, *Inorg.Chem.*, 14, 217 (1975).

50) Metallo-Organic Chemistry, A.J.Pearson, John Wiley and Sons (1985), New York, USA, 21-22.

51) I.Ugi, D.Marquarding, H.Klusacek, and P.Gillespie, *Acc.Chem.Res.*, 4, 288

(1971).

52) L.Kruczynski and J.Takats, *J.Am.Chem.Soc.*, **96**, 932 (1974).

53) P.Bischofberger and H.Hansen, *Helv.Chim.Acta.*, **65**, 721 (1982).

54) A.DeCian and R.Weiss, *Acta.Crystallogr.*, **B28**, 3273 (1972).

55) M.Sacerdoti, V.Bertolasi, and G.Gilli, *Acta.Crystallogr.*, **B36**, 1061 (1980).

56) R.L.Harlow and C.E.Pfluger, *Acta.Crystallogr.B.*, **29**, 2633 (1973).

57) A Guidebook to Mechanism in Organic Chemistry-5th Ed., P.Sykes, Longman Group Ltd., (1981), London, England.

58) A.Samb, B.Demerseman, P.Dixneuf, and C.Mealli, *J.Chem.Soc.,Chem.Comm.*, 1408 (1988).

59) Chemical Reactivity and Reaction Paths, G.Klopman, John Wiley and Sons, (1974), New York, USA.

60) A.J.Pearson and P.R.Raithby, *J.Chem.Soc., Dalton Trans.*, 884 (1981).

61) E.J.S.Vichi, F.Y.Fujiwara, E.Stein, *Inorg.Chem.*, **24**, 286 (1985).

62) C.A.Tolman, *Chem.Rev.*, **77**, 313 (1977).

63) L.J.Todd and J.R.Wilkinson, *J. Organometall.Chem.*, **77**, 1 (1974).

64) Sulphur in Organic and Inorganic Chemistry-3rd Ed., A.Senning, (1972).

65) Y.Tamaru, T.Harada, H.Iwainoto, Z.Yoshida, *J.Am.Chem.Soc.*, **100**, 5221 (1978).

66) G.B.Mpango and V.Snieckus, *Tetrahedron Lett.*, **21**, 4830 (1980).

67) F.Duus, *Tetrahedron*, **32**, 2817 (1976).

68) Comprehensive Heterocyclic Chemistry-Vol.**4**, E.Champaigne, Pergamon Press, (1984), New York, USA.

69) A.Brodie, B.F.Johnson, P.E.Josty, and J.Lewis, *J.Chem.Soc. Dalton Trans.*, 2031 (1972).

70) P.Corrigan, R.Dickson, S.Johnson, G.Pain, and M.Yeoh, *Aust.J.Chem.*, **35**, 2203 (1982).

71) N.Schore, *Chem.Rev.*, **88**, 1081 (1988).

72) L.Liebeskind, S.Baysdon, M.South, S.Ayer, and J.Leeds, *Tetrahedron*, **41**, 5839 (1985).

73) J.L.Davidson and D.W.A.Sharp, *J.Chem.Soc., Dalton Trans.*, 2283 (1975).

74) N.Ngouda, H.LeBozec, and P.Dixneuf, *J.Org.Chem.*, **47**, 4000 (1982).

75) E.Samsel and J.R.Norton, *J.Am.Chem.Soc.*, **106**, 5505 (1984).

76) J.Li, R.Hoffmann, C.Mealli, and J.Silvestre, *Organometallics*, **8**, 1921 (1989).

77) High Resolution NMR Theory and Applications, E.D.Becker, Academic Press (1980), New York, USA.

78) M.F.Semmelhack, J.W.Herndon, and J.K.Liu, *Organometallics*, **2**, 1885 (1983).

79) R.Pettit and J.Mahler, *J.Am.Chem.Soc.*, **85**, 3955 (1963).

80) *Zh.Org.Khim.*, **7**, 411 (1971).

81) C.Bonnans-Plaisance and G.Levesque, *Makromol.Chem. Rapid Comm.*, **6**, 145 (1985).

82) P.Metzner and J.Vialle, *Bull.Chem.Soc. France*, 3739 (1970).

83) A.Tagerman, L.Thijs, A.P.Anker, and B.Zwanenburg, *J.Chem.Soc.Perkin Trans. 2*, 458 (1960).

84) J.Pople, D.Beveridge, and P.Dobosh, *J.Chem.Phys.*, **47**, 2026 (1967).

85) Y.Tamaru, T.Hioki, S.Kawamura, H.Satomi, Z.Yoshida, *J.Am.Chem.Soc.*, **106**, 3876 (1984).

86) Y.Tamaru, T.Harada, and Z.Yoshida, *J.Am.Chem.Soc.*, **101**, 1316 (1979).

87) Y.Tamaru, T.Harada, S.Nishi, and Z.Yoshida,*Tetrahedron Lett.*, **23**, 2383 (1982).

88) S.Murahashi, Y.Imada, Y.Taniguchi, and S.Higashiura, *Tetrahedron Lett.*, **29**, 4945 (1988).

PART II

CHAPTER 5

SILICON ALKOXIDE-HALIDE CARBONYLATION REACTIONS

To contrast the use of organometallics in organic synthesis through stoichiometric reactions, a project involving a catalytic reaction was also investigated. The project focussed on the use of silicon alkoxides, in combination with carbon monoxide, and a rhodium (I) catalyst to convert benzylic halides to esters.

5.1 Introduction

Organometallic carbon-carbon bond formation by carbonylation of organic substrates is one of the most important reactions involving the use of organometallics in organic synthesis[1]. High selectivities in the synthesis of industrially important products such as acetic acid and esters, methyl formate, acetic anhydride, acetaldehyde, ethanol, and ethylene glycol have long been pursued using organometallic catalysts. As well, the bench organic chemist continually seeks improved synthetic procedures in the preparation of various functional groups and, in particular, seeks a general method applicable to a variety of substrates. As both target molecules and as synthetic intermediates, esters have been synthesized by several types of organometallic catalysts using a variety of substrates[2].

The variety of organic substrates that have been used in the organometallic synthesis of esters includes alkyl and aryl halides, thiols, and enol triflates. Enol triflates are readily carbonylated to esters with the catalyst

$[Pd(O_2CMe)_2]$, triphenylphosphine, and triethylamine in methanol/dimethyl formamide[2]. Dicobalt octacarbonyl was an effective catalyst under CO pressure at 180-190°C in the formation of esters from thiols[3][1].

$$RSH + R'OH + CO \xrightarrow[H_2O]{\text{catalyst}} RCO_2R' + H_2S \qquad [1]$$

Perhaps the most versatile organic substrates have been alkyl and aryl halides. Formic esters as well as dialkyl ethers have been used to generate alkyl or aryl esters with carbon monoxide and organometallic catalysts[2,4] [2].

$$RX + HCO_2R' + CO \xrightarrow[KI]{\text{catalyst}} RCO_2R' + HCOX \qquad [2]$$

As well, the use of main group and early transition metal alkoxides in the conversion of benzylic bromides to esters has been the subject of several publications[5,6,7,8]. Specifically, the main group metal alkoxides were borate esters (M=B) and aluminum alkoxides (M=Al) [3].

$$3ArCH_2Br + M(OR)_3 + 3CO \xrightarrow{\text{catalyst}} 3ArCH_2CO_2R + MBr_3 \qquad [3]$$

The early transition metals that have been employed were titanium (M=Ti) or zirconium (M=Zr) alkoxides [4].

$$4ArCH_2Br + M(OR)_4 + 4CO \xrightarrow{\text{catalyst}} 4ArCH_2CO_2R + MBr_3 \qquad [4]$$

Aryl, vinyl, and alkyl bromides produced esters from titanium alkoxides using a palladium catalyst, $[Pd(PPh_3)_4]$, or from zirconium alkoxides using a bimetallic

catalyst, $[Pd(PPh_3)_4]/[(1,5\text{-hexadiene})RhCl]_2$.

In an effort to investigate the scope of alkoxide promoted esterification reactions, a group IV alkoxide, silicon alkoxide, was employed.

5.2 Results and Discussion

Treatment of neat benzylic bromides at 75°C with a silicon alkoxide, 1 atm of carbon monoxide, and a catalytic amount of $[(1,5\text{-hexadiene})RhCl]_2$ (10:1-substrate:catalyst) gave esters in reasonable yields [5]. In some cases the addition of heptane as a cosolvent was required in order to dissolve benzylic substrates and the silicon reagent.

$$ArCH_2Br + XS\ Si(OR)_4 + CO \xrightarrow[1atm\ CO,\ 75°C]{catalyst} ArCH_2CO_2R \qquad [5]$$

The results of reactions using a variety of reagents are shown in Table 9.

Excess silicon alkoxide was required since the use of only a stoichiometric quantity (where the silicon alkoxide is in theory able to deliver four alkoxide groups) gave significantly reduced yields, unlike the results reported in the literature for titanium, zirconium, boron, and aluminum alkoxides.

A variety of substituted benzylic bromides were investigated and the best yields were obtained with benzyl bromide, giving esters **29'-32'**. An aryl bromide, 2-naphthyl bromide, and an alkyl bromide, 1-bromo-2-phenyl-ethane, gave no reaction and only trace amounts of the ester were found for 1-bromo-2-phenyl-ethylene, **42'**, and 1,1-dibromo-2-phenyl-ethylene, **43'**. Sterically hindered 1-bromo-1-phenyl ethane also resulted in only a very low yield of the ester, **41'**.

SUBSTRATE	$Si(OR)_4$ R=	COMMENTS	ISOLATED YIELD OF ESTER (XX')
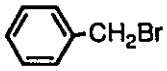	CH_3		81 (29')
	C_2H_5		50 (30')
	n-Bu		76 (31')
	sec-Bu		
	Ph		15 (32')
	C_2H_5	Heptane	0
		KI	56 (30')
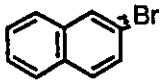	n-Bu	Heptane	0
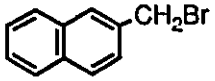	CH_3		49 (33')
	n-Bu	Heptane	34 (34')
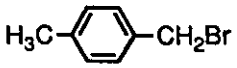	n-Bu		69 (35')
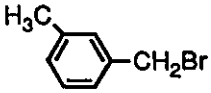	n-Bu		77 (36')
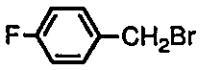	n-Bu		62 (37')
	CH_3		36 (38')
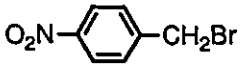	n-Bu	Heptane	56 (39')
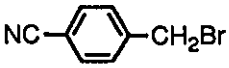	n-Bu	Heptane	61 (40')
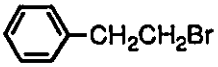	n-Bu		0
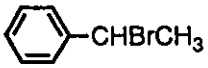	n-Bu		trace (41')
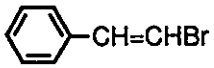	n-Bu		trace (42')
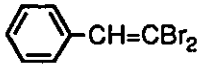	n-Bu		trace (43')
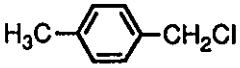	n-Bu		4 (31')

Table 9

The effect of substitution on the aromatic ring was investigated. Substitution of an electron donating alkyl group, (methyl), in the meta position of benzyl bromide had no effect on the yield of the ester obtained using tetra-n-butyl orthosilicate, **36'**. Electron withdrawing groups, fluoro, nitro, and cyano, and an electron donating methyl group in the para position gave esters in good yields, **37'-38'**, **39'**, and **40'** respectively, but they were slightly reduced in comparison to non-substituted benzyl bromide. Therefore, the nature of the substituent and its position on the aromatic ring had no significant effect on the reaction leading to ester formation.

Benzyl chloride resulted in the ester in a reaction with tetra-n-butyl orthosilicate, but the yield of the ester was poor in comparison to the same reaction with benzyl bromide.

The reaction was found to be dependent on the nature of the silicon alkoxide. In the reaction with benzyl bromide, tetra-n-butyl and tetramethyl orthosilicate gave good yields in ester formation, **31'**(76%) and **29'**(81%) respectively, while tetraethyl orthosilicate gave only a moderate yield of the ester, **30'**(50%), and tetra-sec-butyl orthosilicate gave a low isolated yield, **32'**(15%). Tetraphenyl orthosilicate gave no reaction with benzyl bromide. In contrast to the results obtained for benzyl bromide, tetra-n-butyl orthosilicate gave a higher ester yield than did tetramethyl orthosilicate in the reaction with para-fluorobenzyl bromide; (**37'**(62%) and **38'**(36%) respectively).

Several attempts were made to improve the yield in ester formation. Increasing the temperature of the reaction (up to 100°C) did not improve the yield nor did the use of another catalyst, $[Rh(CO)_2(PPh_3)Cl]$. This new catalyst resulted in a decreased yield. As well, increasing the ratio of catalyst to substrate did not improve the yield of ester formation. The use of potassium iodide has

been shown to promote catalytic reactions and has proven effective for the Monsanto acetic acid process, the homologation of acids, ethers, and esters, and in benzyl chloride-borate ester carbonylation reactions[9]. It has been postulated that the role of the iodide ion is to displace chloride in the rhodium chloride catalyst, $[Rh(CO)_2Cl]_2$, generating a new and more active catalyst, $[Rh(CO)_2I]_2$[9]. Unfortunately, there was no significant yield improvement associated with the addition of iodide ion to the silicon alkoxide-benzyl bromide reaction.

5.3 Product Formation Pathway

The pathway outlined in Scheme 1 illustrates a possible route to product formation. The rhodium hexadiene catalyst, I, may be converted to the carbon monoxide substituted catalyst, II, although in a separate experiment, this dichlorodicarbonyl rhodium (I) catalyst was found to catalyze the formation of ester from benzyl bromide and tetra-n-butyl orthosilicate in a slightly lower yield, 48%. Oxidative addition of two moles of benzyl bromide would then give complex III which in the presence of CO could give the acyl complex IV. Reductive elimination of the acid bromide could then lead to alkoxide transfer from the silicon alkoxide leading to the desired ester while at the same time regenerating the carbonyl catalyst, II. This last step was shown in a separate experiment to produce the ester in 23% yield from a mixture of phenylacetyl chloride and tetra-n-butyl orthosilicate.

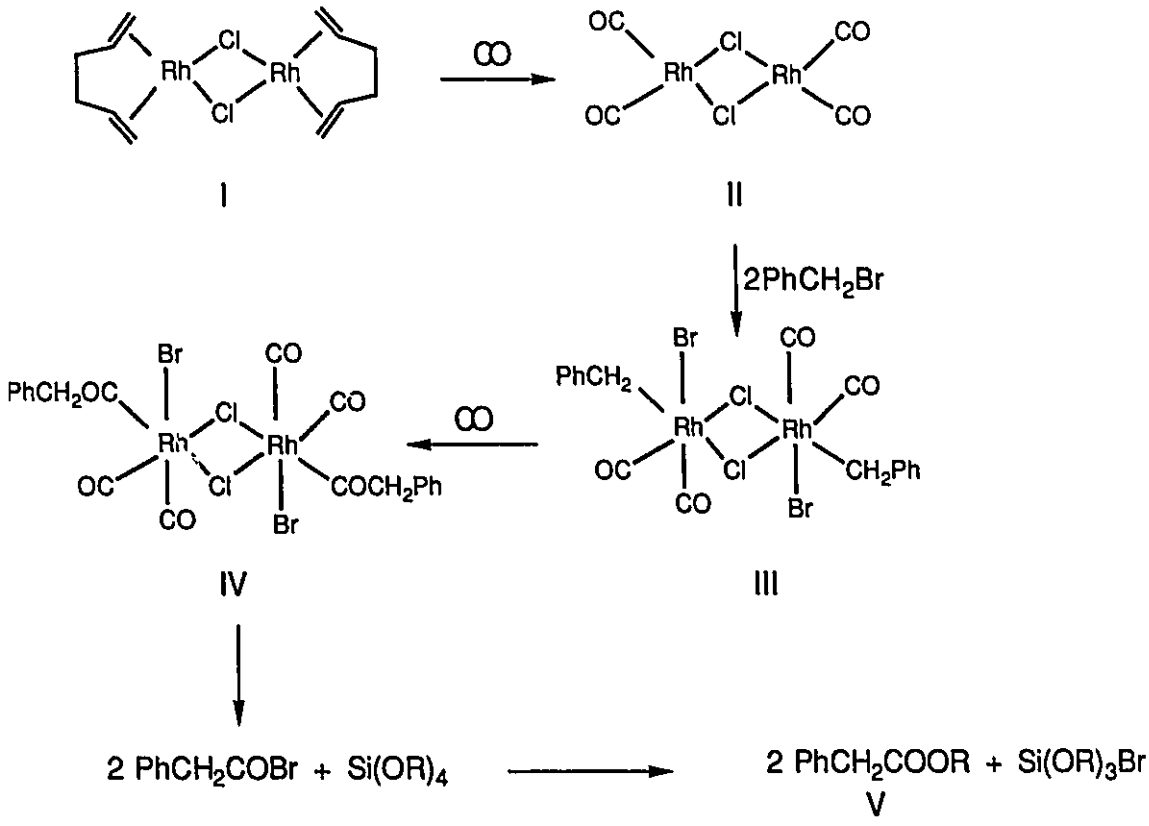

Scheme 1

An alternative mechanism is that which was proposed for the reaction of benzyl bromides with borate esters producing carboxylic esters[5]. Here, silicon alkoxide would initially react with the dichlorodicarbonyl rhodium (I) dimer, II, to yield zwitterion complex IV. Alkoxide migration would give acyl-complex VIII which would then reductively eliminate the ester leaving the complex IX which could then undergo further reaction until all of the alkoxides were transfered.

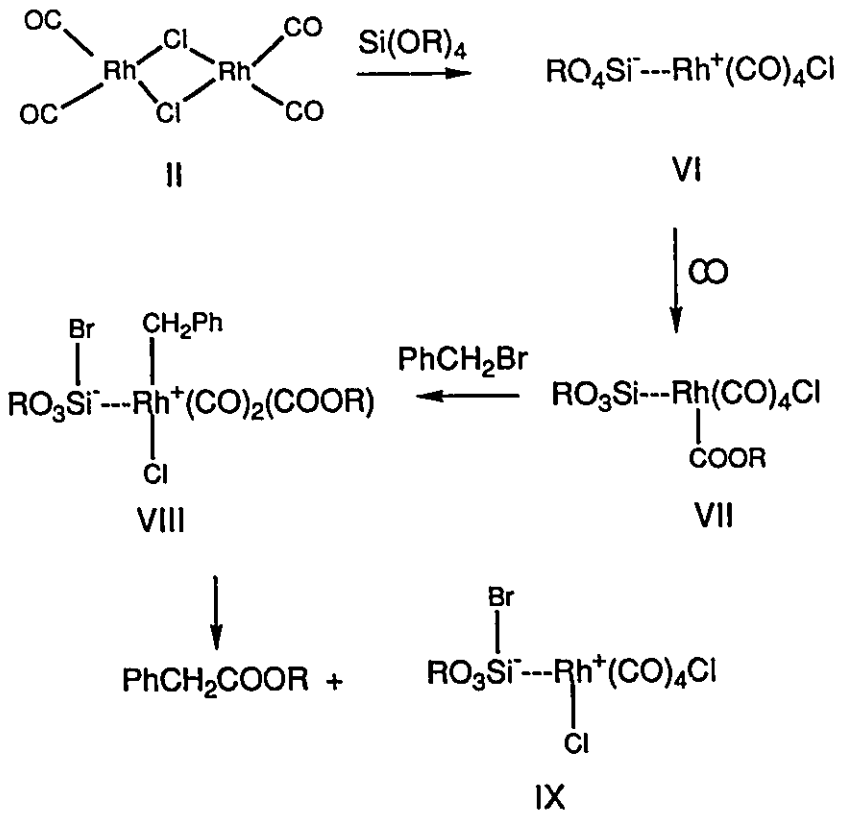

Scheme 2

For the silicon alkoxide-benzyl bromide reaction, this mechanism does not account for the lower yields obtained from a stoichiometric reaction of benzyl bromide to silicon alkoxide.

5.4 Conclusions

In conclusion, silicon alkoxides can be used to prepare carboxylic esters from benzylic bromides and carbon monoxide, catalysed by a rhodium (I) complex, which further demonstrates the 'flexibility' available to the organic chemists in the choice of alkoxides for esterification of benzyl bromides. The reaction proceeds under mild conditions and it is not affected by electron

withdrawing and electron donationg substituents on the aromatic ring, but the yield for ester formation is severely reduced by substituting with an alkyl group at the benzylic carbon. As was found for titanium and zirconium alkoxides, the reaction is sensitive to the nature of the alkoxide group being introduced, although no trends were evident.

5.5 Experimental Details

5.5.0 Solvents and Reagents

Reagents were purchased from Aldrich Chemical Company, Farchan Laboratories, and Fluka. Most were used without further purification.

Ether was dried over sodium prior to each reaction. Hexane was dried over calcium hydride. All of the other solvents were used without further purification. All solvents were purchased from BDH Chemicals or Aldrich Chemical Company.

Columns were packed neutral activated alumina, Brockmann I, and Florisil (60-100 mesh) purchased from Aldrich Chemical Company. Preparatory TLC plates (0.25mm and 1.20mm silica gel and aluminum oxide 60 with fluorescent indicator UV_{254}) were purchased from Chromatographic Specialties Inc.

All of the deuterated solvents were purchased from MSD Isotopes.

5.5.1 Instrumentation

5.5.1.1 Nuclear Magnetic Resonance Spectroscopy

The ^1H NMR spectra were recorded on a Varian EM360A spectrometer. Chemical shifts were reported relative to TMS.

5.5.1.2 Infrared Spectroscopy

Infrared spectra were recorded on a Perkin-Elmer 783 Infrared spectrometer using NaCl disks.

5.5.1.3 Mass Spectrometry

Mass spectra were obtained from a VG7070E mass spectrometer using a PDP8A data system.

5.5.1.4 Mass Balance

Mass determinations were obtained using a Mettler EA100 analytical balance.

5.5.2 General Procedure:

A solution of silicon alkoxide (2.0ml), benzyl halide (2.0mmol), and $[(1,5\text{-hexadiene})RhCl]_2$ (0.2mmol) was stirred overnight at 75°C under an atmosphere of carbon monoxide. After cooling the solution to room temperature, a solution of 6N HCl (10ml) was added and the solution was stirred for 1h to hydrolize the excess silicon alkoxide. The mixture was filtered through Celite and extracted with ether (5X50ml). The combined ether fractions were washed with distilled water (2X50ml), dried over $MgSO_4$, filtered, and the solvent was

removed by rotary evaporation. Purification by column chromatography on alumina using ether gave pure ester as a colourless oil.

5.5.2.1 [Ph-CH_2COOCH_3] **29'**

Yield 81%. M.S.: 150$(M)^+$, 119$(M\text{-}OCH_3)^+$, 119$(PhCH_2CO)^+$, 91$(PhCH_2)^+$ (m/e). IR (neat) υ(CO): 1740(s) cm^{-1}. ^1H NMR ($CDCl_3$) (60MHz): δ 3.7 [m, H5, PhCH_2 and OCH_3]; 7.3 [s, 5H, aromatics] ppm.

5.5.2.2 [Ph-$CH_2COOC_2H_5$] **30'**

Yield 50%. M.S.: 164$(M)^+$, 119$(PhCH_2CO)^+$, 91$(PhCH_2)^+$ (m/e). IR (neat) υ(CO): 1735(s) cm^{-1}. ^1H NMR ($CDCl_3$) (60MHz): δ 1.3 [t, 3H, ^3J=7Hz, OCH_2CH_3]; 3.6 [s, 2H, PhCH_2]; 4.2 [q, 2H, ^3J=7Hz, OCH_2CH_3]; 7.4 [s, 5H, aromatics] ppm.

5.5.2.3 [Ph-$CH_2COOC_4H_9$] **31'**

Yield 76%. M.S.: 192$(M)^+$, 119$(PhCH_2CO)^+$, 91$(PhCH_2)^+$ (m/e). IR (neat) υ(CO): 1735(s) cm^{-1}. ^1H NMR ($CDCl_3$) (60MHz): δ 0.7 [t, 3H, ^3J=7Hz, $O(CH_2)_3CH_3$]; 1.2 [m, 4H, $OCH_2(CH_2)_2CH_3$]; 3.3 [s, 2H, PhCH_2]; 3.8 [m, 2H, O$CH_2(CH_2)_2CH_3$]; 7.2 [s, 5H, aromatics] ppm.

5.5.2.4 [Ph-$CH_2COOCH(CH_3)CH_2CH_3$] **32'**

Yield 15%. M.S.: 192$(M)^+$, 119$(PhCH_2CO)^+$, 91$(PhCH_2)^+$ (m/e). IR (neat) υ(CO): 1735(s) cm^{-1}. ^1H NMR ($CDCl_3$) (60MHz): δ 0.9-1.7 [m, 8H, $OCH(CH_3)CH_2CH_3$]; 3.6 [s, 2H, PhCH_2]; 4.8 [m, 1H, O$CH(CH_3)CH_2CH_3$]; 7.3 [s, 5H, aromatics] ppm.

5.5.2.5 [$C_{10}H_7CH_2COOCH_3$] **33'**

Yield 49%. M.S.: 200$(M)^+$, 141$(C_{10}H_7CH_2)^+$ (m/e). IR (neat) υ(CO): 1735(s) cm^{-1}. ^1H NMR ($CDCl_3$) (60MHz): δ 3.3 [s, 2H, $C_{10}H_7\underline{CH_2}$]; 3.6 [s, 3H, $O\underline{CH_3}$]; 7.1-7.8 [s, 7H, aromatics] ppm.

5.5.2.6 [$\underline{C_{10}H_7CH_2COOC_4H_9}$] **34'**

Yield 34%. M.S.: 242$(M)^+$, 141$(C_{10}H_7CH_2)^+$ (m/e). IR (neat) υ(CO): 1735(s) cm^{-1}. ^1H NMR ($CDCl_3$) (60MHz): δ 0.8 [t, 3H, ^3J=7Hz, $O(CH_2)_3\underline{CH_3}$]; 1.5 [m, 4H, $OCH_2(\underline{CH_2})_2CH_3$]; 3.7 [s, 2H, $C_{10}H_7\underline{CH_2}$]; 4.1 [t, 2H, ^3J=7Hz, $O\underline{CH_2}(CH_2)_2CH_3$]; 7.3-7.8 [s, 7H, aromatics] ppm.

5.5.2.7 [$\underline{p\text{-}CH_3}\text{-}\underline{Ph}\text{-}\underline{CH_2COOC_4H_9}$] **35'**

Yield 69%. M.S.: 206$(M)^+$, 105(p-Me-$PhCH_2)^+$ (m/e). IR (neat) υ(CO): 1735(s) cm^{-1}. ^1H NMR ($CDCl_3$) (60MHz): δ 0.9 [t, 3H, ^3J=7Hz, $O(CH_2)_3\underline{CH_3}$]; 1.4 [m, 4H, $OCH_2(\underline{CH_2})_2CH_3$]; 2.2 [s, 3H, $Ph\underline{CH_3}$]; 3.5 [s, 2H, $Ph\underline{CH_2}$]; 4.0 [t, 2H, ^1J=7Hz, $O\underline{CH_2}(CH_2)_2CH_3$]; 7.2 [m, 4H, aromatics] ppm.

5.5.2.8 [$\underline{m\text{-}CH_3}\text{-}\underline{Ph}\text{-}\underline{CH_2COOC_4H_9}$] **36'**

Yield 77%. M.S.: 206$(M)^+$, 105(m-Me-$PhCH_2)^+$ (m/e). IR (neat) υ(CO): 1735(s) cm^{-1}. ^1H NMR ($CDCl_3$) (60MHz): δ 0.8 [t, 3H, ^3J=7Hz, $O(CH_2)_3\underline{CH_3}$]; 1.4 [m, 4H, $OCH_2(\underline{CH_2})_2CH_3$]; 2.2 [s, 3H, $Ph\underline{CH_3}$]; 3.4 [s, 2H, $Ph\underline{CH_2}$]; 3.9 [m, 2H, $O\underline{CH_2}(CH_2)_2CH_3$]; 7.2 [m, 4H, aromatics] ppm.

5.5.2.9 [$\underline{p\text{-}CN}\text{-}\underline{Ph}\text{-}\underline{CH_2COOC_4H_9}$] **37'**

Yield 62%. M.S.: 210$(M)^+$,109(p-CN-$PhCH_2)^+$ (m/e). IR (neat) υ(CO): 1735(s) cm^{-1}. ^1H NMR ($CDCl_3$) (60MHz): δ 1.0 [t, 3H, ^3J=7Hz, $O(CH_2)_3\underline{CH_3}$]; 1.5 [m, 4H, $OCH_2(\underline{CH_2})_2CH_3$]; 3.6 [s, 2H, $Ph\underline{CH_2}$]; 4.1 [t, 2H, ^1J=7Hz, $O\underline{CH_2}(CH_2)_2CH_3$]; 7.0-7.4 [m, 4H, aromatics] ppm.

5.5.2.10 [p-F-Ph-CH_2COOCH_3] **38'**

Yield 36%. M.S.: 168$(M)^+$, 109(p-F-$PhCH_2)^+$ (m/e). IR (neat) υ(CO): 1735(s) cm^{-1}. ^1H NMR ($CDCl_3$) (60MHz): δ 3.8 [m, 5H, OCH_3 and $PhCH_2$]; 7.1-7.6 [m, 4H, aromatics] ppm.

5.5.2.11 [p-NO_2-Ph-$CH_2COOC_4H_9$] **39'**

Yield 56%. M.S.: 237$(M)^+$, 136(p-NO_2-$PhCH_2)^+$ (m/e). IR (neat) υ(CO): 1735(s), υ(NO_2): 1520(s), 1350(s) cm^{-1}. ^1H NMR ($CDCl_3$) (60MHz): δ 0.9 [t, 3H, ^3J=7Hz, $O(CH_2)_3CH_3$]; 1.4 [m, 4H, $OCH_2(CH_2)_2CH_3$]; 3.7 [s, 2H, $PhCH_2$]; 4.1 [t, 2H, ^1J=7Hz, $OCH_2(CH_2)_2CH_3$]; 7.4-8.3 [m, 4H, aromatics] ppm.

5.5.2.12 [p-CN-Ph-$CH_2COOC_4H_9$] **40'**

Yield 61%. M.S.: 217$(M)^+$, 116(p-CN-$PhCH_2)^+$ (m/e). IR (neat) υ(CO): 1735(s), υ(NO_2): 1520(s), 1350(s) cm^{-1}. ^1H NMR ($CDCl_3$) (60MHz): δ 1.3 [m, 7H, $OCH_3(CH_2)_2CH_3$]; 3.7 [s, 2H, $PhCH_2$]; 4.5 [m, 2H, $OCH_2(CH_2)_2CH_3$]; 7.6 [m, 4H, aromatics] ppm.

5.5.2.13 [Ph-$CH(COOC_4H_9)CH_3$] **41'**

IR (neat) υ(CO): 1735(s) cm^{-1}.

5.5.2.14 [Ph-$CH=CHCOOC_4H_9$] **42'**

IR (neat) υ(CO): 1710(s) cm^{-1}.

5.5.2.15 [p-CH_3-Ph-$CH=C(COOC_4H_9)_2$] **43'**

IR (neat) υ(CO): 1735(s) cm^{-1}.

REFERENCES FOR PART II

1) G.P.Chiusoli, *Transition Met.Chem.*, **12**, 89 (1987).

2) S.Cacchi, E.Morera, and G.Otar, *Tetrahedron Lett.*, **26**, 1109 (1985).

3) S.Shim, S.Antebi, and H.Alper, *J.Org.Chem.*, **50**, 147 (1985);*Tetrahedron Lett.*, **26**, 2609 (1985); S.Antebi and H.Alper, *Organometalics*, **5**, 596 (1986).

4) C.Buchan and H.Alper,*Tetrahedron Lett.*, **26**, 5743 (1985).

5) J.B.Woell and H.Alper,*Tetrahedron Lett.*, **25**, 3791 (1984).

6) K.E.Hashem, J.B.Woell, and H.Alper, *Tetrahedron Lett.*, **25**, 4879 (1984).

7) H.Alper, S.Antebi, and J.B.Woell, *Angew.Chem.Int.Ed.Engl.*, **23**, 732 (1984).

8) J.B.Woell, S.B.Fergusson, and H.Alper, *J.Org.Chem.*, **50**, 2134 (1985).

9) H.Alper, N.Hamel, D.Smith, and J.B.Woell, *Tetrahedron Lett.*, **26**, 2273 (1985).

CHAPTER 6

CLAIMS TO ORIGINAL RESEARCH

1. The first α,β-unsaturated thioamide, thioester, and thione iron tricarbonyl complexes were prepared and characterized and two X-ray crystal structures were obtained.
2. Triphenyphosphine was shown to substitute for a single CO ligand in α,β-unsaturated thioamide and thioester iron tricarbonyl complexes.
3. An α,β-unsaturated thioester iron tricarbonyl complex reacted with strong oxidants affording a sulphine iron tricarbonyl complex.
4. Nucleophiles reacted with α,β-unsaturated thioamide iron tricarbonyl complexes at -78°C generating novel 4-oxo-thioamide products free of metal coordination.
5. An electrophilic alkyl group reacted with an α,β-unsaturated thioester iron tricarbonyl complex produced an S-methyl substituted cationic iron tricarbonyl complex.
6. Alkynes reacted with α,β-unsaturated thioamide iron tricarbonyl complexes forming new thioamide cyclopentenone iron tricarbonyl complexes. One crystal structure was obtained.
7. Silicon alkoxides were used as a source of alkoxide to prepare carboxylic esters in good yields from benzylic bromides and carbon monoxide catalyzed by a rhodium complex under mild conditions.